DISSERTATION

MOLECULAR CHARACTERIZATION OF MACROPHAGE RESPONSE TO MODEL BIOMATERIAL SURFACES *IN VITRO*

Submitted by

Marisha L. Godek

Cell and Molecular Biology Program

In partial fulfillment of the requirements

For the Degree of Doctor of Philosophy

Colorado State University

Fort Collins, CO

Summer 2006

COLORADO STATE UNIVERSITY

May 9, 2006

WE HEREBY RECOMMEND THAT THE DISSERTATION PREPARED UNDER OUR SUPERVISION BY MARISHA L. GODEK ENTITLED "MOLECULAR CHARACTERIZATION OF MACROPHAGE RESPONSE TO MODEL BIOMATERIAL SURFACES *IN VITRO*" BE ACCEPTED AS FULFILLING IN PART REQUIREMENTS FOR THE DEGREE OF DOCTOR OF PHILOSOPHY.

Committee on graduate work

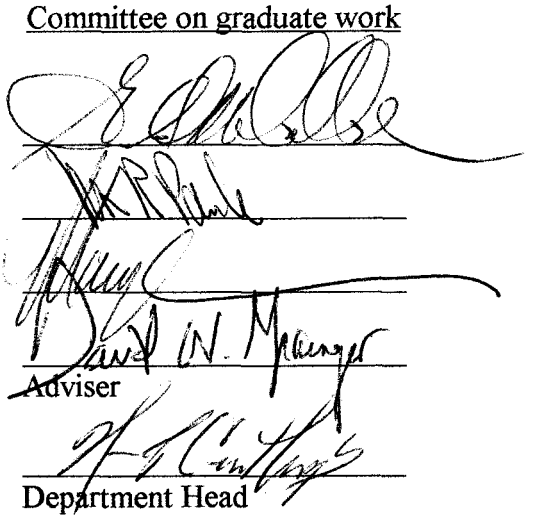

Adviser

Department Head

ABSTRACT OF DISSERTATION

MOLECULAR CHARACTERIZATION OF MACROPHAGE RESPONSE TO MODEL BIOMATERIAL SURFACES *IN VITRO*

Cellular response to various model biomaterials has important fundamental significance to numerous medical device and diagnostic applications. Biomaterial implants are plagued by failure, associated with a host "foreign body" inflammatory reaction, regardless of composition or physiological placement. Underlying the rejection process is a complex dynamic relationship between cells, biomaterials and milieu. *In vivo*, circulating monocytes arrive at a biomaterial surface, attach to it and differentiate to macrophages, the key mediators of the "foreign body" reaction. Macrophage presence signals a chain of events that may result in chronic inflammation, and ultimately implant failure. Understanding the mechanisms by which macrophages are able to adhere to and differentiate on implant surfaces is an important first step toward developing biocompatible implants.

Macrophage response to a diverse group of model biomaterials surfaces was investigated. Gross cellular response was tracked over time, reporting adhesive behavior, proliferative rates, and morphological changes as a function of surface chemistry. Initial studies compared commonly employed cell culture substrates and select model biomaterials with clinical relevance. Subsequently, the study of surface chemistry's effect on cell adhesive

behavior was extended to a large group of plasma-polymerized co-patterned surfaces of distinct chemistries.

Molecular level response to biomaterials was tracked via the Rho GTPase cellular signaling cascade, one integrin-linked outside-in signaling cascade with the ability to affect cell adhesion, proliferation and spreading in response to environmental cues. Expression and activation of the Rho proteins was compared based on cell maturity (pro-monocyte to monocyte to macrophage lineages), cell derivation and by model surface chemistry. Finally, the molecular mechanism by which macrophage cells adhere to and proliferate on albumin selective fluorocarbon surfaces was investigated through integrin blocking studies. Collectively, these experiments represent an important step toward an improved understanding of the unique behaviors exhibited by macrophage cells as part of the natural response to unnatural materials present in the body.

Marisha L. Godek
Cell and Molecular Biology Program
Colorado State University
Fort Collins, CO 80523
Summer 2006

ACKNOWLEDGEMENTS

It is with deep gratitude that I acknowledge the professional and personal contributions of the following individuals to my development as a scientist:

Dr. David Grainger, my adviser, for professional guidance and development. Especially for reading and editing countless abstracts, manuscript drafts and other professional documents.

Current and past committee members: Dr. Marv Paule, Dr. Gerry Callahan, Dr. Mary Weiser-Evans, Dr. Mark Howell and Dr. Tina Rinker.

Technical assistance and advice: Dr. James Anderson, Dr. Andrés García, Dr. Guy Hagen, Dr. Victoria Hitchins, Dr. Mercedes Gonzalez-Juarerro, Dr. W. John Kao, Dr. Amy McNally, Dr. Tim Sit and Dr. Theo van Kooten.

The Grainger lab group: Lisa Chamberlain, Jim Christie, Nikki Duchsherer, Ping Gong, Quinn McElwee, Jennifer Sampson, Terri Stadler and Peng Wu. Special thanks to Dr. Greg Harbers for editing and technical advice.

The Barisas/Roess, Paule, Bamburg and Fisher lab groups.

Dr. Mike Fox and Norma Bulera.

Dr. Ann Maycunich-Gilley, my business mentor, for professional and personal guidance.

David Ellerby. Thank you for recognizing the unifying principles of art and science. "Life beats down and crushes the soul, and art reminds you that you have one."- *Stella Adler.* Thanks for allowing me the indulgence of the reminder.

Special thanks to Mark Grillo---without your persistence and encouragement I would never have made it to Colorado. Thanks for being my original mentor.

Finally, thanks to all friends and family who have supported me throughout this process, especially Corbin, Santano, Nikki, Laurie, Paula, Chuck, Tina, Mike, Sean, Lindsey, Bailey, Patches, Winston and Chloe.

Support provided through NIH funding, grant EB 000894.

DEDICATION

"He said curiosity was necessary to intelligence, and that curiosity never killed the cat. That cat died from stupidity..." *R. Ruark*

For my parents, David and Judy.

I am grateful for the gifts each of you has given me throughout the years, including the countless sacrifices you made so that I could pursue numerous activities and educational endeavors. I am truly blessed to have parents who have always put me first, who encourage without hesitation, and who have boundless faith in my ability to succeed, no matter the circumstances. I believe that scientists are, at heart, naturalists. Scientists examine the world around them and offer explanations for what they see. Their experimentation may be based in thought, action or both. Dad, you were my first scientific mentor. Thank you for encouraging me to mentally engage, to examine my surroundings, to interpret and present what I see in my own voice and medium. Your lessons have served me well in both my scientific and artistic endeavors. Mom, thanks for being an exceptional feminine role-model. You provided me with a strong sense of personal possession, an internal locus of control, a barometer for human kindness, and finally, good fashion sense, despite the fact that I seldom use it.

TABLE OF CONTENTS

CHAPTER 1: INTRODUCTION-MACROPHAGE INTERACTIONS WITH BIOMATERIAL SURFACES

This chapter was written by Marisha L. Godek and edited by David W. Grainger. It is intended to provide information fundamental to an appreciation of the macrophage cell and its role in immuno-modulatory inflammatory processes, particularly the foreign body reaction. This chapter begins with a general introduction, followed by a description of the biointerface, and accompanying surface-protein-cell interactions. Cellular adhesion receptors are briefly introduced. The second section (beginning 1.4) of the chapter is devoted to the physiological responses relevant to biomaterials/biomedical device placement *in vivo*: normal and abnormal (foreign body reaction) wound healing. The third section (beginning 1.6) describes experimental design and conditions and includes working hypotheses addressed in Chapters 2-4.

1.1 Introduction

Biomaterials and associated biomedical devices represent a billion dollar industry in the Unites States alone.[1] *In vivo*, all biomaterials and biomedical devices are plagued by a host inflammatory response, the foreign body reaction[2] (FBR), regardless of material composition or placement.[3,4] The FBR involves components of numerous physiological responses, including wound healing and inflammation, and is characterized by chronic

inflammation, compromised healing at the implant site and biomedical device failure.[5] Significantly, the exceedingly complex FBR is poorly defined at the molecular level.[2,6]

Understanding the FBR elicited by all surgically placed biomaterials[4] is of tremendous importance given that it represents a significant hurdle in biocompatible materials development. Current biomaterials/biomedical devices provide some measure of success, often defined in terms of minimal performance requirements that can be translated to extended or improved quality of life for patients. However, it can be generally stated that medical device performance in many contexts is well below expectations for patients and physicians alike – most implanted devices do not achieve their full potential *in vivo* (as indicated or intended by design), suffer numerous complications, and are merely tolerated by the body. Creating *biocompatible* materials, i.e. materials with the ability to perform with an appropriate host response in a specific application,[1] is inherently challenging due to the tremendous range of physiological locations and conditions where devices must function. This problem is further compounded by a variety of factors including the chemical composition, form and properties of the device itself, the performance requirements and expected lifetime of the device once placed, and the patient's age and health.

The surgical placement of a biomedical device results in the formation of a wound site, and the ensuing ubiquitous FBR represents an aberrant form of wound healing;[5] thus, examination of what is currently known about the progression of the essential "normal" wound healing response is important to distinguishing and understanding components of

the FBR. Current research efforts on the FBR are diverse, crossing immunology, pathology, surgery, cell and molecular biology, materials science, and biomedical engineering. One effort focuses on the biointerface between the implant material and the body, often distilled to studies of "cells on surfaces."[7-9] At the cellular level this response can be examined in terms of key immune cells known to interact with materials and facilitate FBR development, in particular monocytes (MC), macrophages (MΦ), and activated MΦ.[4] These cells are implicated in acute and chronic inflammatory responses to foreign entities of various origins.[5,10,11] Further, the relationships between MC, MΦ and other cells (e.g., fibroblasts, endothelial cells) are significant when considering implanted materials biocompatibility, given that MΦ cells recruit and influence the behavior of other cell types at the implant site, contributing to the development of specific physiological outcomes (e.g., inflammation, thrombosis, fibrosis, angiogenesis).[4,11,12]

The work described here has significant implications for the success of all implantable materials given that immune cells such as the MΦ represent the first line of defense within the body and play a critical role in mobilizing inflammatory responses that impact the ultimate fate (acceptance or rejection) of biomedical implants.[4,5] Additionally, MΦ cells are now employed for *in vitro* diagnostic testing and drug screening (e.g., inflammation, cytotoxicity), and information gleaned from this study is also applicable to improving the reliability of these MΦ-based assays. The global objectives of the work presented here include an improved understanding of the following: 1) the FBR to model biomaterials at the molecular level, 2) the effects of *in vitro* cell culture conditions (e.g., serum, time, exogenous cytokine addition) on MΦ cells employed to recapitulate the

FBR *ex vivo/in vitro* and 3) the equivalence (or non-equivalence) of primary- and secondary-derived MΦ cells commonly employed for *in vitro* assessment of biocompatibility.

1.2 The biointerface

The biointerface is the region where a biomedical device/biomaterial and the body/tissue converge.[13] For practical purposes, the biointerface can often be defined in terms of the diverse interactions between the outermost surface of the material and the cells that contact it through specific and/or non-specific protein-mediated interactions.[13] Biomaterials with a wide range of chemical and physical properties are commonly employed *in vivo*[13] and these properties are important determinants of protein selection and adsorption from complex biological solutions.[14-19] Significantly, adsorbed proteins on a device surface affect cell adhesive behavior, i.e., most mammalian cells attach best to surfaces that are neither too hydrophobic nor too hydrophilic, and of moderate polarity.[13,20,21] Highly hydrophilic (e.g., poly(ethylene glycol), poly(ethylene oxide), dextran) and highly hydrophobic (Teflon®, polystyrene) surfaces are poorly supportive of mammalian cell adhesion *in vitro,*[8,13,21-23] although implant performance cannot be gauged by cell adhesive behavior alone.

Relationships between polymer surfaces and cells depend upon specific surface characteristics such as the chemical composition (surface free energy), related wettability (hydrophobicity/hydrophilicity), charge, topography and specific functionalization or surface modifications.[14,18,24] In turn, these features affect the surface selection of proteins

from complex biological milieu, such as plasma or serum.[25] *In vivo* and *in vitro*, materials are coated by proteins within seconds of exposure;[26] cells never directly contact bare surface chemistry without adsorbed proteins.[16] However, control over protein interfacial events, including adsorbed layer composition, protein conformational maintenance and subsequent interactions with cells and platelets is not possible. Hence, no matter what determinants are asserted for device biocompatibility, interfacial controls on such events are minimal in physiological conditions. Host inflammatory reactions to implanted materials are a direct result of this problem. These reactions are ubiquitous and without a molecular or cellular basis for understanding.

Cell-surface interactions, specifically interactions of MC and MΦ with biomaterial surfaces, are regarded as central to inflammatory responses and the FBR commonly observed around implants *in vivo*.[5] MC and MΦ presence at wound sites is a normal response to wound healing. Indeed, their presence at the device surface in the implant/wound site is essential for progression through various phases of the normal wound healing response (e.g., removal of apoptotic neutrophils, control of infection, recruitment of cells that aid in acute injury response and the production of connective tissue, etc).[5,10,11] Hence, these physiological events are not entirely adverse, and do not necessarily affect implant function and normal wound healing mechanisms. However, acute healing transition to chronic inflammation and departure from normal mechanisms is often observed at implant sites, producing the FBR. Understanding how inflammatory and healing processes can be controlled (and enhanced or curbed as appropriate) and how device design and materials influence these processes could lead to dramatic

improvements in implant function and device-host tissue integration *in vivo*. Ameliorating the FBR to improve implant performance remains an elusive goal in many implant scenarios. Toward this end, improved molecular and cellular understanding of inflammatory and healing processes in biomaterials/biomedical device scenarios is requisite.

1.3 Cell-protein-surface interactions

One approach to understanding the global FBR to biomaterials is to examine key interactions required for FBR development. In addition to the cellular players involved in the FBR and FBGC formation, two important factors influential in FBGC formation are (biomaterial) surface chemistry and protein adsorption that occur prior to cell adhesion. It has been hypothesized that these factors are critical indicators of biomaterials and biomedical device success *in vivo*.[4] This section will focus on cell-protein-surface interactions essential for development of the FBR.

1.3.1 Protein interactions with surfaces

All materials exposed to biological milieu are rapidly coated with proteins.[15] Despite bold assertions to the contrary, materials can influence but not prevent or control this response in physiological milieu. Several thousand different soluble proteins assail an implant surface exposed to physiological milieu, with a dynamic concentration range of 10^{11} and broad range of molecular weights, sizes, and physicochemical characteristics.[27] Most are surface-active. The practical ramification of this phenomenon is that cells must interact with this adsorbed protein layer.[26] Surface chemistry has been shown to play a role in

dictating protein adhesion from complex biological milieu and multi-component protein solutions,[14,18,28] and not all protein species are represented on a given surface proportional to their bulk concentration.[28] Hence, surface chemistry has an indirect effect on cell adhesion through protein interfacial activity, exchange, adsorption and equilibrium composition.[26]

Protein	Plasma Concentration (mg/ml)	Plasma Concentration (μM)	Molecular Weight (kD)	Present in serum
Albumin	40	600	66	Y
IgG	8-17	53-113	150	Y
Fibrinogen	2-3	5.8-8.8	340	N
C3	1.6	8.8	180	Y, active in non-HI serum only
Fibronectin	0.33	0.6	500	Y
Vitronectin	0.2-0.4	2.6-5.3	75	Y

Table 1.1 Characteristics of select plasma proteins[25,29,30].

The rapid initial protein adsorption phase is replaced by multiple slower subsequent phases where protein adsorption is limited by the surface space remaining, displacement and exchange reactions and steady-state kinetics, and typically a steady-state phase is achieved by ≥ 2 hours.[29] A close-packed protein monolayer will have approximately 100-500 ng of protein/cm^2, depending on protein size and orientation.[29] Importantly, competitive adsorption studies indicate that different proteins have different affinities for the same surfaces.[28] Further, mass concentration in solution is an important factor that affects competitive adsorption behavior.[29] The precise position of equilibrium in any given surface system is not predictable. Importantly, the primary serum protein components (albumin, fibrinogen, gamma globulins) influence cell adhesion (platelets, leukocytes, MC and MΦ) that leads to inflammatory response, fibrous encapsulation and potential implant failure.[6,18] The molar plasma concentrations of select plasma proteins

are shown in Table 1.1.[25,30,31] Trace matrix proteins fibronectin and vitronectin can exert a profound cell adhesive effect if present on surfaces at a critical density.

Adsorbed proteins often undergo conformational changes that allow continuous surface associations and/or bonding between the protein and the surface (influenced by the surface composition and the protein species).[24,28] This dynamic rearrangement may stabilize the adsorbed protein layer, reflected in reduced off rates/protein exchange in complex biological solutions (e.g., blood, plasma, serum).[32,33] This is an important factor in biomaterial selection and biomedical device design since material selection can, to some extent, influence the nature of the adsorbed proteins in complex biological milieu, which may in turn influence the ability of cells to interact with the material.[24] For example, highly hydrophobic surfaces (e.g., fluorocarbons) are known to preferentially bind the abundant serum protein, albumin, (Table 1.1) in complex biological milieu.[32-34] Due to favorable interactions between the surface and protein, a low exchange rate between this protein species and others (e.g., fibronectin, vitronectin, fibrinogen, etc.) is observed. Since most cells lack appropriate receptors for interaction with albumin,[13] the adsorbed protein effectively serves as a mask to block cell adhesion. This albumin-masking property is commonly exploited in masking bio-assay surfaces against unwanted cell interactions.

1.3.2 Cellular adhesion receptors

Cells can interact with surfaces using non-specific physical forces (electrostatic or dispersive forces). However, specific interactions between cell adhesion receptors on

cells and the surface-adsorbed protein layer are important for cellular adhesion, growth, proliferation and migration on surfaces.[24] Cells are known to have numerous adhesion receptors (≥ 50 now known) belonging to four basic families: the integrins, cadherins, selectins, and members of the IgG superfamily.[35] Of these, integrins are the most frequently studied; they have recently been identified as the principal regulators of biomaterial-cell interactions.[36] Integrin receptor heterodimers comprise transmembrane α and β subunits that assemble non-covalently by lateral diffusion to form a metal ion-dependent functional unit specific to matrix protein ligand motifs.[37]

More than 25 integrins are currently known, based upon combinations of the 8 β and 18 α subunits.[13] Most cell types express multiple integrin receptors, allowing cell interactions with proteins, generally in adsorbed or insoluble (i.e., crosslinked collagen) forms. Integrin-ligand interaction proceeds through receptor binding of specific matrix protein amino acid sequences, such as the ubiquitous arginine-glycine-aspartic acid (RGD) cell binding motif found in many matrix proteins.[36] Integrins are promiscuous, i.e., one integrin typically has the ability to bind multiple ligands. Recognized integrin ligands include fibronectin, vitronectin, collagens, laminin, tenascin, fibrinogen, C3bi, and many others.[13] Further, it is widely accepted that specific receptor interactions between cells and surfaces are primarily mediated through cell-adhesive proteins such as fibronectin, vitronectin and fibrinogen.[24] MC and MΦ are known to express many integrin receptors, including leukocyte restricted receptors.[38] Integrin families known to be present on leukocytes, include: $\alpha_M\beta_2$ (Cd11b/CD18, Mac-1, CR3), $\alpha_X\beta_2$

(Cd11c/CD18, p150,95), $\alpha_L\beta_2$ (CD11a/CD18, LFA-1), and $\alpha_4\beta_1$ (CD49c/CD29, VLA-4).[39-44]

Integrin-mediated cell interactions with biomaterials may result from deposition of surface-adsorbed proteins from 1) complex biological solutions (e.g., blood, plasma, serum), 2) proteins deposited by cells (e.g., fibronectin, vitronectin, collagen) or 3) pre-adsorbed single or multi-component solutions of adhesive proteins or peptides.[36] In complex solutions, the surface-adsorbed protein composition may change over time due to exchange of surface adsorbed proteins with others in solution (i.e., the Vroman effect).[45] Cell interactions with the surface can lead to dramatic reorganization of the adsorbed protein layer (e.g., via MΦ-based degradation or production of ECM proteins) producing improved or strengthened cell-biomaterial interactions.[36] These interactions may be desired/favorable in normal wound healing and inflammatory responses, or undesired/resulting as in the development of a FBR, often the case for MC/MΦ adhesion to biomaterial surfaces.

1.4 Physiological responses in the absence or presence of biomaterial implants

1.4.1 Normal wound healing, a general description

The normal wound healing process is a concerted effort between multiple cell types including leukocytes (MC, MΦ, platelets, granulocytes, lymphocytes), fibroblasts, endothelial cells and keratinocytes.[10] MΦ play an instrumental role in wound healing: the absence of wound MΦ has been correlated to impaired wound healing.[46] Under normal circumstances (e.g., the absence of a biomaterial) wound healing progresses

through four stages: hemostasis, inflammation, proliferation and resolution.[10] Hemostasis (vasoconstriction and clot formation) occurs first, followed by the inflammatory stage, which begins within hours of injury and may persist for several days. The inflammatory stage is marked by the influx of leukocytes; tissue MΦ in particular play a critical role in wound healing.[47] "Proliferation" is the regenerative stage where protein synthesis, cellular differentiation or replication occur, and the healing process begins. During the resolution stage, wound remodeling, accompanied by regression of newly formed capillaries, takes place.[10]

The sequence of events related to normal wound healing involves several essential cellular players. Neutrophils, comprising 60-70% of the circulating leukocyte population, arrive at the wound site first but are quickly replaced by MC (representing a mere 3% of circulating leukocytes).[48] MC are attracted by a variety of chemokines, platelet-derived factors and complement split products produced locally and transiently.[10] MC are recruited throughout the inflammatory stage, and once at the injury site differentiate to MΦ, becoming the predominant cell type in the wound by day 5 [48] and persisting for up to months.[5] Activated MΦ amplify the inflammatory response by producing chemoattractants for MC and other cell types, resulting in further cellular infiltration of the injury site. MΦ-derived factors play a role in angiogenesis, extracellular matrix deposition[49] and fibroproliferation requisite for wound repair.[11,12] Further, MΦ presence at the wound site is essential for removal of necrotic tissue and apoptotic cells.[47]

1.4.2 Role of the macrophage in normal wound healing

Chief MΦ functions in normal wound sites are 1) phagocytosis of apoptotic cells (e.g., neutrophils) and extracellular debris[47] and the modulation of 2) angiogenesis and 3) fibrogenesis.[10] Phagocytosis of senescent neutrophils is believed to be mediated by specific subsets of lectin (monosaccharide specific), integrin (thrombospondin specific) and lipid (phosphatidylserine specific) receptors found on wound MΦ.[50] Numerous studies report wound MΦ stimulation of capillary growth required to supply nutrients for tissue regeneration.[10] *In situ* studies indicate that wound MΦ produce various pro-angiogenic factors including transforming growth factor-α (TGF-α), platelet-derived growth factor (PDGF), vascular endothelial growth factor (VEGF)[51,52] and others.[10] In addition to producing pro-angiogenic factors MΦ are known to produce several endothelial cell inhibitors (thrombospondin, other-poorly defined factors), suggesting a role in vascular regression and the resolution phase of wound healing.

Similar to their modulation of angiogenesis, wound MΦ have pro- and anti- fibrotic functions.[53] Pro-fibrotic functions include the ability of MΦ to produce ECM components such as fibronectin, thrombospondin and proteoglycans.[54] Further, MΦ-derived growth factors such as transforming growth factor-β (TGF-β) and PDGF directly stimulate collagen synthesis and fibroblast proliferation.[11] In contrast, MΦ produce numerous effectors of ECM-degradation including metalloproteinases and proteinase activators.[55] These findings suggest a role for the wound MΦ in ECM remodeling.

In the context of wound healing two chemokines that affect MC and MΦ participation, monocyte chemotactic protein-1 (MCP-1) and MΦ inflammatory protein 1α (MIP-1α),

have been found to have distinct patterned expression throughout the course of wound repair. MIP-1α levels have been demonstrated to peak concomitant with maximum MΦ levels within the wound site. Further, MIP-1α antibody neutralization was shown to lead to decreased MΦ numbers at the wound site, suggesting that MIP-1α is crucial for MΦ recruitment during wound repair.[56,57]

Limited studies have demonstrated that wound MΦ are phenotypically distinct from other MΦ populations, and these altered phenotypes have both temporal and location-dependent components.[58,59] Based on the role of the wound MΦ in angiogenesis alone, a phenotypic shift from "reparative/proliferative" to "regression/anti-proliferative" should occur.[10] However, a wound-specific phenotype is currently unknown and rigorous investigation toward this end has not been attempted; this type of study is complicated by the heterogeneous wound MΦ population, the pleiotropic nature of wound MΦ function and the overlapping phases of (and functional shifts assumed to accompany) wound healing.

1.4.3 The foreign body reaction, a general description

The FBR is often described as an altered or abnormal wound healing process. The most obvious distinction between normal and abnormal in this context is that in the presence of a foreign entity (e.g., a biomaterial or biomedical device), the response does not progress to or through the normal resolution stage. However, *in the context of implanted biomaterials, the FBR with the development of granulation tissue is considered to be the normal wound healing response.*[5] The FBR is often (although not necessarily) associated

with chronic inflammation, characterized by the presence of MC, MΦ and lymphocytes, angiogenesis and fibrogenesis.[5] Chronic inflammation may result from infection at the implant site, inherent chemical and physical properties or motion of the implant.[5] Chronic inflammation is localized and usually short-lived, but it may persist for years in the presence of a foreign body.[4,5] Generally, inflammation, wound healing processes and the FBR are all facets of the host response to tissue injury that occur upon placement of a biomaterial or biomedical device.[5]

The FBR to biomaterial implants physically comprises the implant, foreign body giant cells (FBGC), and granulation tissue composed of MΦ, fibroblasts and capillaries, in varying amounts.[4,5] The nature of the implant (composition, surface roughness. general shape and physiological placement) influences the structure and thickness of the FBR formed around it.[4] Most, but not all materials are isolated from the adjacent tissue via a fibrous capsule (i.e., dense compacted collagen) that constitutes the outermost layer of the reaction and is typically considered one of the hallmarks of end stage healing in response to a biomaterial.[5] Relatively flat, uniform surfaces may have a FBR only one to two MΦ deep, while rough surfaces have a thicker cellular layer directly adjacent to the implant material, with varying degrees of granulation tissue subadjacent to the cellular layer.[5]

End-stage healing (remodeling) at the implant site may involve either tissue regeneration (new tissue synthesis by parenchymal cells of the same type) or replacement (connective tissue, fibrous capsule formation).[60] The underlying framework of the tissue is one

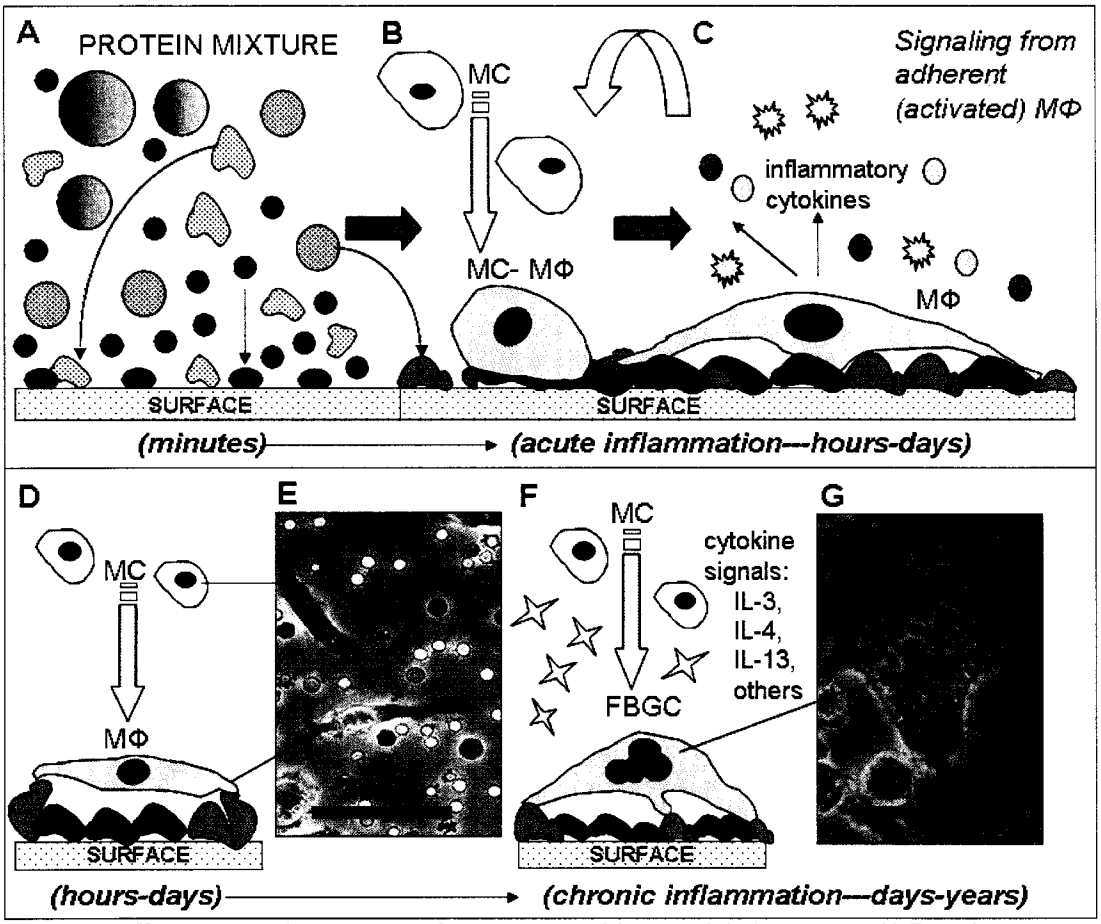

Figure 1.1 The temporal sequence of events upon biomaterial placement. A) Protein adsorption occurs within seconds of material exposure to biological milieu (e.g., blood, serum). Protein surface adsorption is influenced by multiple factors including protein size and abundance, surface free energy, chemical composition, charge and wettability. Significantly, cells never come into contact with a bare surface, all cell-surface interactions are dictated by surface adsorbed proteins. B) *In vivo* circulating monocytes (MC) are recruited to the implant (wound) site by chemokine signals, platelet-derived factors and complement split proteins. MC recruitment occurs early in the inflammatory response (hours) and typically ends within one week. Cell-surface adhesion proceeds largely through integrin-mediated mechanisms, i.e. the specific interactions of distinct integrin subunits with surface adsorbed proteins (fibronectin, vitronectin, laminin, fibrinogen, etc.). MC differentiate/mature to MΦ at the implant site. C) MΦ cytokine signaling (e.g., TNF-α, IL-1, IL-6) leads to an amplified inflammatory response and further MC recruitment. D) *In vitro* cells adhere to surfaces rapidly (approx. 30 minutes) and exhibit migratory phenotypes until space becomes limited. E) Phase contrast photomicrograph of BMMO-derived MC and MΦ grown on tissue culture polystyrene (TCPS, day 2 post-seeding). Microscopically, MC appear as light spherical cells (indicative of a non-adherent phenotype), while MΦ exhibit punctate adhesion sites (adherent phenotype). F) *In vivo* chronic inflammation is indicated by the persistence of activated MΦ and multinucleate foreign body giant cells (FBGC) at the implant site, where they remain for the lifetime of the implant. Multinucleate cells are the product of cytokine-induced fusion of MΦ and MC. *In vitro* colony stimulating factors and IL-3, IL-4, and IL-13 are commonly employed to drive cells to maturity and subsequent fusion. G) Phase contrast photomicrograph of a tetranucleate cell observed in a J774A.1 culture on TCPS treated with exogenous cytokines (10 ng/ml GM-CSF and IL-4), 14 days. Nuclei are indicated by arrows. Note: cartoons are not to scale.

important factor for successful regeneration; without it, fibrosis (the abnormal formation

of fibrous tissue[61]) occurs and normal function is not restored. Altered cellular phenotype(s) within the wound site may lead to the overproduction of collagen and ECM components that contribute to fibrosis and fibrous encapsulation.[4] The FBR fibrous capsule provides an adherent, avascular, impermeable barrier.[62] Thus, implant site remodeling, while unavoidable, is often responsible for biomedical device failure or malfunction.[3,63,64]

1.4.4 Role of the macrophage in the foreign body reaction

MC, the immature circulating form of the MΦ[65], MΦ and activated MΦ cells play important roles in the development of the FBR *in vivo*.[2] MC and MΦ cells are known to fuse into large multinucleated cells in response to a diseased state and/or the presence of foreign entities such as a biomaterial.[66-69] In the presence of a biomaterial implant these multinucleated cells are called *foreign body giant cells* (FBGC), one hallmark of the FBR[66] and are present exclusively at the tissue-implant interface, directly adjacent to the biomaterial.[2,5] Although these cells may persist for the lifetime of the implant, the exact nature of their cellular state (active, phagocytic, quiescent) at extended times *in vivo* remains unknown.[5] Further, the exact molecular signals that regulate FBGC formation and FBR development remain undefined.[2]

Figure 1.1 outlines the events that occur when a biomaterial is placed in the body. The sequence begins with the rapid and immediate adsorption of proteins from blood, serum or plasma (complex biological milieu, containing thousands of proteins).[25] (Neutrophils arrive next, but are neglected for simplicity in this diagram). Neutrophils are rapidly

replaced by circulating MC, which differentiate to mature, adherent, activated MΦ. Subsequently, these MΦ provide signals for further MC/MΦ infiltration, and in response to cytokine cues, MΦ may fuse to form FBGC. Further, MΦ at the implant site play a role in modulation of angiogenesis and fibrogenesis.[11,12] The formation of FBGC is influenced and enhanced by specific cytokines including IL-3, IL-4 and IL-13.[70-73] IL–4 is known to upregulate expression of the macrophage mannose receptor (MMR), a classic phagocytic receptor implicated in fusion to FBGC.[74] Recently, monocyte chemoattractant protein-1 (MCP-1) has been implicated in MC recruitment to biomaterials implanted in the peritoneal cavity, and has been deemed requisite for MΦ fusion to FBGC.[2] Further, MCP-1 has been detected on FBGC at implant sites 2-4 weeks post-implantation, suggesting its role in recruitment of additional MC/MΦ and maintenance or progression of the FBR.[2]

The fusion process is thought to be mediated by the interaction of transiently expressed cell surface proteins.[75] To date, molecular markers implicated in fusion include MMR,[74] (also known as CD 206 or CCR2, the receptor for MCP-1), the macrophage fusion receptor, comprising CD44 and CD47,[75-77] and the dendritic cell-specific transmembrane protein (DC-STAMP).[78] Although significant progress has been made toward describing the effects of numerous factors (cytokines, chemokines, integrins, etc.) on MΦ fusion to FBGC *in vitro* and *in vivo*[2,70,71,73,74,78-80] the detailed mechanism remains elusive.

Vignery *et al* have performed extensive studies on fusing MΦ *in vitro* and *in vivo* and have demonstrated that all cells tested, regardless of origin (species, organ/tissue),

expressed the same functional markers that are characteristic of osteoclasts.[81-85] To date, no molecule has been identified that has an expression restricted either to giant cells or to osteoclasts, although it has been postulated that multinucleated MΦ acquire a tissue-specific molecular repertoire.[75] It is likely that the MΦ present at the biomaterial/implant wound site have similar but altered molecular repertoires when compared to "normal" wound healing MΦ populations, and that the molecular profile of biomaterials-associated MΦ lies somewhere between the "normal" wound healing MΦ populations and that of a giant cell. Unfortunately, none of these cell populations is well-characterized at this time, and substantial effort must be undertaken to progress toward a thorough characterization of these cell types to understand the progression from normal to abnormal wound healing.

1.5 Giant cell formation *in vitro*

In order to further characterize the FBGC, much effort has been devoted to establishing reliable cell fusion protocols for *in vitro* studies. The majority of efforts focus on pooled human blood MC, matured using GM-CSF and subsequently stimulated with IL-4 and IL-13 to produce fused cells.[70,72-74] Numerous factors play into achieving successful fusion: cell source (primary-versus secondary-derived (immortalized) cells), cell maturity (MC versus MΦ), serum source (autologous versus non-autologous), cell age (passage number for secondary cells) and the cytokine cocktail employed to facilitate fusion. Human primary cells represent an expensive and short-lived cell source to form FBGCs *in vitro*, and the use of secondary-derived immortalized macrophage-monocyte cell lines would be greatly beneficial in terms of a readily available cost-effective cell source. To

date, only limited fusion studies have been performed using cell lines,[86] and the high fusion rates typical for primary-derived cells[74] have not been achieved in cell lines.

1.6 Experimental background: Material characteristics and selection

1.6.1 Materials employed in biomedical devices

Numerous materials of varied chemical composition and diverse properties are employed in biomedical devices. Generally, biomaterials can be divided into four classes: natural materials, polymers, ceramics and metals.[87] Frequently, two varieties of materials are combined to create a composite. Polymers represent the largest class of biomaterials.[87] This group comprises natural materials: collagen, hyaluronic acid, cellulose, rubber and others; and synthetic polymeric materials: polyethylene (PE), polypropylene (PP), poly(tetrafluoroethylene) (PTFE, Teflon®),[88] poly(lactic acid), poly(glycolic acid), poly(lactic-glycolic acid) (PLGA) and others. Polymers may be amorphous or semi-crystalline, with the tendency to crystallize enhanced by small side groups and chain regularity.[87]

Many types of biomedical devices and desired functions exist; thus, a broad range of materials with varied properties is employed to achieve specific combinations of desirable properties for the specific device application. Desirable properties may include flexibility, porosity, durability, degradability, biocompatibility, strength, etc. Importantly, the material's surface is the place where the body contacts and samples the material's structure, dictating physiological response to it. The chemical composition and properties

of a material have been shown to affect the structure of its adsorbed protein layer,[24,89] resulting in specific biological outcomes.

Often, materials used as cell culture supports are chemically modified to facilitate more favorable interactions with proteins, thus promoting cellular attachment and growth. One example of this is tissue culture polystyrene (TCPS), a surface generated using a proprietary corona-plasma polymerization treatment to increase the number of oxidized carbon species on the surface, translating to increased hydrophilicity as compared to suspension-culture or bacteriological grade polystyrene (PS).[23] TCPS is widely accepted as the "gold standard" for attachment-dependent cell culture. In comparison, the more hydrophobic PS is less effective at supporting attachment-dependent cell growth and proliferation *in vitro*.[23] PS surfaces are often employed as inexpensive substrates for surface modifications via plasma polymerization.[90]

1.6.2 Biodegradable polymers

Biodegradable polymers, comprising homopolymers, copolymers and stereocomplex blends with varied tunable properties, degrade and eventually dissolve under physiological conditions[91] making them ideally suited for applications requiring a temporary device. Classic examples of biodegradable materials include natural products: gelatin, cellulose, collagen, fibrinogen and fibrin, and synthetic polymers: polyesters, polyanhydrides, poly(ortho esters), poly(amino acids), polyphosphazenes, and polycyanoacrylates.[92]

Polyesters are the most widely used, including the FDA-approved poly(lactic acid) and poly(glycolic acid), that are often combined to create the copolymer, PLGA. The amount of each monomer can be varied to achieve a final material with very specific properties (degradation rate, strength, etc.). These materials are useful for pharmaceutical and biomedical applications including guided tissue regeneration (e.g., scaffolds), orthopedic applications, stents, sutures, barrier membranes, tissue engineering and drug delivery.[92]

From the standpoint of toxicological safety, poly(lactic acid) is an ideal material because its degradation products are intermediates of normal carbohydrate metabolism.[91] L-lactic acid is produced in muscle during anaerobic glycolysis, accumulating in the bloodstream and filtered by the liver where it is converted to glycogen. The metabolic pathway that is responsible for this transformation, (specifically lactate dehydrogenase), only recognizes the L-form,[93] any D-lactic acid present in the bloodstream would be excluded from recycling and excreted unchanged.[94]

Polylactides for implant use are available in either the poly-L-lactide (PLA) or poly-*dl*-lactide forms, and differ in strength and bioabsorbability primarily due to crystallinity.[91] In general, polymer crystallinity has a tremendous influence on the physical properties of the material.[95] Additionally, the molecular weight of the monomeric units used to build the polymer affects strength and bioabsorbability.[91] PLA is a semicrystalline polymer, whereas poly-*dl*-lactide is amorphous. The hydrolysis rate of the amorphous form is more rapid than that of crystalline or semicrystalline polymers, initially due to the availability of ester groups to water in the environment,[96] and subsequently due to the fact that once a

hydrophilic site is introduced into the hydrophobic polymer chain it attracts other hydrophilic species. All of the studies described here employ the lactide form, poly-L-lactide (PLA).

1.6.3 Fluorocarbon materials

Teflon® and Teflon® AF are two polymeric fluorocarbon (FC) materials commercially produced by DuPont for a variety of applications. Teflon® (polytetrafluoroethylene, PTFE) is a highly hydrophobic fluoropolymer[97] with a long history of use in biomaterials implants[9,98] including cardiovascular applications (vascular patches, catheters, cardiac valves), orthopedics (prosthetic hips) and facial reconstruction (maxillary and orbital implants). Teflon® films are often used as device coatings to improve lubricity.[9,98]

The first documented Teflon® implantation and accompanying tissue reactions date to the studies of Leveen and Barbario (1949).[49,99] Initial implants of PTFE were restricted to the peritoneal cavity, but later studies were expanded to include bone, tendons, muscles and the bladder. Compared to other polymers in use at that time, it was thought to be one of the best candidates for implants since it produced less profound tissue reactions than other polymers.[49]

The studies described here do not employ Teflon®, but rather the soluble analog, Teflon® AF ("Amorphous Form"), poly(2, 2-bis (trifluoromethyl)-4,5-difluoro-1,3-dioxide-*co*-tetrafluoroethylene).[97] Unlike PTFE, a highly crystalline, insoluble, poorly processable, opaque solid, Teflon® AF coatings (with thicknesses up to hundreds of

microns) exhibit excellent optical clarity and nearly 100% transmission of visible light[100] making this form an excellent choice for use in cell culture studies employing microscopic evaluation.[101,102]

1.7 Experimental considerations for foreign body reaction *in vitro* studies

The objective of the work described here is an improved understanding of the FBR, a ubiquitous host inflammatory response implicated in biomedical device failure, via cell and molecular level characterizations of this response to select well-characterized model biomaterials relevant to clinical applications. Generally, this work is motivated by 1) the clinical incidence of persistent, chronic inflammation, compromised healing at the implant site and biomedical device failure associated with the FBR, 2) a lack of consensus on valid *in vitro* assay systems to model the FBR and 3) a lack of proven equivalence or non-equivalence of alternative, secondary-derived immortalized cell lines for *in vitro* studies. The ultimate long-term goal of this work is the development of biomaterials with improved biocompatibility. This is likely to result in concomitant improvements in device integration, function and longevity *in vivo*. Toward this end, a careful study of the interactions of MC and MΦ (two key cellular mediators of the FBR associated with implant failure *in vivo*) with select model biomaterial surfaces, was undertaken.

Although utilizing *in vitro* systems to replicate the FBR is desirable, the complex array of variables and problems associated with biomedical device failure *in vivo* translates to *in vitro* studies. Many of these problems are intuitive; for instance, it could be predicted that

cells removed from the body and placed into an *in vitro* system would behave differently than cells *in vivo* due to dramatic differences between these environments. Yet, this type of *ex vivo* system is one strategy that has been advocated for creating or renewing tissues from donors for re-implantation *in vivo.*[103] Further, the limitations of studying and growing cultures in static, two-dimensional environments for biological applications have only recently been acknowledged.[103,104] The work described here underscores some challenges that continue to limit the success of biomaterial implants/biomedical devices.

One significant issue that limits the use of cell lines for *in vitro* FBR and biocompatibility studies is that it is not known how closely the frequently employed immortalized MC- and MΦ-derived secondary cell lines accurately and faithfully represent phenotypic behavior of primary MΦ or MC cells. Complicating this issue is the diverse population of MC and MΦ cells available *in vivo* from which primary cells can be cultured or secondary cell lines can be derived. The small population of MC and MΦ within the body necessitates selective harvest, depending on donor species and size. Murine MΦ cells are most often harvested from the bone marrow or tissues of sacrificial mice while human MC are most often collected from pooled human donor blood,[105] in both cases to yield the maximum number of cells for experimental use. These cells (peripheral MC versus bone marrow or tissue) are generally considered non-equivalent due to differences in cell source, maturity and differentiation state. Thus, uncertainties related to equivalence exist not only between the primary- and secondary- derived populations, but also within them. To investigate the equivalence (or non-equivalence) of secondary-derived immortalized cell lines to primary-derived MΦ grown on model biomaterials surfaces, experiments

utilizing MΦ cells of both primary (BMMO) and secondary (IC-21, RAW 264.7 and J774A.1) origin were performed. These studies (described in Chapters 2 and 3) addressed our first working hypothesis: ***Macrophage cells of primary and secondary origin will exhibit analogous responses to control (TCPS, PS) and model biomaterial (PLA and Teflon® AF) surfaces.***

This investigation began with an evaluation of cellular behavior on surfaces with varied composition and properties: TCPS, PS, PLA and Teflon® AF. The cellular evaluation was designed to include MC, MΦ and fibroblast cells, as each contributes significantly to the FBR in different, highly specialized ways.[5] (Whereas MC and MΦ contribute to the initial mobilization of the FBR, fibroblast cells play a role in end-stage fibrosis associated with the FBR). This comparison was advantageous based on the fact that fibroblasts, like most mammalian cell types, are poorly or non-adherent to FC surfaces.[20-22,106,107] Thus, the fibroblast cell line NIH 3T3 served as a convenient control for non-adhesion in the FC based experiments performed with MC and MΦ. Initial experiments assessed MC, MΦ and fibroblast viability, adhesion, growth and proliferation on control (TCPS, PS) or model surfaces created using plasma polymerization (pp) techniques (pp-FC and others) or evaporation deposition (PLA, Teflon® AF) methods.

While many studies examine the behavior of MΦ on biomaterial-relevant surface chemistries,[7,8,86,108-112] few report results for side-by-side comparisons on a single surface of alternating chemistries. To directly assess MΦ behavior in this format, an investigation of MΦ response to macro- and micro- patterned surfaces with distinct regions of

alternating adhesive (hydrophilic) and non-adhesive (hydrophobic) surface chemistries was undertaken. This group of experiments (described in Chapter 2) addressed our second working hypothesis: ***Unlike many attachment-dependent cell types, macrophages bind to highly hydrophobic regions of substrates when presented with alternating hydrophobic and hydrophilic composition.***

Generally, microscopic methods were employed to evaluate cell-surface interactions, and these results are reported in Chapters 2-4. The intriguing result that MC and MΦ were able to adhere to and efficiently colonize FC surfaces led to two additional sets of experiments. First, phenotypic changes (an increased number of morphological features--filopodia, membrane ruffles) were observed on Teflon® AF FC surfaces. These features have been linked to the Rho GTPase family of proteins, and specifically to Rho, Rac and Cdc. We subsequently investigated the possible link between surface chemistry induced morphological changes and Rho GTPase expression and activation in cells (described in Chapter 3), related to our third working hypothesis: ***Macrophages utilize integrin-based signaling pathways, including the Rho GTPases, when bound to biomaterial surfaces. Further, Rho GTPase expression and /or activation correlates to predominant morphological features (i.e. filopodia, membrane ruffles) present on cells.***

Finally, an investigation of proposed integrin-based mechanisms by which MC and MΦ may adhere, grow and proliferate on FC surfaces (described in Chapter 4), related to our fourth working hypothesis: ***Monocytes and macrophages adhere to fluorocarbon biomaterial surfaces through integrin-mediated interactions.***

Collectively, these experiments were performed to provide new insight into MC/MΦ behavior on model biomaterials surfaces, toward an improved understanding of the cellular and molecular mechanisms that underlie the FBR and determine biomedical device fate *in vivo*, and to determine if employing secondary-derived MΦ immortalized cell lines is a viable alternative to MΦ cells of primary-derivation for FBR studies *in vitro*.

1.8 References

1. Ratner BD, Hoffman AS, Schoen FJ, Lemons JE. Biomaterials Science: A Multidisciplinary Endeavor. In: Ratner BD, Hoffman AS, Schoen FJ, Lemons JE, eds. *Biomaterials Science: An Introduction to Materials in Medicine*. New York: Elsevier Academic Press, 2004:1-9.

2. Kyriakides TR, Foster MJ, Keeney GE, Tsai A, Giachelli CM, Clark-Lewis I, Rollins BJ, Bornstein P. The CC chemokine ligand, CCL2/MCP1, participates in macrophage fusion and foreign body giant cell formation. *Am J Pathol* 2004;**165**:2157-66.

3. Tang L, Eaton JW. Inflammatory responses to biomaterials. *Am J Clin Pathol* 1995;**103**:466-71.

4. Anderson JM. Biological responses to materials. *Annu Rev Mater Res* 2001;**31**:81-110.

5. Anderson JM. Inflammation, wound healing and the foreign body response. In: Ratner BD, Hoffman AS, Schoen FJ, Lemons JE, eds. Biomaterials Science: An Introduction to Materials in Medicine. New York: Elsevier Academic Press, 2004:296-304.

6. Tang L, Eaton JW. Natural responses to unnatural materials: A molecular mechanism for foreign body reactions. *Mol Med* 1999;**5**:351-8.

7. Brodbeck WG, Nakayama Y, Matsuda T, Colton E, Ziats NP, Anderson JM. Biomaterial surface chemistry dictates adherent monocyte/macrophage cytokine expression in vitro. *Cytokine* 2002;**18**:311-9.

8. Collier TO, Thomas CH, Anderson JM, Healy KE. Surface chemistry control of monocyte and macrophage adhesion, morphology, and fusion. *J Biomed Mater Res* 2000;**49**:141-5.

9. Desai NP, Hubbell JA. Tissue response to intraperitoneal implants of polyethylene oxide-modified polyethylene terephthalate. *Biomaterials* 1992;**13**:505-10.

10. DiPietro LA, Strieter RM. Macrophages in wound healing. In: Burke B, Lewis CE, eds. The Macrophage. Oxford: Oxford University Press, 2002:434-56.

11. Hunt TK, Knighton DR, Thakral KK, Goodson WH, 3rd, Andrews WS. Studies on inflammation and wound healing: angiogenesis and collagen synthesis stimulated in vivo by resident and activated wound macrophages. *Surgery* 1984;**96**:48-54.

12. Clark RA, Stone RD, Leung DY, Silver I, Hohn DC, Hunt TK. Role of macrophages in would healing. *Surg Forum* 1976;**27**:16-8.

13. Harbers GM, Grainger DW. Cell-Material Interactions: Fundamental Design Issues for Tissue Engineering and Clinical Considerations. In: Guelcher SA, Hollinger JO, eds. An Introduction to Biomaterials. Boca Raton: CRC Press, 2006:15-45.

14. Baszkin A, Lyman DJ. The interaction of plasma proteins with polymers. I. Relationship between polymer surface energy and protein adsorption/desorption. *J Biomed Mater Res* 1980;**14**:393-403.

15. Andrade JD. Interfacial phenomena and biomaterials. *Med Instrum* 1973;**7**:110-9.

16. Andrade JD. Surface and interfacial aspects of biomedical polymers: Protein adsorption. New York, NY: Plenum, 1985.

17. Gray JJ. The interaction of proteins with solid surfaces. *Curr Opin Struct Biol* 2004;**14**:110-5.

18. Horbett TA. Biological activity of adsorbed proteins. *Surfactant Science Series* 2003;**110**:393-413.

19. Sethuraman A, Han M, Kane RS, Belfort G. Effect of surface wettability on the adhesion of proteins. *Langmuir* 2004;**20**:7779-88.

20. Dewez JL, Doren A, Schneider YJ, Rouxhet PG. Competitive adsorption of proteins: key of the relationship between substratum surface properties and adhesion of epithelial cells. *Biomaterials* 1999;**20**:547-59.

21. Webb K, Hlady V, Tresco PA. Relative importance of surface wettability and charged functional groups on NIH 3T3 fibroblast attachment, spreading, and cytoskeletal organization. *J Biomed Mater Res* 1998;**41**:422-30.

22. Rich A, Harris AK. Anomalous preferences of cultured macrophages for hydrophobic and roughened substrata. *J Cell Sci* 1981;**50**:1-7.

23. van Kooten TG. Growth of cells on polymer surfaces Encyclopedia of Surface and Colloid Science. New York, NY: Marcel Dekker, Inc., 2004:1-19.

24. Horbett TA. The role of adsorbed proteins in animal cell adhesion. *Surf Coll B* 1994;**2**:225-40.

25. Andrade JD, Hlady V. Plasma protein adsorption: the big twelve. *Ann NY Acad Sci* 1987;**516**:158-72.

26. Baier RE, Weiss L. Demonstration of the involvement of adsorbed proteins in cell adhesion and cell growth on solid surfaces. *Adv Chem Ser* 1975;**145**:300-307.

27. Anderson NL, Anderson NG. The human plasma proteome: history, character, and diagnostic prospects. *Mol Cell Proteomics* 2002;**1**:845-67.

28. Horbett TA. Principles underlying the role of adsorbed plasma proteins in blood interactions with foreign materials *Cardiovasc Pathol* 1993;**2**:137S-148S.

29. Eskin SG, Horbett TA, McIntire LV, Mitchell RN, Ratner BD, Schoen FJ, Yee A. Some background concepts. In: Ratner BD, Hoffman AS, Schoen FJ, Lemons JE, eds. Biomaterials Science: An Introduction to Materials in Medicine. New York: Elsevier Academic Press, 2004:237-246.

30. Conlan MG, Tomasini BR, Schultz RL, Mosher DF. Plasma vitronectin polymorphism in normal subjects and patients with disseminated intravascular coagulation. *Blood* 1988;**72**:185-90.

31. Moser TL, Enghild JJ, Pizzo SV, Stack MS. The extracellular matrix proteins laminin and fibronectin contain binding domains for human plasminogen and tissue plasminogen activator. *J Biol Chem* 1993;**268**:18917-23.

32. Lassen B, Malmsten M. Competitive protein adsorption at radio frequency plasma polymer surfaces. *J Mater Sci Mater Med* 1994;**5**:662-665.

33. McFarland CD, De Filippis C, Jenkins M, Tunstell A, Rhodes NP, Williams DF, Steele JG. Albumin-binding surfaces: in vitro activity. *J Biomater Sci Polym Ed* 1998;**9**:1227-39.

34. Grainger DW, Pavon-Djavid G, Migonney V, Josefowicz M. Assessment of fibronectin conformation adsorbed to polytetrafluoroethylene surfaces from serum protein mixtures and correlation to support of cell attachment in culture. *J Biomater Sci Polym Ed* 2003;**14**:973-88.

35. Hynes RO, Lander AD. Contact and adhesive specificities in the associations, migrations, and targeting of cells and axons. *Cell* 1992;**68**:303-22.

36. Garcia AJ. Get a grip: integrins in cell-biomaterial interactions. *Biomaterials* 2005;**26**:7525-9.

37. Hynes RO. Integrins: bidirectional, allosteric signaling machines. *Cell* 2002;**110**:673-87.

38. Taylor PR, Martinez-Pomares L, Stacey M, Lin HH, Brown GD, Gordon S. Macrophage receptors and immune recognition. *Annu Rev Immunol* 2005;**23**:901-44.

39. Arnaout MA. Structure and function of the leukocyte adhesion molecules CD11/CD18. *Blood* 1990;**75**:1037-50.

40. Corbi AL, Kishimoto TK, Miller LJ, Springer TA. The human leukocyte adhesion glycoprotein Mac-1 (complement receptor type 3, CD11b) alpha subunit. Cloning, primary structure, and relation to the integrins, von Willebrand factor and factor B. *J Biol Chem* 1988;**263**:12403-11.

41. Jongstra-Bilen J, Harrison R, Grinstein S. Fcgamma-receptors induce Mac-1 (CD11b/CD18) mobilization and accumulation in the phagocytic cup for optimal phagocytosis. *J Biol Chem* 2003;**278**:45720-9. Epub 2003 Aug 26.

42. Springer TA. Traffic signals for lymphocyte recirculation and leukocyte emigration: the multistep paradigm. *Cell* 1994;**76**:301-14.

43. Stewart M, Thiel M, Hogg N. Leukocyte integrins. *Curr Opin Cell Biol* 1995;7:690-6.

44. Dustin ML, Rothlein R, Bhan AK, Dinarello CA, Springer TA. Induction by IL 1 and interferon-gamma: tissue distribution, biochemistry, and function of a natural adherence molecule (ICAM-1). *J Immunol* 1986;**137**:245-54.

45. Leonard EF, Vroman L. Is the Vroman effect of importance in the interaction of blood with artificial materials? *J Biomater Sci Polym Ed* 1991;**3**:95-107.

46. Subramaniam M, Saffaripour S, Van De Water L, Frenette PS, Mayadas TN, Hynes RO, Wagner DD. Role of endothelial selectins in wound repair. *Am J Pathol* 1997;**150**:1701-9.

47. Leibovich SJ, Ross R. The role of the macrophage in wound repair. A study with hydrocortisone and antimacrophage serum. *Am J Pathol* 1975;**78**:71-100.

48. Ross R, Odland G. Human wound repair. II. Inflammatory cells, epithelial-mesenchymal interrelations, and fibrogenesis. *J Cell Biol* 1968;**39**:152-68.

49. Laustriat S, Geiss S, Becmeur F, Bientz J, Marcellin L, Sauvage P. Medical history of Teflon. *Eur Urol* 1990;**17**:301-3.

50. Savill J, Fadok V, Henson P, Haslett C. Phagocyte recognition of cells undergoing apoptosis. *Immunol Today* 1993;**14**:131-6.

51. Brown LF, Yeo KT, Berse B, Yeo TK, Senger DR, Dvorak HF, van de Water L. Expression of vascular permeability factor (vascular endothelial growth factor) by epidermal keratinocytes during wound healing. *J Exp Med* 1992;**176**:1375-9.

52. Nissen NN, Polverini PJ, Koch AE, Volin MV, Gamelli RL, DiPietro LA. Vascular endothelial growth factor mediates angiogenic activity during the proliferative phase of wound healing. *Am J Pathol* 1998;**152**:1445-52.

53. Kovacs EJ, DiPietro LA. Fibrogenic cytokines and connective tissue production. *Faseb J* 1994;**8**:854-61.

54. Nathan CF. Secretory products of macrophages. *J Clin Invest* 1987;**79**:319-326.

55. Fukasawa M, Campeau JD, Yanagihara DL, Rodgers KE, Dizerega GS. Mitogenic and protein synthetic activity of tissue repair cells: control by the postsurgical macrophage. *J Invest Surg* 1989;**2**:169-80.

56. DiPietro LA, Polverini PJ, Rahbe SM, Kovacs EJ. Modulation of JE/MCP-1 expression in dermal wound repair. *Am J Pathol* 1995;**146**:868-75.

57. DiPietro LA, Burdick M, Low QE, Kunkel SL, Strieter RM. MIP-1alpha as a critical macrophage chemoattractant in murine wound repair. *J Clin Invest* 1998;**101**:1693-8.

58. Nessel CC, Henry WL, Jr., Mastrofrancesco B, Reichner JS, Albina JE. Vestigial respiratory burst activity in wound macrophages. *Am J Physiol* 1999;**276**:R1587-94.

59. Reichner JS, Meszaros AJ, Louis CA, Henry WL, Jr., Mastrofrancesco B, Martin BA, Albina JE. Molecular and metabolic evidence for the restricted expression of inducible nitric oxide synthase in healing wounds. *Am J Pathol* 1999;**154**:1097-104.

60. Cotran RZ, Kumar V, Robbins SL. *Pathological Basis of Disease*. Philadelphia: Saunders, 1999:50-112.

61. Thomas CL. *Taber's Cyclopedic Medical Dictionary*. Philadelphia: F.A. Davis Co., 1989.

62. Woodward SC. How fibroblasts and giant cells encapsulate implants: considerations in design of glucose sensors. *Diabetes Care* 1982;**5**:278-81.

63. Ratner BD. New ideas in biomaterials science--a path to engineered biomaterials. *J Biomed Mater Res* 1993;**27**:837-50.

64. Ratner BD. The engineering of biomaterials exhibiting recognition and specificity. *J Mol Recognit* 1996;**9**:617-25.

65. Ross JA, Auger MJ. The biology of the macrophage. In: Burke B, Lewis CE, eds. The Macrophage. Oxford: Oxford University Press, 2002:3-72.

66. Anderson JM. Multinucleated giant cells. *Curr Opin Hematol* 2000;**7**:40-7.

67. Langhans T. *Uber Riesenzellen mit Wandstandigen Kernen in Tuberkeln und die fibrose Form des Tuberkels. Arch Pathol Anat* 1868;**42**:382-404.

68. Lewis MR. Origin of phagocytic cells of the lung of the frog. *Bull Johns Hopkins Hosp* 1925;**36**:361-75.

69. Lewis WH. The formation of giant cells in tissue cultures and their similarities to those in tuberculosis lesions. *Ann Rev Tuberc* 1927;**15**:616-28.

70. McNally AK, Anderson JM. Interleukin-4 induces foreign body giant cells from human monocytes/macrophages. Differential lymphokine regulation of macrophage fusion leads to morphological variants of multinucleated giant cells. *Am J Pathol* 1995;**147**:1487-99.

71. McNally AK, Anderson JM. Foreign body-type multinucleated giant cell formation is potently induced by alpha-tocopherol and prevented by the diacylglycerol kinase inhibitor R59022. *Am J Pathol* 2003;**163**:1147-56.

72. Kao WJ, McNally AK, Hiltner A, Anderson JM. Role for interleukin-4 in foreign-body giant cell formation on a poly(etherurethane urea) in vivo. *J Biomed Mater Res* 1995;**29**:1267-75.

73. DeFife KM, Jenney CR, McNally AK, Colton E, Anderson JM. Interleukin-13 induces human monocyte/macrophage fusion and macrophage mannose receptor expression. *J Immunol* 1997;**158**:3385-90.

74. McNally AK, DeFife KM, Anderson JM. Interleukin-4-induced macrophage fusion is prevented by inhibitors of mannose receptor activity. *Am J Pathol* 1996;**149**:975-85.

75. Vignery A. Osteoclasts and giant cells: macrophage-macrophage fusion mechanism. *Int J Exp Pathol* 2000;**81**:291-304.

76. Cui W, Ke JZ, Zhang Q, Ke HZ, Chalouni C, Vignery A. The intracellular domain of CD44 promotes the fusion of macrophages. *Blood* 2006;**107**:796-805. Epub 2005 Sep 29.

77. Han X, Sterling H, Chen Y, Saginario C, Brown EJ, Frazier WA, Lindberg FP, Vignery A. CD47, a ligand for the macrophage fusion receptor, participates in macrophage multinucleation. *J Biol Chem* 2000;**275**:37984-92.

78. Yagi M, Miyamoto T, Sawatani Y, Iwamoto K, Hosogane N, Fujita N, Morita K, Ninomiya K, Suzuki T, Miyamoto K, Oike Y, Takeya M, Toyama Y, Suda T. DC-STAMP is essential for cell-cell fusion in osteoclasts and foreign body giant cells. *J Exp Med* 2005;**202**:345-51.

79. McNally AK, Anderson JM. Beta1 and beta2 integrins mediate adhesion during macrophage fusion and multinucleated foreign body giant cell formation. *Am J Pathol* 2002;**160**:621-30.

80. Lambert RA. The production of foreign body giant cells *in vitro*. *J Exp Med* 1912;**15**:510-515.

81. Baron R. Molecular mechanisms of bone resorption. An update. *Acta Orthop Scand Suppl* 1995;**266**:66-70.

82. Vignery A, Niven-Fairchild T, Ingbar DH, Caplan M. Polarized distribution of Na+,K+-ATPase in giant cells elicited in vivo and in vitro. *J Histochem Cytochem* 1989;**37**:1265-71.

83. Vignery A, Raymond MJ, Qian HY, Wang F, Rosenzweig SA. Multinucleated rat alveolar macrophages express functional receptors for calcitonin. *Am J Physiol* 1991;**261**:F1026-32.

84. Vignery A, Wang F, Qian HY, Benz EJ, Jr., Gilmore-Hebert M. Detection of the Na(+)-K(+)-ATPase alpha 3-isoform in multinucleated macrophages. *Am J Physiol* 1991;**260**:F704-9.

85. Vignery A, Wang F, Ganz MB. Macrophages express functional receptors for calcitonin-gene-related peptide. *J Cell Physiol* 1991;**149**:301-6.

86. Godek ML, Duchsherer NL, McElwee Q, Grainger DW. Morphology and growth of murine cell lines on model biomaterials *Biomed Sci Instrum* 2004;**40**:7-12.

87. Cooper SL, Visser SA, Hegenrother RW, Lamba NMK. Polymers. In: Ratner BD, Hoffman AS, Schoen FJ, Lemons JE, eds. Biomaterials Science: An Introduction to Materials in Medicine. New York: Elsevier Academic Press, 2004:67-79.

88. Arthur WT, Petch LA, Burridge K. Integrin engagement suppresses RhoA activity via a c-Src-dependent mechanism. *Curr Biol* 2000;**10**:719-22.

89. Norde W. Adsorption of proteins from solution at the solid-liquid interface. *Adv Colloid Interface Sci* 1986;**25**:267-340.

90. Malkov G, Martin IT, Schwisow WB, Chandler JP, Fisher ER. Pulsed plasma-induced micropatterning with alternating hydrophilic and hydrophobic surface chemistries. *Chem Mater* 2006, submitted.

91. Barrows TH. Synthetic Bioabsorbable Polymers. In: Szycher M, ed. High Performance Biomaterials: A Comprehensive Guide to Medical and Pharmaceutical Applications. Lancaster: Technomic Publishing Company, Inc., 1991:243-257.

92. Kohn J, Abramson S, Langer R. Bioresorbable and Bioerodible Materials. In: Ratner BD, Hoffman AS, Schoen FJ, Lemons JE, eds. Biomaterials Science: An Introduction to Materials in Medicine. New York: Elsevier Academic Press, 2004:115-126.

93. Mahler HR, Cordes EH. *Biological Chemistry*. Harper and Row, 1966:430.

94. Jamshidi K, Hyon SH, Nakamura T, Ikada Y, Shimizu K, Teramatsu T. *In vitro* and *in vivo* Degradation of Poly-L-Lactide Fibers. In: Christel P, Meunier A, Lee AJC, eds. Biological and Biochemical Performance of Biomaterials. Amersterdam: Elsevier, 1986:227-232.

95. Van Krevelan DW. Crystallinity of polymers and the manes to influence the crystallization process. *Chimia* 1978;**32**:279-294.

96. Chu CC. The study of thermal and gross morphological properties of polyglycolic acid upon annealing and degradation treatments. *J Biomed Mater Res* 1985;**22**:699-712.

97. Zhao H, Ismail K, Weber SG. How fluorous is poly(2,2-bis(trifluoromethyl)-4,5-difluoro-1,3-dioxide-co-tetrafluoroethyl ene) (Teflon AF)? *J Am Chem Soc* 2004;**126**:13184-5.

98. Kossovsky N, Millett D, Juma S, Little N, Briggs PC, Raz S, Berg E. In vivo characterization of the inflammatory properties of poly(tetrafluoroethylene) particulates. *J Biomed Mater Res* 1991;**25**:1287-301.

99. Williams DF, Homsy CA. Biocompatibility of Clinical Implant Materials. Cro Press, 1981:60-77.

100. Teflon AF Processing, DuPont, 2006. http://www2.dupont.com/Teflon_Industrial/en_US/products/product_by_name/teflon_af/index.html

101. Anamelechi CC, Truskey GA, Reichert WM. Mylar and Teflon-AF as cell culture substrates for studying endothelial cell adhesion. *Biomaterials* 2005;**26**:6887-96.

102. Makohliso SA, Giovangrandi L, Leonard D, Mathieu HJ, Ilegems M, Aebischer P. Application of Teflon-AF thin films for bio-patterning of neural cell adhesion. *Biosens Bioelectron* 1998;**13**:1227-35.

103. Godbey WT, Atala A. *In vitro* systems for tissue engineering. *Ann N Y Acad Sci* 2002;**961**:10-26.

104. Folch A, Toner M. Microengineering of cellular interactions. *Annu Rev Biomed Eng* 2000;**2**:227-56.

105. McNally AK, Anderson JM. Interleukin-4 induces foreign body giant cells from human monocytes/macrophages. Differential lymphokine regulation of macrophage fusion leads to morphological variants of multinucleated giant cells. *Am J Pathol* 1995;**147**:1487-99.

106. McClary KB, Ugarova T, Grainger DW. Modulating fibroblast adhesion, spreading, and proliferation using self-assembled monolayer films of alkylthiolates on gold. *J Biomed Mater Res* 2000;**50**:428-39.

107. Schakenraad JM, Busscher HJ, Wildevuur CR, Arends J. The influence of substratum surface free energy on growth and spreading of human fibroblasts in the presence and absence of serum proteins. *J Biomed Mater Res* 1986;**20**:773-84.

108. Shen M, Horbett TA. The effects of surface chemistry and adsorbed proteins on monocyte/macrophage adhesion to chemically modified polystyrene surfaces. *J Biomed Mater Res* 2001;**57**:336-45.

109. McNally AK, Anderson JM. Complement C3 participation in monocyte adhesion to different surfaces. *Proc Natl Acad Sci U S A* 1994;**91**:10119-23.

110. Anderson JM, Defife K, McNally A, Collier T, Jenney C. Monocyte, macrophage and foreign body giant cell interactions with molecularly engineered surfaces. *J Mater Sci Mater Med* 1999;**10**:579-88.

111. Jones JA, Dadsetan M, Collier TO, Ebert M, Stokes KS, Ward RS, Hiltner PA, Anderson JM. Macrophage behavior on surface-modified polyurethanes. *J Biomater Sci Polym Ed* 2004;**15**:567-84.

112. Kao WJ. Evaluation of protein-modulated macrophage behavior on biomaterials: designing biomimetic materials for cellular engineering. *Biomaterials* 1999;**20**:2213-21.

CHAPTER 2: MACROPHAGE SERUM-BASED ADHESION TO PLASMA PROCESSED-SURFACE CHEMISTRY IS DISTINCT FROM THAT EXHIBITED BY FIBROBLASTS

This chapter was written by Marisha L. Godek, edited by David W. Grainger and Ellen R. Fisher and contains contributions from Galiya Sh. Malkov. It has been accepted for publication in *Plasma Processes and Polymers*, 2006.

2.1 Abstract

Plasma-polymerized films deposited from allylamine (AlAm), hexylamine (HxAm), N-vinyl-2-pyrrolidine (NVP), N-vinyl formamide (NVFA), acrylic acid (AA) and C_3F_8 (fluorocarbon or FC) were compared to tissue culture polystyrene (TCPS) and polystyrene (PS) surfaces in supporting cellular attachment, viability, and proliferation in serum-based culture *in vitro* for extended periods of time (>7 days). Surface patterns were created using multi-step depositions with physical masks. Cell adhesion in the presence of serum was compared for (MC-) MΦ and fibroblast cell lines. Cellular response was tracked over time, reporting adhesive behavior, proliferative rates, and morphological changes as a function of surface chemistry. Micropatterned surfaces containing different surface chemistries and functional groups (e.g. $-NH_2$, -COOH, $-CF_3$) produced differential cell adhesive patterns for NIH 3T3 fibroblasts compared to

J774A.1, RAW 264.7 or IC-21 (MC-) MΦ cell types. Significantly, MΦ adhesion is substantial on surfaces where fibroblasts do not adhere under identical culture conditions.

2.2 Introduction

Surface chemistry is well known to exert profound effects over interfacial biological processes *in vitro* relevant to biomedical device designs and applications.[1-4] Interfacial behaviors of both proteins and cell types are known to result from combined effects of surface chemical composition and physical topology.[5-10] Plasma polymerization (pp) is frequently employed to generate stable, sterile surfaces or coatings with varied chemical, topological and physical characteristics, facilitating such measurements.[11,12] Patterned surfaces representing regular arrangements of two or more chemically distinct materials can be readily generated, providing both spatial and chemical control of the interface useful for examining and producing differential biological responses.

Surface pattern deposition methods include soft (stamping) lithography, photolithography, ion milling and plasma patterning. Plasma polymerization techniques have been employed for numerous applications including deposition of Si-based materials for microelectronics applications,[13-15] hard coatings such as diamond-like carbon and carbon nitride films,[4,16,17] and organic polymer films for modifying substrates with complicated geometries.[18-23] Plasma polymerization techniques provide a facile preparation method for generation of diverse surface chemistries on a variety of substrates. The resultant surfaces are sterile, stable under ambient storage conditions and amenable to use with cultured cells.

Cell patterning studies to date have examined the effects of specific substrate chemistries and microfabrication techniques on the modulation of cell-substrate and cell-cell contacts.[25-28] Frequently, differential cell fidelity to underlying pattern chemistry is a determinant for distinguishing success of these approaches to elucidate cell-surface interaction mechanisms. Numerous methods for cellular micropatterning have been employed, with varied levels of success for specific substrate-substrate and substrate-cell combinations.[6,10,12,22-25] Many strategies have exploited unique combinations of surface chemistries or deposition techniques to achieve alternating cell adhesive and non-adhesive regions, often correlated with the presence or absence of surface-adsorbed cell adhesive matrix proteins,[24,26-28] thus modulating cell-substrate interactions.

Although many combinations of surfaces, patterns and cells have been tested to date, one important distinction is the ability to produce spontaneous cell pattern fidelity in serum protein-based culture versus that resulting from pre-adsorbed matrix protein (e.g., collagen, fibronectin) adsorption to surface patterns prior to cell seeding. Biased (e.g., pure mono-component extra-cellular matrix, ECM) protein pre-adsorption to patterned chemistry readily produces protein patterns templated by the surface chemistry to which cells adhere. However, spontaneous cell pattern formation and long-term fidelity from serum media is less reported, understood or controlled because of difficulties in control of ECM protein surface selection from serum (a milieu of > 500 proteins). Yet, this serum-based cell-surface scenario is much more relevant to cell response to implanted biomaterials than biased ECM protein adsorption templated control of cell patterning.

Numerous surface chemistries have been studied to date for cell patterning.[22-26] A broad general characterization of the conclusions from this exhaustive survey is that surface chemistries conducive to cell adhesion have specific chemical and physical parameters that endow them with a propensity to adsorb cell matrix proteins at sufficient density, and with sufficient adhesion strength, to support cell receptor and cell surface engagement successfully enough to produce cell adhesion, spreading and proliferative responses.[4,29] Frequently, this correlates with moderate surface polarity and mechanical modulus (neither extreme hydrophilicity nor extreme surface elasticity).[29]

Various cell types have been employed in cell patterning studies, including epithelial,[7] endothelial,[30] capillary endothelial,[31] MC-MΦ,[26,32] osteoblast,[24,33] fibroblast[34] and numerous others.[3] Interestingly, few studies report pattern responses of inflammatory cell types, including lymphocytes, or leukocytes such as MC and differentiated MΦ. This current contribution describes the use of plasma-patterned surface chemistry to contrast the adhesive and proliferative behavior of fibroblasts and MΦ cell lines cultured in serum-containing media. Few studies compare these distinct cell behaviors. This present study

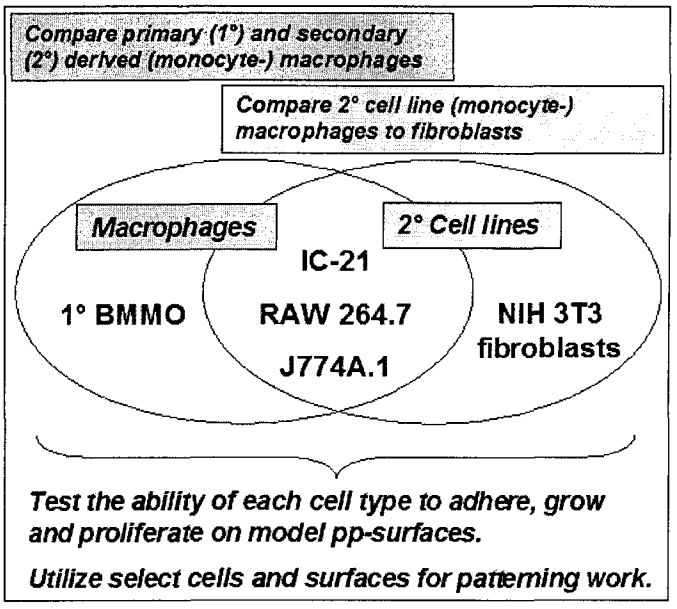

Figure 2.1 Schematic of relationships among cultured

includes biologically relevant cell types of primary and secondary derivation for comparison: primary bone marrow-derived MΦ, three secondary (MC-) MΦ cell lines (IC-21, RAW 264.7 and J774A.1), and one fibroblast cell line (NIH 3T3) frequently employed in patterning studies[34-36] (Figure 2.1). Results point to intrinsic differences in the responses of these cell types to identical chemistries and suggest important distinctions in phenotypic mechanisms for recognizing surfaces relevant to cell based drug testing *in vitro* (e.g., anti-fibrotic, anti-inflammatory drugs) and inflammatory processes with implanted biomaterials and surgical devices.

2.3 Materials and Methods

Preparation of culture surfaces using plasma deposition

All pp-films were deposited as described previously.[37] Acrylic acid (99%), N-vinyl-2-pyrrolidinone (99%), and N-vinylformamide (98%) were obtained from Aldrich Chemical Company. Allylamine (98%) and hexylamine (99%) were obtained from Acros Organics. Tissue culture polystyrene (TCPS, Falcon) and polystyrene (PS) suspension culture dishes (Corning), and glass coverslips (VWR Scientific) were used as substrates for pp deposition reactions. One macro (30 mm diameter) solid disk mask and copper TEM grids (Ted Pella, Inc.) of various dimensions and with distinctly different internal patterns (grids, circles and bullet shapes) were used as masters for pp-film patterning on TCPS, PS and glass substrates. All substrates were cleaned with methanol immediately before pp-deposition. Surface analysis was performed on patterned and unpatterned samples treated identically. Deposition times ranged from 5 to 90 minutes and deposition rates varied from 1.3Å/minute to 129.3Å/minute. Adhesion tests revealed successful

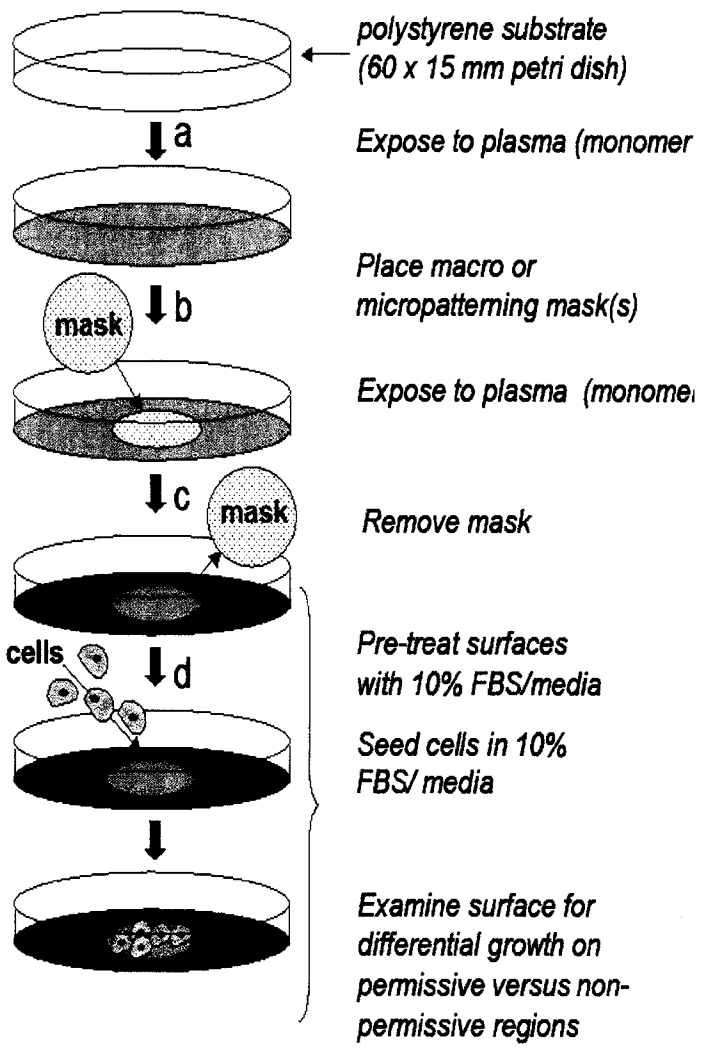

Figure 2.2 Schematic illustration of the patterning procedure using masks and sequential plasma polymerization techniques. (a) Polystyrene petri dishes were exposed to the first of two sequential plasma polymerization depositions. (b) One macro (30 mm diameter solid disk) or multiple micropatterning (3 mm diameter copper TEM grid) mask(s) of various patterns (grids, circles and bullet shapes) were placed onto the plasma-deposited substrates and the (c) second plasma deposition (different chemistry) was performed. The mask(s) were then removed. (d) Plates were treated with 70% ethanol and UV light for twenty minutes. Plates were subsequently exposed to 10% serum containing media for 3-24 hours before cell seeding. Plates were seeded with NIH 3T3 fibroblasts and (MC-) MΦ cells at various densities as described in Materials and Methods.

layering (i.e. no delamination) of pp-films on PS and PS coated with pp-C_3F_8. After deposition, samples were stored in petri dishes under ambient conditions until cell culture use (1-14 days). All pp-surface chemistries employed here are listed in Table 2.1.

Prior to use in cell studies, pp-surfaces were first thoroughly misted with 70% ethanol and then UV irradiated for twenty minutes in a biosafety cabinet. This process was previously shown to reliably produce sterility for cell culture with minimal changes to surface chemistry.[38] XPS analysis[37]

performed on samples before and after this treatment demonstrated that the pp-deposited surface chemistry was not affected (data not shown).

Patterned substrate deposition by plasma polymerization

Patterned substrates comprising two different surface chemistries for cell culture were produced by a previously reported plasma deposition technique.[37] Plasma deposition for patterns occurred sequentially as described in Figure 2.2, and was then reversed in a separate preparation to create two analogous inverse macropatterned surfaces for each combination of surface chemistries employed (Table 2.2).

Materials surface characterization

Surfaces of plasma-deposited polymeric materials were characterized as described previously using angle-resolved XPS, spectroscopic ellipsometry (SE) and measurement of static water contact angles.[37] Similarly, surface pattern fidelity was confirmed with scanning electron microscopy (SEM), scanning Auger microscopy (SAM), XPS imaging, and time-of-flight secondary ion mass spectroscopy (ToF-SIMS).[37] Aging studies were performed on nitrogen-containing materials by allowing exposure to atmosphere for 10-14 days, with subsequent reprobing of surfaces via XPS.[37]

Cell culture

Murine fibroblast NIH 3T3, murine MC-MΦ RAW 264.7 and J774A.1, and murine MΦ IC-21 cell lines were obtained from the American Type Culture Collection (Manassas, VA). Cells were cultured in Dulbecco's modification of Eagle's medium (DMEM,

Mediatech, for NIH 3T3 and J774A.1), or RPMI 1640 (Mediatech, for IC-21 and RAW 264.7) supplemented with 10% fetal bovine serum (FBS, HyClone, Inc.) and 1% penicillin-streptomycin (Life Technologies). Cultures were maintained in T-175 TCPS flasks (Nunc™) under standard conditions: incubation at 37° C, 98% humidity and 5% CO_2. Cells were dissociated from culture flasks by incubation with Ca^{2+}- and Mg^{2+}- free cell culture grade Hank's balanced salt solution (HBSS, Life Technologies) (NIH 3T3, J774A.1 and RAW 264.7), or by scraping with a rubber policeman (IC-21).

Primary cell harvest

Bone marrow derived macrophages (BMMO) were prepared from bone marrow cells harvested from the femurs and tibias of C57BL/6 mice.[39] To differentiate bone marrow precursors into MΦ, bone marrow-extracted cells were cultured in DMEM supplemented with 10% L929 fibroblast-conditioned medium, 2 mM L-glutamine, 0.01% HEPES, 1% penicillin-streptomycin, and 2 mM non-essential amino acids (Sigma-Aldrich). Cells were grown under standard conditions (*vida supra*) with media changes every two days. This method has been shown to produce differentiated MΦ.[39]

Cell culture on patterned surfaces

Cell seeding densities were adjusted, depending on observed cell-specific culture doubling times. Seeding densities were varied for each cell type to allow similar growth kinetics toward confluent density for comparison of cell types as follows: murine (MC-) MΦ cell lines were seeded at a density of 50,000 to 250,000 cells; NIH 3T3 murine fibroblasts at 150,000-200,000 cells; and primary-derived BMMO cells at 6.2 x 10^6 cells;

all per 15 x 60 mm culture surface. Cell line passage number ranged from 2-22 (beyond original stock subculture as obtained from the ATCC) and varied depending on the cell line employed. Cells counts were performed with a hemacytometer and viability was assessed using the standard Trypan blue dye exclusion test.[43] Surfaces were conditioned for up to 24 hours with 10% FBS-containing media (RPMI 1640 or DMEM) prior to seeding. After seeding, surfaces were incubated at 37°C, 98% humidity and 5% CO_2 and media changes were performed as necessary. Cell attachment, growth and proliferation were studied by phase contrast (light) and fluorescent microscopy techniques.

Protein pre-adsorption and cell culture on pp-FC surfaces

IC-21, NIH 3T3 or BMMO cells were seeded onto control PS suspension culture dishes and pp-FC surfaces that were treated for 24 hours with one of the following solutions: 3 mg/ml bovine serum albumin (BSA Fraction V, OmniPur®, Sigma) in sterile Dulbecco's phosphate buffered saline (DPBS, HyClone), 100% FBS, or 10% FBS in DPBS. At 24 hours, the protein solution or serum was removed by aspiration and cells were immediately seeded in an appropriate cell culture media containing 10% FBS. Culture conditions proceeded as described above.

Phase contrast microscopy

Images were obtained on either a Nikon Eclipse TS100 or a Nikon TMS inverted microscope using Nikon objectives. A Kodak DC290 camera was used to capture images that were subsequently processed in Adobe Photoshop 6.0 (Adobe Systems, Inc.).

Fluorescence microscopy

Cells were stained with fluorescein diacetate (Molecular Probes). Briefly, culture media was aspirated from the surfaces, which were then rinsed once with sterile DPBS. A dilute fluorescein diacetate solution (0.01 mg/ml in PBS) was added and surfaces with cells were allowed to stand for 15 minutes. Images were obtained on a Zeiss Axiomat® inverted microscope with Zeiss filter sets for fluorescein with a Dage 300 CCD camera (Zeiss Plan 2.5X objective, NA of 0.08, and 0.63 reducing lens). A DPS PVR digital recorder was used to digitize the video output of the camera.

2.4 Results

Previously, a series of micropatterned substrates was created and characterized where the underlying substrate was first coated with one type of plasma polymer (most commonly a highly hydrophobic FC) and then patterned with a second type of plasma polymer (usually a relatively hydrophilic hydrocarbon).[37] This diverse group of polymer films was subsequently employed in patterning experiments using fibroblastic and (MC-) MΦ cell types, as reported here. Included in this group were the cell adhesion-promoting pp-AA films[41] containing carboxylic acid groups; the unique NVP monomer, a heterocyclic nitrogen-containing compound; the amide-containing NVFA monomer, an isomer of acrylamide that exhibits low toxicity; the extensively studied and employed nitrogen-containing AlAm; and the saturated amine monomer HxAm, thought to be promising for the production of films with high concentrations of primary amines.[37] Since material hydrophilicity is a critical factor in promoting protein adhesion and subsequent cellular adhesion, static aqueous contact angle measurements were performed on non-patterned

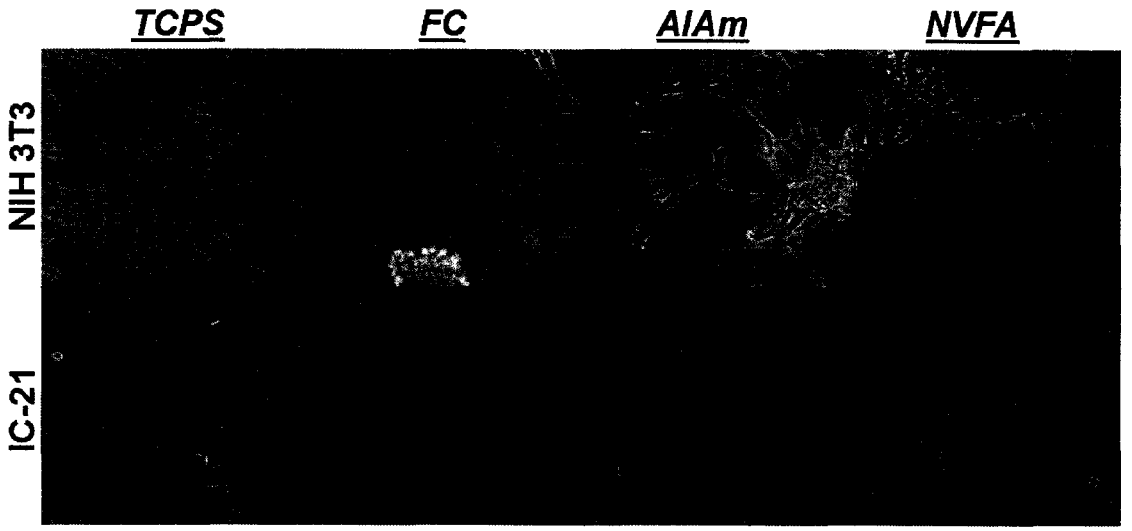

Figure 2.3 Phase contrast microscopy images of NIH 3T3 (A-D) and IC-21 [2] cell morphologies observed on control (TCPS) and FC, AlAm and NVFA pp-surfaces at sub-confluent culture conditions (time in culture varied based on cell type and substrate). Images shown are representative of results obtained for multiple fields (> 5) and plates (≥ 2) for each surface and cell line. Arrow (B) indicates an anomalous adherent cell that has likely attached to a surface defect.

plasma polymerized films created on Si substrates[37] with the materials ranging from hydrophilic to very hydrophobic in nature: NVFA (43 ± 1°), AlAm (46 ± 1°), NVP (53 ± 1°), HxAm (77 ± 6°), AA (74 ± 3°), FC (114± 1°).

2.4.1 Cell attachment and proliferation on plasma-polymerized culture substrates in serum containing media

First, each unpatterned pp-surface was assessed for its ability to support cell attachment and proliferation *in vitro* in 10% FBS using the following cell types: NIH 3T3 (fibroblast), RAW 264.7 and J774A.1 (MC-MΦ), IC-21 (MΦ) and primary-derived BMMO. Two dissimilar cell types were selected [fibroblast versus (MC-) MΦ] to determine differential surface responses based on cell type. On each unpatterned surface chemistry, at least one (MC-) MΦ cell line was compared to the NIH 3T3 fibroblast cell

line. Results for control surfaces (PS and TCPS) and pp-film chemistries studied over 2-7 day culture times are shown in Table 2.1. Each surface tested supported the attachment and proliferation of all (MC-) MΦ cell lines, and all surfaces except the FC chemistry supported attachment and proliferation of NIH 3T3 fibroblasts, similar to fibroblast behavior observed on Teflon® AF FC surfaces.[42,43] Representative phase contrast microscopy images for the IC-21 and NIH 3T3 cell lines are shown in Figures 2.3 and 2.4. Figure 2.3 shows results for control (TCPS) and three of the pp-surfaces tested: FC, AlAm and NVFA. Due to differences in doubling times, cell lines were seeded at varied densities on each substrate (as described in Materials and Methods) to facilitate comparative analysis over virtually equivalent culture time periods, based on predicted time to reach 100% confluence on TCPS. Results from Figure 2.3 B and Figure 2.4 D-F show minimal fibroblast attachment and survival, supporting previous assertions that albumin's natural abundance in cell culture media prevents fibroblast-surface interactions required for attachment, growth and proliferation on FC surfaces.[30,42-44]

Table 2.1 Cell attachment and proliferation on uniform plasma-deposited substrates.

Surface description[a]	NIH 3T3[b]	RAW 264.7[b]	J774A.1[b]	IC-21[b]	BMMO[b]	Duration (days)[c]
FC	-	+	+	+	+	2-5
AA	+	+	ND	ND	ND	2
AlAm	+	+	+	+	ND	4
HxAm	+	ND	+	+	ND	4
NVFA	+	ND	ND	+	ND	4
NVP	+	+	+	+	ND	4
PS control	+	ND	+	+	+	7
TCPS control	+	+	+	+	+	7

[a] Abbreviations as used in text. See text for detailed description of patterning method.
[b] + (supportive of cell growth), – (no adherence or proliferation), ND (not determined). See ref. 37 for full surface analytical characterization. [c] Duration differences due to different seeding concentrations, doubling times, and affinity for surfaces.

Table 2.2 Cell attachment and proliferation on plasma-macropatterned substrates.

Surface description[a]	NIH 3T3[b]	RAW 264.7[b]	J774A.1[b]	IC-21[b]	Cell pattern fidelity (days)[c]
NVP-FC	+/-	ND	ND	+/+	7
FC-NVP	-/+	ND	ND	+/+	7
AlAm-FC	+/-	+/+	ND	+/+	7
FC-AlAm	-/+	ND	+/+	+/+	5

[a] Abbreviations as used in text. See text for detailed description of patterning method.
[b] + (supportive of cell growth), – (no adherence or proliferation); order of "surface description" matches reported + or - order, respectively. ND (not determined). See ref. 37 for full surface analytical characterization. See text for a detailed description of successful combinations of surface chemistries for macropatterning based on cell line. [c] Cell pattern fidelity differences due to different seeding concentrations, doubling times, and affinity for surfaces.

To determine whether the noteworthy result of growth of (MC-) MΦ cell lines on FC surfaces was a cell line-dependent phenomenon, we performed limited experiments on FC surfaces with murine primary-derived BMMO. Significantly, BMMO cells readily adhered, grew and proliferated on FC surfaces (Figure 2.4 G-L). Although at 24 hours the majority of BMMO cells remained undifferentiated (monocytic) and either non-adherent or loosely adherent (indicated by a round shape), several cells with surface contacts and short filopodia can be seen even at this early time point (Figure 2.4 J-L).

Surfaces prepared with AlAm (Figure 2.3 C, G), HxAm (data not shown) and NVFA (Figure 2.3 D, H) readily promoted cell adhesion and proliferation for fibroblast and (MC-) MΦ cell types. Cells elongated and spread at early time points suggestive of a motile phenotype, but as the cultures progressed, adherent cells adopted characteristic tightly packed cobblestone growth patterns associated with limited surface space (exemplified by cells grown on TCPS, Figure 2.3 A). Fibroblasts exhibited normal morphology on AlAm (Figure 2.3 C), HxAm (data not shown) and NVFA (Figure 2.3 D)

Table 2.3 Cell attachment and proliferation on plasma-micropatterned substrates.

Surface description[a]	NIH 3T3[b]	IC-21[b]	Cell pattern fidelity (days)[c]
HxAm-FC	+/-	+/+	9
NVP-FC	+/-	+/+	9
NVFA-FC	+/-	+/+	9
AlAm-FC	+/-	+/+	7
FC-AlAm	-/+	+/+	7

[a] Abbreviations as used in text. See text for detailed description of patterning method.
[b] + (supportive of cell growth), – (no adherence or proliferation); order of "surface description" matches reported + or - order, respectively. ND (not determined). See ref. 37 for full surface analytical characterization. See text for a detailed description of successful combinations of surface chemistries for micropatterning based on cell line. [c] Cell pattern fidelity differences due to different seeding concentrations, doubling times, and affinity for surfaces.

surfaces by comparison to TCPS (Figure 2.3 A) with multiple attachment sites on these surfaces. Cultures progressed to 100% confluence if allowed (Day 4), and cells remained adherent throughout the culture lifetime. No delamination of the cells was observed at any time.

On AlAm, HxAm and NVFA substrates, (MC-) MΦ cells also adopted typical adherent morphologies, which differed slightly based on the cell line. Representative data for IC-21 cells are shown in Figure 2.3 E-H. J774A.1 and RAW 264.7 cultures exhibited similar results (data not shown), with the appearance of characteristic features such as lamellipodia, filopodia, and membrane ruffles as the cells adhered to and spread on surfaces. These features have been previously reported for surfaces of varied chemical composition and hydrophilicity.[43] Surfaces comprising NVP were also observed to be generally cell-conducive for all cell lineages tested, with slightly slower proliferation rates compared to AlAm, HxAm and NVFA surfaces (unpublished

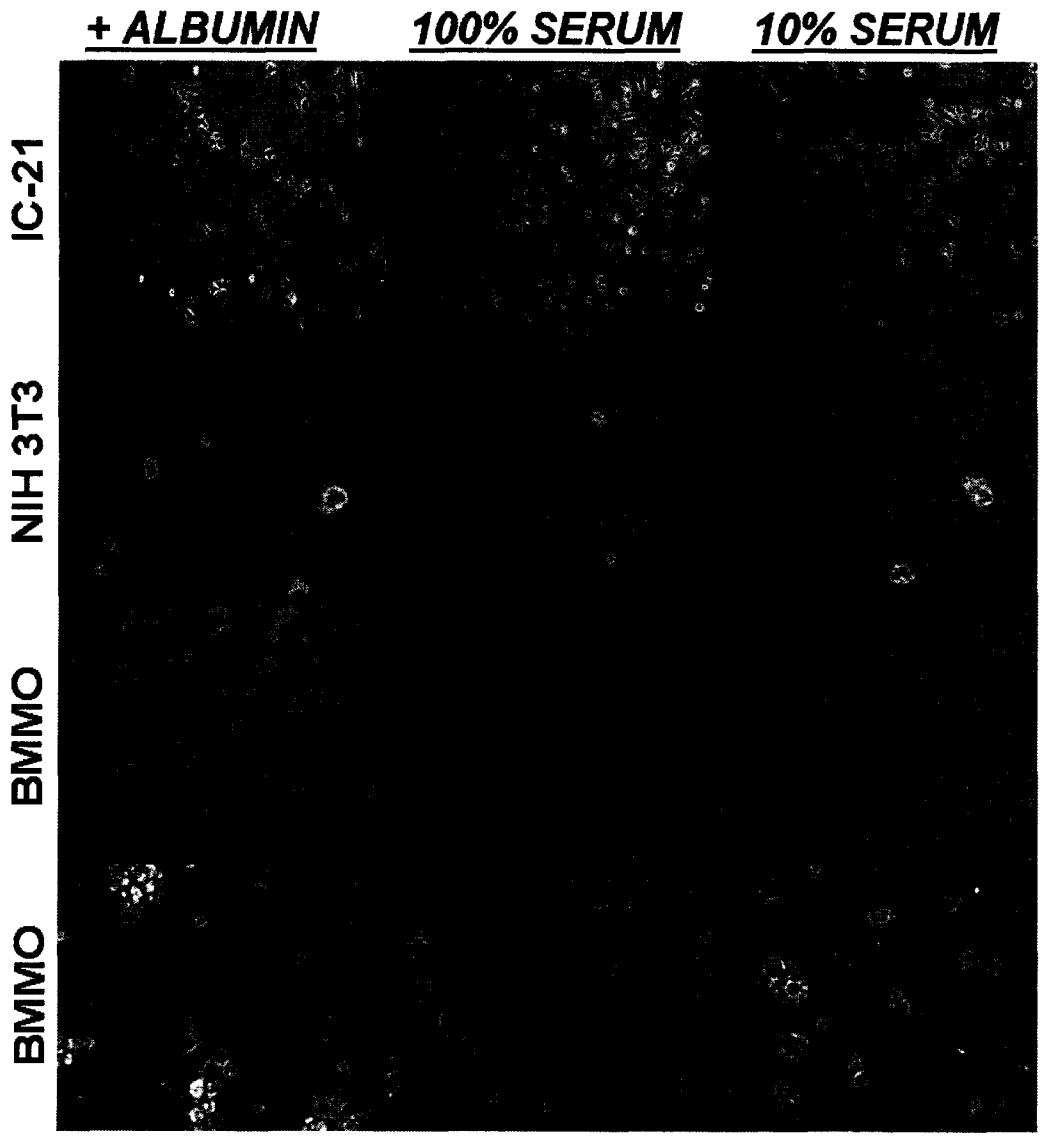

Figure 2.4 Phase contrast microscopy comparison of IC-21 MΦ, NIH 3T3 fibroblast and BMMO cell growth at 24 hours post-seeding in 10% serum containing media on uniform FC surfaces pre-treated with pure (3 mg/ml) albumin (A, D, G and J), 100% (B, E, H and K) or 10% serum (C, F, I and L). NIH 3T3 fibroblasts fail to adhere to FC surfaces under any of the conditions tested (D-F). IC-21 (A-C) and BMMO (G-L) cells adhere and proliferate to nearly confluent cultures (data not shown) on FC surfaces under all test conditions. Images are representative of multiple fields (> 5) and multiple plates (2) for each test condition. Since BMMO cells are significantly smaller than IC-21 and NIH 3T3 cells, BMMO images were further magnified (J-L) to allow visualization of differences in adherent (dark circular and angular with extensions) and non-adherent (light circular) cell morphologies.

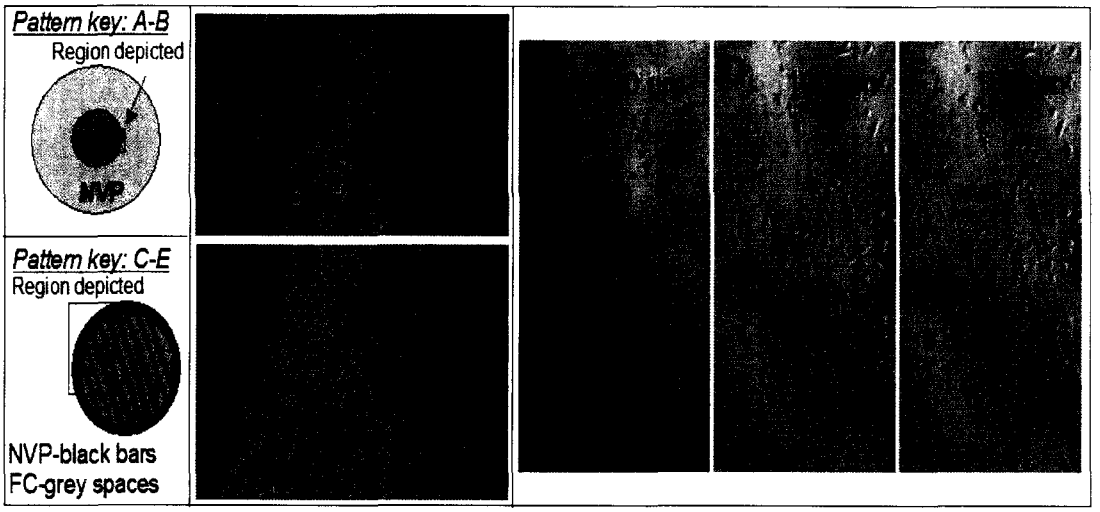

Figure 2.5 Patterning of IC-21 murine MΦ (A, C-E) and NIH 3T3 fibroblasts (B) on FC-NVP surfaces with macro (A-B) and micro (C-E, striped TEM grid) masks. Note: pattern cartoons are not to scale. Striped TEM grid (C-E) bars are184 μm, spaces are 92 μm. A) IC-21 MΦ moderately and evenly populated the FC center of the pattern, while fewer cells attached to NVP regions (72 hours). A small annulus (partially shown, bold arrow) was visible at the chemistry boundary. B) NIH 3T3 fibroblasts attached exclusively to the NVP region, with a ring forming at the margin between the NVP and FC chemistries (bold arrow, 72 hours). Cells were loosely adherent at this boundary (an edge effect) with some cells floating above other adherent cells, attached on the NVP side only. C-E) Edge effect observed with IC-21 cells on NVP-FC micropatterns at 48 hours (bold arrows). MΦ cells grew preferentially at the interface of the surface chemistries at early time points. (D and E are the same image with E labeled for clarity).

observations). Limited culture performed on AA surfaces supported attachment and proliferation of both RAW 264.7 and NIH 3T3 cells, consistent with previous reports.[45,46]

2.4.2 Media influences on cell proliferation on protein pre-adsorbed surfaces

Effects of serum protein-surface deposition from a pure albumin solution (at 10% of physiological concentration, 3 mg/ml, consistent with tissue culture conditions of 10% FBS) versus surface protein selection from complex cell culture milieu (10% or 100% FBS) on cellular attachment and proliferation, were assessed using NIH 3T3 fibroblasts, IC-21 MΦ and BMMO under the aforementioned culture conditions on moderately and very hydrophobic surfaces (PS and pp-FC, respectively). Surfaces were exposed to one of

three protein pre-adsorption test conditions: 1) pure albumin solution (3 mg/ml albumin in DPBS), 2) 100% FBS, or 3) 10% FBS in DPBS, for 24 hours prior to seeding with either fibroblast or MΦ cells in an appropriate culture media also containing 10% FBS.

Murine NIH 3T3 fibroblasts failed to adhere and proliferate up to 48 hours on FC surfaces under any of the pre-adsorbed test conditions. Instead, fibroblast cells displayed spherical morphologies characteristic of non-adherent/non-spreading phenotypes[3,38] or adhered to each other, forming cell clusters (Figure 2.4, D-F, 24 hours after seeding). Significantly, IC-21 MΦ readily adhered to and proliferated on FC surfaces under all test conditions (Figure 2.4, A-C) with no apparent differences in proliferative rate or morphological behavior as compared to growth on PS (data not shown). These cells progressed to near confluent (data not shown) conditions in culture and exhibited varied morphology including astral shapes, filopodia, lamellipodia and membrane ruffling, consistent with our previous observations of MΦ growth on Teflon® AF FC surfaces.[42,43] BMMO cells also adhered, grew and proliferated regardless of test conditions (Figure 2.4, G-L), and at later time points (data not shown) achieved cell morphologies similar to that observed for the IC-21 cell line on these surfaces under identical conditions. The morphologies observed for the BMMO at 24 hours (Figure 2.4 J-L) are typical for mixed cell population primary-derived BMMO cultures that have been recently collected. Light spherical cells are non-adherent (for BMMO cultures, typically immature monocytic) cells. Dark spherical cells are assumed to be in proximity to the surface, and are likely establishing adhesive contacts. Cells with astral or elongated morphologies are adherent.

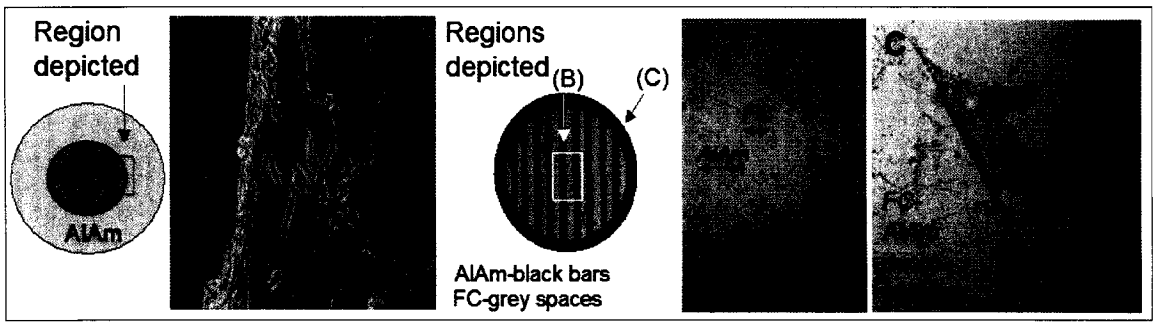

Figure 2.6. Patterning of NIH 3T3 fibroblasts on FC-AlAm surfaces with macro (A) and micro (B-C) masks. Striped TEM grid (B), bars are 184 μm, spaces are 92 μm. A) NIH 3T3 cells adhered to and proliferated on AlAm [1], but not on FC (left). Patterned growth fidelity appeared within 24 hours and was maintained through day 7. An "edge effect" (see text for description, bold arrow) was noted at margins of masked regions. B) NIH 3T3 cell growth was confined to the region of the TEM grid (see also C, left), but not to the AlAm region exclusively (arrows indicate approximate widths of each polymer chemistry) C) NIH 3T3 cells did not grow on the larger FC background region [1] of the plates with micropatterns. Arrows indicate a large sheet of cells that are loosely adherent at the boundary (bold arrow) between the FC background and the FC-AlAm micropatterned region. Note: pattern cartoons are not to scale.

Only a small percentage of the cell population exhibits filopodia at this early time point on this substrate.

2.4.3 Cell attachment and proliferation on macropatterns in serum-culture

Cell growth on macropatterned surfaces was tested using multiple combinations of two dissimilar plasma-deposited surfaces (Table 2.2); one surface generally observed to be cell-adhesive in serum-based culture (e.g., NVP, AlAm) was paired with another surface characterized as generally non-cell adhesive (e.g., FC). Plasma deposition of patterns occurred sequentially, and was then reversed in a separate preparation to create two analogous macropatterned surfaces for each polymer combination studied (Figure 2.2). Representative results for macropattern cultures using IC-21 murine MΦ (Figure 2.5 A) and NIH 3T3 murine fibroblasts (Figures 2.5 B and 2.6 A) are shown.

For either the NVP-FC or AlAm-FC macropatterns, NIH 3T3 fibroblasts adhered exclusively to and proliferated on the NVP (Figure 2.5 B) or the AlAm (Figure 2.6 A) regions. Cell patterns with fidelity to the anticipated surface chemistry pattern appeared within 24 hours of seeding. The NIH 3T3 cells exhibited normal growth characteristics, kinetics and morphology in cell-supportive regions, and progressed to 100% confluence over the time course of the experiment, 7 days, in these regions. The boundary between the two co-patterned chemistries was also maintained for the duration of the culture experiment. At the boundary, cells would frequently grow parallel to the non-supportive chemistry boundary or extend toward and over the non-supportive (FC) region, surface-adherent only by cell contacts made in the cell-supportive (AlAm or NVP) region (Figures 2.5 B and 2.6 A). Many loosely adherent cells were observed at the pattern boundary. These cells were partially attached to the adherent NVP (or AlAm) chemistry zone, and floated above the non-adherent FC zone. Collectively, this behavior at the margin can be described as an "edge effect", attributed both to topological and chemical distinctions by cultured cells across the adherent/non-adherent pattern boundaries. The pp-film thickness for each deposition was calculated from the deposition rates and exposure times. For each experiment, deposited film thicknesses were: FC, 100 nm; NVP, 26 nm; AlAm, 90 nm; HxAm 47 nm.

By contrast, serum cultured IC-21 murine MΦ preferentially adhered to the FC region of the FC-NVP surfaces. These cells were evenly distributed over the FC substrate chemistry, suggesting that adherence was not due to a surface defect or topographical feature (Figure 2.5 A). Initially upon seeding, cell morphology was markedly different on

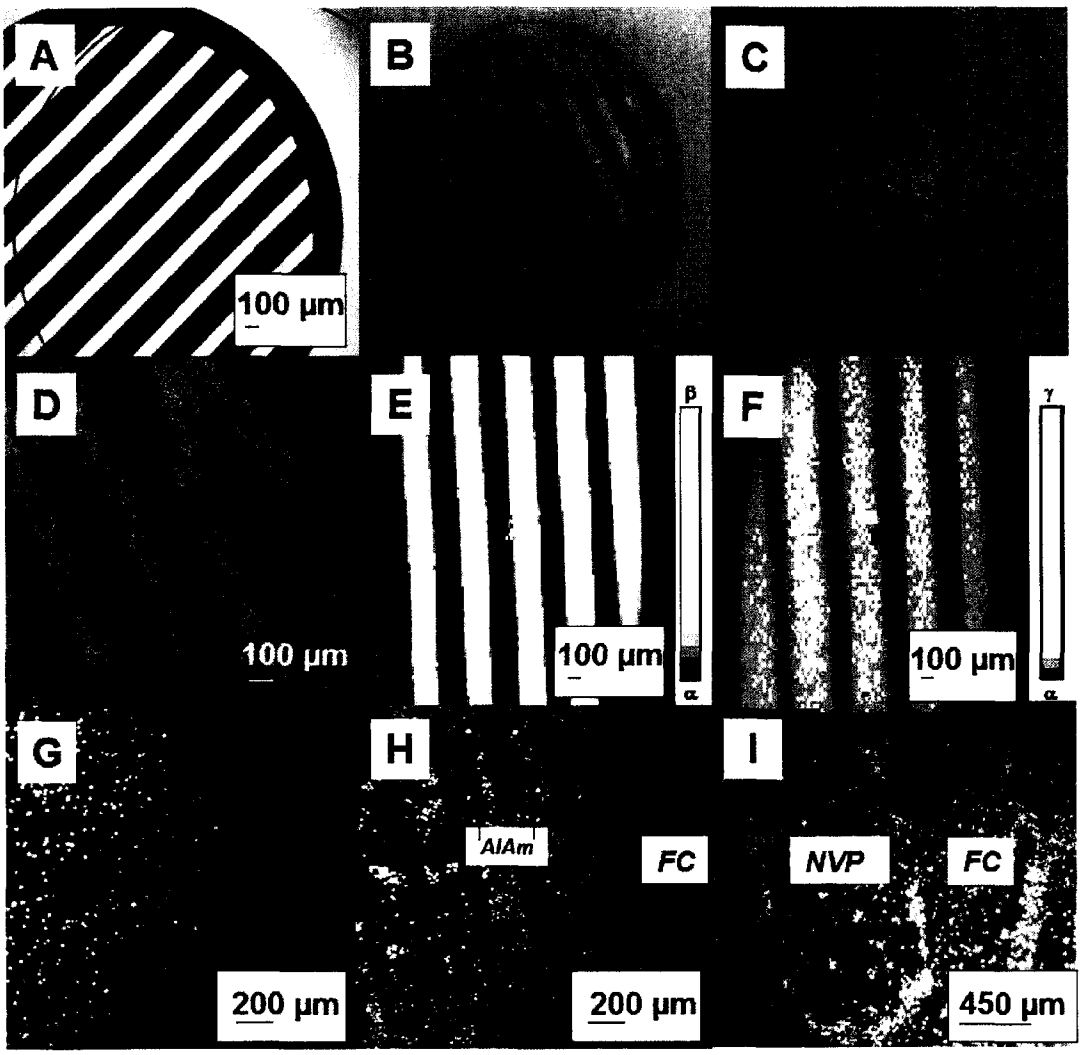

Figure 2.7 Micropatterning and control images. A) Phase contrast microscopy image of one type of (striped) TEM grid employed as a mask. Bars, 184 µm; spaces 92 µm. B-C) Electron microscopy images of the same grid. D) Phase contrast microscopy image of IC-21 cells grown on micropatterned HxAl-FC. Majority of cells shown are adhered to the HxAl bars. Patterns appeared by day 7 and were maintained through day 9, when the experiment was terminated. Cell seeding density was 100,000 cells per 15 x 60 mm plate. E-F) Scanning Auger maps of a pattern generated using a striped TEM grid identical to those used for preparing samples for use in cell culture experiments. Areas of most intensity (lightest) are strongest Auger signal. Intensity scales shown in E and F: α= 0, β= 281400, γ= 520633. E) Auger fluorine map (from the KLL signal) and F) Auger nitrogen map (from the KLL signal). G) Fluorescence microscopy of a non-patterned control FC surface showing an even and random distribution of IC-21 cells. H) Fluorescence microscopy of IC-21 cells on an AlAm-FC striped micropattern. Preferential growth was observed on the AlAm region (thicker bar) of the pattern at day 2, although cells also grew on the FC regions (thinner bar and background). Seeding density was 136,000 cells per 15 x 60 mm plate. I) Phase contrast images of IC-21 cells grown on a bullet shaped micropattern of NVP-FC, dimensions 1 x 2 mm, 4 days post-seeding at a density of 250,000 cells per plate.

each chemistry; cells in the center of the FC pattern were more closely packed and exhibited primarily astral morphology, whereas the fewer cells scattered across the NVP

region exhibited spreading behavior. Adherent MΦ cells exhibited characteristic membrane ruffling, lamellipodia and filopodia on both chemistries.[43] Although initial cell adherent densities indicated cell preference for FC regions, these cells progressed with a normal proliferative rate and eventually populated the entire surface (> 7 days) with no discernible differences in cell behavior or morphology based on surface chemistry. However, over short time frames post-seeding (24-72 hours), the IC-21 cells were observed to preferentially bind to the FC surfaces rather than the NVP, a behavior distinct from that previously documented in cultures of most other cell lines on similar FC or substantially hydrophobic surfaces,[30,38] but similar to that reported by Rich and Harris.[32]

Since the IC-21 MΦ represents the most physiologically relevant MΦ model within this study, use of the more monocytic RAW 264.7 and J774A.1 cell lines in macropatterning studies was limited. However, RAW 264.7 and J774A.1 behavior was examined on AlAm-FC and FC-AlAm, respectively. Both cell types attached to the FC and AlAm surface chemistries; neither demonstrated any discernible preference for either chemistry throughout the culture period, analogous to results obtained for the IC-21 cells (data not shown).

2.4.4 Cell attachment and proliferation on micropatterned surfaces

Cell behavior on micropatterned surfaces (see masks, Figure 2.7 A-C) was tested using multiple combinations of five plasma-deposited polymers (Table 2.3), representing four adhesive (e.g., NVP, AlAm, HxAm, NVFA) and one non-adhesive (e.g., FC) cell culture surfaces. Plasma deposition was performed in a sequential manner (Figure 2.2) and all

cell cultured micropatterning experiments were performed in media supplemented with 10% FBS.

Micropattern cell pattern fidelity for the MΦ-derived IC-21 cell line was generally successful, although not absolute for cell exclusion versus adherence on the different chemistries where registration of patterned substrate chemistry and cell adhesion was directly observable in culture from 2-9 days (Figures 2.5 C-E and 2.7 D, H, I). Cell adhesive patterns became evident at different time points. Generally, at early time points, few cells adhered to both regions regardless of surface chemistry (illustrated in Figure 2.7 H for cells grown on AlAm-FC chemistries Day 2). At later time points, discernible preferences for one chemistry were observed on select surfaces (e.g., Day 7 of culture for HxAm-FC, Figure 2.7 D). Patterns were typically maintained for 2-5 days before the cells overgrew the pattern. Such fidelity to substrate micropatterned chemistry was less successful for NIH 3T3 fibroblasts. Although cell patterns developed on these surfaces (Figure 2.6 B), as fibroblast cultures progressed, cellular delamination occurred readily, originating from the margins of the chemistry interfaces (Figure 2.6 C). These results indicate that strong cell-cell contacts dominate over cell-surface interactions. As cells multiplied and adhesive space became limiting, strong cell-cell contacts allowed surface-bound cells to be pulled off of their patterns (during rinsing) by attached cells "hanging" off pattern edges bound only by cell-cell contacts. Additionally, after completely rinsing cells from the surface, cells repopulated the patterned region, but again could be rinsed away once space became limiting.

Representative results for micropatterning with IC-21 murine MΦ (Figure 2.5 C-E, Figure 2.7 D, H and I) indicate that cell patterns develop for these cells on AlAm-FC (Figure 2.7 H), NVP-FC (Figure 2.5 C-E, Figure 2.7 I) and HxAm-FC (Figure 2.7 D), but not on NVFA-FC (data not shown) where no preferential growth based on chemistries was observed. Phase contrast microscopy results for striped and bullet shaped TEM grid-patterns, HxAm-FC and NVP-FC respectively, are shown in Figure 2.7 D and I. Multiple examples of such pattern fidelity were detected on each plate. Additionally, at early culture times (48 hours), an edge effect was observed for micropatterned IC-21 cells (Figure 2.5 C-E), likely a response to topological features (roughness) at the margin of the two chemistries.[32]

2.5 Discussion

Cellular response to various model materials has important fundamental significance to numerous biotechnological medical devices, diagnostic high-throughput cell-based screening and environmental applications. Specifically, surface interactions with leukocytes and lymphocytes are particularly important for understanding inflammatory responses to implanted device materials and soluble drug candidates. We have previously described the morphological and proliferative characteristics of a fibroblast and MΦ inclusive group cultured on model biomaterials surfaces.[42,43] This initial study has been extended here to a large group of previously characterized plasma-deposited co-patterned surfaces of distinct chemistries.[37]

Two important considerations distinguishing cell-surface behavior for *in vitro*-based cell adhesion studies are the presence of serum as opposed to biased pre-adsorption of ECM proteins, and the influence of cell phenotype.[3] MC-MΦ and fibroblast cells have markedly different functions *in vivo*, and consequently their interactions with surfaces reflect these highly specialized phenotypic roles. Although typically considered non-adhesive *in vivo* unless activated by non-host materials (e.g., foreign bodies) MΦ, the sentinels of the immune system, are uniquely equipped to identify and respond to surfaces. The complex MΦ-mediated host response includes biomaterials attachment reactions,[47] interactions with lymphocytes[48] and cell-cell fusion to form FBGC.[49-51] Curiously, materials typically considered non-permissive to cell attachment and growth in culture unless pre-adsorbed with matrix proteins (e.g., hydrophobic surfaces), have been shown to promote MΦ attachment in serum cultures *in vitro*.[32,42,43,52] One major unresolved issue is the mechanism by which this occurs, compared to well-known integrin attachment mechanisms employed by most cell types.[53,54] Additionally, there is the question of how closely the frequently employed immortalized MC/MΦ-derived secondary cell lines accurately and faithfully represent phenotypic behavior of primary MΦ or monocytic cells under *in vitro* assay conditions. This has significant implications for *in vitro* pharmacological assays employing adherent cells as predictive indicators of inflammatory activation *in vivo*.

Given that MΦ adhesion to biomaterials plays a key role in mediating immune response to foreign materials,[47] adhesive behavior on surfaces designed to be non-fouling is of great interest. However, primary cells represent an expensive cell source with a short

lifetime and uncertain phenotypic stability in culture. Therefore, we focused on the most physiologically relevant cell line, IC-21, as it shares many characteristics with normal peritoneal MΦ,[55] yet as an immortalized cell line it can be grown successfully over extended culture periods. In the case of our most interesting result, i.e. proficient growth on FC surfaces, we compared the behavior of primary sourced and secondary-derived cell lines. Results for the (MC-) MΦ cell lines indicated similar behaviors for these cells on all pp-generated surfaces tested. The IC-21 and J774A.1 lines grew well on HxAm, and all three MC/MΦ cell lines successfully colonized FC, AlAm and NVP surfaces (Table 2.1).

Data demonstrate that IC-21, J774A.1 and RAW 264.7 secondary (MC-) MΦ cell lines tested in serum cultures adhered to and proliferated on all pp-surfaces, regardless of surface chemistry. In addition, limited tests with primary derived bone marrow MΦ (FC and PS controls) showed similar results, indicating that both the immortalized lineages and the primary MΦ behave consistently with respect to surface response within this select group of cells and surfaces.

Poor cell culture results on FC surfaces have been previously reported for numerous cell lines and conditions.[3,26,30,32,38,56,57] Extremely hydrophobic perfluorocarbon surfaces (e.g., poly(vinylidene fluorine), PVDF; poly(tetrafluoroethylene), PTFE) typically hinder cellular attachment from serum media.[3,44] This observed resistance to cell adhesion has been shown to be mediated by preferential albumin deposition onto these surfaces, blocking recognition by cell integrin receptors of trace matrix protein motifs on the

surface required for cell adhesion.[44,57,58] Interestingly, our FC surfaces supported the attachment and proliferation of all (MC-) MΦ cell lines tested, but not the NIH 3T3 fibroblasts (Figures 2.3 and 2.4).[3,38] In addition, pre-treatment of surfaces for 24 hours with either 3 mg/ml albumin, 10% or 100% serum, to adsorb protein from a single biased or complex protein mixture, had no significant effect on the ability of cells to adhere to and proliferate on this surface (Figure 2.4). Despite little observable adhesion from other cell lines cultured on similar FC surfaces in serum-containing media,[3,30,38,56] murine MΦ were observed to grow well on various types of FC surfaces: all three MΦ-derived cell lines and primary-derived bone marrow MΦ adhered readily to FC patterns in the presence of serum. This distinct attachment capability from fibroblasts could result from: (1) different classes of cell adhesion receptors on MΦ compared to other cell types that typically rely on integrins and matrix proteins, (2) MΦ use of an integrin-independent surface attachment process that is not receptor-driven (i.e., protein-independent, electrostatic, membrane glycosylation-dependent), (3) much lower surface density requirements of adsorbed trace matrix proteins (e.g., fibronectin, collagens, vitronectin) for MΦ as compared to cells that attach to surfaces using their integrin classes, or (4) rapid up-regulation of endogenous matrix protein expression in these cells that facilitates surface attachment.

Grainger and coworkers recently showed that poly(tetrafluoroethylene) FC surfaces overwhelmingly adsorb excess albumin from serum[44] compared to other trace matrix proteins (e.g., fibronectin) essential for attachment of most cell types.[53,54] This result correlated with lack of observed probe antibody reactivity to several fibronectin-epitopes

after serum exposure, as well as observed low endothelial cell adhesion. Biased surface selection of albumin seems to be a natural tendency of FC surfaces,[58] hindering cellular attachment in the presence of serum via an albumin blocking mechanism that either limits matrix protein deposition or masks its recognition by adhering cells. Therefore, cell-surface chemistry selection preference should result for specific surface chemistries patterned side-by-side. For example, this rationale applied to cell attachment to HxAm co-patterned with FC in serum predicts that albumin adsorption to the more apolar FC surface precludes cell adhesion to these areas, whereas increased matrix protein adsorbed abundance on HxAm promotes cell adhesion. This is in fact what is observed in studies reported here for MΦ and supported in several other analogous literature reports.[3,35,36] Typical cell pattern development from serum media relies on consistent cell adhesion preference for an attachment-permissive surface (e.g., HxAm, NVP, TCPS) adsorbing sufficient matrix proteins over non-permissive (e.g., FC) surfaces blocked by preferential albumin adsorption.

This predicted preferential behavior was evident in the NIH 3T3 fibroblast culture results, where cells bound exclusively and definitively to permissive regions of macropatterned plates (Figure 2.5 B and 2.6 A; analogous results obtained for inverse patterned chemistry, data not shown). These patterns were evident at early culture times (24 hours) and maintained even if cells were allowed to progress to 100% confluence on the permissive substrate. In contrast, MΦ did not exhibit this distinct patterning behavior: they did not adhere exclusively to the predicted permissive regions. Although (MC-) MΦ consistently demonstrated the ability to adhere to and proliferate on all homogenous

surface chemistries tested, they did exhibit preferences for specific chemistries within combinations of co-patterned substrates. Examples include the combination of FC and HxAm (Figure 2.7 D) where IC-21 MΦ adhered preferentially to the HxAm over the FC, resulting in a pattern. This pattern evolved slowly with time, fully developed seven days after cells were applied to the plates, and was maintained through day nine when the experiment was terminated. By contrast, at early time points (24 hours), IC-21 MΦ attached preferentially to FC regions of FC-NVP macropatterns (Figure 2.5 A). In some cases no surface chemistry preference was discernible due to similar surface selection (e.g., J774A.1 and RAW 264.7 cultures on AlAm-FC and FC-AlAm, respectively, data not shown).

Numerous previous studies of cell adhesion to materials have utilized fibroblastic cell lines of diverse types.[3,32,35,36,38] The ability of fibroblasts to attach to and proliferate on, or in the presence of specific substrate chemistries in serum-containing milieu or pre-adsorbed with matrix proteins, is often used as a basic indicator of materials "biotolerance". Fibroblasts adhere to more hydrophobic substrate chemistries with difficulty[3,32,34,38,56,57] unless pre-adsorbed with purified matrix proteins prior to culture. Their attachment-dependent phenotype, adherent morphology and surface matrix protein requirements are distinct from MC/MΦ cells. In addition, the cell-cell contacts formed in cells grown on hydrophobic surfaces are stronger than the cell-surface contacts, exemplified by delamination of large intact sheets of cells (Figure 2.6 C).

NIH 3T3 fibroblast cultures attached to and grew readily on all attachment-permissive surfaces tested--AlAm, HxAm, NVP and NVFA. This is consistent with previous reports[59-61] and leads to an interpretation that these adhesion-permissive surface chemistries (1) adsorb sufficient matrix proteins from serum to support cell integrin-dependent attachment, and (2) are not cytotoxic. In contrast to MΦ cultures, fibroblasts were non-adherent or poorly adherent to the FC surfaces in the presence of either serum (as previously observed by others)[3,38,56] or pure albumin solution pre-adsorption. Most cells were unable to adhere and remained free-floating in the media. Any observed fibroblast attachment was attributed to small surface coating defects in the plates (Figure 2.3 B, arrow). Ultimately, the NIH 3T3 fibroblast cells were not able to colonize the plates effectively, with only small, isolated areas of attachment, and no observed cell pattern development in any case, consistent over various cell-seeding densities. Limited fibroblast attachment and growth on non-permissive plasma-treated substrates was most frequently observed at the pattern edges (Figure 2.6 B) where FC deposition was likely affected or disrupted by the pattern transition or walls of the plate.

2.6 Conclusions

Biomaterials design has become more sophisticated with numerous techniques currently available to develop surfaces with improved biocompatibility. Plasma-derived chemical functionalization of biomaterials is one commonly employed method for improving implant surface characteristics. We have examined a diverse group of pp-surfaces and the responses of two phenotypically distinct cell types to these surfaces *in vitro*.

NIH 3T3 fibroblast cell lineage adherence, growth and proliferation on pp-substrates in serum proceeds as expected based on known surface chemistry trends. MC-MΦ cells derived from both primary and secondary cell sources show consistent adherence, growth and proliferation on all pp-surfaces tested, including FC shown refractory to cell adhesion in many previous studies. Results suggest that these phenotypically distinct cell types have different requirements for successful surface adherence and proliferation. Cell-cell contacts on FC surfaces are stronger than cell-surface contacts made by fibroblast cultures, whereas (MC-) MΦ cells establish strong cell-surface contacts, even in serum on FC.

The demonstrated ability of cultured, secondary-derived immortalized cells to attach to non-adhesive substrates such as FC is unusual. Equivalence with the more biologically significant primary-derived BMMO cells to adhere and proliferate on these surfaces suggests that the many elegant micropatterns designed for use in implantable devices and scaffolds may not be practically useful *in vivo* due to the attachment of immunogenic cells which not only elicit a FBR, but also preclude the attachment and growth of desirable cell types. Additionally, use of apolar surfaces and albumin masking agents in common *in vitro* assays of anti-inflammatory drugs with cultured MΦ may not be sufficient to block cell-surface activation, thus confounding pharmacological assay results. Consequently, the interactions of MΦ as key cellular mediators must be carefully considered in an appropriate biologically relevant context.

2.7 References

1. Andrade JD. Interfacial phenomena and biomaterials. *Med Instrum* 1973;**7**:110-9.

2. Hubbell JA. Biomaterials in tissue engineering. *Biotechnology (N Y)* 1995;**13**:565-76.

3. van Kooten TG. Growth of cells on polymer surfaces. *Encyclopedia of Surface and Colloid Science*. New York, NY: Marcel Dekker, Inc., 2004:1-19.

4. Liu WF, Chen CS. Engineering biomaterials to control cell function. *Mater Today* 2005;**8**:28-35.

5. Andrade JD. *Surface and interfacial aspects of biomedical polymers: Protein adsorption.* New York, NY: Plenum, 1985.

6. Mrksich M, Whitesides GM. Using self-assembled monolayers to understand the interactions of man-made surfaces with proteins and cells. *Annu Rev Biophys Biomol Struct* 1996;**25**:55-78.

7. Dewez JL, Doren A, Schneider YJ, Rouxhet PG. Competitive adsorption of proteins: key of the relationship between substratum surface properties and adhesion of epithelial cells. *Biomaterials* 1999;**20**:547-59.

8. Baszkin A, Lyman DJ. The interaction of plasma proteins with polymers. I. Relationship between polymer surface energy and protein adsorption/desorption. *J Biomed Mater Res* 1980;**14**:393-403.

9. Sethuraman A, Han M, Kane RS, Belfort G. Effect of surface wettability on the adhesion of proteins. *Langmuir* 2004;**20**:7779-88.

10. Curtis A, Wilkinson C. Topographical control of cells. *Biomaterials* 1997;**18**:1573-83.

11. Poncin-Epaillard F, Legeay G. Surface engineering of biomaterials with plasma techniques. *J Biomater Sci Polym Ed* 2003;**14**:1005-28.

12. Schroder K, Meyer-Plath A, Keller D, Ohl A. On the applicability of plasma assisted chemical micropatterning to different polymeric biomaterials. *Plasmas Polym* 2002;**7**:103-124.

13. Bouyer E, Schiller G, Muller M, Henne RH. Thermal plasma chemical vapor deposition of Si-based ceramic coatings from liquid precursors. *Plasma Chem Plasma Proc* 2001;**21**:532-546.

14. Meaudre R, Butte R, Vignoli S, Meaudre M, Saviot L, Marty O, Rocai I, Cabarrocas P. Structural properties and recombination processes in hydrogenated polymorphous silicon. *Eur Phys J Appl Phys* 2003; **22**:171-178.

15. Sopori B. Dielectric films for Si solar cell applications. *J Electron Mater* 2005;**34**:564-570.

16. Cicala G, Bruno P, Losacco AM, Mattei G. Plasma deposition of hydrogenated diamond-like carbon films from CH4-Ar mixtures. *Surf Coat Technol* 2004;**180-181**:222-226.

17. Mutsukura N, Handa Y. Deposition of diamond-like carbon film in a closed-space CH4 RF plasma. *Plasma Chem Plasma Proc* 2002;**22**:607-617. .

18. Dhar R, Pedrow PD, Liddell K, C. N, Ming Q, Moeller TM, Osman MA. Plasma-enhanced metal-organic chemical vapor deposition (PEMOCVD) of catalytic coatings for fuel cell reformers. *IEEE Trans Plasma Sci* 2005;**33**:138-146.

19. Luting Y, Wenjie S, Hezhuo M, Wei H, Zhigang G, Yikang P. Surface modification of ultrafine ceramic powders by low temperature plasma polymerization. *Key Eng Mater* 2004;**264-268**:109-112.

20. Steen ML, Flory WC, Capps NE, Fisher ER. Plasma modification of porous structures for formation of composite materials. *Chem Mater* 2001;**13**:2749-2752.

21. Tang JX, Li YQ, Dong X, Wang SD, Lee CS, Hung LS, Lee ST. Photoemission and vibrational studies of metal/organic interfaces modified by plasma-polymerized fluorocarbon films. *Appl Surf Sci* 2004;**239**:117-124.

22. Folch A, Toner M. Microengineering of cellular interactions. *Annu Rev Biomed Eng* 2000;**2**:227-56.

23. Singhvi R, Kumar A, Lopez GP, Stephanopoulos GN, Wang DI, Whitesides GM, Ingber DE. Engineering cell shape and function. *Science* 1994;**264**:696-8.

24. McFarland CD, Thomas CH, DeFilippis C, Steele JG, Healy KE. Protein adsorption and cell attachment to patterned surfaces. *J Biomed Mater Res* 2000;**49**:200-10.

25. Mitchell SA, Emmison, N. and A.G. Shard. Spatial control of cell attachment using plasma micropatterned polymers. *Surf Interface Anal* 2002;**33**:742-747.

26. Collier TO, Thomas CH, Anderson JM, Healy KE. Surface chemistry control of monocyte and macrophage adhesion, morphology, and fusion. *J Biomed Mater Res* 2000;**49**:141-5.

27. Thomas CH, McFarland CD, Jenkins ML, Rezania A, Steele JG, Healy KE. The role of vitronectin in the attachment and spatial distribution of bone-derived cells on materials with patterned surface chemistry. *J Biomed Mater Res* 1997;**37**:81-93.

28. Folch A, Jo BH, Hurtado O, Beebe DJ, Toner M. Microfabricated elastomeric stencils for micropatterning cell cultures. *J Biomed Mater Res* 2000;**52**:346-53.

29. Harbers GM, Grainger DW. Cell-Material Interactions: Fundamental Design Issues for Tissue Engineering and Clinical Considerations. In: Guelcher SA, Hollinger JO, eds. *An Introduction to Biomaterials*. Boca Raton: CRC Press, 2006:15-45.

30. Koenig AL, Gambillara V, Grainger DW. Correlating fibronectin adsorption with endothelial cell adhesion and signaling on polymer substrates. *J Biomed Mater Res A* 2003;**64**:20-37.

31. Mrksich M, Dike LE, Tien J, Ingber DE, Whitesides GM. Using microcontact printing to pattern the attachment of mammalian cells to self-assembled monolayers of alkanethiolates on transparent films of gold and silver. *Exp Cell Res* 1997;**235**:305-13.

32. Rich A, Harris AK. Anomalous preferences of cultured macrophages for hydrophobic and roughened substrata. *J Cell Sci* 1981;**50**:1-7.

33. Scotchford CA, Gilmore CP, Cooper E, Leggett GJ, Downes S. Protein adsorption and human osteoblast-like cell attachment and growth on alkylthiol on gold self-assembled monolayers. *J Biomed Mater Res* 2002;**59**:84-99.

34. Ruardy TG, Schakenraad JM, van der Mei HC, Busscher HJ. Adhesion and spreading of human skin fibroblasts on physicochemically characterized gradient surfaces. *J Biomed Mater Res* 1995;**29**:1415-23.

35. Gallant ND, Capadona JR, Frazier AB, Collard DM, Garcia AJ. Micropatterned surfaces to engineer focal adhesions for analysis of cell adhesion strengthening. *Langmuir* 2002;**18**:5579-5584.

36. Tourovskaia A, Barber T, Wickes BT, Hirdes D, Grin B, Castner DG, Healy KE, Folch A. Micropatterns of chemisorbed cell adhesion-repellent films using oxygen plasma etching and elastomeric masks. *Langmuir* 2003;**19**:4754-4764.

37. Malkov G, Martin IT, Schwisow WB, Chandler JP, Fisher ER. Pulsed plasma-induced micropatterning with alternating hydrophilic and hydrophobic surface chemistries. *Chem Mater* 2006, submitted.

38. McClary KB, Ugarova T, Grainger DW. Modulating fibroblast adhesion, spreading, and proliferation using self-assembled monolayer films of alkylthiolates on gold. *J Biomed Mater Res* 2000;**50**:428-39.

39. Rhoades ER, Orme IM. Similar responses by macrophages from young and old mice infected with Mycobacterium tuberculosis. *Mech Ageing Dev* 1998;**106**:145-53.

40. Kaltenbach JP, Kaltenbach MH, Lyons WB. Nigrosin as a dye for differentiating live and dead ascites cells. *Exp Cell Res* 1958;**15**:112-7.

41. Daw R, Candan S, Beck AJ, Devlin AJ, Brook IM, MacNeil S, Dawson RA, Short RD. Plasma copolymer surfaces of acrylic acid/1,7 octadiene: Surface characterisation and the attachment of ROS 17/2.8 osteoblast-like cells. *Biomaterials* 1998;**19**:1717-1725.

42. Godek ML, Duchsherer, N. L., McElwee, Q., Grainger, D. W. Morphology and growth of murine cell lines on model biomaterials. *Biomed Sci Instrum* 2004;**40**:7-12.

43. Godek ML, Michel R, Grainger DW. Adsorbed serum albumin is permissive to macrophage attachment to polymer surfaces in culture. 2006 (Manuscript in preparation).

44. Grainger DW, Pavon-Djavid G, Migonney V, Josefowicz M. Assessment of fibronectin conformation adsorbed to polytetrafluoroethylene surfaces from serum protein mixtures and correlation to support of cell attachment in culture. *J Biomater Sci Polym Ed* 2003;**14**:973-88.

45. Haddow DB, France RM, Short RD, MacNeil S, Dawson RA, Leggett GJ, Cooper E. Comparison of proliferation and growth of human keratinocytes on plasma copolymers of acrylic acid/1,7-octadiene and self-assembled monolayers. *J Biomed Mater Res* 1999;**47**:379-87.

46. Haddow DB, Steele DA, Short RD, Dawson RA, Macneil S. Plasma-polymerized surfaces for culture of human keratinocytes and transfer of cells to an in vitro wound-bed model. *J Biomed Mater Res A* 2003;**64**:80-7.

47. Anderson JM. Mechanisms of Inflammation and Infection With Implanted Devices. *Cardiovasc Pathol* 1993;**2**:33S-41S.

48. MacEwan MR, Brodbeck WG, Matsuda T, Anderson JM. Student Research Award in the Undergraduate Degree Candidate category, 30th Annual Meeting of the Society for Biomaterials, Memphis, Tennessee, April 27-30, 2005. Monocyte/lymphocyte interactions and the foreign body response: in vitro effects of biomaterial surface chemistry. *J Biomed Mater Res A* 2005;**74**:285-93.

49. Anderson JM. Multinucleated giant cells. *Curr Opin Hematol* 2000;**7**:40-7.

50. Kyriakides TR, Foster MJ, Keeney GE, Tsai A, Giachelli CM, Clark-Lewis I, Rollins BJ, Bornstein P. The CC chemokine ligand, CCL2/MCP1, participates in macrophage fusion and foreign body giant cell formation. *Am J Pathol* 2004;**165**:2157-66.

51. McNally AK, Anderson JM. Interleukin-4 induces foreign body giant cells from human monocytes/macrophages. Differential lymphokine regulation of macrophage fusion leads to morphological variants of multinucleated giant cells. *Am J Pathol* 1995;**147**:1487-99.

52. Davis GE. The Mac-1 and p150,95 beta 2 integrins bind denatured proteins to mediate leukocyte cell-substrate adhesion. *Exp Cell Res* 1992;**200**:242-52.

53. Garcia AJ. Get a grip: integrins in cell-biomaterial interactions. *Biomaterials* 2005;**26**:7525-9.

54. Hynes RO. Integrins: bidirectional, allosteric signaling machines. *Cell* 2002;**110**:673-87.

55. Mauel J, Defendi V. Infection and transformation of mouse peritoneal macrophages by simian virus 40. *J Exp Med* 1971;**134**:335-50.

56. Schakenraad JM, Busscher HJ, Wildevuur CR, Arends J. The influence of substratum surface free energy on growth and spreading of human fibroblasts in the presence and absence of serum proteins. *J Biomed Mater Res* 1986;**20**:773-84.

57. Webb K, Hlady V, Tresco PA. Relative importance of surface wettability and charged functional groups on NIH 3T3 fibroblast attachment, spreading, and cytoskeletal organization. *J Biomed Mater Res* 1998;**41**:422-30.

58. Kiaei D, Hoffman AS, Horbett TA. Tight binding of albumin to glow discharge treated polymers. *J Biomater Sci Polym Ed* 1992;**4**:35-44.

59. Griesser HJ, Chatelier RC, Gengenbach TR, Johnson G, Steele JG. Growth of human cells on plasma polymers: putative role of amine and amide groups. *J Biomater Sci Polym Ed* 1994;**5**:531-54.

60. Marchant RE, Johnson SD, Schneider BH, Agger MP, Anderson JM. A hydrophilic plasma polymerized film composite with potential application as an interface for biomaterials. *J Biomed Mater Res* 1990;**24**:1521-37.

61. Morra M, Cassinelli C. Cell adhesion micropatterning by plasma treatment of alginate coated surfaces. *Plasmas Polym* 2002;**7**:89-101.

CHAPTER 3: RHO GTPASE PROTEIN EXPRESSION AND ACTIVATION IN MURINE MONOCYTE/MACROPHAGES ARE NOT MODULATED BY MODEL BIOMATERIAL CULTURE SURFACES IN SERUM-CONTAINING *IN VITRO* CULTURES

This chapter was written by Marisha L. Godek, edited by David W. Grainger and contains contributions from Jennifer A. Sampson, Nichole L. Duchsherer and Quinn McElwee. It has been accepted for publication in the Journal of Biomaterials Science, Polymer Edition, 2006.

3.1 Abstract

The Rho GTPase cellular signaling cascade was investigated in pro-monocyte and (MC-) MΦ cells by examining GTPase expression and activation in serum-containing cultures on model biomaterials. Abundance of Rho GDI and the Rho GTPase proteins RhoA, Cdc42 and Rac1 was determined in cells grown on TCPS, PS, PLA and Teflon® AF surfaces. Protein expression was compared based on cell maturity (pro-monocyte to MC to MΦ lineages) and by model surface chemistry: Rho proteins were present in the majority of MΦ cells tested on model surfaces suggesting that a pool of Rho proteins is readily available for signaling events in response to numerous activating cues, including

biomaterials surface encounter. Rho GTPase activation profiles in these cell lines indicate active Cdc42 and Rho proteins in RAW 264.7, Rac1 and Rho in J774A.1, and Cdc42 and Rac1 in IC-21 cell lines, respectively. Collectively, these proteins are known to play critical roles in all actin-based cytoskeletal rearrangement necessary for cell adhesion, spreading and motility, and remain important to establishing cellular responses required for FBR *in vivo*. Differences in Rho GTPase protein expression levels based on cell sourcing (primary versus secondary-derived cell source), or as a function of surface chemistry were insignificant. Rho GTPase expression profiles varied between pro-monocytic non-adherent precursor cells and mature adherent (MC-) MΦ cells. The active GTP-bound forms of the Rho GTPase proteins were detected from MC-MΦ cell lines RAW 264.7 and J774A.1 on all polymer surfaces, suggesting that while these proteins are central to cell adhesive behavior, differences in surface chemistry are insufficient to differentially regulate GTPase activation in these cell types. Active Cdc42 was detected from cells cultured on the more-polar TCPS and PLA surfaces after several days, but absent from those grown on apolar PS and Teflon® AF, indicating some surface influence on this GTPase in serum-containing cultures.

3.2 Introduction

The Rho GTPase family of intracellular signaling proteins is implicated in numerous cellular behaviors, including cytoskeletal reorganization and resultant cell adhesion, shape and motility changes, membrane trafficking, cellular proliferation and transcriptional regulation in mammalian cells.[1,2] Rho GTPases are key enzymes positioned at signal convergence points from numerous receptors, and when activated,

mobilize groups of functionally divergent molecules to elicit diverse responses.[3] Numerous interactions of Rho GTPase proteins with upstream regulators and downstream targets create a complex cell-signaling network.

Rho, Rac and Cdc are the most frequently studied Rho GTPase proteins and, like other G proteins, function as intracellular molecular switches, cycling between active (GTP bound) and inactive (GDP bound) forms. Cellular regulation of these proteins, based on the exchange of substrate GDP for GTP, is complex and affected by multiple regulatory factors including GEFs (Guanine Nucleotide Exchange Factors) that catalyze the exchange of bound GDP for GTP[1], GAPs (Guanine Activating Proteins) that increase the intrinsic Rho protein GTPase activity, and Rho GDIs (GDP-Dissociation Inhibitors) that prevent release of bound GDP, stabilizing inactive forms of Rho proteins.[4,5]

Rho GTPases influence the ability of many cell types to adhere, proliferate and spread, mobilizing elements of the cytoskeleton in response to environmental stimuli that are both physical and chemical in nature.[5,6] Significant environmental cues in the context of biomaterials include both (solid) physical and (soluble) chemical stimuli such as culture plastics and implantable materials interfaced with host tissues, as well as altered physiological states of tissues adjacent to a biomaterial (hypoxia, edema, mechanical and chemokine gradients, etc) . Many attachment-dependent cell types require surface contact, haptotaxis, adhesion, spreading and migration to initiate proliferative and phenotypic responses.[7,8] Other cells (e.g., leukocytes), while not requiring attachment for normal functions, use outside-inside receptor-initiated interrogation of both natural and

synthetic surfaces in homeostatic and immuno-modulatory responses. Rho GTPases are implicated in these cells' phenotypic functions and signaling.[9-12]

Implanted biomaterials initiate a host FBR reaction involving a series of cell-materials surface-mediated interactions.[13,14] Rho GTPases are likely involved in mediating this ubiquitous host cell-materials interaction. MC, MΦ, and fibroblast recruitment to and presence at biomaterial implant sites correlate with histological events producing implant-associated fibrosis and unresolved wound healing.[13] Gross cellular responses to biomaterials surfaces such as morphological changes in cytoskeletal features can be directly observed,[15] yet cell-surface signaling mechanisms underlying propagation of key events in this context remain poorly understood. Ultimate control of this adverse host inflammatory response requires an improved understanding of implant surface reactions with various cell types crucial to healing response mechanisms. In particular, MC and MΦ recruitment, followed by cell-surface attachment, maturation to differentiated MΦ phenotypes, and ensuing signaling events initiating the FBR, including characteristic FBGC development [13,14,16,17] all plausibly involve Rho GTPases.

Directly relevant to implant-associated cell types, Rho GTPases have been studied extensively in adherent Swiss 3T3 fibroblast and Bac1.2F5 MΦ cell lines.[1-4,18] Less work is reported for other cell lines, including J774A.1 (MC-MΦ)[12] and a sub-line of the RAW 264.7 MC-MΦ, RAW LR/FMLPR 2.[19] In these cells, Rho GTPase expression has been linked to regulation of specific cytoskeletal features: RhoA is associated with control of stress fiber formation (fibroblasts) and actin and myosin attachment to the cell membrane

at focal adhesion sites.[1,2] Rac controls lamellipodial protrusion and membrane ruffle formation[18] and Cdc42 induces formation of microspikes and filopodia, and influences cell polarity.[4] In Swiss 3T3 fibroblasts, a hierarchical signaling cascade exists beginning with Cdc activation, then Rac, and subsequent activation of Rho.[20] Rho GTPase contributions to MΦ phagocytic behavior have also been reported.[19,21] Recently, the Rho/ROCK (Rho activated kinase) signaling proteins have been implicated in the ability of fibroblasts to "sense" rigidity in their adhesion environment.[22] These effects have profound implications for elucidating cell-based mechanisms in wound healing, tissue regeneration and neogenesis.

The FBR is characterized by chronic unresolved wound healing,[13] is mediated by MΦ cells *in vivo*. Rho GTPase involvement in key cellular responses to biomaterials such as MΦ activation and differentiation at the implant site is therefore a significant issue. Hence, expression and activation profiles of Rho GTPases Rho, Rac1 and Cdc42 in primary-derived murine pro-monocytes and differentiated BMMO, and in three murine (MC-) MΦ[1] derived cell lines in culture are compared here. Specifically, Rho GTPase expression (e.g., presence or absence of this protein) and activation (e.g., presence or absence of the GTP-bound protein) profiles were compared for: 1) primary-derived MΦ to secondary-derived immortalized (MC-) MΦ cell line populations, 2) cellular maturity, ranging from the (non-adherent) pro-monocytic mixed population bone marrow precursor cells to the fully differentiated (adherent) BMMO, and 3) ability of cells to adhere to,

[1] The use of "(MC-) MΦ" is meant to describe the three cell lines J774A.1, RAW 264.7 and IC-21 collectively despite their presumed phenotypic differences and lineage maturity, and may refer to any combination of the MC-MΦ cell lines J774A.1 and RAW 264.7 with each other and/or the MΦ cell line IC-21.

grow (enlarge), proliferate and spread on control and model biomaterial polymer surfaces. We have previously reported the ability of BMMO and RAW 264.7, J774A.1 and IC-21 murine (MC-) MΦ cells to adhere to, proliferate and spread on these surfaces.[15] New findings here relate to key signaling events in the context of specific model biomaterials and MΦ cell culture systems to progress toward an improved understanding of events underlying MΦ attachment to and proliferation on biomaterials. We hypothesized that surface chemistry would influence Rho GTPase expression and/or activation profiles based on observations of varied gross cell morphologies on the substrates selected. Interestingly, we found that Rho GTPase expression is not significantly different in cultured cells based on either cell sourcing or culture surface chemistries tested. Rho GTPase activation in the MC-MΦ cell lines RAW 264.7 and J774A.1 was not modulated in a surface-dependent manner. In contrast, activated Cdc42 was detected in the IC-21 MΦ cell line on more polar surfaces (TCPS and PLA) after several days in culture, and absent from less polar PS and Teflon® surfaces, correlated to observations of distinct cell morphologies based on surface polarity.

3.3 Materials and Methods

Primary cell harvest

Bone marrow cells were harvested from the femurs and tibias of C57/BL-6 mice (Jackson Laboratories) as previously described.[23] Proteins were either extracted from these isolated cells immediately upon harvest from bones and labeled "naïve pro-monocytic" due to the immature nature of the cells present, or these cells were plated in 10 ml of complete BMMO media (10% heat inactivated FBS, 10% L929 fibroblast conditioned medium, 1%

penicillin-streptomycin, 1% HEPES, 1% non-essential amino acids, and 1% sodium pyruvate in Dulbecco's modified Eagle's medium, DMEM) to promote maturation to the MΦ phenotype for 10 days before collection and protein extraction.[23]

Cell culture

Murine MC-MΦ cell lines RAW 264.7 and J774A.1, and the MΦ IC-21 cell line were obtained from the ATCC (Manassas, VA). Cells were cultured in DMEM (Mediatech, for J774A.1) or RPMI 1640 (Mediatech, for IC-21 and RAW 264.7) supplemented with 10% FBS (HyClone) and 1% penicillin-streptomycin (Life Technologies) or complete BMMO media. Cultures were maintained in T175 TCPS flasks (Nunc™) under standard conditions: incubation at 37°C, 98% humidity and 5% CO_2. Cells were dissociated from culture flasks by incubation with Ca^{2+}- and Mg^{2+}- free cell culture grade Hank's balanced salt solution (HBSS, Life Technologies) (J774A.1 and RAW 264.7), or by scraping with a rubber policeman (IC-21). Cell concentration and viability was assessed using trypan blue dye exclusion (BioWhittaker) and a hemacytometer. All cell line subcultures were ≤ 41 beyond the passage number as received from ATCC.

Cell culture on model surfaces

TCPS (Falcon®, Becton Dickinson) and PS (Corning Inc.) 15 x 100 mm dishes were utilized for both control and experimental conditions. Glass plates (20 x 100 mm) were treated in a potassium hydroxide solution overnight and rinsed copiously with 18 MΩ "Nanopure-grade" water prior to use. Fluoropolymer culture surfaces were prepared by coating PS dishes with 0.1 wt. % Teflon® AF (DuPont Fluoroproducts) in FC-40 solvent

(3M Corp). Coated surfaces were incubated in vacuum overnight to remove residual solvent, and plates were misted with 70% ethanol, dried, and treated with biosafety cabinet UV light for 20 minutes immediately before culture use, a process shown benign to cell culture surface chemistry.[24] PLA (mol. wt. 50,000 or 100,000, Polysciences, Inc; 0.2% solution in methylene chloride) was pipetted into glass plates and air-dried (covered). Plates were sterilized with a 70% ethanol solution and biosafety cabinet UV light immediately before use. Plates were tested for the presence of contaminating endotoxin using a Pyrogene™ Assay kit (Cambrex), and endotoxin levels were determined to be below the kit detection limit (0.02 EU/ml). Plates were subsequently pre-treated with appropriate media containing 10% FBS for a minimum of six hours before cell seeding. This media was then removed and cells were seeded at concentrations ranging from 5.0×10^4-1×10^6 cells per plate, and grown to a specified point of sub-confluence (to avoid profiling staged or quiescent cells). Initial seeding densities varied slightly for each cell type, due to surface-dependent differences in cell adhesion and growth rates, and in order to create roughly equivalent culture time endpoints whenever possible (see Figure 3.1.S for experimental outline).

Phase contrast microscopy

Images were obtained on either a Nikon Eclipse TS100 or a Nikon TMS inverted microscope using Nikon objectives. A Kodak DC290 camera was used to capture field images that were subsequently processed in Adobe Photoshop 6.0 (Adobe Systems, Inc.).

Contact angle analysis

Static water contact angles were measured with a contact angle goniometer (Krüss DSA 10). Reported contact angle measurements are the mean of 4 measurements on each of 3 samples for each experimental condition. The water drop profiles were fit using the tangent method drawn from the three-phase contact point along the drop/air phase boundary.

Protein harvest for Rho GTPase expression and activation assays from cells cultured on control and model biomaterials surfaces

Upon reaching a predetermined sub-confluent density (<90%) in culture, cells were rinsed once with Dulbecco's phosphate buffered saline (DPBS, HyClone) to remove residual media, and 0.75 ml of cell lysis buffer was applied. Protease inhibitors (1 μg/ml aprotinin, 1 μg/ml leupeptin and 1 mM (final) phenylmethylsulfonyl fluoride) were added to the lysis buffer [M-PER® (expression only; Pierce Biotechnology, Inc) or 25 mM Tris-HCl with 150 mM NaCl, 5 mM $MgCl_2$, 1% NP-40, 5% glycerol and 1 mM dithiothreitol (DTT) (combined expression/activation assays)] immediately before use. Cell lysates were removed with the aid of a rubber policeman and lysates were pipetted into sterile microcentrifuge tubes on ice. Samples were vortexed briefly and kept cold (4°C) throughout the harvesting and activation assay procedures. Rho GTPase expression samples were clarified at 16,000 x g, 4°C for 15 minutes and stored at -20°C.

Active (GTP-bound) Rho proteins were pulled down using commercially available affinity columns (Pierce EZ-Detect™ Activation Kits) with specificity for Rac1, Cdc 42 and Rho. The Rho pulldown is not specific for RhoA exclusively, but is known to detect

three common (A, B and C) isoforms, which are highly homologous. Appropriate positive and negative control treatments (GTPγS or GDP) were carried out (per manufacturer's instructions) to ensure that the affinity capture procedures functioned properly. To avoid GTP hydrolysis, cell lysates were immediately loaded onto affinity columns preincubated with the appropriate binding protein for the target of interest: 20μg of GST-Pak1-PBD (Cdc42 capture), or GST-human Pak1-PBD (Rac1 capture), or 400 μg of GST-Rhotekin-RBD (Rho capture). All binding and rinsing steps were carried out per manufacturer's instructions. Protein was eluted with 2x SDS Laemmli sample buffer with β-mercaptoethanol (β-ME, Sigma-Aldrich) and heat. Samples were centrifuged at 7200 x g for 2 minutes and stored at -20°C until analysis.

Total protein quantification

Total cellular protein was quantified per manufacturer's instructions using the Bio-Rad Protein microassay (Bio-Rad Laboratories, linear range of 0.05 to 0.5 mg/ml) and a microplate reader (Phenix Research Products).

Rho GTPase expression analysis by immunoblotting

Commercial preparations of whole cell lysates (WCL; Santa Cruz Biotechnology) were used as positive controls for expression of each protein of interest: HeLa WCL for Cdc42, RhoA and Rho GDI; KNRK WCL for Rac1; and K562 WCL for Cdc42 and Rac1. Equivalent amounts (25 μg) of total cell lysate from each expression sample and controls were analyzed via standard Western blot techniques. Equivalent loading of samples based on amount or volume was confirmed by SDS-PAGE (Figure 3.2.S), and

equivalent and optimized transfer conditions were confirmed by post-electrotransfer staining of nitrocellulose (NC) membranes (Bio-Rad Laboratories) and gels (data not shown).

Briefly, samples were electrophoresed on a 12% SDS-polyacrylamide gel and electrotransferred to a 0.2 μm NC membrane (Bio-Rad Laboratories). Membranes were blocked with 3% BSA (Sigma-Aldrich) in Tris-buffered saline (TBS, Bio-Rad Laboratories) and washed with 0.05% TBST (Tween®-20 (Sigma-Aldrich) in TBS). Blotting conditions were optimized for each protein separately. Primary antibody solutions (all rabbit polyclonal, Santa Cruz Biotechnology) at concentrations ranging from 1:100-1:1000 were applied to membranes (individually) for RhoA (clone 119, goat polyclonal), Rac1 (clone C-14), Cdc42 (clone P1) or Rho GDI (cloneA-20). Optimum detection was achieved using a 1:100 dilution for RhoA and a 1:500 dilution for Rac 1 and Cdc42. Horse radish peroxidase (HRP)-conjugated secondary antibodies (Santa Cruz Biotechnology, goat anti-rabbit IgG-HRP or mouse anti-goat IgG-HRP) were applied at concentrations of 1:500 (RhoA) or 1:5000 (Cdc42 and Rac1). Blots were developed using Supersignal® West Pico Chemiluminescent Substrate or SuperSignal® West Dura Extended Duration Substrate (Pierce Biotechnology) and membranes were quantified on either a BioChemi Imaging System using LabWorks software (UVP) or a ChemiDoc™ XRS System using Quantity One® software (Bio-Rad Laboratories).

Each blot contained one or more positive control lysate sample(s) (WCL, *vida supra*) known to contain the protein analyte of interest. All sample values obtained from

chemiluminescent imaging techniques were normalized to the positive control WCL value of the same blot to minimize effects attributed to variation between blots due to slight differences in electrophoretic conditions. Generally, blots were not stripped and re-probed with multiple antibodies. However, when protein supply was limited (e.g. IC-21) blots were stripped with Restore™ Western Blot Stripping Buffer (Pierce Biotechnologies) prior to re-probing.

Protein activation analysis by immunoblotting

As noted above, the Rho pull-down assay employed here is not specific for RhoA exclusively, but detects the common, highly homologous A, B and C isoforms. Subsequent RhoA specific probing of these samples was attempted with the same antibody used in expression analyses (Santa Cruz Biotechnology, clone 119) with only marginal success, likely due to the small amount of active protein isolated. Further, this RhoA antibody was compared to numerous commercially supplied RhoA antibodies (different species, different suppliers, etc), and was found to be, by far, the most effective RhoA antibody available for this assay. Due to these difficulties, the less-specific "Rho" antibody was used for activation assays. Thus, Rho activation results are reported as "Rho", in contrast to protein expression data reported as "RhoA".

Up to 50 µl of cell-derived activation lysate and 25 µg of WCL controls were analyzed via standard Western blot techniques as described (*vida supra*). Primary antibody solutions (Pierce Biotechnology) at concentrations of 1:100 (RhoA) or 1:250 (Rac1 and Cdc42) were applied to the membranes individually for Rho (mouse monoclonal IgG_1),

Rac1 (mouse monoclonal IgG_{2b}) and Cdc42 (mouse monoclonal IgG_1). Immunopure® Goat Anti-Mouse IgG (H + L) peroxidase-conjugated secondary antibody (Pierce Biotechnology) was applied at a concentration of 1:1000 and blots were developed and quantified as described above.

Statistical analysis

To determine statistically significant differences in protein expression, split plot analysis of variance was performed on data, where the whole plot effects were cell line and protein, and the split plot effect was surface chemistry. The whole plot error was trial by cell line and by protein. The split plot error was the surface by the whole plot error interaction. Error was represented as ± one standard error of the mean (SEM).

3.4 Results

Microscopic evaluation of each cell type in serum cultures, with attention to characteristic morphological features (filopodia, membrane ruffles) exhibited by cells on each control and model surface revealed distinct features based on cell type and surface. Culture surfaces represent a wide wettability range, as determined by static aqueous contact angle measurement: hydrophilic TCPS (54° ± 2),[25] moderately hydrophobic PS (92° ± 1)[25] and PLA (82° ± 1),[25,26] and very hydrophobic Teflon® AF (116° ± 2),[26] consistent with values previously reported. Cell adhesive and proliferative behavior was expected to vary on these different substrates related to surface chemistry effects on protein selection from complex biological milieu (serum). Morphological features exhibited by cells on each surface provided basic information about general cell

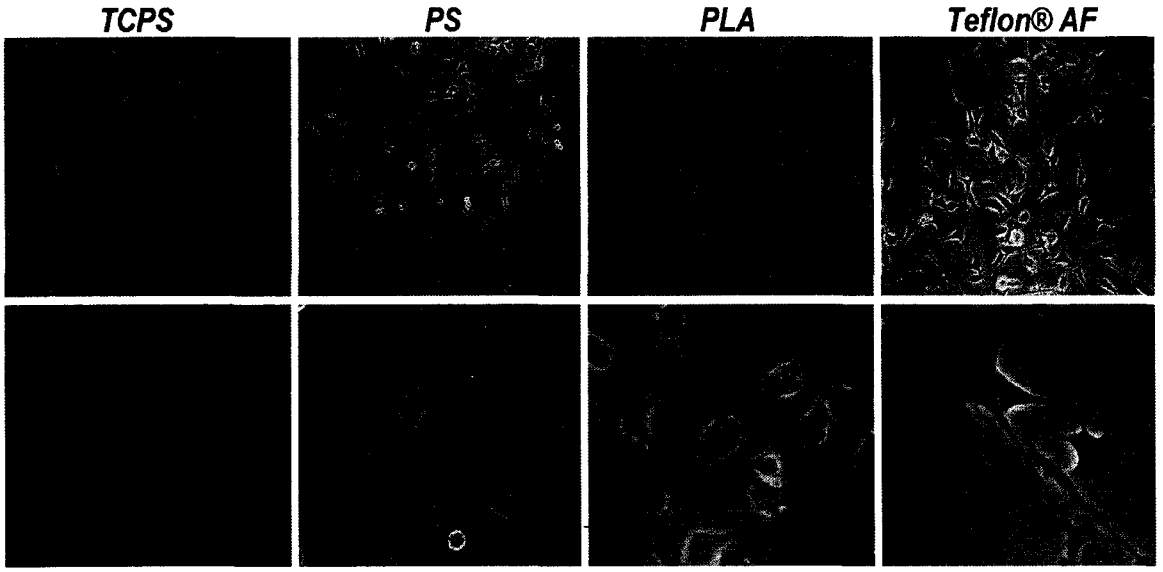

Figure 3.1 Phase contrast photomicrographs of various morphologies exhibited by populations of IC-21 MΦ cells on polymer surfaces at early (< 50% confluent) culture times. Cells exhibit primarily astral morphology with some filopodial extensions (E, bold arrow) at sub-confluent culture conditions on TCPS (A, E). However, as these cultures progress to 100% confluence cells adopt a typical "cobblestone-like" pattern of cell growth with fewer extensions (data not shown). On PS (B, F) cells exhibit membrane ruffling (F, arrows) and filopodia, similar to (but to a lesser extent than) behavior observed on Teflon® AF. Morphology is more compact on PLA surfaces (C, G), in contrast to the lengthy filopodia and large areas of membrane ruffling (D and H, arrows) observed on Teflon® AF. Results are representative of numerous (>3) fields and (>3) trials.

responsiveness to surfaces, including establishment of focal adhesions required for surface colonization, a requisite step in inflammatory response induction at implant sites. Further, cell morphology has been associated with expression and/or activation of specific Rho GTPases.[27]

Phase contrast microscopy observation of MC-MΦ cells revealed populations exhibiting different morphologies based on surface chemistry (Figures 3.1, 3.2, 3.3.S and 3.4.S). Hydrophilic TCPS promoted attachment, growth and proliferation for all cells tested, and cells exhibited adherent (punctate, astral) morphology indicative of numerous cell-adhesive sites (Figure 3.1 A and E; Figure 3.3.S, A; Figure 3.4.S, A and C). At early time points cells exhibited motile phenotypes on all surfaces, as indicated by the presence of

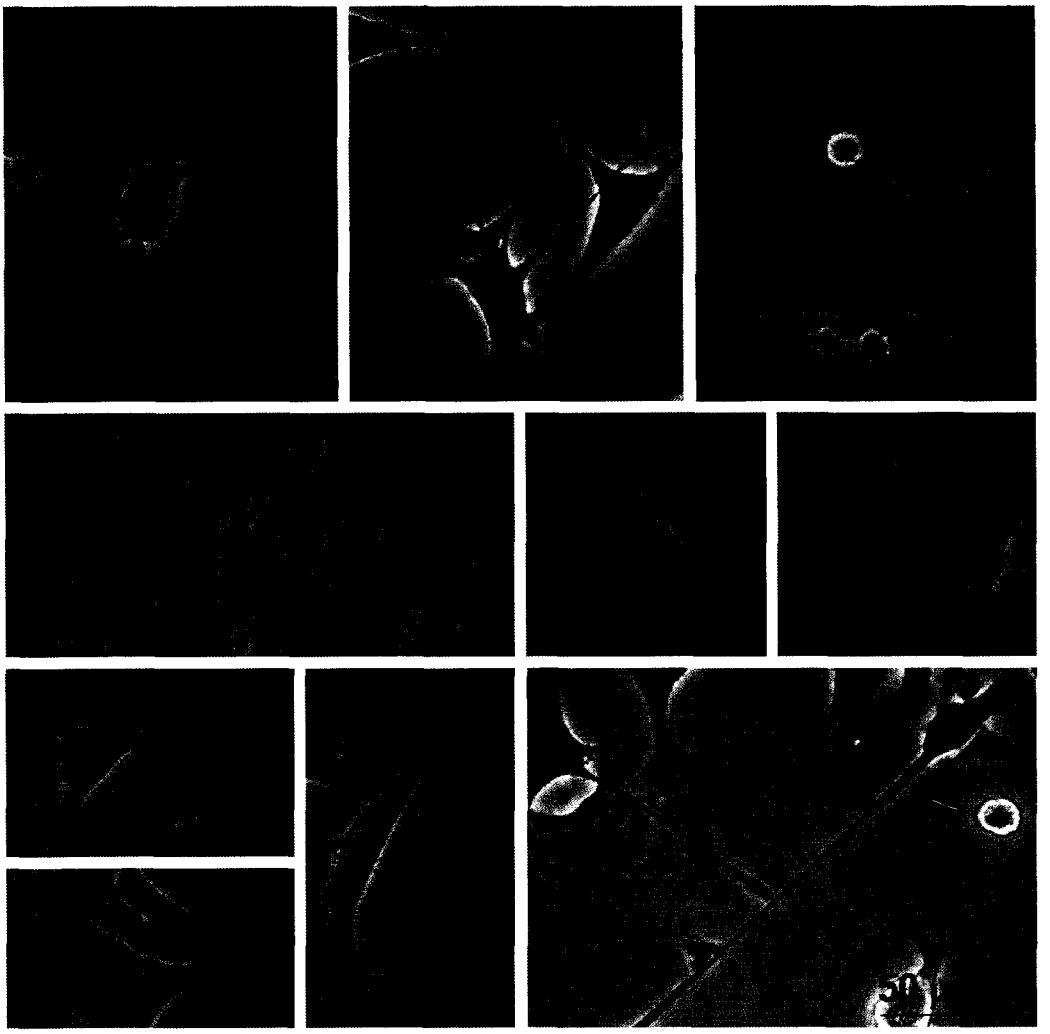

Figure 3.2 Phase contrast photomicrographs of IC-21 MΦ cell morphologies on Teflon® AF surfaces. A) Cells commonly exhibit loosely adherent cell bodies (circle) with numerous filopodia, sometimes in a circular arrangement. B) Distinct from cultures on all other surface chemistries, filopodial extensions are often observed to cross one another (bold arrows), or to terminate in proximity to attachment sites of other cells. C) Cell populations on Teflon® AF surfaces show a mixture of actin-based cytoskeletal features (filopodia, lamellipodia, membrane ruffling), often with numerous features on a single cell, as illustrated by all 3 cells in this field. Note differences in cell size, shape and features. D) Filopodia are frequently lengthy, extending hundreds of microns from the cell body [bold arrows indicate cell body (right) and filopodium terminus (left)]. E-F) Cells showing characteristic membrane ruffling, indicative of the "lagging edge" of a motile cell. G-H) Less typical morphologies observed on Teflon® AF include cells with numerous bulbous attachment sites (G) and tree-trunk-like morphologies (H). I) This field illustrates the diversity of the cell population observed: cell "1" has multiple lengthy filopodia that cross over cell "2", and that are diffuse rather than punctate at their termini, possibly indicative of active surface probing. Cell "2" has a diffuse cytoplasm, with large areas if membrane ruffling. Cell "3" has a small well-defined cell body with one lengthy filopodium. J) Occasionally, cells with multiple nuclei (3-5) have been observed on Teflon® AF without the addition of exogenous cytokines that promote fusion events. Results are representative of numerous (>3) experiments.

filopodia and membrane ruffling (Figure 3.1, E-H). However, as cultures progressed to

nearly confluent conditions cells adopted a tightly packed "cobblestone-like" growth pattern allowing maximal use of surface area (data not shown). Morphology on PLA surfaces (Figure 3.1, C and G) was highly similar to TCPS. Typically, cells grown on PS (Figure 3.1, B and F; Figure 3.3.S, B and F), and Teflon® AF (Figure 3.1, D and H; Figure 3.3.S, D and H; Figure 3.4.S, B and D) exhibited lengthy filopodia and large areas of membrane ruffling; these effects were always more pronounced on Teflon® AF surfaces.

Pronounced morphological variation was observed for the most MΦ-like cell line tested, IC-21, on Teflon® AF (Figure 3.2) At early time points (24 hours), cells with loosely adherent cell bodies and multiple attachment sites at the termini of lengthy filopodia were frequently observed. Filopodia often extended radially from the cell body (Figure 3.2 A-C). Alternatively, filopodia extended in a direction opposite that of an area of membrane ruffling (Figure 3.2 D and I, cell #1). Collectively, the arrangement of filopodia suggests that cells first send out filopodia to sample the surrounding surface in all directions, and subsequently respond to environmental cues by moving toward a "desirable" region [indicated by the development of a cellular "leading edge"(designated by the presence of filopodia) and a "lagging edge" (designated by the presence of membrane ruffling)]. Characteristic membrane ruffling is shown in Figure 3.2 E and F, and less typical morphological variants and multinucleation are shown in panels G, H and J, respectively. Regardless of cell lineage or derivation, the (MC-) MΦ cells grown on Teflon® AF exhibited a mixture of phenotypic features such as membrane ruffles and filopodia within the same culture and in proximity to one another (Figure 3.2 D and I). Significantly, cell

behavior on Teflon® AF was different from predicted cell growth patterns. For example, IC-21 cells grown on Teflon® AF sent out unusually lengthy (hundreds of microns) filopodia (Figure 3.2 D, arrows), indicating a lack of appropriate adhesive contact sites on these highly hydrophobic surfaces in serum. Equally unusual, filopodia were repeatedly seen crossing over one another (Figure 3.2 B, C, D; Figure 3.3.S, H) or over other cell bodies (Figure 3.2 I, cell #s 1 and 2). Figure 3.2 I shows cells moving in directions opposite one another, but nearly on top of one another (cell #s 1 and 2). In proximity to cell #s 1 and 2, cell # 3 exhibits a very different morphology, a compact cell body with a single filopodium. Importantly, these features are maintained as cell culture progresses to near 100% confluence on Teflon® AF, in contrast to all other surface chemistries where adherent cell shape is modified as progression toward confluence occurs, most notably observed in IC-21 cells and mature, differentiated BMMO. In general, these cell types responded to surfaces in a more pronounced and morphologically similar fashion than either of the MC-MΦ cell lines (J774A.1 and RAW 264.7).

To correlate observed morphological features (filopodia, membrane ruffling) and Rho GTPase signaling proteins in (MC-) MΦ cells grown on these surfaces, Rho protein 1) expression, and 2) activation assays were performed. Lysate samples from cells of increasing maturity (e.g., primary pro-monocytes, secondary (MC-) MΦ cell lines J774A.1 and RAW 264.7, secondary MΦ IC-21 and primary BMMO) were analyzed for expression of the regulatory factor Rho GDI, and Rho GTPase proteins, RhoA, Rac1 and Cdc42 (Figures 3.3, 3.5.S, 3.6.S and 3.7.S).

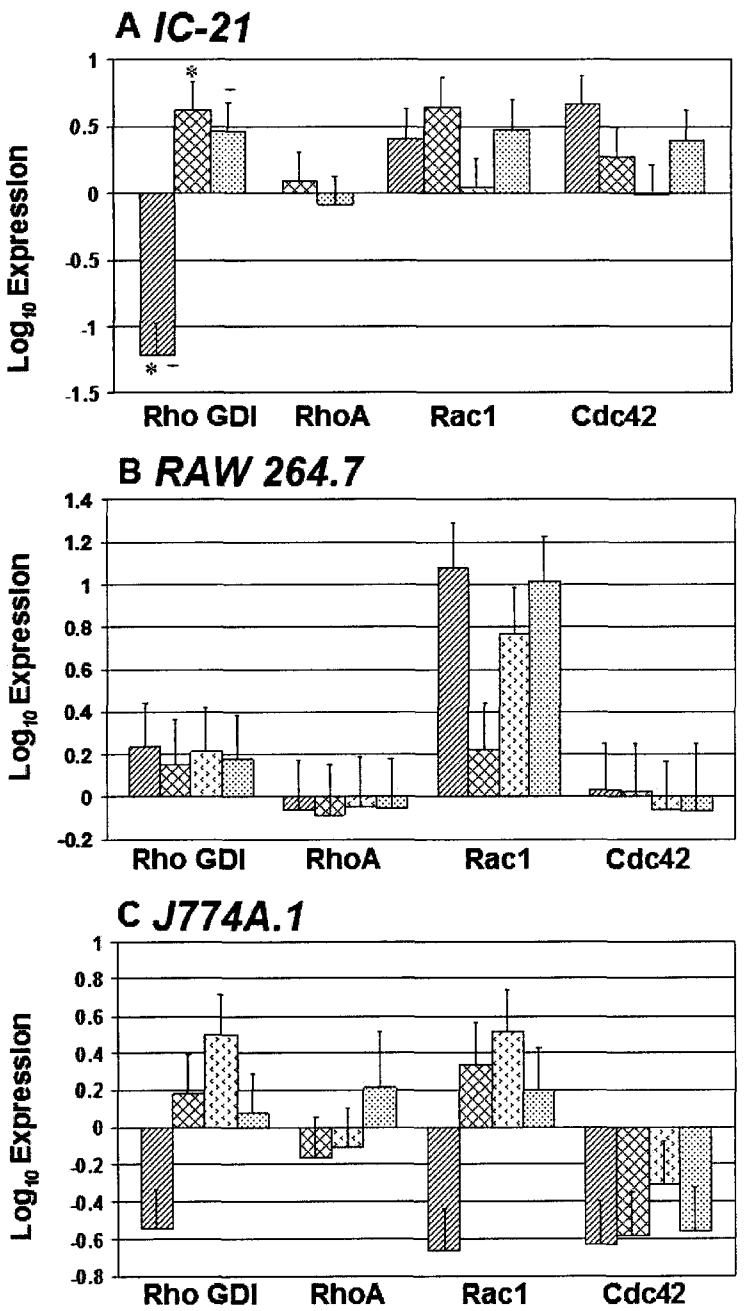

Figure 3.3 Rho GTPase expression comparison for (MC-) MΦ cell lines cultured on control (TCPS, PS) and model (PLA, Teflon® AF) surfaces. Protein expression was normalized to a whole cell lysate for the protein of interest. Error bars represent standard error of the mean, n= 3-8. Only two significant pairings ($p < 0.05$) were noted, and they are indicated by a * or a $^{+}$, respectively (panel A). Key:
TCPS, PS, PLA, Teflon® AF.

The least mature cell group tested, non-adherent pro-monocytic samples containing a mixed population of bone marrow-derived cells, had detectable levels of Rho GDI protein, but none of the probed Rho GTPases (data not shown). This was attributed to their immature (poorly-phagocytic) and non-adherent status, inducing less Rho GTPase production. Indeed, when this population was plated and allowed to mature for ten days to BMMO, cells expressed detectable levels of all Rho GTPase proteins

probed except Rac1 (data not shown). The adherent (MC-) MΦ cell lines, J774A.1, RAW 264.7 and IC-21, exhibited similar expression profiles; the majority of Rho GTPase proteins were expressed on most surfaces tested (Figure 3.3 A-C); RhoA was absent on TCPS from both the J774A.1 and IC-21 cell lines (Figure 3.3, A and C), and both RhoA and Rho GDI were non-detectable in IC-21 cells cultured on PLA (Figure 3.3 A). A comparison of each Rho protein expression profile within each cell type based on surface chemistry alone (control: TCPS, PS, versus model: PLA, Teflon® AF surfaces) revealed only two significant pairings, IC-21, Rho GDI on TCPS versus either PLA or Teflon® AF (Figure 3.3 A).

Table 3.1 Rho GTPase activation summary for (MC-) MΦ cell lines.

Protein & Culture Surface		Cell Line		
		RAW 264.7	**J774A.1**	**IC-21**
Rho[a,b]	TCPS	+	+	-
	PS	+	+	-
	PLA	+	+	-
	Teflon AF	+	+	-
Rac1[a]	TCPS	-	+	+
	PS	-	+	-
	PLA	-	+	-
	Teflon AF	-	+	-
Cdc42[a]	TCPS	+	-	+
	PS	+	-	-
	PLA	+	-	+
	Teflon AF	+	-	-

[a] + indicates the presence of the GTP-bound form of the protein(s), - indicates the absence of the GTP-bound form of the protein(s). [b]The Rho pulldown and probe is not specific for RhoA, but rather detects Rho isoforms A, B and C. See Materials and Methods for a detailed explanation.

Close examination of Rac1 expression (Figures 3.5.S and 3.6.S), which appeared to be most variable among the Rho GTPases tested, revealed that comparatively no statistically significant differences based on cell line or surface chemistry were observed. Comparison

of Rho GTPase expression profiles on the most different polymer surfaces (based on polarity, chemistry and cell morphological response), TCPS and Teflon® AF, revealed only one statistically significant pairing for Rho GDI expression (Figure 3.3 A). Similar results were obtained for a comparison of Rho GTPase expression profiles on TCPS and PLA surfaces (data not shown).

Activation assays performed under identical conditions (for all cells and all surfaces) indicate active (GTP-bound) Cdc42 and Rho proteins in RAW 264.7, Rac1 and Rho in J774A.1, and Cdc42 and Rac1 in IC-21 cell lines, respectively (Table 1 and Figure 3.7.S). No modulation of Rho or Cdc42 activation in RAW 264.7 cells as a function of culture surface was observed, as indicated by detectable amounts of active protein on each surface tested. A similar result was obtained for the J774A.1 cell line, except that the active proteins in this cell type are Rho and Rac1, rather than Rho and Cdc42. In the IC-21 cells no active Rho was detected on any culture surface, and active fractions of Rac1 and Cdc42 were only detected on TCPS (both proteins) and PLA (Cdc42 only).

3.5 Discussion

In this study, culture surfaces with various properties were selected as models to determine effects of surface chemistry on MΦ adhesion and subsequent changes in expression levels and/or activation states of select Rho GTPases. Chemistries selected included: TCPS, the current "gold standard" for adherent cell culture, PS, commonly employed for suspension culture, PLA an FDA-approved synthetic bioerodible polymer and Teflon® AF ("Amorphous Form"), (4,5-difluoro-2, 2-bis (trifluoromethyl)-1,3-

dioxole copolymerized with tetrafluoroethylene) the soluble analog of Teflon®, a highly hydrophobic fluoropolymer with a long history of use in biomaterials implants.[28,29] Our previous work characterized these surface chemistries using x-ray photoelectron spectroscopy and correlated surface characteristics to endothelial cell culture support. For this attachment dependent cell type, adhesion from serum and contact angle were proportional to surface oxygen content.[25]

Until a decade ago, the primary role of Rho GTPases was believed to be regulation of cytoskeletal organization in response to extracellular growth factors. Recent evidence indicates that these proteins are key mediators of many critical cellular events such as cell cycle progression and apoptosis, and are often implicated in disease.[1,3] Rho GTPases respond not only to growth factors,[6,20,30] but to many molecular signals often found at biomaterial implant sites: cytokines, antigens, hormone neurotransmitters, and extracellular matrix (ECM) cues.[5,15,22] Particularly important in the context of biomaterials, integrin interactions with ECM proteins have been shown to regulate RhoA, Rac1 and Cdc42,[30-35] and specific integrin β subunits are known to differentially activate specific Rho GTPases (β3, Rho and β1, Rac/Cdc) through outside-inside signaling.[36,37] Different cell lineages express distinctive groups of integrins that facilitate ECM protein mediated adhesion and other interactions.[38,39]

Given that surface chemistry dictates protein selection from complex biological milieu[40] (represented here by serum-containing cultures), and subsequent cell adhesion, growth, proliferation and spreading relies on the establishment of these protein mediated

interactions,[41] surface chemistry influences on Rho GTPase expression and activation in various (MC-) MΦ cells were studied. Interestingly, these cells have the unique ability to proliferate efficiently on fluorocarbon surfaces (Figures 3.1-3.2) that are non- or poorly supportive of most mammalian cell adhesion (e.g., endothelial cells, fibroblasts).[25,42] Furthermore, cell morphologies were markedly different on control versus Teflon® AF surfaces[15] suggesting that expression of specific Rho proteins related to the most commonly observed morphological features could be differentially regulated by the surface. Previous reports using Swiss 3T3 fibroblasts indicated that surface chemistry affected RhoA activation.[42]

As cell response to extracellular signals requires regulation of actin polymerization, largely orchestrated by Rho GTPases,[1-3] correlation of cytoskeletal regulation through adherent morphology to Rho GTPase activity should be possible. The actin cytoskeleton comprises filamentous actin organized into discrete structures: filopodia, lamellipodia and membrane ruffles, all features commonly observed in (MC-) MΦ grown on various culture surfaces.[15] Observations of these features is correlated to multiple factors: 1) cell maturity; mature MΦ (e.g., IC-21 cell line, Figure 3.1) exhibit more filopodia and membrane ruffles on control and model surfaces than less mature RAW 264.7 and J774A.1 cell lines on the same surfaces (data not shown); 2) surface area; greater areas available for cell spreading correlate to the presence of filopodia and a motile phenotype; 3) surface chemistry; cells cultured on very hydrophobic substrates have been observed to exhibit more filopodia per cell (up to 6) and extremely lengthy (400-500 μm) filopodial protrusions (Figure 3.1 D and H) even when surface area becomes limiting.

Despite differences in gross adherent cell morphologies on polymer surfaces (Figure 3.1), protein expression data was not statistically significantly different for expression of RhoA, Rac1, Cdc42 or Rho GDI on these surfaces (Figure 3.3). Although Rac1 expression appears to vary when compared to the other Rho proteins no statistically significant differences ($p<0.05$) based on either surface chemistry or cell line were observed. Both Cdc and Rac are necessary for cell spreading: disruption of expression of either protein has been shown to inhibit spreading.[5,35] Integrin activation of Cdc42 is linked to a mobile phenotype and increased cellular migration, while Rac is associated with membrane ruffles and lamellipodial formation important to cellular polarization,[1-3] and Rho is known to increase cell contractility and focal adhesions necessary to establish adherence.[6,43] Samples tested here for protein expression represent mixed populations of cells exhibiting all of these morphological features (e.g., Figure 3.2 D, I). Collectively, expression of each of these proteins was expected in the adherent MC-MΦ cells due to their observed proliferative and motile phenotypes on all materials tested at the time of protein collection.

Gross cell morphologies and size were different for cell cultures on TCPS and Teflon® AF (e.g., Figure 3.1, A and E versus D and H). However, a detailed comparison of expression values for Rho GTPases (Rho GDI, RhoA, Cdc42 and Rac1) on these surfaces revealed only one statistically significant difference: Rho GDI expression on TCPS compared to Teflon®AF (Figure 3.3 A). Possible explanations for lack of predicted modulation of Rho GTPases based on polymer surface chemistry can be attributed to

both cellular and molecular events. First, the adherent MΦ phenotype, regardless of source (primary or secondary derived cells) interacts with the surface (regardless of chemistry) to attach, grow, proliferate and spread upon it. All such behaviors require cytoskeletal rearrangement, orchestrated by Rho GTPases. Further, cultures on both control and model surfaces contained diverse cell populations, even at late culture time points where surface space was limited and cell spreading reduced. This heterogeneous cell population may lead to a net "averaging" of contributions from any single protein correlated to specific membrane features when pooled lysates are analyzed. Finally, the (MC-) MΦ is a dynamic cell type with the ability to mature and differentiate in many ways in response to various stimuli. Membrane trafficking and antigen presentation are crucial MΦ behaviors to which the Rho GTPases contribute. Thus, mature MΦ cells likely maintain Rho GTPase expression levels of sufficient quantity such that a population of these proteins is continuously present and poised for rapid activation in response to extracellular cues.

Rho GDI is known to be ubiquitously expressed in many cell types,[1,44] and is measurable even in pro-monocytic cells where RhoA, Rac1 and Cdc42 were undetectable (data not shown). Detection of Rho GDI expression in the absence of RhoA, Cdc42 and Rac1 expression may be attributed to the fact that Rho GDI complexes with numerous Rho proteins to stabilize them in their inactive form in the cytoplasm. Thus, significantly greater amounts of Rho GDI are likely to be present, placing it within detectable limits. Further, the immature and non-adherent status of these cells may contribute to low Rho GTPase expression levels.

Active (GTP-bound) forms of Rho, Rac1 and Cdc42 were detected J774A.1, RAW 264.7 and IC-21 cells as shown in Table 1, with active Rho detectable in both MC- MΦ cell lines. Rho activation by integrins is known to be biphasic.[5,31] Immediately upon cell binding to a surface, Rho is inhibited to allow cell attachment and spreading, and is subsequently reactivated to enhance the formation of focal adhesions.[31] This understanding is consistent with the observation of Rho expression and activation (where detected) in cells cultured on model biomaterial surfaces, since cells are collected at time points where focal adhesion formation is likely ongoing. Further, MC differentiation to a MΦ phenotype is accompanied by growth and cytoskeletal changes, to which the active Rho form may contribute. Active Rho was absent in the mature MΦ IC-21 cell line, consistent with the highly motile phenotype observed even at advanced culture time points.

Although the RAW 264.7 and J774A.1 cells share common Rho GTPase activation profiles, they diverge at Cdc42/Rac1 activation. Yet, active Rac and Cdc42 share a downstream effector, PAK,[30] that is implicated in both proliferative signaling and cytoskeletal regulation.[45] Therefore, the outcome of these apparently different activation profiles may be functionally equivalent in terms of cell attachment and spreading on biomaterials surfaces. Active Cdc42 fractions were detected in IC-21 on both TCPS and PLA surfaces, which may be related to surface chemistry given that these polymers exhibit more polar surface chemistries-TCPS initially,[25] and PLA as surface hydrolysis occurs over the time course of the experiment. Further, active Cdc42 was absent on the

apolar PS and Teflon® AF surfaces. This result correlates to similarities observed in gross cellular morphologies on TCPS (Figure 3.1 A, E) and PLA (Figure 3.1 C, G) versus the morphologies observed on the more apolar hydrophobic surfaces PS (Figure 3.1 B, D) and Teflon® AF (Figure 3.1 F, H). Active Rac and Cdc have been implicated in regulation of "strong versus weak" cell adhesion through binding to IQGAP, a Rho binding protein that plays a role in E cadherin-mediated cell-cell adhesion.[46] Active Rac1 detection in both J774A.1 and IC-21 cultures on TCPS could be related to the rapid and facile population of this surface with cells, with a concomitant increase in cell-cell adhesion as the population of cells approaches 100% confluence on this surface.

3.6 Conclusions

Despite gross morphological differences observed in (MC-) MΦ cell cultures on various polymer substrates, no statistically significant differences in expression levels of Rho GTPases RhoA, Cdc42 or Rac1 were detected as a function of either cell lineage (primary versus secondary-derived cell source), or surface chemistry. Pro-monocytic primary bone marrow-derived cells were found to contain ample Rho GDI protein, but expression of Rho GTPases RhoA, Rac1 and Cdc42 was not detectable, suggesting these proteins were below the detection threshold commonly achieved by more mature, adherent cell types. Rho GTPase expression profiles (based on cell maturity from the non-adherent pro-monocytic precursor cells to the adherent, mature (MC-) MΦ phenotypes) were implicitly different and likely affected by both cell adhesion and maturity states.

Activation of specific Rho GTPase proteins was detected on all polymer surfaces for the RAW 264.7 and J774A.1 cells, suggesting that while these proteins are important to cell behaviors on polymer surfaces, differences in surface chemistry are not sufficient to differentially modulate GTPase activation in these cell types. The IC-21 activation profile was markedly different from either of the less mature MC-MΦ cell lines. However, as it is the most mature, biologically relevant cell line examined, it may possibly be the most sensitive to differential activation by surface chemistry. Overall, specific non-equivalences of different MΦ sources in expression and activation patterns of Rho signaling proteins on different surfaces are shown. These differences should be carefully considered for *in vitro* experiments attempting to probe or recapitulate inflammatory events in cells on surfaces. This would be particularly important to *in vitro* cell-based assays (e.g., for inflammatory drug screening) where such casual MΦ surface contact might induce cell activation, phenotypic changes and assay artifacts in this cell type typically considered non-attachment dependent.

Accordingly, implant surfaces may be considered generally "activating" to MΦ cells; differences in downstream signaling may relate only to the specific integrin subunits and other receptors expressed by different cell types and utilized in interactions with key ECM proteins adsorbed on different surface chemistries. Further effects of growth factors and cytokines relevant to FBGC formation at biomaterial implant surfaces on Rho GTPase expression and activation have not been explored in this context. Since these factors play a crucial role in cytoskeletal rearrangement, an obligatory step in cell fusion to FBGCs, they should be worthwhile targets for future investigation.

3.7 Acknowledgements

The authors acknowledge Dr. J. Bamburg, Dr. S. Summers and Dr. A. García for helpful technical guidance, Dr. J. zumBrunnen for assistance with statistical analysis, and Dr. M. Gonzalez-Juarerro (CSU), for assistance with primary BMMO harvests. This work was supported by NIH grant EB 000894.

3.8 References

1. Van Aelst L, D'Souza-Schorey C. Rho GTPases and signaling networks. *Genes Dev* 1997;**11**:2295-322.

2. Mackay DJ, Hall A. Rho GTPases. *J Biol Chem* 1998;**273**:20685-8.

3. Karnoub AE, Symons M, Campbell SL, Der CJ. Molecular basis for Rho GTPase signaling specificity. *Breast Cancer Res Treat* 2004;**84**:61-71.

4. Dumontier M, Hocht P, Mintert U, Faix J. Rac1 GTPases control filopodia formation, cell motility, endocytosis, cytokinesis and development in Dictyostelium. *J Cell Sci* 2000;**113**:2253-65.

5. Berrier AL, Martinez R, Bokoch GM, LaFlamme SE. The integrin beta tail is required and sufficient to regulate adhesion signaling to Rac1. *J Cell Sci* 2002;**115**:4285-91.

6. Ridley AJ, Hall A. The small GTP-binding protein rho regulates the assembly of focal adhesions and actin stress fibers in response to growth factors. *Cell* 1992;**70**:389-99.

7. Ruoslahti E. RGD and other recognition sequences for integrins. *Annu Rev Cell Dev Biol* 1996;**12**:697-715.

8. Akiyama SK, Nagata K, Yamada KM. Cell surface receptors for extracellular matrix components. *Biochim Biophys Acta* 1990;**1031**:91-110.

9. Ridley AJ, Allen WE, Peppelenbosch M, Jones GE. Rho family proteins and cell migration. *Biochem Soc Symp* 1999;**65**:111-23.

10. Ridley AJ. Rho proteins, PI 3-kinases, and monocyte/macrophage motility. *FEBS Lett* 2001;**498**:168-71.

11. Leverrier Y, Ridley AJ. Requirement for Rho GTPases and PI 3-kinases during apoptotic cell phagocytosis by macrophages. *Curr Biol* 2001;**11**:195-9.

12. Patel JC, Hall A, Caron E. Rho GTPases and macrophage phagocytosis. *Meth Enzymol* 2000;**325**:462-73.

13. Anderson JM. Mechanisms of inflammation and infection with implanted devices. *Cardiovasc Pathol* 1993;**2**:33S-41S.

14. McNally AK, Anderson JM. Beta1 and beta2 integrins mediate adhesion during macrophage fusion and multinucleated foreign body giant cell formation. *Am J Pathol* 2002;**160**:621-30.

15. Godek ML, Duchsherer NL, McElwee Q, Grainger DW. Morphology and growth of murine cell lines on model biomaterials. *Biomed Sci Instrum* 2004;**40**:7-12.

16. Tang L, Eaton JW. Natural responses to unnatural materials: a molecular mechanism for foreign body reactions. *Mol Med* 1999;**5**:351-8.

17. Kyriakides TR, Foster MJ, Keeney GE, Tsai A, Giachelli CM, Clark-Lewis I, Rollins BJ, Bornstein P. The CC chemokine ligand, CCL2/MCP1, participates in macrophage fusion and foreign body giant cell formation. *Am J Pathol* 2004;**165**:2157-66.

18. Wittmann T, Waterman-Storer CM. Cell motility: can Rho GTPases and microtubules point the way? *J Cell Sci* 2001;**114**:3795-803.

19. Lee DJ, Cox D, Li J, Greenberg S. Rac1 and Cdc42 are required for phagocytosis, but not NF-kappaB-dependent gene expression, in macrophages challenged with Pseudomonas aeruginosa. *J Biol Chem* 2000;**275**:141-6.

20. Nobes CD, Hall A. Rho, rac, and cdc42 GTPases regulate the assembly of multimolecular focal complexes associated with actin stress fibers, lamellipodia, and filopodia. *Cell* 1995;**81**:53-62.

21. Caron E, Hall A. Identification of two distinct mechanisms of phagocytosis controlled by different Rho GTPases. *Science* 1998;**282**:1717-21.

22. Giannone G, Dubin-Thaler BJ, Dobereiner HG, Kieffer N, Bresnick AR, Sheetz MP. Periodic lamellipodial contractions correlate with rearward actin waves. *Cell* 2004;**116**:431-43.

23. Rhoades ER, Orme IM. Similar responses by macrophages from young and old mice infected with Mycobacterium tuberculosis. *Mech Ageing Dev* 1998;**106**:145-53.

24. Malkov G, Martin IT, Schwisow WB, Chandler JP, Fisher ER. Pulsed plasma-induced micropatterning with alternating hydrophilic and hydrophobic surface chemistries. *Chem Mater* 2006, submitted.

25. Koenig AL, Gambillara V, Grainger DW. Correlating fibronectin adsorption with endothelial cell adhesion and signaling on polymer substrates. *J Biomed Mater Res A* 2003;**64**:20-37.

26. Guruvenket S, Komath M, Vijayalakshmi SP, Raichur AM, Rao GM. Wettabilility enhamcement of polystyrene with electron cyclotron resonance plasma with argon. *J Appl Polym Sci* 2003;**90**:1618-23.

27. Ridley AJ, Hall A. Distinct patterns of actin organization regulated by the small GTP-binding proteins Rac and Rho. *Cold Spring Harb Symp Quant Biol* 1992;**57**:661-71.

28. Kossovsky N, Millett D, Juma S, Little N, Briggs PC, Raz S, Berg E. In vivo characterization of the inflammatory properties of poly(tetrafluoroethylene) particulates. *J Biomed Mater Res* 1991;**25**:1287-301.

29. Desai NP, Hubbell JA. Tissue response to intraperitoneal implants of polyethylene oxide-modified polyethylene terephthalate. *Biomaterials* 1992;**13**:505-10.

30. del Pozo MA, Price LS, Alderson NB, Ren XD, Schwartz MA. Adhesion to the extracellular matrix regulates the coupling of the small GTPase Rac to its effector PAK. *Embo J* 2000;**19**:2008-14.

31. Ren XD, Kiosses WB, Schwartz MA. Regulation of the small GTP-binding protein Rho by cell adhesion and the cytoskeleton. *Embo J* 1999;**18**:578-85.

32. Arthur WT, Petch LA, Burridge K. Integrin engagement suppresses RhoA activity via a c-Src-dependent mechanism. *Curr Biol* 2000;**10**:719-22.

33. Danen EH, Sonneveld P, Sonnenberg A, Yamada KM. Dual stimulation of Ras/mitogen-activated protein kinase and RhoA by cell adhesion to fibronectin supports growth factor-stimulated cell cycle progression. *J Cell Biol* 2000;**151**:1413-22.

34. Etienne-Manneville S, Hall A. Integrin-mediated activation of Cdc42 controls cell polarity in migrating astrocytes through PKCzeta. *Cell* 2001;**106**:489-98.

35. Price LS, Leng J, Schwartz MA, Bokoch GM. Activation of Rac and Cdc42 by integrins mediates cell spreading. *Mol Biol Cell* 1998;**9**:1863-71.

36. Miao H, Li S, Hu YL, Yuan S, Zhao Y, Chen BP, Puzon-McLaughlin W, Tarui T, Shyy JY, Takada Y, Usami S, Chien S. Differential regulation of Rho GTPases by beta1 and beta3 integrins: the role of an extracellular domain of integrin in intracellular signaling. *J Cell Sci* 2002;**115**:2199-206.

37. Salsmann A, Schaffner-Reckinger E, Kieffer N. RGD, the Rho'd to cell spreading. *Eur J Cell Biol* 2006;**85**:249-54.

38. Hynes RO. Integrins: bidirectional, allosteric signaling machines. *Cell* 2002;**110**:673-87.

39. Larson RS, Springer TA. Structure and function of leukocyte integrins. *Immunol Rev* 1990;**114**:181-217.

40. Andrade JD, Hlady V. Plasma protein adsorption: the big twelve. *Ann N Y Acad Sci* 1987;**516**:158-72.

41. Horbett TA. The role of adsorbed proteins in animal cell adhesion. *Surf Coll B* 1994;**2**:225-40.

42. McClary KB, Grainger DW. RhoA-induced changes in fibroblasts cultured on organic monolayers. *Biomaterials* 1999;**20**:2435-46.

43. Hotchin NA, Hall A. The assembly of integrin adhesion complexes requires both extracellular matrix and intracellular rho/rac GTPases. *J Cell Biol* 1995;**131**:1857-65.

44. Zalcman G, Closson V, Camonis J, Honore N, Rousseau-Merck MF, Tavitian A, Olofsson B. RhoGDI-3 is a new GDP dissociation inhibitor (GDI). Identification of a non-cytosolic GDI protein interacting with the small GTP-binding proteins RhoB and RhoG. *J Biol Chem* 1996;**271**:30366-74.

45. Puto LA, Pestonjamasp K, King CC, Bokoch GM. p21-activated kinase 1 (PAK1) interacts with the Grb2 adapter protein to couple to growth factor signaling. *J Biol Chem* 2003;**278**:9388-93.

46. Kaibuchi K, Kuroda S, Fukata M, Nakagawa M. Regulation of cadherin-mediated cell-cell adhesion by the Rho family GTPases. *Curr Opin Cell Biol* 1999;**11**:591-6.

3.9 Supplemental Figures

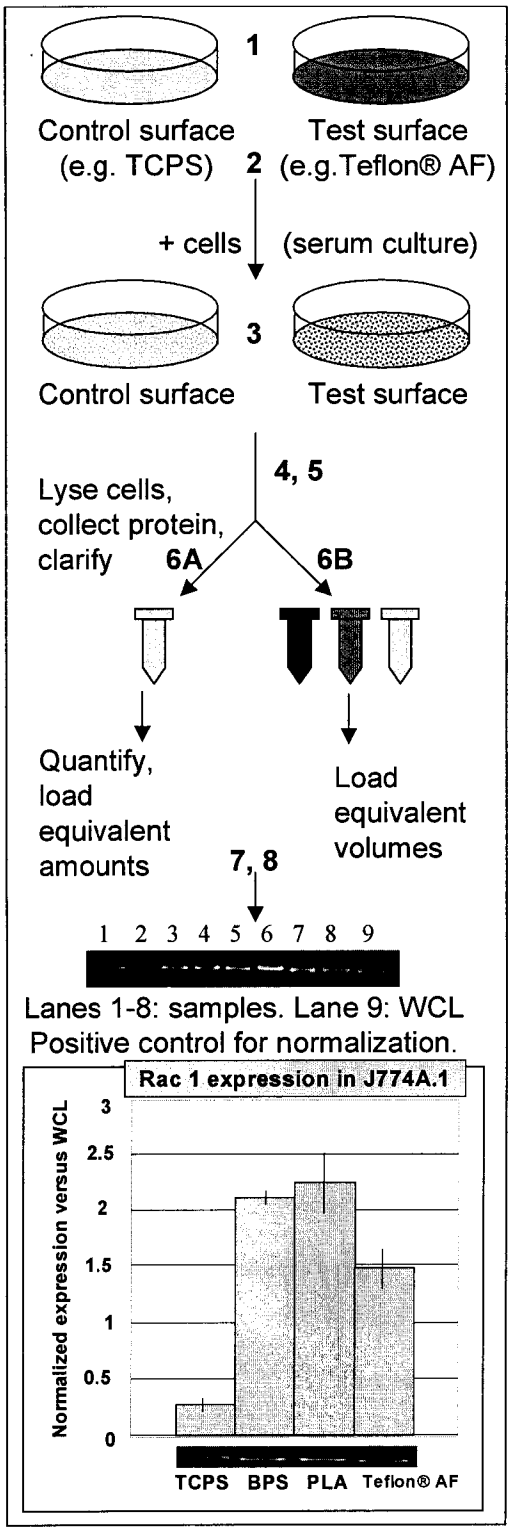

1) *Replicates of each surface type are pre-conditioned with 10% serum-containing media.*

2) *Seed cells in appropriate media containing 10% serum.*

3) *Examine surfaces for differential growth.*

4) *Lyse sub-confluent cells and extract proteins (on ice).*

5) *Clarify samples. Then, A) freeze proteins until expression analysis, or B) load immediately onto Pierce EZ Detect™ Activation Kit columns to select the active (GTP) form of the protein of interest i) Rho, ii) Rac1 or iii) Cd42. Store denatured products at -20° until analysis.*

6) *A) Quantify total protein using Bio-Rad protein assay. Adjust volumes to 25 µg total protein per well, or B) load equivalent volumes of the selected protein product from step 6B onto SDS-PAGE for Western blot analysis.*

7) *Analyze multiple samples (≥ 4) from multiple (≥ 2) experimental trials for each cell type and surface tested via standard Western blot techniques. Positive control whole cell lysate included as + control for expression & as an internal standard for band normalization.*

8) *Quantify sample and control bands (chemiluminescent detection). Normalize sample intensities to control intensities for each gel.*

9) *Statistical and graphical analysis.*

Figure 3.1.S Schematic of experimental procedures.

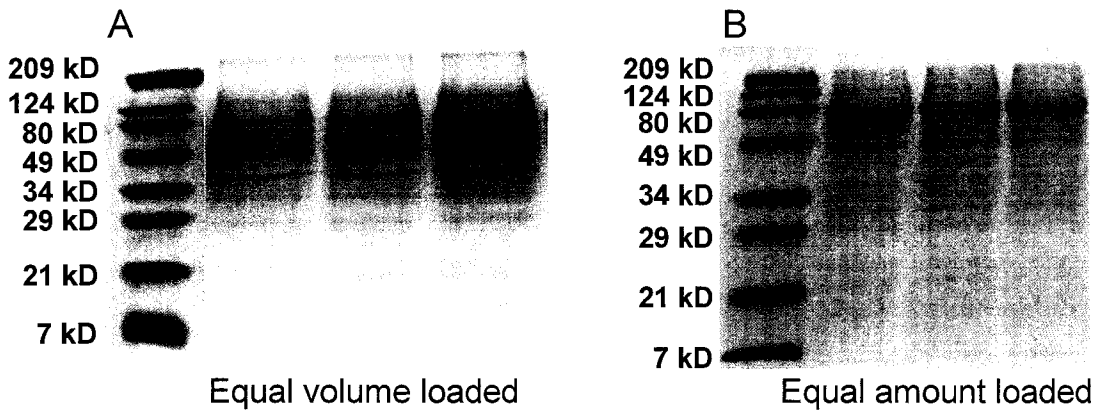

Figure 3.2.S Representative SDS-PAGE results of samples loaded as (A) equal volumes of cell lysate or as (B) equal amounts of protein as quantified using the Bio-Rad protein assay. A) Lane 1, MWM (Bio-Rad), lanes 2-4, BMMO cells grown on TCPS, 30 µl volumes. B) Lane 1 MWM (Bio-Rad), lanes 2-4, IC-21 murine macrophage cells grown on 0.1% PLA, 25 µg of each sample. 12% SDS-PAGE stained with Coomassie blue.

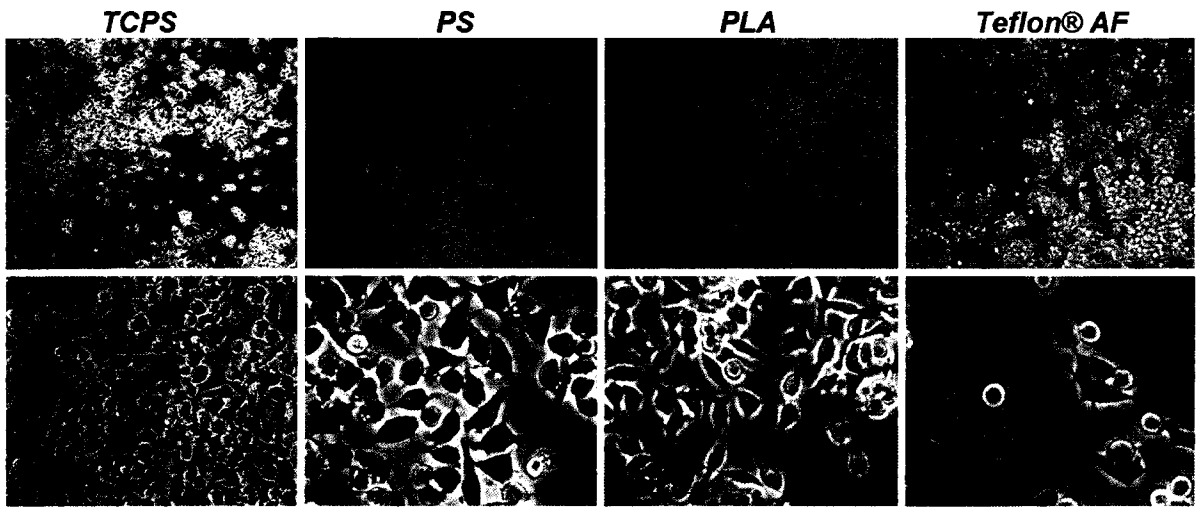

Figure 3.3.S Phase contrast photomicrographs of morphologies exhibited by RAW 264.7 MC-MΦ on polymer surfaces as indicated at sub-confluent culture times. Cells exhibited adherent morphology (astral shapes) with short filopodia on TCPS (A, E), PS (B.F), and PLA (C, G). More non-adherent cells and cells with lengthy filopodia were observed on Teflon® AF substrates (H, arrows). Results are representative of numerous (>3) fields and trails.

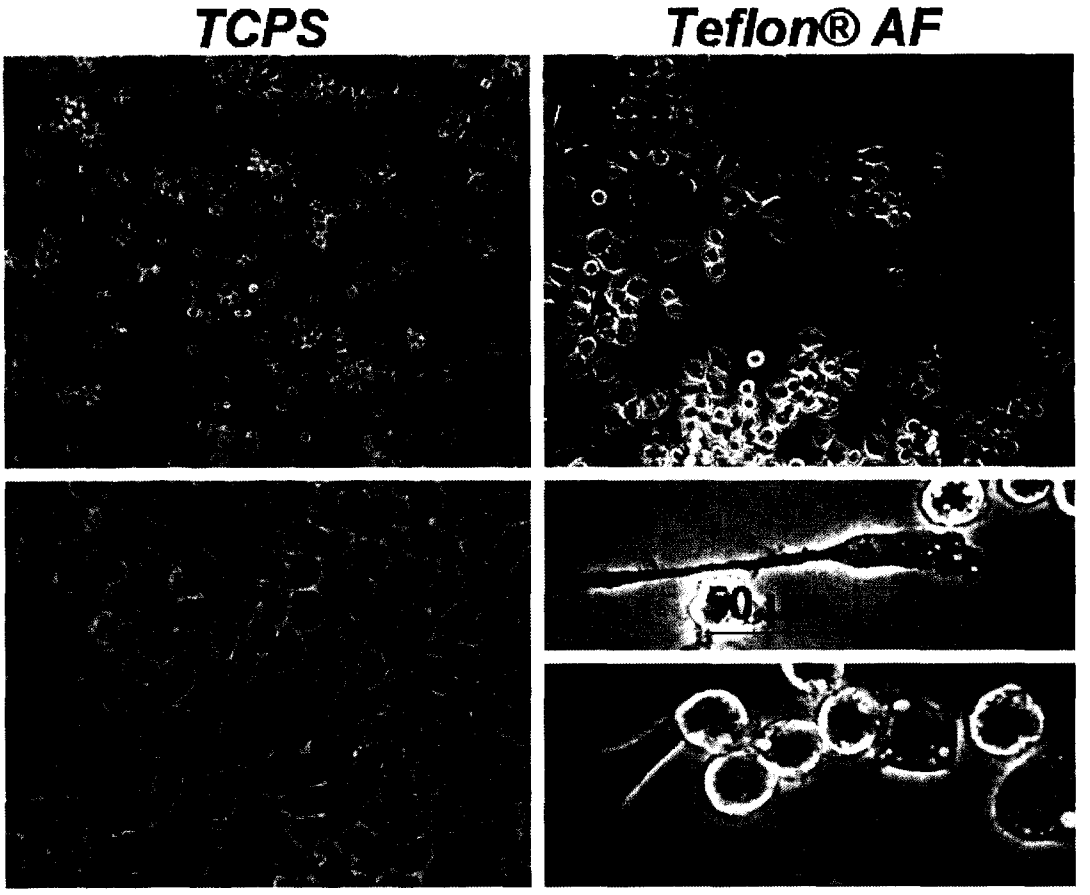

Figure 3.4.S Phase contrast photomicrographs of morphologies exhibited by J774A.1 monocyte-macrophages on select polymer surfaces at sub-confluent culture times. Cells exhibit adherent (spherical and astral shaped) morphologies with short filopodial extensions on TCPS (A, C). Cell morphology is more elongated, with lengthy filopodia (B, D, arrows) and large regions of membrane ruffling (D, E, grouped arrows) on Teflon® AF substrates. Results are representative of numerous (>3) fields and (>3) trials.

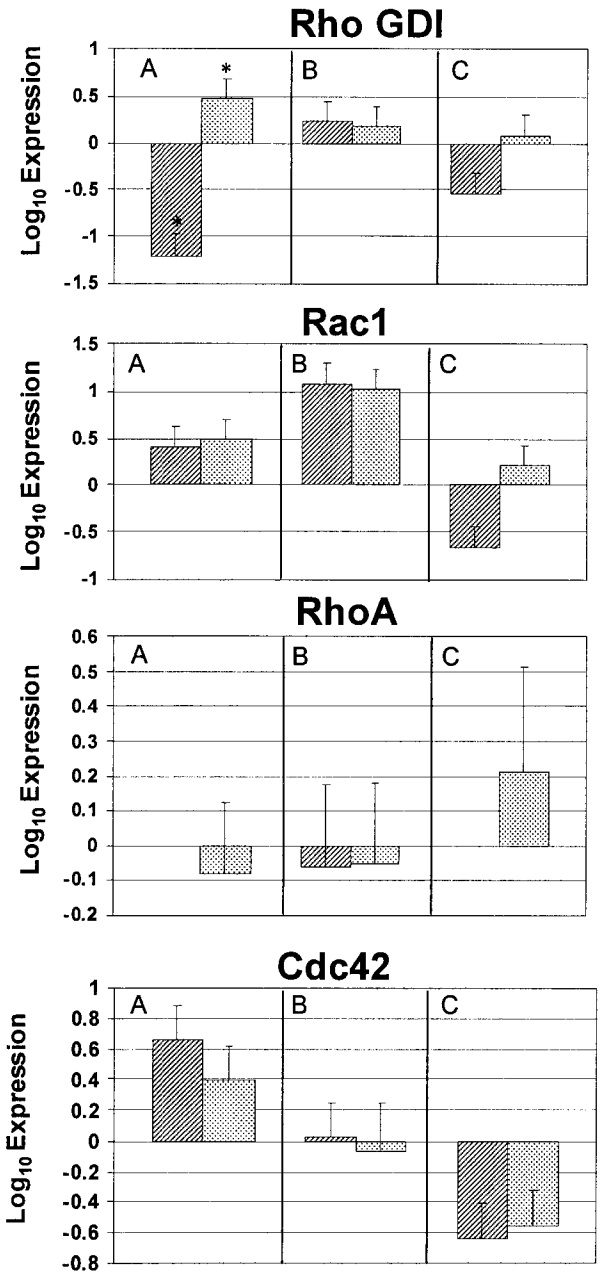

Figure 3.5.S Rho GTPase expression comparison for IC-21 (A), RAW 264.7 (B) and J774A.1 (C) on control TCPS and model Teflon® AF surfaces. Error bars represent standard error of the mean, n= 3-8. Hatched bars: TCPS (left), dotted bars Teflon® AF (right). The only significant pairing ($p < 0.05$) is noted, indicated by a * (top panel, A).

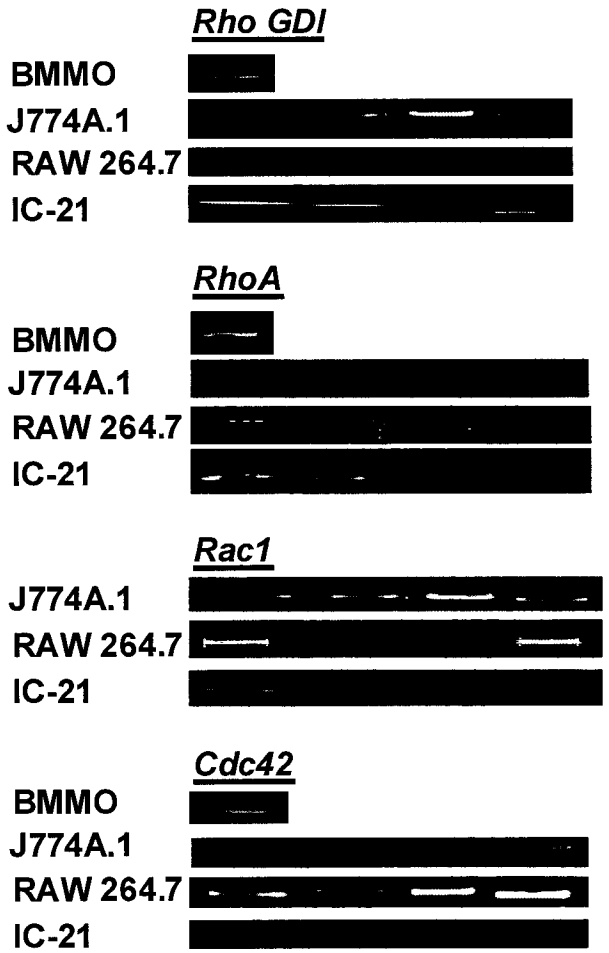

Figure 3.6.S Representative Western blot expression data for all proteins tested. Some RAW 267.4 data was highly pixilated due to imaging limitations. All bands were normalized to an appropriate internal standard (WCL) on each gel corresponding to the protein(s) of interest, standards not shown. Molecular weights of proteins detected: Rho GDI 30 kD, RhoA 24 kD, Rac1 25 kD, Cdc42 25 kD.

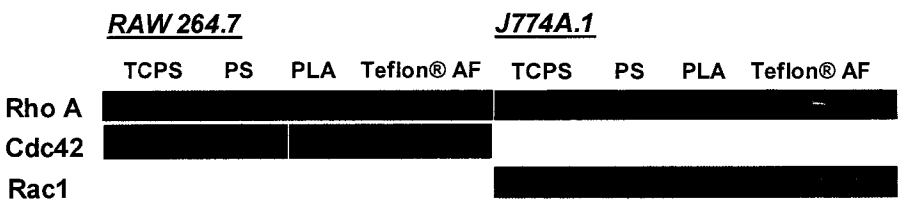

Figure 3.7.S Representative Western blot activation data for positive samples in the RAW 264.7 and J774A.1 cell lines. Molecular weights of proteins detected: RhoA 24 kD, Rac1 25 kD, Cdc42 25 kD.

CHAPTER 4: ADHESION OF MACROPHAGES TO ALBUMIN-COATED SURFACES *IN VITRO* IS DISTINCT FROM OTHER CELL TYPES

This chapter was written by Marisha L. Godek, edited by David W. Grainger and contains contributions from Roger Michel, Lisa Chamberlain and David Castner. It is a manuscript in preparation for submission to the *Journal of Biomedical Materials Research.*

4.1 Abstract

In vivo, the ubiquitous FBR, a complex inflammatory reaction orchestrated by the MΦ, continues to plague biomedical implants of diverse chemical composition, design and physiological placement. MC-MΦ adhesion to biomaterial surfaces, an obligate step in the development of the FBR, is typically achieved through adhesive protein-integrin mediated interactions. Highly hydrophobic albumin-selective fluorocarbon chemistries often employed in biomedical devices are generally considered poorly cell-inductive due to a lack of appropriate adhesive recognition sites for receptor-mediated cellular interaction. Yet, *in vitro* reports indicate MΦ-derived cells can bind to albumin-coated substrates and bind *preferentially* to highly hydrophobic surfaces.

This investigation was undertaken to compare and contrast the behavior of primary (BMMO) and secondary-derived immortalized (IC-21) murine MΦ cells grown on model FC biomaterial surfaces. First, protein deposition onto two chemically distinct FC surfaces (plasma-polymerized (pp-FC) and commercial cast Teflon® AF coatings) from complex and single-component solutions was tracked using fluorescence (labeled albumin and fibronectin), and time-of-flight secondary ion mass spectrometry (ToF-SIMS) methods. Second, cellular adhesion, growth and proliferation were tracked using light microscopy. Finally, the mechanism of cellular adhesion to these FC surfaces was explored using flow cytometry and integrin-directed monoclonal antibody (mAb) blocking for select cell membrane receptors deemed critical for establishing MC and MΦ adhesion *in vitro*.

Albumin was shown to be the predominant protein adsorbed onto pp-FC and Teflon® AF surfaces, even from complex biological milieu (10% serum). In cultures on both FC surfaces pre-adsorbed with albumin only, or serum-dilutions, BMMO cells responded similar to the murine cell line IC-21 at early time points in culture, and grew well for extensive periods of time (to 36 days) on Teflon® AF surfaces. The pp-FC surfaces were less permissive to extended cell growth and proliferation, suggesting that differences in FC surface chemistry may affect long-term cell viability *in vitro*. Integrin blocking results indicate that β_2 integrins, a component of the Mac-1 MΦ receptor, play a major role in MΦ adhesion to these surfaces given that blocking significantly disrupted this cellular behavior.

4.2 Introduction

MΦ cells are key mediators of host inflammatory responses to surgically placed biomedical devices, implicated in an abnormal wound healing response commonly observed around implanted materials known as the FBR.[1-3] MΦ cells represent a highly adaptable, dynamic cell population that respond to activating cues of both chemical and physical nature present in their local environment. FBGC, the fusion product of MC and MΦ and one cellular hallmark of the FBR to implantable materials,[4] are frequently found at surfaces of biomaterial implants. and material surface chemistries have been shown to influence fusion.[5,6] Modulating the events that facilitate progression of the FBR at implant sites is of substantial interest toward improved biomedical device performance and host integration. To date, little *in vivo* control over this complex reaction to implanted materials has been demonstrated.

In vivo, biomaterials surfaces are instantly and continuously bombarded with thousands of different host proteins,[7-11] and surface chemistry is well-known to exert an influence on adsorbed protein layer composition, exchange dynamics and structural conformations.[12-14] Subsequent cell adhesion is influenced indirectly by surface chemistry, and by the surface adsorbed protein layer.[5,15,16] Albumin is the predominant plasma protein[7,8] and albumin's interaction with surfaces has been studied extensively[17-22] due to albumin's propensity to reduce platelet reactivity to and thrombogenicity of certain implant materials, such as polyurethanes.[23] Albumin's presence at implants has been reported to decrease bacterial adhesion and device-centered infections[23] and reduced platelet adhesion has been reported by numerous

groups.[24-26] "Fatty acid-like" alkyl-grafting surface modifications have been employed to exploit albumin's natural affinity for free fatty acids and produce albumin-binding device surfaces.[27-29] However, these surfaces have not been entirely successful in terms of improved thromboresistance associated with 100% albumin-selection[23], possibly due to the highly hydrophobic nature of the material, resulting in a denatured protein adsorbate at the surface.[8] *In vitro*, denatured proteins have been correlated to increased MC (circulating immature MΦ) adhesion,[30] the first step in a sequence of events that may ultimately result in development of a FBR *in vivo*.

Albumin adsorption to and desorption from surfaces has been studied extensively *in vitro.* [17,18,23,31-37] Some studies indicate that albumin preadsorption on hydrophobic surfaces (i.e., surfaces of aqueous contact angle ≥ 100°) dramatically reduces amounts of bound IgG and fibrinogen from mixed component solutions, and this phenomenon is attributed to the irreversible adsorption of albumin, accompanied by adsorbed-state globular protein conformational changes[32,35,36] that occur readily at most surfaces.[10] Further, on perfluorinated (i.e., plasma-deposited and PTFE) surfaces, albumin has been shown to bind strongly and selectively,[36] out-competing the cell-adhesive ECM protein, fibronectin, in adsorption from binary solutions and serum dilutions, even when fibronectin bulk concentration is biased 10-100 fold higher than found physiologically.[38] Albumin apparently can out-compete and "mask" adsorbed fibronectin, and low rates of endothelial cell adhesion have been correlated to the limited adsorbed fibronectin surface density as probed by anti-fibronectin antibodies.[38] Thus, increased density of surface-adsorbed albumin should correlate to

reduced mammalian cell adhesion[39] given that the majority of cells are not known to have specific receptors to actively engage albumin, with the exception of hepatocytes,[40] vascular endothelial cells[41] and MC, MΦ and DC.[42,43] Importantly the FcRN receptor, identified as an albumin-binding protein present on MC, MΦ and DC,[43] binds exclusively at pHs below 6.5. and is not a known cell-adhesive receptor.[42] In the context of the FBR, highly albumin-adsorbed perfluorinated surfaces might be predicted to elicit reduced inflammatory cell activation if their surface adhesion is inhibited. This has been one motivation for clinical use of PTFE, although *in vivo* results are equivocal.

Specific integrin receptor families expressed on leukocytes include: $\alpha_M\beta_2$ (Cd11b/CD18, Mac-1, CR3), $\alpha_X\beta_2$ (Cd11c/CD18, p150,95), $\alpha_L\beta_2$ (CD11a/CD18, LFA-1), and $\alpha_4\beta_1$ (CD49c/CD29, VLA-4).[44-49] contributing to leukocyte surface adhesion.[50] Mac-1, expressed primarily in neutrophils, MC and MΦ, plays a role in several important aspects of innate immunity, including phagocytosis of complement-opsonized particles, and adhesion and migration[46] on ECM components and the endothelial lining.[51] Like other integrins, Mac-1 requires priming by an agonist that induces conformational changes, mobilization and clustering.[52] It has been demonstrated that Mac-1 binds numerous ligands including fibrinogen,[53,54] C3bi[45] and ICAM1,[55] but not albumin. Both Mac-1 and p150,95 have been implicated in mediating leukocyte adhesion to denatured proteins, including albumin[56] and denatured albumin[30], facilitating interactions of cells with solid substrates *in vitro.*

In vitro "biocompatibility" testing and cell-based drug screening often employ immortalized, secondary-derived (MC-) MΦ cell lines due to their availability and cost-effectiveness, despite the fact that these cells exhibit varied adhesion patterns, culture requirements, longevity and unknown "equivalence" to primary cells. The goals of this study were to 1) examine and compare aspects of cell behavior for murine cells of primary- (BMMO) and secondary- (IC-21) origins when grown on perfluorinated (i.e., fluorocarbon, FC) surfaces *in vitro*, and 2) to propose a mechanism by which initial MC/MΦ cell adhesion events could occur in the context of establishing a FBR to biomaterials. For practical purposes and to allow an appropriate equivalence comparison between primary and secondary derived MΦ, this study focused on responses of BMMO and IC-21 cells exclusively. Of the three secondary cell lines initially tested IC-21 was selected as a best match for comparison to primary BMMO because: 1) IC-21 represents the most physiologically relevant cell line within this group.[57] and 2) mature IC-21 cell size, morphology, adhesion and spreading behaviors were very similar to BMMO. To contrast (MC-) MΦ cell behavior on FC surfaces, one alternate adhesive cell type known to be non-adhesive to FC surfaces *in vitro*, NIH 3T3 fibroblasts,[58,59] was included in these assessments.

Two different FC surface chemistries (pp-FC and Teflon® AF) were used to verify cellular adhesion to FC surfaces. Teflon® AF has been employed in previous studies employing MC/MΦ,[59-61] neuronal[62] and endothelial[63] cells due to its solubility and nearly 100% transmissibility of light, allowing facile microscopic evaluation of cell cultures. Based on our preliminary findings related to cell adhesive behavior,[59-61] both

FC surface chemistries utilized were predicted to produce similar protein adsorption and cell adhesive patterns, regardless of MΦ cell origin. The β_2 integrin family, vital to the development of an effective inflammatory response *in vivo*[47] and known to interact with specific ECM proteins as well as denatured proteins at surfaces,[30] was hypothesized to be the primary mediator of any observed initial MΦ adhesion to FC surfaces exposed to biological milieu *in vitro*. Further, as MΦ are known to secrete fibronectin,[64-67] this may facilitate MC and MΦ adhesion to FC surfaces via endogenous ECM production, deposition and cell-based remodeling of the pre-existing adsorbed protein layer.

4.3 Materials and Methods

Sample preparation for ToF-SIMS

PS dishes were cut into pieces with dimensions not greater than 1 cm x 1 cm, labeled to indicate "bottom" and affixed to the bottom of PS petri dishes using double-sided tape, or left unfixed to free-float in protein milieu. Sufficient Teflon® AF (DuPont Fluoroproducts) solution (0.1 wt. % in FC-40 solvent, 3M Corp.) was added to these petri dishes to completely cover all PS pieces. Coated PS surfaces were then incubated in a vacuum oven overnight at 65°C to remove residual solvent, and plates were misted with 70% ethanol, dried, and treated with biosafety cabinet UV light for 20 minutes immediately before culture use, a process shown to sterilize reliably while remaining benign to cell culture surface chemistry.[68] A number of Teflon® AF samples were reserved as controls. Following sterilization, samples were immersed in either a 3 mg/ml BSA solution (fraction V, OmniPur®, Sigma, ≥ 98% pure by gel

electrophoresis) or 10% FBS solution, both in sterile Dulbecco's phosphate buffered saline with Ca^{++} and Mg^{++} (PBS^{++}), and incubated at 37°C for 24 hours. Samples were removed, rinsed twice with PBS^{++}, three times with 18 MΩ "Nanopure-grade" ASTM I water and dried under a stream of nitrogen. These samples were subjected to surface analysis as described below.

Preparation of fluoropolymer culture surfaces using plasma deposition

All plasma-prepared (pp) fluorocarbon surfaces employed in these studies were the gift of Dr. E. Fisher and Dr. G. Malkov (Colorado State University). pp-FC surfaces utilized in these studies were prepared and characterized as previously described.[68] This method produces a robust (100 nm) thick film of crosslinked perfluorocarbon highly enriched in $-CF_2$ and $-CF_3$ groups. Briefly, all films were deposited in a home-built inductively coupled radio frequency (RF) (13.56 MHz) plasma reactor[69]. The pulse duty cycle was varied using the internal pulse generator of an RF Power Products power supply. The peak applied RF pulse power (P) was kept constant at 300 W for fluorocarbon film. The duty cycle (d.c.) is the ratio of pulse on time to the total cycle time; thus, a pulse sequence of 10/190 ms has a 5% d.c. A 10 ms on time was used in all experiments; pulse off time was varied to achieve different d.c.'s, ranging from 5-50%. For all experiments, the gas flow was kept constant at 10.0 sccm (standard cubic centimeters per minute), resulting in a reactor pressure of ~200 mTorr. The C_3F_8 (Air Products, 99%) was used without further purification.

ToF-SIMS analysis

ToF-SIMS analysis used a Physical Electronics 7200 instrument for static data acquisition, exploiting an 8 keV Cs^+ ion source, a reflectron time-of-flight mass analyzer, chevron-type multi-channel plates, and a time-to-digital converter. Data was acquired for the Teflon® AF samples incubated (as described) with 3 mg/ml BSA or 10% FBS; other protein spectra for comparison were collected previously.[34,70] Positive secondary ions mass spectra were acquired over a mass range from $m/z = 0$ to 1000. Negative ion ToF-SIMS spectra were not considered here due to a lack of unique peaks for the different amino acids.[71] The area of analysis for each spectrum was 100 μm x 100 μm, and the total ion dose used to acquire each spectrum was less than 1×10^{12} ions/cm^2. The mass resolution ($m/\Delta m$) of the secondary ion peaks in the positive spectra was typically between 3000 and 5000. The ion beam was moved to a different spot on the sample for each acquisition. Positive spectra were calibrated to the CH_3^+, $C_2H_3^+$, $C_3H_5^+$, and $C_5H_{10}N^+$ peaks before any further analysis. At least two replicates were prepared for each sample type, with three spectra acquired from each replicate.

Principal Components Analysis (PCA) of ToF-SIMS data

PCA was used to analyze the positive ToF-SIMS spectra projected into a previously established dataset,[34] and was performed using scripts written at NESAC/BIO (University of Washington, USA) for MATLAB (The MathWorks, Inc.). All spectra were mean-centered before running PCA, capturing the linear combination of peaks that describe the majority of variation in the dataset. In this study, a previously established model of various proteins adsorbed to PTFE was used for analysis.[34]

Briefly, each amino acid was assigned a distinct mass peak, and the abundance of each peak, or amino acid, respectively, was used as input for the dataset. PCA yields an output of both a "scores" and a "loadings" plot. Wagner *et al*[34] demonstrated that proteins present at a surface can be identified through unique amino acid fragmentation patterns in the ToF-SIMS positive ion spectra. Here, the same data set (Wagner *et al*[34]) was used for comparison to new data collected in experiments evaluating BSA and 10% FBS sample adsorption to Teflon® AF surfaces.

Fluorescence labeling of proteins for detection of surface adsorption

Fibronectin (from bovine plasma, Sigma) and BSA solutions were fluorescently labeled and subsequently purified per manufacturer's instructions using Alexa Fluor 555® and Alexa Fluor 647® protein labeling kits (Invitrogen). Protein and dye concentrations were determined by optical density using UV-vis spectroscopy. Subsequently, samples of pp-FC, Teflon® AF, negative control Codelink™ Activated hydrogel-coated slides (Amersham Biosciences) or glass coverslips (positive control) were either completely covered with dye-labeled protein solution (depending on the substrate size: small samples were completely immersed, while wax pencil "wells" were drawn on larger slides), or spotted with 30 μl drops (confined within a wax pencil-defined well). Samples were exposed to: 1) single component solutions of fluorescently labeled albumin or fibronectin, or 2) a mixture of both dye-labeled proteins (each with a different fluorescent label) in a range of sample concentrations (albumin, from 1.5 μg/ml to 1.5 mg/ml; fibronectin, from 1.9 μg/ml to 1.9 mg/ml) or 3) a mixture of both proteins with only one dye-labeled protein in the same range of

sample concentrations (*vida supra*). Coverslips were transferred to petri dishes and incubated at 37°C, 98% humidity for 24 hours. No differences in 30 μl spot sizes were discernable after the 24 hour incubation period. At the end of the incubation period, the remaining solution was rinsed from the surface using PBS^{++}. Surfaces were rinsed copiously with PBS^{++}, dried under a stream of nitrogen and affixed to glass slides using double-sided tape (at the edges only). Samples were scanned for fluorescence signal using a Perkin Elmer ScanArray Express™ Microarray Scanner employing appropriate filters and wavelengths for each dye employed. Gain and power settings were consistently controlled for sample comparisons. Images were processed for relative fluorescence intensity using ImagePro™ software, and quantified using Quantity One® (Bio-Rad) and MS™ Excel software.

Cell culture

All cell lines were obtained from the ATCC (Manassas, VA). Cells were cultured in DMEM (Mediatech, for NIH 3T3), or RPMI 1640 (Mediatech, for IC-21) supplemented with 10% FBS (HyClone, Inc.), and 1% penicillin-streptomycin (Life Technologies) except IC-21. Cultures were maintained in T-175 TCPS flasks (Nunc™) under standard conditions: incubation at 37° C, 98% humidity and 5% CO_2. Cells were dissociated from culture flasks by incubation with Ca^{2+}- and Mg^{2+}- free cell culture grade HBSS (Life Technologies) (NIH 3T3), or by scraping with a rubber policeman (IC-21). Cell concentration and viability was assessed using standard trypan blue (BioWhittaker) dye exclusion assay and a hemacytometer.[72] All cell line subcultures were ≤ 25 beyond the passage number as received from ATCC.

Primary cell harvest

BMMO were prepared from bone marrow cells harvested from the femurs and tibias of C57BL/6 mice.[73] To differentiate bone marrow stromal precursors into MΦ, bone marrow-extracted cells were cultured in "complete" bone marrow medium: DMEM supplemented with 10% L929 fibroblast-conditioned medium, 2 mM L-glutamine, 0.01% HEPES, 1% penicillin-streptomycin, and 2 mM non-essential amino acids (Sigma-Aldrich). Cells were grown under standard conditions (*vida supra*) with media changes every two days. This method has been shown to reliably produce differentiated MΦ.[73]

Cell culture on model surfaces

TCPS (Falcon®, Becton Dickinson) and suspension culture PS (Corning Inc.) 15 x 100 mm dishes and 24-well plates were utilized for both control and experimental conditions. Teflon® AF fluoropolymer culture surfaces were prepared by coating PS surfaces as previously described (*vida supra*). Plates were tested for the presence of contaminating endotoxin using a Pyrogene™ Assay kit (Cambrex), and endotoxin levels were determined to be below the kit detection limit (0.02 EU/ml). Plates were subsequently preconditioned with appropriate medium containing 10% FBS for a minimum of six hours before cell seeding unless otherwise indicated. Cells were seeded at concentrations ranging from 5.0×10^4-3×10^6 cells per plate in fresh medium unless otherwise indicated. Initial seeding densities varied slightly for each

cell type, due to surface-dependent differences in cell adhesion and growth rates, and in order to create roughly equivalent culture time endpoints whenever possible.

Protein pre-conditioning and cell culture on select surfaces

FC surfaces were incubated at 37°C for 24 hours with one of the following solutions: PBS^{++}, 3 mg/ml BSA in PBS^{++}, 0.3 mg/ml fibrinogen (bovine fraction 1, 75% clottable, ICN Biomedical), 10% FBS in PBS^{++}, 10% heat inactivated (HI, 56°C, 1 hour) FBS in PBS^{++}, 100% FBS or (cell specific) medium containing 10% FBS. At 24 hours, the protein solution or serum was removed by aspiration and cells were immediately seeded in an appropriate cell culture medium containing 10% FBS. Cell culture conditions proceeded as described above.

Phase contrast microscopy

Images of cells on surfaces were obtained with either a Nikon Eclipse TS100 or a Nikon TMS inverted microscope using Nikon objectives. A Kodak DC290 camera was used to capture field images that were subsequently processed in Adobe Photoshop 6.0 (Adobe Systems, Inc.).

Flow cytometry

Cells were pelleted by centrifugation (300 x g, 5 minutes) and resuspended in 100 µl of staining solution (1% FBS, 0.01% NaN_3 in PBS^{++}) with 1 µg of anti-CD16/32 (clone 93) mAb (eBioscience, F_c receptor block). Cell F_c receptors were blocked for 15 minutes at 4°C. Subsequently, cells were rinsed twice and resuspended in staining

solution without antibodies. Cells were transferred to a 96-well plate for subsequent staining with 0.1 μg/ml of one of the following fluorescently conjugated (allophycocyanin, APC or fluorescein isothiocyanate, FITC) mAb per experiment: anti-CD11b (clone M1/70, APC), anti-IgG2a (clone eBR2a, FITC), anti-CD18 (clone M18/2, FITC), all eBioscience). Cells were stained for 30 minutes at 4°C, rinsed twice and resuspended in 500 μl staining solution without antibodies. Cell suspensions were transferred to 15 x 100 mm tubes for flow cytometry analysis (BD FACSCalibur™ flow cytometer).

Integrin blocking studies

Function-blocking monoclonal antibodies (mAb, all sterile-filtered, azide-free, low endotoxin) directed against the murine integrin β2 (M18/2) chain and a non-specific isotype-matched control (Rat IgG2a, κ) were purchased from eBioscience. BMMO (matured 7 days) and IC-21 cells were pre-incubated for 30 minutes at 4°C with either an integrin-directed mAb or an appropriate isotype control (both 100 μg/ml). Samples were seeded into Teflon® AF-coated wells (2 cm^2) previously treated for 24 hours with 10% FBS in PBS^{++} at a density of 500 cells/mm^2 and allowed to adhere for 1 hour. After the 1 hour incubation period, non-adherent cells were removed with two 0.65 ml washes of warm (37°C) PBS^{++}. Cells were fixed and stained according to the Wright-Giemsa method[74] using a commercially available kit (Hema 3® Staining System, Fisher). For each sample, adhesion blocking was evaluated by counting the number of cells in three lower-power fields and expressing the result as a percentage of untreated cells (Teflon® AF control). For each cell type, 4 independent

experiments were performed, and data presented is the average of the 4 trials. Error was reported as standard error of the mean.

Reverse transcriptase-polymerase chain reaction (RT-PCR)

Total RNA from BMMO and IC-21 cells grown on either TCPS or Teflon® AF surfaces was extracted and purified at various time points using RNeasy™ kits (Qiagen) per the manufacturer's instructions. First strand cDNA was synthesized from up to 4 μg of total RNA using Superscript II™ reverse transcriptase (Invitrogen) as recommended by the supplier. Both poly dT (Invitrogen) and murine fibronectin-specific primers[75] (5'-AGCAGTGGGAACGGACCTAC-3', 5'-CGTAGGACGTCCCAGCAGC-3', IDT), 100 pmol per reaction, were used (in separate reactions) to obtain total and fibronectin-specific product cDNA, respectively. Primer-specific PCR amplifications of glyceraldehyde-3-phosphate dehydrogenase (GAPDH) served as "housekeeping" controls for each sample (5'-AACTTTGGCATTGTGGAAGGGCTC-3', 5'-TGGAAGAGTGGGAGTTGCTGTTGA-3'). Primers were either designed using Primerquest^{SM} software (GAPDH) or as described previously (fibronectin).[75] All PCR amplifications were performed using an iTaq™ DNA polymerase kit (Bio-Rad) per manufacturer's instructions, on an iCycler thermal cycler (Bio-Rad). Each experiment was performed with ≥ 2 separate RNA isolations. PCR products were analyzed on 2% agarose gels, stained with ethidium bromide, and visualized/analyzed using a ChemiDoc XRS system (Bio-Rad) and Quantity One® software (Bio-Rad).

4.4 Results

ToF-SIMS and PCA

ToF-SIMS and PCA methods previously described have been frequently employed to classify and distinguish surface adsorbed proteins.[34] ToF-SIMS spectra are challenging to interpret due to the highly energetic SIMS ion fragmentation process, which leads to extensive protein fragment production from surfaces during analysis. This fragmentation translates to a multitude of small peptides, reflected in SIMS-spectral data in the form of hundreds of peaks in the 0-200 m/z (i.e., mass/charge ratio) range. To facilitate protein identification under these experimental conditions, each amino acid can be assigned one characteristic mass peak; a standard table of mass peaks assigned to specific amino acids has been established.[71]

PCA is a convenient method for simplifying large, complex data sets and identifying trends. Previous reported created a PCA-based model useful for identifying proteins adsorbed to surfaces, (Wagner *et al.*)[29] This model included the analysis of numerous proteins including BSA, fibrinogen, fibronectin, IgG and others (Figure 4.1 A). PCA involves a mathematical transformation that relates a large number of (potentially) correlated variables into a smaller number of uncorrelated variables, i.e. the principal components. The first principal component (x axis) accounts for as much of the variability in the data set as possible (in the cases reported here, 51%), and the second principal component (y axis) accounts for as much of the remaining variability as possible (here, 17%). In Wagner's model,[34] as presented here, this allows for

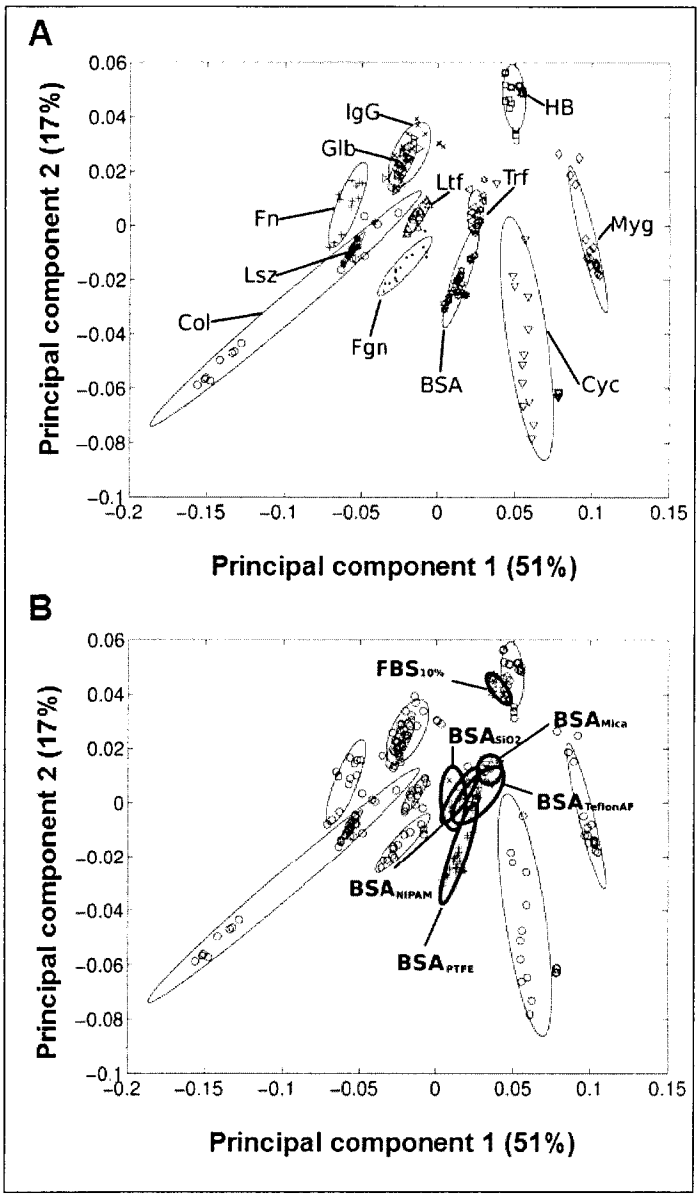

Figure 4.1 Principal component analysis performed on BSA and 10% FBS treated Teflon® AF surfaces, projected into the model of Wagner *et al.*[34] A) Wagner's PCA-based model identifying and grouping various proteins adsorbed to different substrates. B) Samples of 3 mg/ml BSA and 10% FBS on Teflon® AF substrates projected into Wagner's BSA model. Figure and PCA analysis, courtesy Dr. Roger Michel and Dr. David Castner.

qualitative statements to be made about the presence (or absence) of specific protein species present on tested surfaces.

In this set of experiments, the PCA model of Wagner *et al*[34] was utilized for analysis of a new data set for protein(s) of interest (e.g., albumin) on Teflon® AF surfaces pre-treated with either complex (10% FBS) or biased single component (BSA) protein solutions. Data obtained for BSA were compared to the results obtained by Wagner *et al*[34] (Figure 4.1 A) for numerous single proteins adsorbed to a PTFE surface. In this model the ellipses represent the 95% confidence interval for each protein, and most of the proteins (differing in amino acid composition) can be

separated from each other based on the two principal components shown (Figure 4.1 A). By comparison, it can be stated that the BSA present on Teflon® AF surfaces exposed to a single component BSA solution (indicated as $BSA_{Teflon\ AF}$) is highly similar to BSA results for PTFE and BSA on other surfaces (Figure 4.1 B). In fact, the data for all BSA samples shown (0.1 mg/ml BSA solution on mica, silica (SiO_2), and plasma-polymerized poly(*N*-isopropyl acrylamide, ppNIPAM) are within the 95% confidence limits of BSA on Teflon® AF. In contrast, the 10% FBS (multi-component protein solution) on Teflon® AF ($FBS_{10\%}$) showed a slightly different localization from the BSA samples (Figure 4.1 B). By examining the first principal component (51% of all the variance in the dataset) exclusively, co-localization of the $FBS_{10\%}$ with the $BSA_{Teflon®AF}$ and other BSA samples is noted. Examining the second principal component (17% of the overall variance) exclusively, reveals a higher value for the $FBS_{10\%}$ compared to the BSA samples.

To examine precise distances between these groups of proteins, a group distance-calculating program was employed to measure distances between the PCA-generated ellipse centers of each sample protein. The average normalized distance of the $BSA_{Teflon®AF}$ to BSA on other substrates was 0.0168, while the distance of the $BSA_{Teflon®AF}$ to the other proteins was 0.0615. The $FBS_{10\%}$ distance from the BSA samples was 0.0456, while the average normalized distance to the rest of the proteins was 0.817. Although this experiment cannot distinguish between proteins *per se*, the location of the $FBS_{10\%}$ is likely an indication that albumin derived from the FBS

solution (BSA) is the major component adsorbed to the Teflon® AF surface from this complex solution.

Fluorescence scanning detection of surface adsorbed proteins

Results of fluorescence scanning experiments probing protein adsorption to various surfaces are show in Figure 4.2. Results presented are equivalent protein concentrations and fluorescence label by species across experimental trials, i.e., 4 μg/ml fibronectin-Alexa Fluor 555® and 37 μg/ml albumin-Alexa Fluor 647®. Significantly, the concentration of fibronectin employed here is roughly equivalent to the concentration of fibronectin in 10% FBS (i.e., 10% physiological concentration), whereas the albumin concentration is considerably less than encountered in either circumstance (1% of that in 10% FBS, 0.1% of physiological concentration) due to the complications from preliminary experiments performed with albumin at physiological concentration and 1:10 or 1:100 dilutions that were not quantifiable due to saturation of fluorescence signal.

The highly hydrophilic Codelink™ hydrogel control surfaces showed minimal protein adsorption (background levels) compared to both glass and highly hydrophobic FC surfaces (Figure 4.2). As a hydrated, uncharged polyacrylamide-based coating, this commercial microarraying surface is designed to repel serum proteins.[76] Protein adsorption was not significantly different on the Codelink™ surface based on the protein species (albumin versus fibronectin, Figure 4.2 insert). Further, these results were very close to background levels of fluorescence (unlabeled

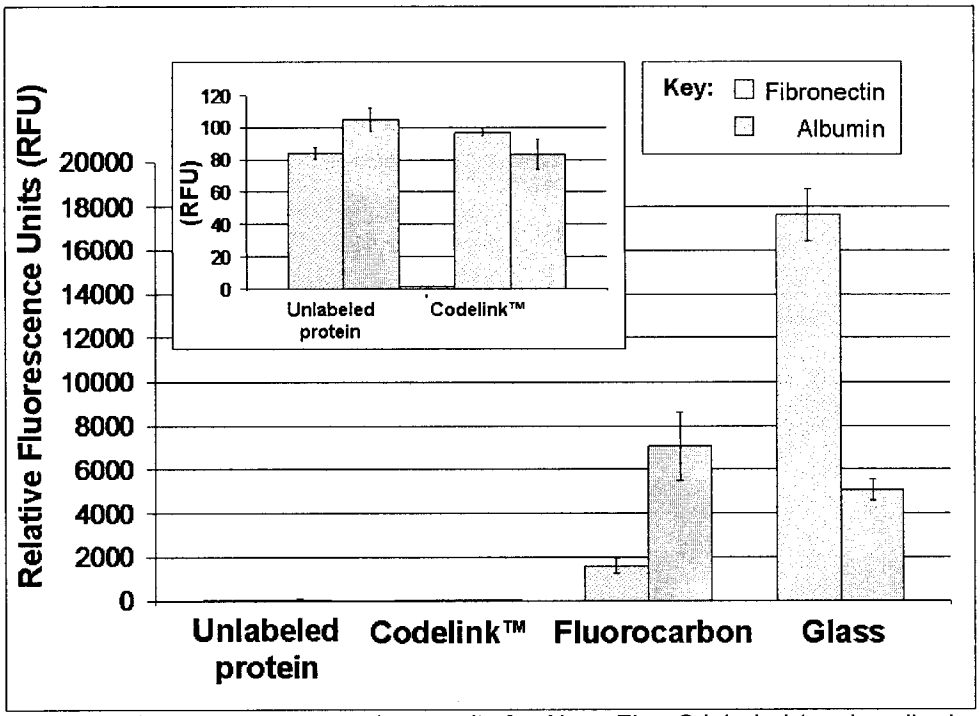

Figure 4.2 Fluorescence scanning results for Alexa Fluor® labeled (as described in Material and Methods) fibronectin and albumin protein samples exposed to surfaces with a wide range of wettabilities for 24 hours: Codelink™ and glass (very hydrophilic), FC (very hydrophobic). Unlabeled proteins were incubated with FC surfaces as a negative control. Results shown in all tests are for 37 μg/ml albumin-Alexa Fluor 647®, and 4 μg/ml fibronectin-Alexa Fluor 555®. Insert: Close up of results for unlabeled protein samples and proteins exposed to hydrophilic Codelink™ substrates.

protein, Figure 4.2 insert), reflecting minimal protein adsorption on the Codelink™ surface. Fluorescence-based adsorption results for FC surfaces show minimal fibronectin adsorption when compared to albumin on the same substrate (Figure 4.2) in contrast to adsorption profiles on glass substrates where fibronectin signal is significantly higher than that from albumin.

Cell adhesion, growth and proliferation on control and fluorocarbon surfaces

Adhesion, growth and proliferation of (MC-) MΦ and fibroblast immortalized cell lines and primary-derived BMMO cultured on FC (Teflon® AF and pp-FC) surfaces were characterized using light microscopy techniques. Cells were tracked live and/or

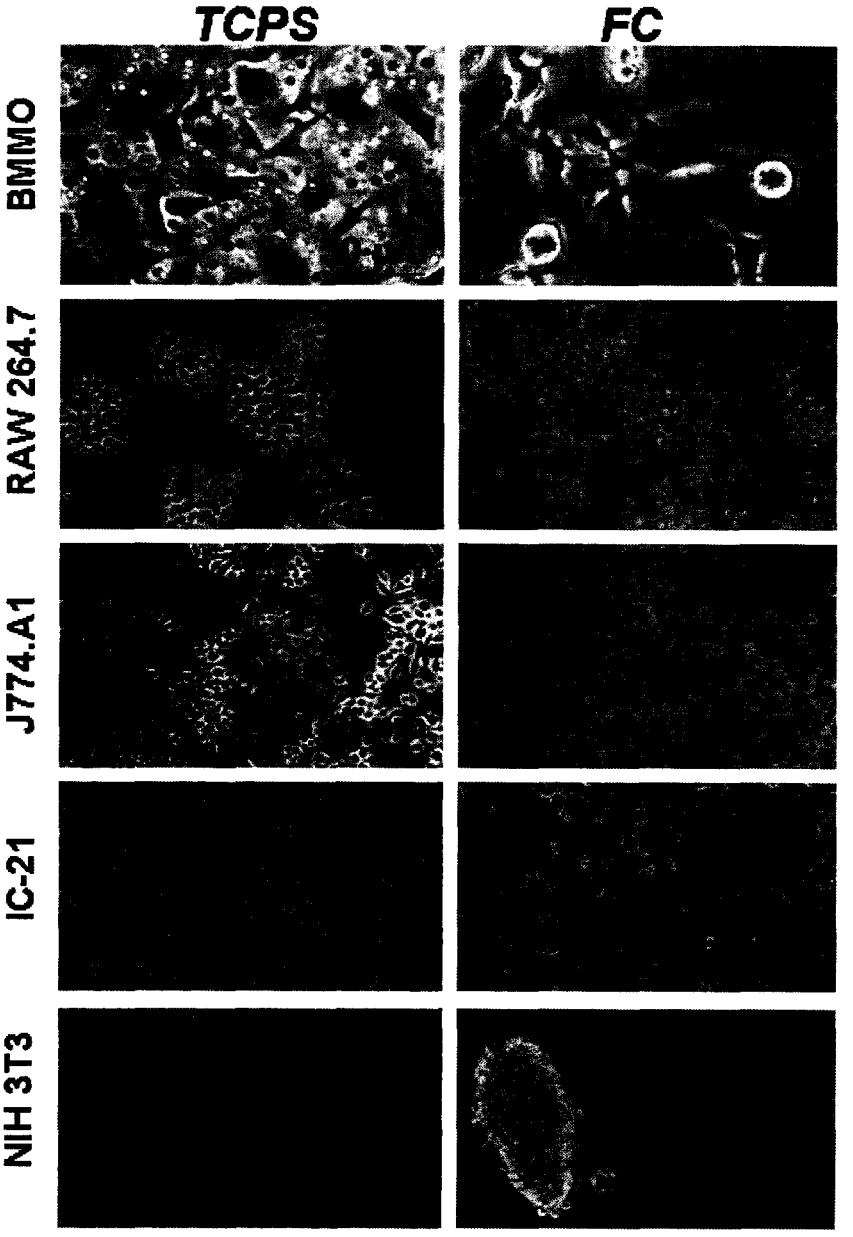

Figure 4.3 Phase contrast photomicrographs of live cells on control (TCPS) and FC surfaces for primary-derived cells (BMMO) and secondary-derived immortalized cell lines of monocyte/macrophage (RAW 264.7, J774A.1, IC-21) and fibroblast (NIH 3T3) origin. Cell seeding density varied, as described in Materials and Methods. Cultures depicted represent 2-4 days post-seeding on each surface and represent the typical sub-confluent growth pattern observed for each cell type (except J). Images are representative of multiple fields (≥ 3) and multiple replicates (≥ 2) for each test condition.

after fixation and staining using the Wright-Giemsa technique.[74] As expected, all cells were able to efficiently colonize TCPS surfaces (Figure 4.3 A, C, E, G, I). All (MC-)

MΦ cells tested achieved proficient growth, although cell adhesion was not 100% (Figure 4.3 B, D, F and H, spherical cell body morphologies are non-adherent). Adherent cells were not easily removed by rinsing and exhibited motile phenotypes, often displaying lengthy filopodia (up to hundreds of microns from the cell body) which appeared to be "probing" the surface in search of adhesive sites[61]. IC-21[61] and BMMO (Figure 4.4 M-O, Figure 4.5) cell populations on FC surfaces showed a mixture of actin-based cytoskeletal features (filopodia, lamellipodia, membrane ruffling), often with numerous features on a single cell.

A temporal series of phase contrast photomicrographs for BMMO cell adhesion, growth and proliferation on pp-FC surfaces exposed to pre-conditioning with 3 mg/ml BSA, 100% serum or 10% serum is shown in Figure 4.4. By 24 hours, cells had attached to surfaces and adopted characteristic adherent MΦ morphologies: astral shapes with short filopodia (Figure 4.4 A-C). By Day 8, adherent MΦ had approximately doubled in size (Figure 4.4 D-F, note scale bar difference) and filopodia and membrane ruffles were observed features of the majority of cells, comparable to previous observations on model biomaterials surfaces.[59,61] Similar surface coverage and growth patterns were observed for each test condition (Figure 4.4 G-I). By Day 12 a substantial portion of the FC surface was covered with cells (Figure 4.4 J, L), although some areas were more sparsely populated (Figure 4.4 K). BMMO morphologies and growth patterns on FC surfaces were consistent with those previously observed for the IC-21 MΦ cell line on FC and Teflon® AF FC surfaces.[61]

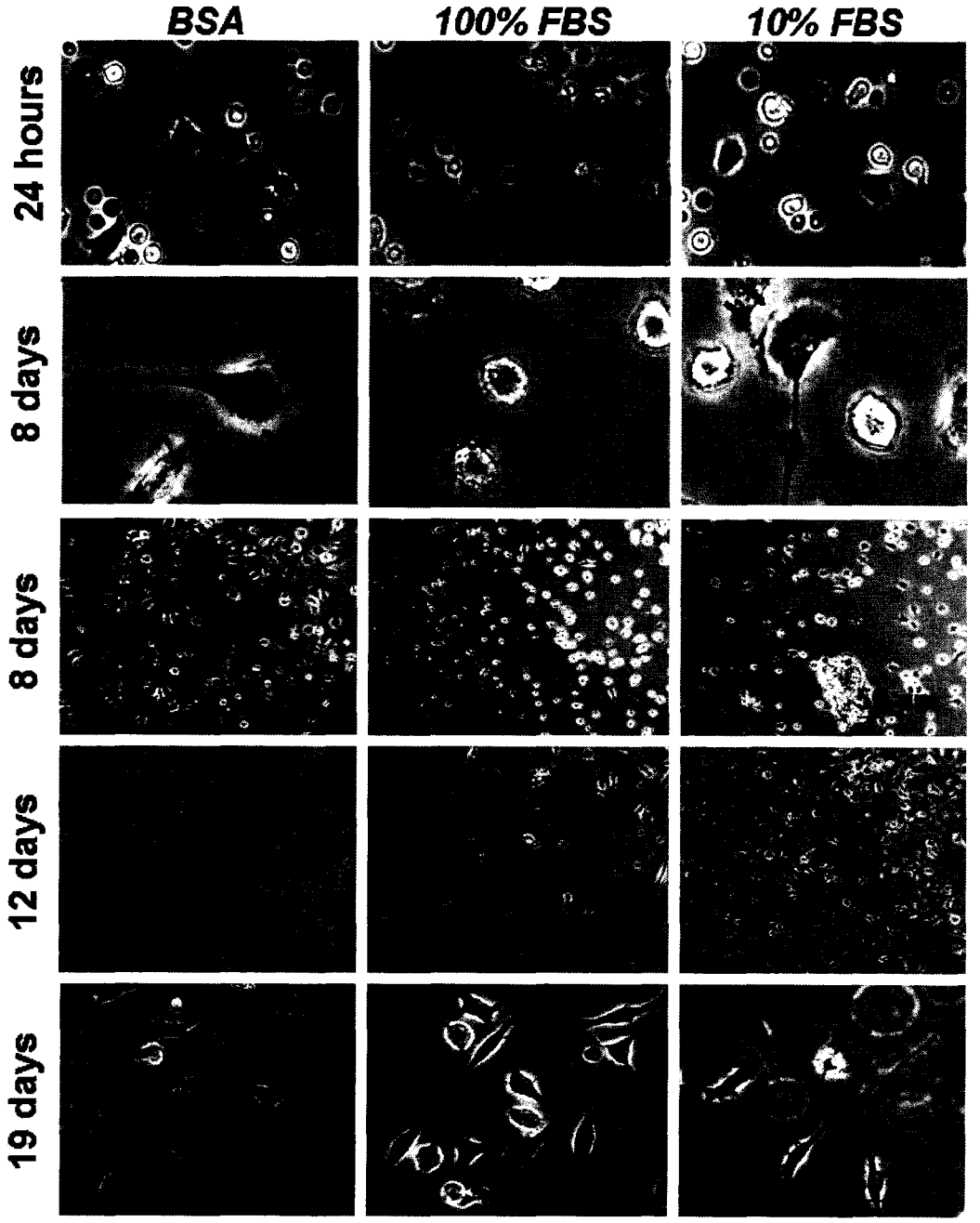

Figure 4.4 Phase contrast photomicrographs of live BMMO grown on uniform pp-FC surfaces preconditioned with pure (3 mg/ml) albumin (BSA), 100% FBS or 10% FBS. Images of cells are at times indicated for each condition and scale bars are relevant for each row. Cells were seeded at densities of 1500 cells/mm^2. Circles indicate astral morphology (A, E), arrows indicate filopodia (D, M, O) and bold arrows indicate membrane ruffling (D, F). Note that multiple cytoskeletal features (filopodia and membrane ruffling) are common features on many cells, as illustrated by examples shown in D and F. Images are representative of multiple fields ($\geq$ 3) and multiple replicates ($\geq$ 2) for each test condition.

For all time points, the results for FC surfaces exposed to 3 mg/ml BSA or 10%

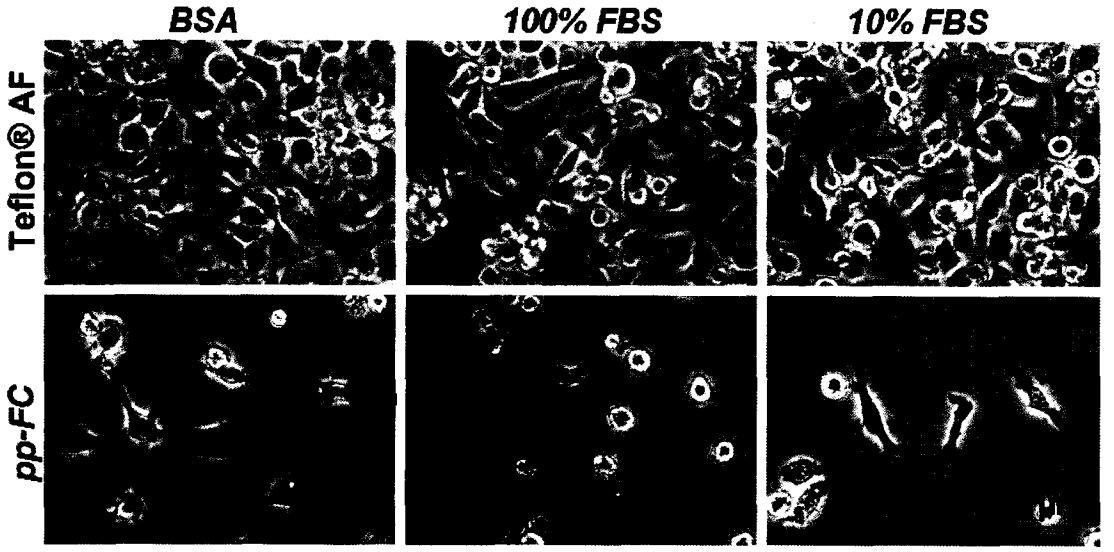

Figure 4.5 Phase contrast photomicrographs of live BMMO (Day 8 in culture) on FC surfaces exposed to preconditioning treatments as indicated. Cells were seeded at densities of 600 cells/mm ^{2} on Teflon® AF and 1500 cells/mm^2 on pp-FC. Circles indicate astral morphology (C-E), arrows indicate filopodia (A-D, F) and bold arrows indicate membrane ruffling (D). Scale bar shown in F is relevant for all images. Images are representative of multiple fields (≥ 3) and multiple replicates (≥ 2) for each test condition.

serum were comparable, suggestive of albumin biasing of the protein-adsorbed surface, regardless of whether a complex mixture of serum proteins (e.g., FBS) or pure BSA was used to condition the FC surface prior to cell culture. By Day 19, individual cells adopted MΦ morphologies typically observed on FC surfaces[59,61]: lengthy filopodia, membrane ruffling, unusual shapes and clustered growth with overlapping regions (Figure 4.4 M-O). Results shown in Figure 4.3 are for cells on pp-FC surfaces. These surfaces supported cell growth and proliferation, but when compared to Teflon® AF (Figure 4.5), a significant difference in BMMO response was observed. Although numerous non-adherent cells were observed on each type of surface (i.e., spherical cells with a haloed appearance), Teflon® AF was more permissive to BMMO attachment and spreading, this behavior was observed from 8-

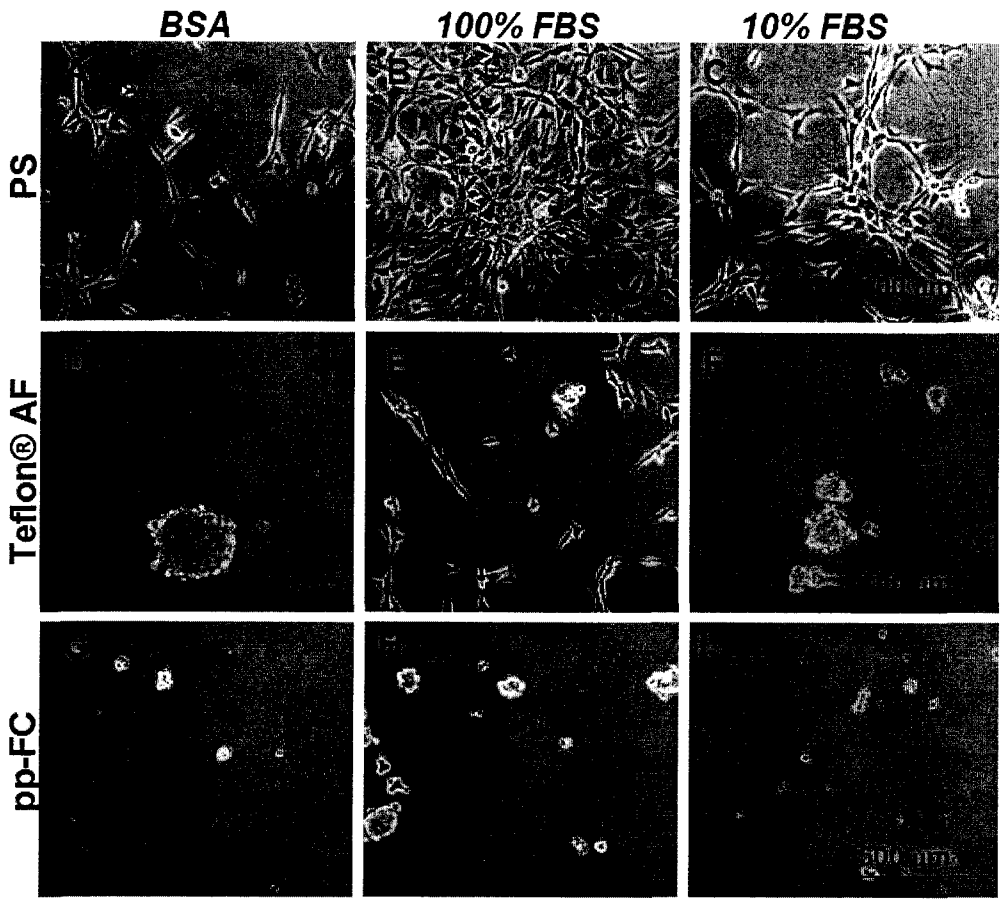

Figure 4.6 Phase contrast photomicrographs of live NIH 3T3 cells 48 hours post-seeding in 10% serum containing media on uniform pp-FC surfaces pre-treated with (3 mg/ml) BSA (A, D and G), 100% (B, E and H) or 10% serum (C, F and I). NIH 3T3 fibroblasts fail to effectively colonize FC surfaces under any of the conditions tested (D-I). Scale bars are relevant for each row. Images are representative of multiple fields (> 5) and multiple plates (2) for each test condition.

36 days of culture. On pp-FC BMMO grew and proliferated until approximately Day 21 of culture, when cells began to die/detach.

In contrast, NIH 3T3 fibroblast cells were unable to colonize identically treated FC surfaces (Figures 4.3 J and 4.6 D-I) at any time point. On PS surfaces (Figure 4.6 A-C) cell proliferative kinetics were approximately equivalent for the 3 mg/ml BSA and 10% serum samples. PS surfaces preconditioned with 100% serum (Figure 4.6 B) showed substantial improvement in cell proliferation at early time points (through 72

hours). Eventually, the cell populations on all three PS pre-conditioned surfaces reached 100% confluence (data not shown), but large confluent "sheets" of fibroblasts delaminated easily from PS, suggesting that cell-cell contacts were stronger than cell-surface interactions on this surface. On Teflon® AF surfaces, BSA and 10% serum pre-conditioning treatments (Figure 4.6 D and F) also exhibit similar results, with only the 100% treatment (Figure 4.6 E) supporting limited NIH 3T3 cell adhesion. The pp-FC surfaces were non-supportive of cell adhesion regardless of pre-conditioning (Figure 4.6 G-I) and this was maintained until NIH 3T3 cultures were terminated (Day 6 post-seeding).

Pre-conditioning treatments also included PBS^{++}, 0.3 mg/ml fibrinogen, 10% HI FBS in PBS^{++} and cell-specific medium containing 10% FBS. Regardless of treatment, BMMO (data not shown) and IC-21 cells adhered rapidly and spread on the FC surfaces, exhibiting great variance in cell size (Figure 4.1.S). Results for the most frequently employed pre-conditioning treatments for BMMO and IC-21 cells are shown in Figure 4.7. Generally, IC-21 cells exhibited more motile phenotypic features (i.e., filopodia and membrane ruffles) on Teflon® AF surfaces (Figure 4.7 E, G and I) when compared to TCPS (Figure 4.7 A and C), which exhibited a more even distribution of adherent cells. In contrast, BMMO cells were larger with more motile phenotypes on TCPS surfaces versus Teflon® AF at one hour time points (Figure 4.7, B and D versus F, H and J). In general, the adhesion of BMMO cells was lower on Teflon® AF surfaces than TCPS, whereas IC-21 adhesion was comparable on both surfaces regardless of protein pre-conditioning (Figure 4.2.S).

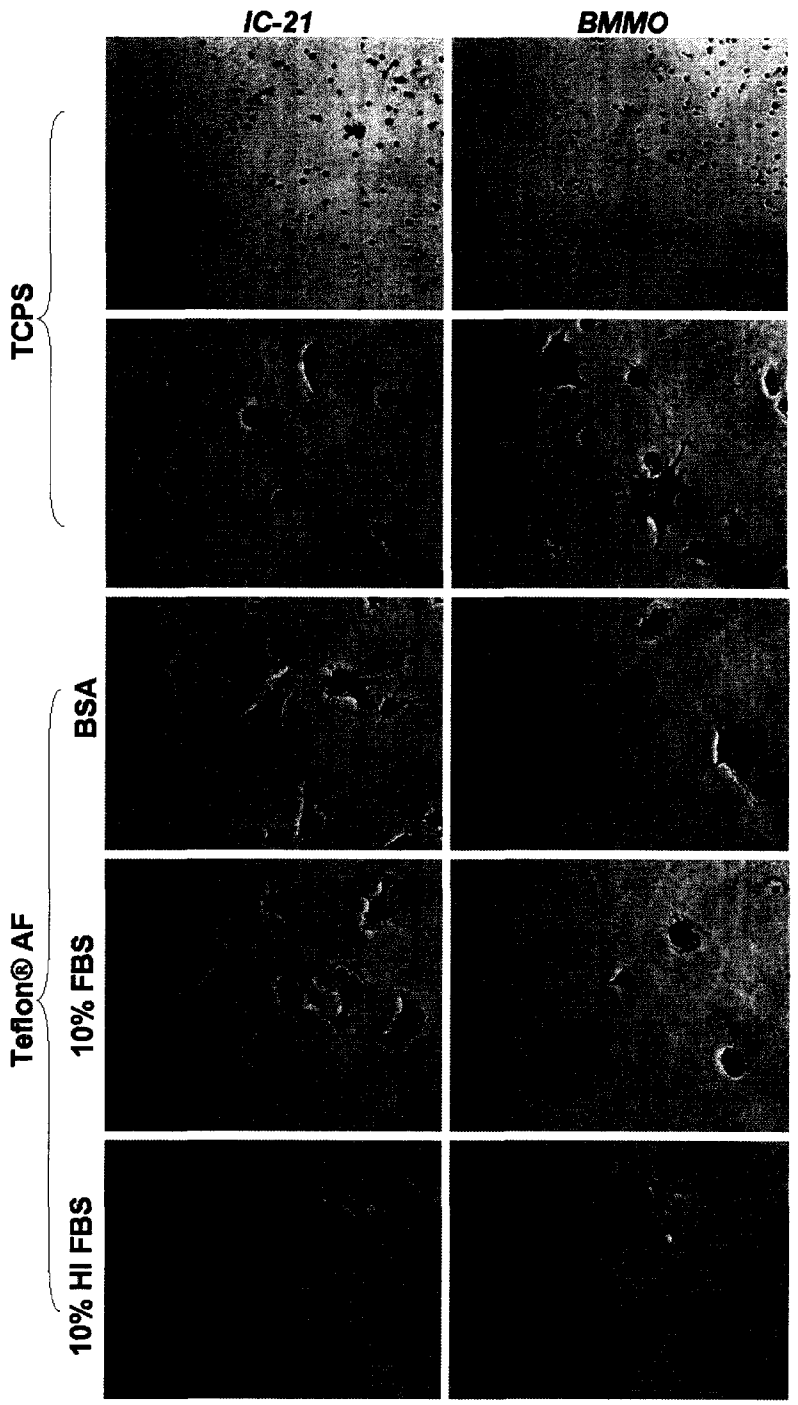

Figure 4.7 Phase contrast photomicrographs of IC-21 and BMMO cells on control (TCPS) and Teflon® AF surfaces with preconditioning treatments (Teflon® AF only) as indicated. Cells were seeded at a density of 500 cells/mm^2, fixed and stained after one hour. Scale bars in D and J are equivalent, and relative for all panels except A and B. Images are representative of multiple fields (≥ 3) and multiple replicates (≥ 2) for each test condition.

Flow cytometry and integrin blocking studies

Flow cytometry experiments were performed to determine fractions of cells in BMMO and IC-21 populations expressing β_2 and α_M subunits of the Mac-1 integrin receptor. Results (Figure 4.8) indicate that 76 ± 13% of the IC-21 and 80 ± 5% of the BMMO cells express β_2 (CD18), and 90 ± 1% of the IC-21 and 87 ± 3% of the BMMO populations express α_M (CD11b). mAb blocking experiments included controls for 1) the surface, Teflon® AF (Figure 4.9 A and D) and 2) non-specific binding (isotype matched control, Rat IgG2a, κ; Figure 4.9 B and E). mAb blocking against integrin β_2 produced significant cell adhesion blocking (i.e., reduced cell adhesion) for both the IC-21 (reduced 88 ± 6%) and BMMO (reduced 80 ± 9%) cells on Teflon® AF surfaces (Figure 4.9 C and F) compared to untreated cells seeded under identical conditions. Further, at one hour post-seeding, β_2-blocked seeded cells (Figure 4.9 C and F) exhibit altered morphologies when compared to those unblocked on Teflon® AF (Figure 4.9 A and D) and isotype controls (Figure 4.9 B and E). Post-blocking adherent cell morphology is more spherical with fewer obvious adhesion sites, fewer filopodia and less extensive membrane ruffling.

RT-PCR for fibronectin transcript production

Fibronectin mRNA production in both BMMO (Figure 4.10 A) and IC-21 (Figure 4.10 B) cells grown on TCPS and Teflon® AF surfaces was confirmed at various time points (up to 24-hours post-seeding). Figure 4.10 shows representative agarose gel electrophoresis results for amplifications of fibronectin cDNA (Figure 4.10 A, Lanes 2-5; B Lanes 2-4), which yielded a 400 bp band (Figure 4.10 A and B, arrows).

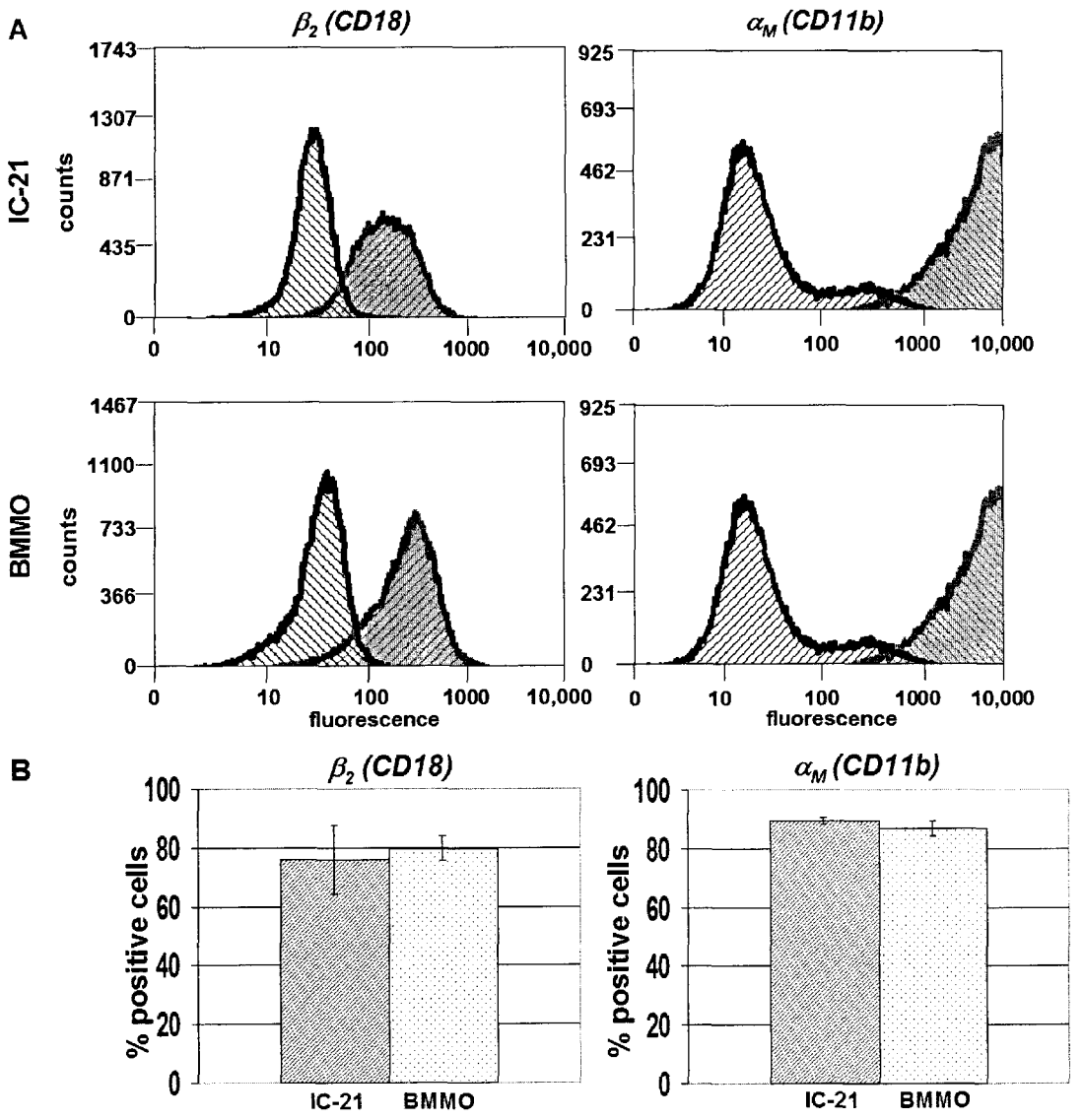

Figure 4.8 Flow cytometry analysis of integrin β_2 (CD18) and α_M (CD11b) expression on populations of IC-21 and BMMO cells grown on TCPS under standard conditions. A) Raw data showing specific integrin labeling. B) Bar graphs representation of data shown in A, indicating the percent of total sampled cell population positive for the integrin indicated. Error bars represent standard error of the mean. Data provided by Lisa M. Chamberlain.

Each sample was also tested for the presence of GAPDH (all positive, data not shown) to monitor the quality of RNA purification and cDNA synthesis. BMMO cells were positive for fibronectin transcript production at 30 and 60 minutes on control (TCPS) and model biomaterial (Teflon® AF FC) surfaces (Figure 4.10 A, Lanes 2-5); IC-21 cells were also positive for fibronectin transcript production at 30 minutes and

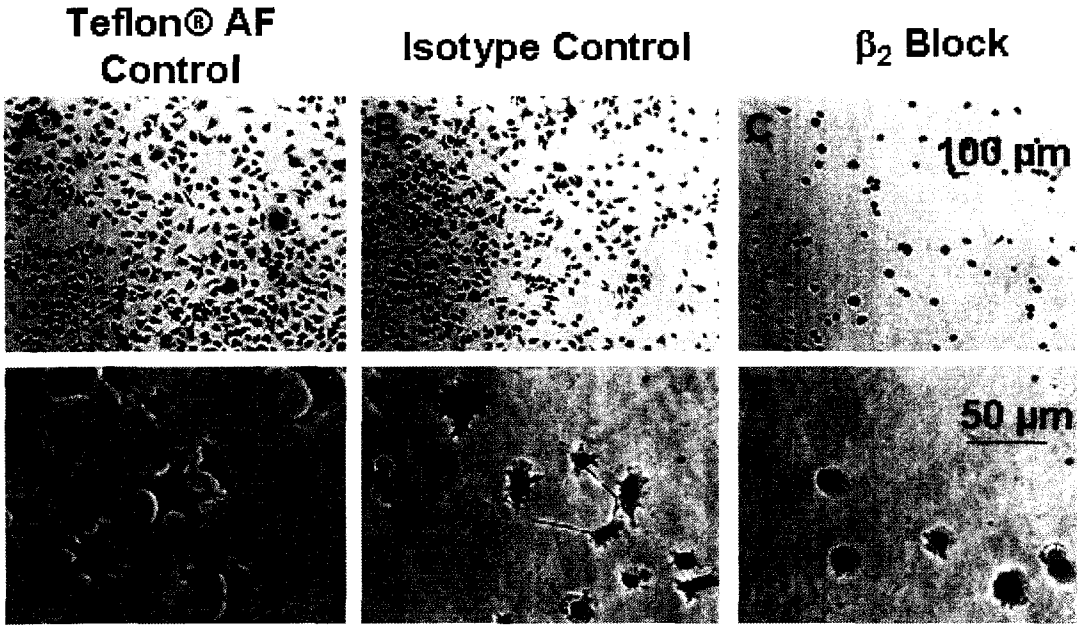

Figure 4.9 Representative phase contrast photomicrographs of integrin blocking experiments for IC-21 cells incubated on Teflon® AF surfaces after treatments as indicated: A) Teflon® AF negative control (no antibodies), B) Isotype control (non-β_2 directed antibodies) and C) β_2-directed monoclonal antibody block. Cells were incubated with control or blocking antibodies at a concentration of 100 µg/ml for 30 minutes prior to seeding at a density of 500 cells/mm^2. Cells were fixed and stained at one hour post-seeding. Scale bars are relevant for each row. Images are representative of multiple fields (≥ 3) and multiple replicates (≥ 2) for each test condition.

two hours post-seeding (60 minute time point was omitted in this experiment to allow a longer sampling time) on TCPS (Figure 4.10 B, Lanes 2-3) but not Teflon® AF (data not shown). IC-21 cells were positive for fibronectin production on Teflon® AF, but only at the 24 hour time point shown in Figure 4.10 B, lane 4.

4.5 Discussion

MΦ adhesive behavior to FC surfaces is interesting since these surfaces are shown to be heavily albumin-adsorbed – a condition that should inhibit cell adhesion as shown by substantial previous work on related surfaces.[77-79] Indeed, control NIH 3T3 fibroblasts show poor FC adhesion, consistent with these previous results for

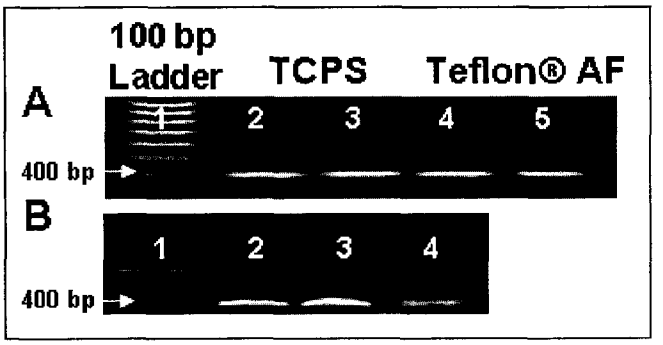

Figure 4.10 RT-PCR amplification of murine fibronectin cDNA from BMMO (A) and IC-21 (B) cells grown on TCPS and Teflon® AF surfaces, as indicated. Lane 1 A and B: 100 bp marker (Bio-Rad). BMMO cells collected from TCPS (lanes 2 and 3) or Teflon® AF (lanes 4 and 5) surfaces at 30 and 60 minutes post-seeding, respectively. IC-21 cells collected from TCPS (lanes 2 and 3) at 30 and 120 minutes after seeding, respectively or Teflon ® AF (lane 4) 24 hours after seeding.

fibroblasts[58,80,81] as well as several other attachment-dependent cell lines.[14,78] Hence, because cell-surface interactions are primarily due to integrin-ECM mediated interactions, mechanisms for consistent MΦ attachment, growth and proliferation observed on albumin-coated surfaces are intriguing. MΦ adhesive behavior on two FC surfaces, pp-FC and Teflon® AF was described in preliminary studies.[60,68,82] This current study compares the response of select MΦ and fibroblast cells on two FC surfaces subjected to protein pre-conditioning treatments for biased protein adsorption, and investigates a possible mechanism for initial integrin-based MΦ adhesion to these surfaces. The culture surface test set included controls (TCPS, the current "gold standard" for attachment-dependent cell culture; PS, a substrate commonly employed for surface modifications) and two FC surfaces (pp-FC, a plasma deposited film of C_3F_8 monomer; Teflon® AF ("Amorphous Form", poly(2,2-bis (trifluoromethyl)-4,5-difluoro-1,3-dioxide-*co*-tetrafluoroethylene)), a stable fluorinated polymer[83] and the soluble analog of Teflon® (PTFE), a highly hydrophobic fluoropolymer with a long history of use in biomaterials implants.[84,85] Surface characterization of these substrates by static aqueous contact angle measurements[69,82] and XPS has been

reported.[69,78] The two FC surfaces likely exhibit different surface and bulk FC chain arrangements: PTFE (corresponding to segments of Teflon® AF) is known to have a helical conformation,[86] with $-CF_2-$ monomer units oriented parallel and in-plane at the surface, and very few $-CF_3$ groups (i.e.., only from chain ends on very high molecular weight polymers). Teflon® AF, by stark contrast, has amorphous segments of $-CF_2-$ chemistries alternating with segments of the 2,2-bis (trifluoromethyl)-4,5-difluoro-1,3-dioxide monomer that present higher concentrations of $-CF_3$ groups at the surface (see XPS spectra in Ref. 71). In further contrast, pp-C_3F_8 is an amorphous, crosslinked thin film,[87,88] with different plasma preparation conditions producing differing amounts of $-CF_2-$ units oriented both in- and out of- plane at the surface, and varying amounts of co-existing $-CF_3$ terminal groups, but certainly measurable amounts of both.[87] The reported static aqueous contact angle for pp-FC (112°)[69] suggests the terminating surface layer is composed largely of $-CF_3$ groups. Hence, these pp-FC surfaces also present surfaces rich with different mixtures of $-CF_2-$ and $-CF_3$ chemistry. These structural differences likely translate to non-equivalent adsorbed protein densities[36] and/or conformations,[89,90] common phenomena on synthetic polymers. Since albumin retention on various glow-discharge treated polymer surfaces is linked to surface free energy (lower surface energy correlated to higher albumin retention),[36] and specifically, FC surfaces are known to both sequester albumin and exhibit poor cell adhesion, different adhesive behaviors observed for BMMO cells (the most naïve and perhaps the most biologically-relevant/stimulus sensitive cell type explored here) on pp-FC versus Teflon® AF surfaces may be related to albumin adsorbed states on surfaces over time in culture. Thus, the different

adhesive behaviors observed for BMMO cells (the most naïve and perhaps the most biologically-relevant/stimulus sensitive cell type explored here) on pp-FC versus Teflon® AF surfaces, may be related to the amount and conformation of albumin adsorbed to (and retained by) surfaces over time in culture.

Prior to cell culture experiments, surfaces were assayed using several analytical techniques to verify protein deposition. XPS was employed to verify general presence of protein on FC surfaces (i.e., specific presence of protein nitrogen N1s signal, data not shown). Fluorescently labeled BSA and fibronectin samples (adsorbed singly per surface or from binary mixtures) were incubated with FC surfaces under conditions identical to those employed in cell culture experiments. Fluorescence intensity measurements indicate that albumin inundates these surfaces, even well below physiological ($1/1000^{th}$) or standard cell culture condition ($1/100^{th}$) levels of protein (Figure 4.2). Fibronectin is barely detectable in FC samples exposed to binary solutions of fibronectin and albumin (data not shown), consistent with previous reports.[31,32,38] Finally, ToF-SIMS and PCA analyses compared protein deposition from BSA and 10% FBS solutions onto Teflon® AF substrates using previously established models for protein surface adsorption described by Wagner *et al.*[34] Since ToF-SIMS methods employed here sample only the outermost 1.0-1.5 nm of the surface,[29] this is extremely selective for protein surface analysis. Additionally, ToF-SIMS fragments from underlying FC surfaces are readily distinguished from any protein.[86] Significantly, PCA analysis of these data strongly supports BSA abundance on Teflon® AF both from single component BSA and multi-component (10% FBS)

solutions, consistent with similar studies.[31,32] Collectively, these techniques indicate that albumin represents the major protein constituent at the FC surface, suggesting that MC/MΦ must initially interact with an albumin-rich surface in order to efficiently adhere and grow.

Typical (sub-confluent) cell adhesive responses to FC surfaces from serum-containing cultures are shown in Figure 4.3. Adherent cells appear darker, with punctate adhesion sites and typically exhibit filopodia and membrane ruffling (examples shown in Figure 4.4 D and F). Non-adherent surface-resident cells appear lighter ("haloed") and rounded. The BMMO shown are immature (i.e., 24 hour cultures), and thus represent a mixed MC-MΦ culture. BMMO cell size varies significantly in immature cultures, but generally all BMMO cells are smaller than any cell line examined here. When comparing all cell types, magnified BMMO images were selected to more clearly illustrate adherent cells (Figure 4.3 A and B). For all other cell types (where adherent cells are more obvious) low magnification images were selected to depict typical growth patterns (Figure 4.3 C-J).

All cell types except NIH 3T3 fibroblasts readily adhered to and, over time (days), efficiently colonized FC surfaces in all treatment conditions. All MC-MΦ cultures grew to nearly 100% confluence on Teflon® AF substrates, and BMMO and IC-21 cells grew to nearly 100% confluence on pp-FC. These results are consistent with previous reports of MC and MΦ adhesion and migration on albumin-coated surfaces.[50,56,91-95] Generally, growth kinetics observed for all MC-MΦ cells tested

were comparable (to each other) on either TCPS or Teflon® AF substrates. The primary observed difference between cells grown on these surfaces was that cells cultured on FC surfaces exhibited lengthy filopodia maintained even when surface space became limiting (Figure 4.5 A-C).

Comparing BMMO growth on Teflon® AF and pp-FC (Figure 4.5) it is evident that Teflon® AF is the more supportive substrate. Pre-biasing the FC surface with adsorbed BSA or 10% or 100% FBS had no effect on the ability of these cells to adhere, grow and proliferate (Figure 4.5 A-C). Cells on both substrates exhibited motile phenotypes with characteristic features (Figure 4.5 A-C-filopodia, arrows; D-membrane ruffling, bold arrows). On pp-FC, BMMO cells reached maximum confluence at 19-20 days post-seeding, and cells began to detach and die at 20-21 days. It is unlikely that cell age was the primary factor in cell death/detachment on pp-FC since the same cells seeded onto Teflon® AF surfaces were still growing well on Day 36, when the culture was terminated.

Observed differences in BMMO cell adhesive behavior observed on the two different FC substrates employed here could be attributed to different FC surface chemistry influences on adsorbed protein conformation and composition, which in turn influence cell adhesive behavior. Methods employed here indicate only the presence or absence of proteins, and provide no information about accessibility or orientation of cell receptor ligands available for binding interactions. Previous studies show unique behavior for proteins in general and albumin specifically on FC surfaces.[30-32]

Albumin, the most abundant serum protein (55% of total serum mass),[8] binds to FC surfaces with high affinity and retention, resisting surfactant elution.[17,36,38] This albumin-binding characteristic has been correlated with improved surface resistance to cell adhesion, related to the ability of albumin to effectively block recognition of adhesive protein motifs present on these surfaces via integrin receptor-mediated interactions.[28,29,36,38,58] This is significant since albumin is likely the primary adsorbed protein on many of the surfaces shown here to allow MΦ adhesion. Other potential adsorbed protein mediators of MC/MΦ adhesion to FC surfaces *in vitro* include the complement protein C3,[96] trace fibrinogen,[53,97] and trace matrix proteins such as fibronectin and vitronectin.[98,99] Each of these proteins is known to interact with cells via specific integrin receptor interactions. However, previous serum-based adsorption studies have indicated that negligible adsorbed fibronectin is detectable on PTFE[34] or Teflon AF.[69] Also, since fibrinogen should be effectively removed from serum during standard commercial preparation, it should not represent a significant fraction of protein adsorbed to FC surfaces under the test conditions described here.

Surfaces treated with either 10% FBS or 3 mg/ml BSA solutions are expected to represent approximately equivalent amounts of albumin and roughly 10% of physiological concentration (plasma/serum concentration 35-50 mg/ml),[8] allowing facile comparison of albumin deposition from a pure, biased solution (BSA) versus a cell culture-relevant multi-component solution (10% FBS). Limited tests were performed in 100% serum (Figures 4.4-4.6), admittedly the most biologically relevant solution, but not representative of *in vitro* conditions and overwhelming in terms of protein deposition, leading to difficulty in parsing out individual protein contributions

and cellular behaviors on these surfaces. Therefore, pre-biasing conditions (10% FBS, BSA) relevant to *in vitro* assay conditions were of more interest.

NIH 3T3 fibroblast cells exposed to a range of hydrophobic substrates (moderately hydrophobic PS and very hydrophobic pp-FC and Teflon® AF) demonstrate predicted non-adhesive behavior on these substrates (Figure 4.6) consistent with numerous previous reports of poor cell adhesion on FC surfaces.[58,77-79] Compared to TCPS, PS is well known to have less adsorbed vitronectin and fibronectin, resulting in decreased fibroblast cell attachment.[100,101] Consistent with these reports, NIH 3T3 cells grown on PS under conditions typically employed *in vitro* (Figure 4.6 C) exhibited only moderate adhesion.[16,79] When substrates were pre-biased with 100% FBS, NIH 3T3 cell adhesion improved dramatically (Figure 4.6 B), likely related to an increase in the amount of trace adhesive proteins present at the substrate surface.[78] Notably, NIH 3T3 cells were able to colonize PS after several days regardless of protein pre-biasing, although the 100% FBS treatment progressed most rapidly (data not shown). In contrast, NIH 3T3 cells were unable to colonize the FC substrates (Figure 4.6 D, F, G-I) at any time points under any of the test conditions except for scant adhesion on the 100% FBS treatment of Teflon® AF (Figure 4.6 E), similar to results reported for endothelial cell adhesion on Teflon® AF.[78]

Pre-conditioning treatments of PBS^{++} (negative control), 0.3 mg/ml fibrinogen (positive control for MΦ adhesion, approximately equivalent to 10% of physiological concentration, but non-equivalent to 10% serum since serum should be fibrinogen-

free), 10% HI FBS in PBS^{++} (control for removing complement protein C3) and cell-specific media containing 10% FBS (negative control for media effects). The adhesive behavior of IC-21 and BMMO on Teflon® AF substrates did not change significantly in response to pre-conditioning with albumin-containing solutions (BSA, 10% FBS, 10% HI FBS, Figure 4.2.S C-H). However, BMMO adhesion favored TCPS chemistry to Teflon® AF at short culture time points; 30 minutes (data not shown), and one hour (Figure 4.2.S A versus C, E and G). Further, on substrates pre-biased with fibrinogen, an increase in adhesion at these short time points was noted. Both of these observations are consistent with results reported by Shen *et al.*[6] In contrast, IC-21 cells exhibited comparable adhesion rates on TCPS and Teflon® AF surfaces (Figure 4.2.S B, D, F, H).

Results for the most frequently employed pre-conditioning treatments for BMMO and IC-21 cells are shown in Figure 4.7. Generally, IC-21 cells exhibited more motile phenotypic features (filopodia, membrane ruffles) on Teflon® AF surfaces (Figure 4.7 E, G and I) compared to TCPS (Figure 4.7 A and C), on which cells were more evenly distributed. Interestingly, both cell types exhibited a range of cell sizes and motile phenotypes on both substrates, suggesting that BMMO and IC-21 populations employ similar mechanisms to attach and probe surfaces *in vitro*.

Investigation of integrin-related mechanisms facilitating initial MΦ adhesion to FC surfaces focused on integrin β_2, often implicated in MΦ adhesion[96] and extravasation.[102] Leukocyte-specific β_2 receptors include α_L/β_2, α_D/β_2, α_x/β_2 and

α_M/β_2, and receptor α_M/β_2 (CD11b/CD18, Mac-1) is well-known to interact with numerous ligands, including complement protein C3, fibrinogen, ICAM-1, -2 and -3, VCAM-1 and factor X.[103] Based on flow cytometry analysis (Figure 4.8), the majority of BMMO cells present α_M (CD11b) and β_2 (CD18). Other reports indicate that the Mac-1 β_2 integrin subunit contributes most significantly ($>\alpha_M$, $>\alpha_X >\alpha_L$) to MΦ adhesion on protein-coated glass surfaces and latex beads.[50] Davis reported that activated MC bind to denatured and native protein-coated substrates via a β_2 mechanism, and that activated MC bind faster and to a greater extent on surfaces coated with denatured proteins *in vitro*.[30] Based on these findings this integrin was selected as a target for monoclonal antibody (mAb)-directed blocking studies for cells on FC surfaces. Blocking experiments employing mAb directed toward β_2 show 88 ± 6% adhesion blocking in IC-21 cells and 80 ± 9% in BMMO cells, suggesting that β_2 integrins play an important role in establishing initial surface contacts on FC. Previous results for an analogous assay on peripheral blood-derived MC showed 70-100% cell adhesion blocking with the variation attributed to differences in β_2-directed mAb efficiency.[96] The higher (100%) adhesion blocking may reflect the naïve, non-adherent nature of the peripheral blood MC. Adherent cells cultured on solid two-dimensional substrates for extended periods of time (such as immortalized cell lines and the mature BMMO utilized here) likely exhibit an altered, diversified integrin expression profile that may contribute to lower adhesion blocking rates.

However, the incomplete block observed suggests a(n) additional mechanism(s) for cell attachment, given that flow cytometry shows 20-24% of the cell populations lack

a β_2 receptor, and blocking efficiency directed against β_2 is less than 100%. Other integrins may contribute to MC/MΦ adhesion. Analogous assay of β_1 integrin-mediated adhesion was unsuccessful due to high levels of non-specific binding for isotype controls. Non-integrin mediated cell attachment mechanisms may include non-specific binding, hydrophobic interactions and interactions (primarily electrostatic in nature) between heparin- (or heparin-like) binding domain ands proteoglycans or glycoproteins found on cells/surfaces.[103] However, that these are specific to MΦ adhesion on FC, and not other cell types shown refractory to FC binding, seems implausible. Additionally, endogenous MΦ fibronectin production demonstrated at early culture time points (30 minutes in some cases, Figure 4.10) may increase adsorbed matrix protein density sufficiently to increase numbers of cell adhesive sites available for cell interactions, resulting in cell-enhanced remodeling of the pre-existing adsorbed protein layer at the surface and facilitating additional MC/MΦ adhesion as cultures progress temporally. Finally, presence of surface-adsorbed fibronectin or other ECM protein sufficient to accommodate integrin attachment cannot be ruled out (except in the 100% BSA pre-adsorbed cultures), despite the lack of evidence from fluorescence studies and the strong supporting evidence for a predominantly albumin-covered surfaces.

4.6 Conclusions

Significant to the reported development of the FBR *in vivo* with implanted fluorinated polymers,[3,104] MΦ cultures were found to efficiently adhere to and colonize FC surfaces of two different chemical compositions *in vitro*. This distinct adhesive

behavior was exhibited by cells of both primary- (BMMO) and secondary- (IC-21) origin. At early time points, BMMO colonization was more successful on standard tissue culture substrates designed to promote cell adhesion, growth and proliferation compared to FC. However, BMMO cells were able to achieve nearly 100% confluent surface coverage on FC substrates as cultures progressed. Both FC substrate cultures were allowed to progress to extended (36 Day) time points not typically assayed *in vitro*. Some previous reports assay "non-adhesive" albuminated substrates such as FC for very short (~24 hours) time periods,[6] perhaps missing a more long-term efficient colonization of FC surfaces described here. Findings confirm numerous previous reports of "anomalous" MC/MΦ growth and motility on hydrophobic surfaces[30,56,79] that contrast the better-known poor adhesion characteristics typical of numerous cultured mammalian cell types on FC surfaces.[14,58,80,81]

Several protein pre-conditioning treatments had little effect on the consistent MΦ adhesion and colonization of FC substrates, although slightly improved cell adhesion was noted for FC surfaces pre-biased with known MΦ-adhesive protein[1,54] fibrinogen. Interestingly, despite presumed albumin dominance of this FC surface in culture media, pp-C3F8 surfaces were less permissive than Teflon® AF surfaces to BMMO cultures, suggesting that variations in FC surface chemical composition or architecture translate to altered protein conformations that affect these naïve cells in culture. Previous findings indicate that MC and activated MΦ cell lines adhere proficiently to denatured proteins, including albumin,[30,56] with direct relevance to the scenario described here given that 1) highly hydrophobic surfaces such as FC have

been shown to be albumin selective, 2) albumin was shown to be the major protein adsorbed to both FC surfaces tested here and 3) the mechanism of adhesion to FC surfaces was consistent with the findings of Davis,[30] i.e., functional blocking of the Mac-1 β_2 integrin significantly impaired the ability of BMMO and IC-21 cells to adhere to FC substrates. This suggests that the MΦ cells examined here primarily utilize integrin-mediated binding mechanisms to adhere to denatured proteins present on FC surfaces, and that this interaction may proceed via integrin interactions with epitopes exposed only after albumin denaturation or altered conformational state(s) are achieved.

Although mAb blocking experiments directed toward the β_2 integrin subunit of the Mac-1 receptor reduced cell adhesion substantially for both primary- and secondary-derived cells on FC substrates, limited adhesion was still observed, indicating that other interactions play a role in MΦ adhesion to FC surfaces. Collectively, these studies demonstrate that primary BMMO and secondary-derived IC-21 cells behave in a very similar manner with respect to adhesive capacity and mechanism, and cell morphology, motility and proliferative behavior on FC surfaces regardless of protein biasing. Yet, one difference was observed for the comparative case of BMMO cells grown to extended culture time (36 days) on pp-FC and Teflon® AF surfaces, which may reflect important phenotypic differences of these cell types that may be enhanced by extended culture times. Since many secondary cells lines are selected for their ability to grow in adhesion-dependent cultures, phenotypic differences between

primary (i.e., surface naïve) MΦ and those of secondary origin might be attributed to this selection bias.

4.7 Acknowledgements

The authors acknowledge Dr. A. García, Dr. G. Hagen, Dr. P. Gong, Dr. P. Wu and Dr. M. Gonzalez-Juarerro for helpful technical guidance. This work was funded by NIH grant EB 000894.

4.8 References

1. Tang L, Eaton JW. Inflammatory responses to biomaterials. *Am J Clin Pathol* 1995;**103**:466-71.

2. Anderson JM. Inflammatory response to implants. *ASAIO Trans* 1988;**34**:101-7.

3. Anderson JM. Biological responses to materials. *Annu Rev Mater Res* 2001;**31**:81-110.

4. Anderson JM. Multinucleated giant cells. *Curr Opin Hematol* 2000;**7**:40-7.

5. Dadsetan M, Jones JA, Hiltner A, Anderson JM. Surface chemistry mediates adhesive structure, cytoskeletal organization, and fusion of macrophages. *J Biomed Mater Res A* 2004;**71**:439-48.

6. Shen M, Horbett TA. The effects of surface chemistry and adsorbed proteins on monocyte/macrophage adhesion to chemically modified polystyrene surfaces. *J Biomed Mater Res* 2001;**57**:336-45.

7. Anderson NL, Anderson NG. The human plasma proteome: history, character, and diagnostic prospects. *Mol Cell Proteomics* 2002;**1**:845-67.

8. Andrade JD, Hlady V. Plasma protein adsorption: the big twelve. *Ann N Y Acad Sci* 1987;**516**:158-72.

9. Haynes CA, Norde W. Globular proteins at solid/liquid interfaces. *Coll Surf B* 1994;**2**:517-66.

10. Horbett TA. Principles underlying the role of adsorbed plasma proteins in blood interactions with foreign materials *Cardiovasc Pathol* 1993;**2**:137S-148S.

11. Norde W. Adsorption of proteins from solution at the solid-liquid interface. *Adv Colloid Interface Sci* 1986;**25**:267-340.

12. Garcia AJ, Vega MD, Boettiger D. Modulation of cell proliferation and differentiation through substrate-dependent changes in fibronectin conformation. *Mol Biol Cell* 1999;**10**:785-98.

13. Iuliano DJ, Saavedra SS, Truskey GA. Effect of the conformation and orientation of adsorbed fibronectin on endothelial cell spreading and the strength of adhesion. *J Biomed Mater Res* 1993;**27**:1103-13.

14. Dewez JL, Doren A, Schneider YJ, Rouxhet PG. Competitive adsorption of proteins: key of the relationship between substratum surface properties and adhesion of epithelial cells. *Biomaterials* 1999;**20**:547-59.

15. Horbett TA. The role of adsorbed proteins in animal cell adhesion. *Surf Coll B* 1994;**2**:225-40.

16. Sethuraman A, Han M, Kane RS, Belfort G. Effect of surface wettability on the adhesion of proteins. *Langmuir* 2004;**20**:7779-88.

17. Bohnert JL, Fowler BC, Horbett TA, Hoffman AS. Plasma gas discharge deposited fluorocarbon polymers exhibit reduced elutability of adsorbed albumin and fibrinogen. *J Biomater Sci Polym Ed* 1990;**1**:279-97.

18. Eberhart RC, Prokop LD, Wissenger J, Wilkov MA. Observation of albumin deposits on teflon surfaces. *Trans Am Soc Artif Intern Organs* 1977;**23**:134-40.

19. Eberhart RC, Munro MS, Frautschi JR, Lubin M, Clubb FJ, Jr., Miller CW, Sevastianov VI. Influence of endogenous albumin binding on blood-material interactions. *Ann N Y Acad Sci* 1987;**516**:78-95.

20. Eberhart RC, Munro MS, Williams GB, Kulkarni PV, Shannon WA, Jr., Brink BE, Fry WJ. Albumin adsorption and retention on C18-alkyl-derivatized polyurethane vascular grafts. *Artif Organs* 1987;**11**:375-82.

21. Keogh JR, Eaton JW. Albumin binding surfaces for biomaterials. *J Lab Clin Med* 1994;**124**:537-45.

22. Keogh JR, Velander FF, Eaton JW. Albumin-binding surfaces for implantable devices. *J Biomed Mater Res* 1992;**26**:441-56.

23. Keogh J, Eaton J. Albumin affinity for biomaterial surfaces. *Cells and Materials* 1996;**6**:209-220.

24. Absolom DR, Zingg W, Neumann AW. Protein adsorption to polymer particles: role of surface properties. *J Biomed Mater Res* 1987;**21**:161-71.

25. Kim SW, Lee RG, Oster H, Coleman D, Andrade JD, Lentz DJ, Olsen D. Platelet adhesion to polymer surfaces. *Trans Am Soc Artif Intern Organs* 1974;**20**:449-55.

26. Zucker MB, Vroman L. Platelet adhesion induced by fibrinogen adsorbed onto glass. *Proc Soc Exp Biol Med* 1969;**131**:318-20.

27. Munro MS, Quattrone AJ, Ellsworth SR, Kulkarni P, Eberhart RC. Alkyl substituted polymers with enhanced albumin affinity. *Trans Am Soc Artif Intern Organs* 1981;**27**:499-503.

28. Pitt WG, Cooper SL. Albumin adsorption on alkyl chain derivatized polyurethanes: I. The effect of C-18 alkylation. *J Biomed Mater Res* 1988;**22**:359-82.

29. Pitt WG, Grasel TG, Cooper SL. Albumin adsorption on alkyl chain derivatized polyurethanes. II. The effect of alkyl chain length. *Biomaterials* 1988;**9**:36-46.

30. Davis GE. The Mac-1 and p150,95 beta 2 integrins bind denatured proteins to mediate leukocyte cell-substrate adhesion. *Exp Cell Res* 1992;**200**:242-52.

31. Baszkin A, Lyman DJ. The interaction of plasma proteins with polymers. I. Relationship between polymer surface energy and protein adsorption/desorption. *J Biomed Mater Res* 1980;**14**:393-403.

32. Lassen B, Malmsten M. Competitive protein adsorption at radio frequency plasma polymer surfaces. *J Mater Sci Mater Med* 1994;**5**:662-665.

33. Wagner MS, Horbett TA, Castner DG. Characterization of the structure of binary and ternary adsorbed protein films using electron spectroscopy for chemical analysis, time-of-flight- secondary ion mass spectrometry, and radiolabeling. *Langmuir* 2003;**19**:1708-15.

34. Wagner MS, Castner DG. Characterization of adsorbed protein films by time-of-flight secondary ion mass spectrometry with principal component analysis. *Langmuir* 2001;**17**:4649-4660.

35. McFarland CD, De Filippis C, Jenkins M, Tunstell A, Rhodes NP, Williams DF, Steele JG. Albumin-binding surfaces: in vitro activity. *J Biomater Sci Polym Ed* 1998;**9**:1227-39.

36. Kiaei D, Hoffman AS, Horbett TA. Tight binding of albumin to glow discharge treated polymers. *J Biomater Sci Polym Ed* 1992;**4**:35-44.

37. Eberhart RC. Albumin adsorption and retention on C18-alkyl-derivatized polyurethane vascular grafts. *Artif Organs* 1987;**11**:375-82.

38. Grainger DW, Pavon-Djavid G, Migonney V, Josefowicz M. Assessment of fibronectin conformation adsorbed to polytetrafluoroethylene surfaces from serum

protein mixtures and correlation to support of cell attachment in culture. *J Biomater Sci Polym Ed* 2003;**14**:973-88.

39. Lateef S, Boateng S, Ahluwalia N, Hartman T, Russell B, Hanley L. Three-dimensional chemical structures by protein functionalized micron-sized beads bound to polylysine-coated silicone surfaces. *J Biomed Mater Res* 2005;**72A**:373-380.

40. Weisiger R, Gollan J, Ockner R. Receptor for albumin on the liver cell surface may mediate uptake of fatty acids and other albumin-bound substances. *Science* 1981;**211**:1048-51.

41. Tiruppathi C, Finnegan A, Malik AB. Isolation and characterization of a cell surface albumin-binding protein from vascular endothelial cells. *Proc Natl Acad Sci U S A* 1996;**93**:250-4.

42. Chaudhury C, Mehnaz S, Robinson JM, Hayton WL, Pearl DK, Roopenian DC, Anderson CL. The major histocompatibility complex-related Fc receptor for IgG (FcRn) binds albumin and prolongs its lifespan. *J Exp Med* 2003;**197**:315-22.

43. Zhu X, Meng G, Dickinson BL, Li X, Mizoguchi E, Miao L, Wang Y, Robert C, Wu B, Smith PD, Lencer WI, Blumberg RS. MHC class I-related neonatal Fc receptor for IgG is functionally expressed in monocytes, intestinal macrophages, and dendritic cells. *J Immunol* 2001;**166**:3266-76.

44. Arnaout MA. Structure and function of the leukocyte adhesion molecules CD11/CD18. *Blood* 1990;**75**:1037-50.

45. Corbi AL, Kishimoto TK, Miller LJ, Springer TA. The human leukocyte adhesion glycoprotein Mac-1 (complement receptor type 3, CD11b) alpha subunit. Cloning, primary structure, and relation to the integrins, von Willebrand factor and factor B. *J Biol Chem* 1988;**263**:12403-11.

46. Jongstra-Bilen J, Harrison R, Grinstein S. Fcgamma-receptors induce Mac-1 (CD11b/CD18) mobilization and accumulation in the phagocytic cup for optimal phagocytosis. *J Biol Chem* 2003;**278**:45720-9. Epub 2003 Aug 26.

47. Springer TA. Traffic signals for lymphocyte recirculation and leukocyte emigration: the multistep paradigm. *Cell* 1994;**76**:301-14.

48. Stewart M, Thiel M, Hogg N. Leukocyte integrins. *Curr Opin Cell Biol* 1995;**7**:690-6.

49. Springer TA. Adhesion receptors of the immune system. *Nature* 1990;**346**:425-34.

50. Anderson DC, Miller LJ, Schmalstieg FC, Rothlein R, Springer TA. Contributions of the Mac-1 glycoprotein family to adherence-dependent granulocyte

functions: structure-function assessments employing subunit-specific monoclonal antibodies. *J Immunol* 1986;**137**:15-27.

51. Lundahl J, Hallden G, Skold CM. Human blood monocytes, but not alveolar macrophages, reveal increased CD11b/CD18 expression and adhesion properties upon receptor-dependent activation. *Eur Respir J.* 1996;**9**:1188-94.

52. Gonzalez-Amaro R, Sanchez-Madrid F. Cell adhesion molecules: selectins and integrins. *Crit Rev Immunol* 1999;**19**:389-429.

53. Tang L, Eaton JW. Natural responses to unnatural materials: A molecular mechanism for foreign body reactions. *Mol Med* 1999;**5**:351-8.

54. Altieri DC, Agbanyo FR, Plescia J, Ginsberg MH, Edgington TS, Plow EF. A unique recognition site mediates the interaction of fibrinogen with the leukocyte integrin Mac-1 (CD11b/CD18). *J Biol Chem* 1990;**265**:12119-22.

55. Diamond MS, Staunton DE, Marlin SD, Springer TA. Binding of the integrin Mac-1 (CD11b/CD18) to the third immunoglobulin-like domain of ICAM-1 (CD54) and its regulation by glycosylation. *Cell* 1991;**65**:961-71.

56. Koyama Y, Norose-Toyoda K, Hirano S, Kobayashi M, Ebihara T, Someki I, Fujisaki H, Irie S. Type I collagen is a non-adhesive extracellular matrix for macrophages. *Arch Histol Cytol.* 2000;**63**:71-9.

57. Mauel J, Defendi V. Infection and transformation of mouse peritoneal macrophages by simian virus 40. *J Exp Med* 1971;**134**:335-50.

58. Webb K, Hlady V, Tresco PA. Relative importance of surface wettability and charged functional groups on NIH 3T3 fibroblast attachment, spreading, and cytoskeletal organization. *J Biomed Mater Res* 1998;**41**:422-30.

59. Godek ML, Malkov GM, Fisher ER, Grainger DW. Macrophage serum-based adhesion to surface chemistry is distinct from that exhibited by fibroblasts. *Plasma Proc Polym* 2006.

60. Godek ML, Duchsherer NL, McElwee Q, Grainger DW. Morphology and growth of murine cell lines on model biomaterials *Biomed Sci Instrum* 2004;**40**:7-12.

61. Godek ML, Sampson JA, Duchsherer ML, McElwee Q, Grainger DW. Rho GTPase protein expression and activation in murine monocyte/macrophages is not modulated by model biomaterial culture surfaces *in vitro*. *J Biomater Sci Polym Ed* 2006 (in press).

62. Makohliso SA, Giovangrandi L, Leonard D, Mathieu HJ, Ilegems M, Aebischer P. Application of Teflon-AF thin films for bio-patterning of neural cell adhesion. *Biosens Bioelectron.* 1998;**13**:1227-35.

63. Anamelechi CC, Truskey GA, Reichert WM. Mylar and Teflon-AF as cell culture substrates for studying endothelial cell adhesion. *Biomaterials.* 2005;**26**:6887-96.

64. Hershkoviz R, Alon R, Gilat D, Lider O. Activated T lymphocytes and macrophages secrete fibronectin which strongly supports cell adhesion. *Cell Immunol* 1992;**141**:352-61.

65. Alitalo K, Hovi T, Vaheri A. Fibronectin is produced by human macrophages. *J Exp Med* 1980;**151**:602-13.

66. Nathan CF. Secretory Products of Macrophages. *J Clin Invest* 1987;**79**:319-326.

67. Lewis C, McCarthy S, Lorenzen J, McGee Jd. Differential effects of LPS, IFN-gamma and TNFalpha on the secretion of lysozyme by individual human mononuclear phagocytes: relationship to cell maturity. *Immunology* 1990;**69**:402-408.

68. Godek ML, Malkov GM, Fisher ER, Grainger DW. Macrophage serum-based adhesion to surface chemistry is distinct from that exhibited by fibroblasts. *Plasma Proc. Polym.* 2006.

69. Malkov G, Martin IT, Schwisow WB, Chandler JP, Fisher ER. Pulsed plasma-induced micropatterning with alternating hydrophilic and hydrophobic surface chemistries. *Chem Mater* 2006, submitted.

70. Canavan HE, Graham DJ, Cheng X, Ratner BD, Castner DG. Comparison of the Extracellular Matrix with Adsorbed Protein Films using Mass Spectrometry. *Langmuir* To be sumbitted.

71. Lhoest JB, Wagner MS, Tidwell CD, Castner DG. Characterization of adsorbed protein films by time of flight secondary ion mass spectrometry. *J Biomed Mater Res* 2001;**57**:432-40.

72. Kaltenbach JP, Kaltenbach MH, Lyons WB. Nigrosin as a dye for differentiating live and dead ascites cells. *Exp Cell Res* 1958;**15**:112-7.

73. Rhoades ER, Orme IM. Similar responses by macrophages from young and old mice infected with Mycobacterium tuberculosis. *Mech Ageing Dev* 1998;**106**:145-53.

74. Woronzoff-Dashkoff KK. The wright-giemsa stain. Secrets revealed. *Clin Lab Med* 2002;**22**:15-23.

75. Bohnsack BL, Lai L, Dolle P, Hirschi KK. Signaling hierarchy downstream of retinoic acid that independently regulates vascular remodeling and endothelial cell proliferation. *Genes Dev* 2004;**18**:1345-58.

76. Gong P, Harbers GM, Grainger DW. Multi-technique comparison of immobilized and hybridized oligonucleotide surface density on commercial amine-reactive microarray slides. *Anal Chem* 2006;**78**:2342-51.

77. Collier TO, Thomas CH, Anderson JM, Healy KE. Surface chemistry control of monocyte and macrophage adhesion, morphology, and fusion. *J Biomed Mater Res* 2000;**49**:141-5.

78. Koenig AL, Gambillara V, Grainger DW. Correlating fibronectin adsorption with endothelial cell adhesion and signaling on polymer substrates. *J Biomed Mater Res A* 2003;**64**:20-37.

79. Rich A, Harris AK. Anomalous preferences of cultured macrophages for hydrophobic and roughened substrata. *J Cell Sci* 1981;**50**:1-7.

80. McClary KB, Ugarova T, Grainger DW. Modulating fibroblast adhesion, spreading, and proliferation using self-assembled monolayer films of alkylthiolates on gold. *J Biomed Mater Res* 2000;**50**:428-39.

81. Ruardy TG, Schakenraad JM, van der Mei HC, Busscher HJ. Adhesion and spreading of human skin fibroblasts on physicochemically characterized gradient surfaces. *J Biomed Mater Res* 1995;**29**:1415-23.

82. Godek ML, Sampson JA, Duchsherer ML, McElwee Q, Grainger DW. Rho GTPase protein expression and activation in murine monocyte/macrophages is not modulated by model biomaterial culture surfaces *in vitro*. *J. Biomater. Sci., Polym. Ed.* 2006 (submitted).

83. Zhao H, Ismail K, Weber SG. How fluorous is poly(2,2-bis(trifluoromethyl)-4,5-difluoro-1,3-dioxide-co-tetrafluoroethyl ene) (Teflon AF)? *J Am Chem Soc* 2004;**126**:13184-5.

84. Desai NP, Hubbell JA. Tissue response to intraperitoneal implants of polyethylene oxide-modified polyethylene terephthalate. *Biomaterials* 1992;**13**:505-10.

85. Kossovsky N, Millett D, Juma S, Little N, Briggs PC, Raz S, Berg E. In vivo characterization of the inflammatory properties of poly(tetrafluoroethylene) particulates. *J Biomed Mater Res* 1991;**25**:1287-301.

86. Gamble LJ, Ravel B, Fischer DA, Castner DG. Surface structure and orientation of PTFE films determined by experimental and FEFF8-calculated NEXAFS spectra. *Langmuir* 2002;**18**:2183-89.

87. Martin IT, Malkov G, Butoi CI, Fisher ER. Comparison of pulsed and downstream deposition of fluorocarbon materials from C_3F_8 and c-C_4F_8 plasmas. *J Vac Sci Technol* 2004;**22**:227-235.

88. Haidopoulos M, Turgeon S, Laroche G, Mantovani D. Chemical and morphological characterization of ultra-thin fluorocarbon plasma-polymer deposition on 316 stainless steel substrates: a first step toward the improvement of the long-term safety of coated stents. *Plasma Proc. Polym.* 2004;**2**:424-440.

89. Lewis D, Whateley TL. Adsorption of enzymes at the solid-liquid interface. I. Trypsin on polystyrene latex. *Biomaterials* 1988;**9**:71-5.

90. Sandwick R, Schray K. Conformational states of enzymes bound to surfaces. *J Coll Interface Sci* 1988;**121**:1-12.

91. Dana N, Styrt B, Griffin JD, Todd RF, 3rd, Klempner MS, Arnaout MA. Two functional domains in the phagocyte membrane glycoprotein Mo1 identified with monoclonal antibodies. *J Immunol.* 1986;**137**:3259-63.

92. Davis GE, Martin BM. A latent Mr 94,000 gelatin-degrading metalloprotease induced during differentiation of HL-60 promyelocytic leukemia cells: a member of the collagenase family of enzymes. *Cancer Res.* 1990;**50**:1113-20.

93. Falk W, Goodwin RH, Jr., Leonard EJ. A 48-well micro chemotaxis assembly for rapid and accurate measurement of leukocyte migration. *J Immunol Methods* 1980;**33**:239-47.

94. Loike J, Sodeik B, Cao L, Leucona S, Weitz J, Detmers P, Wright S, Silverstein S. CD11c/CD18 on neutrophils recognizes a domain at the N terminus of the A alpha chain of fibrinogen. *Proc. Natl. Acad. Sci. USA* 1991;**88**:1044-1084.

95. Marks PW, Hendey B, Maxfield FR. Attachment to fibronectin or vitronectin makes human neutrophil migration sensitive to alterations in cytosolic free calcium concentration. *J Cell Biol.* 1991;**112**:149-58.

96. McNally AK, Anderson JM. Beta1 and beta2 integrins mediate adhesion during macrophage fusion and multinucleated foreign body giant cell formation. *Am J Pathol.* 2002;**160**:621-30.

97. Flick MJ, Du X, Witte DP, Jirouskova M, Soloviev DA, Busuttil SJ, Plow EF, Degen JL. Leukocyte engagement of fibrin(ogen) via the integrin receptor alphaMbeta2/Mac-1 is critical for host inflammatory response in vivo. *J Clin Invest* 2004;**113**:1596-606.

98. Underwood PA, Bennett FA. A comparison of the biological activities of the cell-adhesive proteins vitronectin and fibronectin. *J Cell Sci.* 1989;**93**:641-9.

99. Hayman EG, Pierschbacher MD, Suzuki S, Ruoslahti E. Vitronectin--a major cell attachment-promoting protein in fetal bovine serum. *Exp Cell Res.* 1985;**160**:245-58.

100. Steele JG, Dalton BA, Johnson G, Underwood PA. Polystyrene chemistry affects vitronectin activity: an explanation for cell attachment to tissue culture polystyrene but not to unmodified polystyrene. *J Biomed Mater Res* 1993;**27**:927-40.

101. Grinnell F, Feld MK. Adsorption characteristics of plasma fibronectin in relationship to biological activity. *J Biomed Mater Res* 1981;**15**:363-81.

102. Luscinskas FW, Kansas GS, Ding H, Pizcueta P, Schleiffenbaum BE, Tedder TF, Gimbrone MA, Jr. Monocyte rolling, arrest and spreading on IL-4-activated vascular endothelium under flow is mediated via sequential action of L-selectin, beta 1-integrins, and beta 2-integrins. *J Cell Biol* 1994;**125**:1417-27.

103. Harbers GM, Grainger DW. Cell-Material Interactions: Fundamental Design Issues for Tissue Engineering and Clinical Considerations. In: Guelcher SA, Hollinger JO, eds. An Introduction to Biomaterials. Boca Raton: CRC Press, 2006:15-45.

104. Williams DF, Homsy CA. Biocompatibility of Clinical Implant Materials. Cro Press, 1981:60-77.

4.9 Supplemental Figures

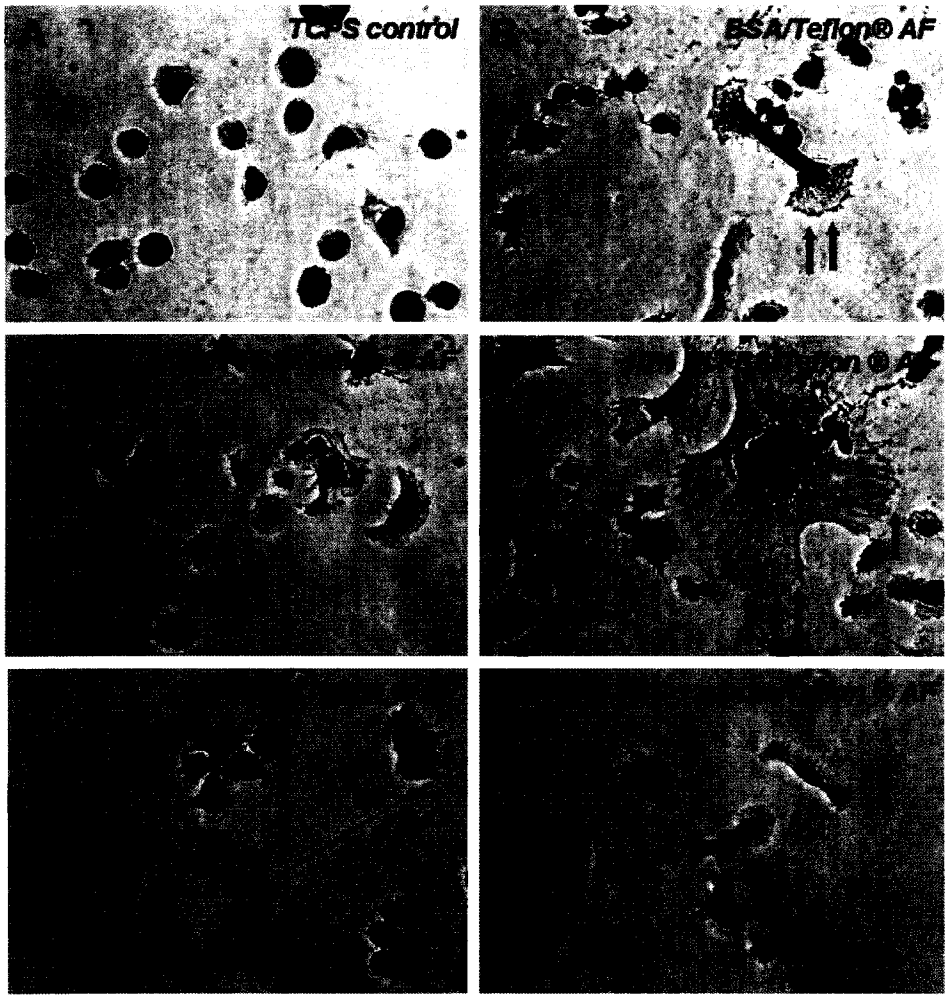

Figure 4.1.S Phase contrast photomicrographs of fixed, stained IC-21 cells one hour after seeding onto Teflon® AF surfaces exposed to preconditioning treatments as indicated. Cells were seeded at a density of 500 cells/mm^2. Bold arrows indicate membrane ruffling. Images are representative of multiple fields (≥ 3) and multiple replicates (≥ 2) for each test condition. Scale bar shown in F is relevant for all images. Images are labeled with letters to simplify references in the text.

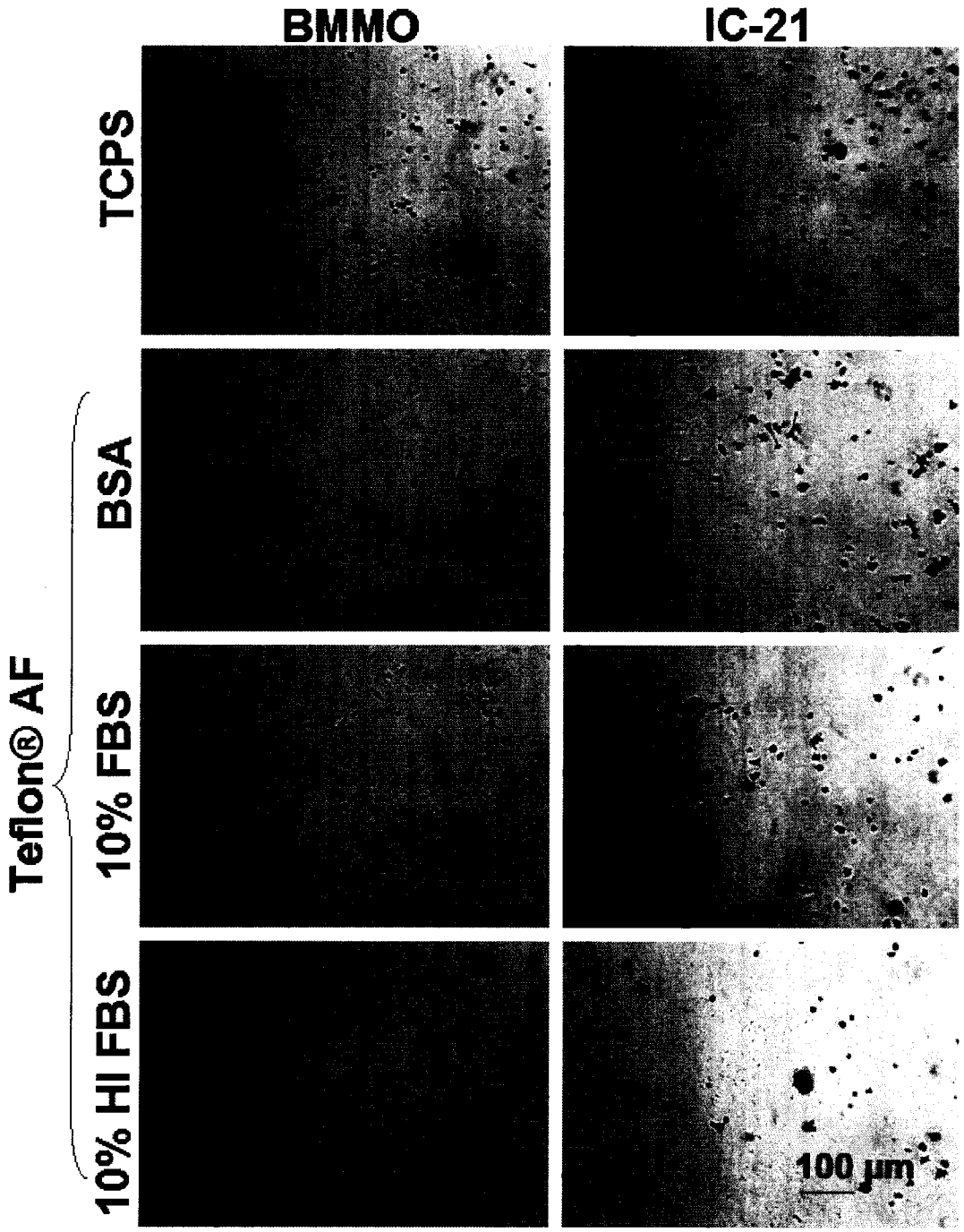

Supplemental Figure 4.2.S Phase contrast photomicrographs of fixed, stained BMMO and IC-21 cells one hour after seeding onto TCPS and Teflon® AF surfaces exposed to preconditioning treatments as indicated. Cells were seeded at a density of 500 cells/mm^2. BMMO results are typical (differences in number of adherent cells) for one hour evaluation, i.e., cells adhere, grow and proliferate on all surfaces over time-see Figure 4.4 for examples. Images are representative of multiple fields (≥ 3) and multiple replicates (≥ 2) for each test condition. Scale bar shown in H is relevant for all images.

CHAPTER 5: SUMMARY AND FUTURE DIRECTIONS

5.1 Summary

The work described here explored (MC-) MΦ cell behavior to select biomedically-relevant polymer surfaces under standard *in vitro* culture conditions. Initially, observations and comparisons of (MC-) MΦ cell behavior on control and model polymer surfaces were made. Differences in gross morphological features have previously been linked to changes in DNA synthesis and cell growth in primary cells,[1] and our observations of cell morphology influenced selection of specific molecular-level targets such as the Rho GTPases, in an effort to provide insight to the basic molecular level events governing (MC-) MΦ cell adhesion, spreading and proliferation, necessary to the establishment of a foreign body inflammatory reaction. Significant findings of this work include:

- (MC-) MΦ cells adhered to and efficiently colonized substrates that are considered non- or poorly permissive for mammalian cell adhesion, growth and proliferation *in vitro* (i.e., PS, Teflon® AF, pp-FC). This behavior was exhibited by cells of both primary and secondary derivation, and of varying maturity.

- When cultured on substrates with alternating hydrophilic and hydrophobic regions, (MC-) MΦ cells preferentially bound to hydrophobic substrates that are refractory to the growth of other cell types (endothelial, fibroblasts, etc.) until surface space became limiting.

- Surfaces were generally activating to (MC-) MΦ cells *in vitro*, likely due to the presence of (denatured) adsorbed proteins.

- BMMO and IC-21 MΦ adhesion to Teflon® AF FC surfaces was found to be significantly reduced by blocking the β_2 integrin of the Mac-1 receptor.

- Cells of primary origin (BMMO) behaved in similar and dissimilar manners to cell lines (IC-21, RAW 264.7 and J774A.1), depending on the specific experimental context.

- Cell lines IC-21, RAW 264.7 and J774A.1 may behave in a similar or dissimilar manner to each other, depending on the specific context

5.2 Future Work

Numerous previous studies of materials utilized for biomedical device construction employ (MC-) MΦ cells to examine cytotoxicity, inflammatory response and general "biotolerance". The selection of the specific cells employed to this end is often limited by what is available, inexpensive and practical, typically excluding primary cells. Numerous

cell lines of MC and/or MΦ origin from human and murine sources are available, each with different morphologies, adhesion patterns and growth requirements. For instance, the IC-21 murine cell line is an adherent, trypsin-sensitive cell line. Thus, it grows readily on surfaces without the addition of activating agents such as phorbol esters, yet is cannot be trypsinized from surfaces like other cells. In contrast, human MC lines such as U937 require a stimulus for initial adherence *in vitro*. Both cell types are oft employed in biomaterial studies, but comparison of results for cells types from different species, of varied maturity and with different growth, subculture and harvesting requirements is problematic. A thorough characterization of each cell type would support some comparison, but consensus is lacking in terms of what markers are appropriate for distinguishing maturity and differentiation, especially between the closely related MΦ and dendritic cell. Characterization via surface marker detection is commonly employed, but often it relies on relative levels of expression rather than presence or absence of markers to distinguish between cells of the mononuclear phagocyte system. This begs the question-- are these cells truly different or rather specialized adaptive states? [2] Further, no single marker can be used to define a MΦ. It has been suggested by Hume that based on new insight provided by detailed characterizations of cells of the mononuclear system in recent years that a revised system for classifying immune cells of this lineage is overdue.[2]

Considering many different types of cell culture supports and their effects on MΦ, it is evident that there is no unambiguous culture substrate to which other materials can be compared,[3] and results reported here (Chapter 3) suggest that all surfaces tested were activating to MΦ (see also Appendix B.7). The activating nature of the surface may result

from denatured or partially denatured proteins adsorbed to the surface that act as attractants and/or provide MΦ activating cues. Previous reports indicate that denatured proteins serve as non-specific attractants for granulocytes.[4] Recently, efforts to develop and employ new materials that mimic the three-dimensional environment more natural to cells have led to commercial synthetic support production (e.g., Ultra-Web® Synthetic ECM, SurModics/Donaldson®) for use in static cultures.[5] Culture methods have seen some advances, examples include roller bottle systems (designed to more closely represent cell growth in the presence of shear forces) and spinner flasks (designed to support suspended cell growth). Advances represent efforts to more accurately mimic *in vivo* conditions for *in vitro* studies.[6] Additional considerations for appropriate design of *in vitro* studies require the use of serum, given that serum proteins play a determinant role in cell interaction with surfaces *in vivo*. MΦ studies can be complicated by the presence of contaminating levels of endotoxins produced by bacteria. Therefore, all studies that employ MΦ should also describe measures taken to test for and reduce endotoxin contamination.

In order to advance in our quest for biocompatible materials we must first develop a thorough understanding of the FRB, which necessitates a detailed understanding of MΦ phenotype and function in this unique context. With the advent of new molecular characterization techniques and the likely discovery of novel MΦ markers the relative relationships between cells of the mononuclear phagocyte system should be clarified. Additionally, understanding of the role of relatively new markers related to MΦ fusion

(e.g., CD 47),[7] and comparison to MΦ specific (maturity) markers should allow a more detailed picture of the MΦ phenotype found at biomaterials surfaces.

Given that cell lines are certain to remain in use for practical purposes, improved phenotypic characterization should aid in the selection of specific cell lines that most faithfully represent primary cells within the experimental context. Specific guidelines for appropriate experimental design (serum inclusion, endotoxin testing, etc.) in the context of biomaterials testing must be followed to collect meaningful data. Relevant to *in vitro* work, characterization and comparison of immature and mature (aged) primary-derived cells to MΦ cell lines with respect to integrin expression on both standard tissue culture supports and model biomaterial surfaces would provide insight to the suitability of employing (aged, immortalized) adherent MΦ cultures that may be "prebiased" with respect to integrin expression based solely on culture methods. The same argument could be applied to MΦ activation and inflammatory cytokine production.

Studies must be carefully designed to be relevant to FBR progress *in vivo*, and full FBR modeling requires an understanding of relationships between specific subsets of MC-MΦ as well as MΦ interaction with other cell types (e.g., fibroblasts, lymphocytes). Future work should address a thorough characterization of all MΦ phenotypes present at implant sites (adherent, activated or fused MΦ). This could be attempted *in situ* using specific markers directed toward surface antigens or soluble chemokine/cytokine products, or using techniques that allow cell sorting based on size and various surface markers. A combination of techniques will likely yield the most convincing results in terms of FBR

event sequelae. Understanding the molecular events underlying the FBR should allow for improved biocompatibility through modification and modulation of both materials and host inflammatory response.

5.3 References

1. Folkman J, Moscona A. Role of cell shape in growth control. *Nature* 1978;**273**:345-9.

2. Hume DA. The mononuclear phagocyte system. *Curr Opin Immunol* 2006;**18**:49-53.

3. van Kooten TG. Growth of cells on polymer surfaces Encyclopedia of Surface and Colloid Science. New York, NY: Marcel Dekker, Inc., 2004:1-19.

4. Davis GE. The Mac-1 and p150,95 beta 2 integrins bind denatured proteins to mediate leukocyte cell-substrate adhesion. *Exp Cell Res* 1992;**200**:242-52.

5. Schindler M, Ahmed I, Kamal J, Nur EKA, Grafe TH, Young Chung H, Meiners S. A synthetic nanofibrillar matrix promotes in vivo-like organization and morphogenesis for cells in culture. *Biomaterials* 2005;**26**:5624-31.

6. Folch A, Toner M. Microengineering of cellular interactions. *Annu Rev Biomed Eng* 2000;**2**:227-56.

7. Han X, Sterling H, Chen Y, Saginario C, Brown EJ, Frazier WA, Lindberg FP, Vignery A. CD47, a ligand for the macrophage fusion receptor, participates in macrophage multinucleation. *J Biol Chem* 2000;**275**:37984-92.

APPENDICES

APPENDIX A: BACKGROUND-MACROPHAGE ORIGIN, CHARACTERISTICS AND FUSION PRODUCTS

A.1 Macrophage origin

Macrophages (MΦ) represent the major differentiated cell of the mononuclear phagocyte system, are widely distributed throughout the body and exhibit a broad range of structural and functional heterogeneity, often associated with "immunocompetency" and localization within specific tissues.[1] The mononuclear phagocyte system, comprising bone marrow monoblasts and promonocytes, circulating peripheral blood monocytes, and tissue-resident MΦ (Figure A.1), is largely responsible for protecting the body from insulting entities of various origins. MΦ can be found in the skin, synovium, central nervous system, gastrointestinal tract, liver, lungs, serous cavities, and the lymphoid organs where they participate in physiological and pathological processes of great variety.[1] MΦ cells represent a highly adaptable and dynamic cell population with the ability to alter their physical appearance and biochemical profile in response to activating cues present in their local environment.

The MΦ originates in the bone marrow, where the cell population includes not only resident MΦ but also precursors including monoblasts, promonocytes and monocytes (MC). MC and neutrophils are thought to share a common progenitor cell, the "colony forming unit, granulocyte-macrophage" (CFU-GM).[3] MC progress through several stages

of maturity, each associated with increased functionality, before reaching their terminally differentiated states in tissues (Figure A.1). It is likely that MC remain in the bone marrow for less than 24 hours before entering the peripheral blood, where they distribute between the circulating and marginating pools.[4,5] MC have a half-life of 17.4 hours in mice,[6] up to 70 hours in humans,[7] and constitute between one and six percent of the of the total white blood cell count, approximately 300-700 cells per microliter of blood.[1] This circulating form is frequently harvested and differentiated to MΦ that serve as a primary culture in experimental models. MC may migrate into extravascular tissues where they differentiate to MΦ, relying on local cues for phenotype. After transition, MC do not return to circulation, but reside in the organ, tissue or implant site for several months as mature, terminally differentiated MΦ.[1] Approximately 95% of tissue-resident MΦ derive from MC; the remaining 5% derive from local division of mononuclear

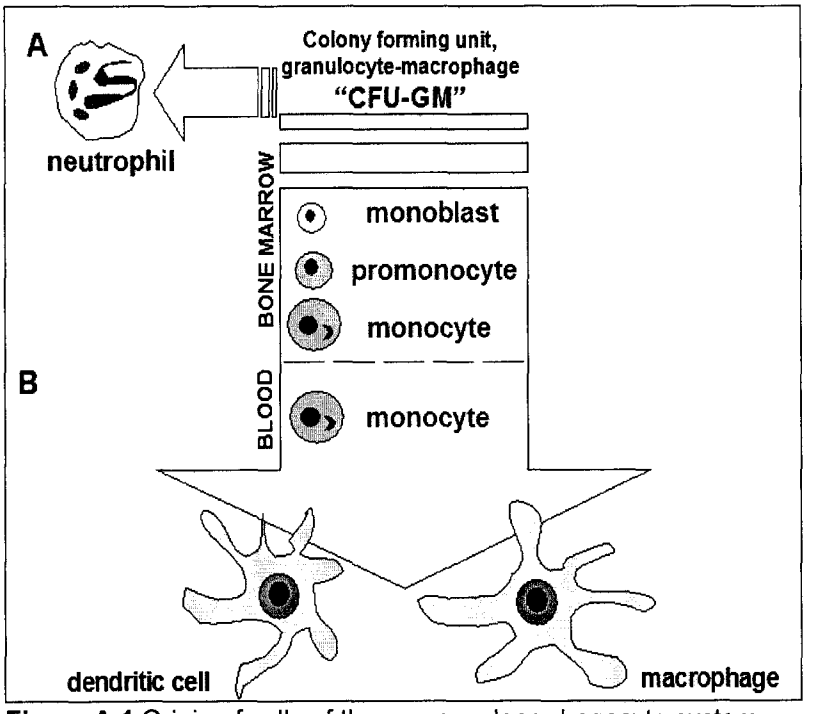

Figure A.1 Origin of cells of the mononuclear phagocyte system. A) Neutrophils and monoblasts derive from a common precursor, the colony forming unit, granulocyte-macrophage, "CFU-GM". Promonocytes precede monocytes (MC) in maturity. MC originate in the bone marrow and pass into the blood and tissues. B) MC mature to dendritic cells (DC) or macrophages (MΦ) in response to local chemical cues. Note: cartoons are not to scale.

phagocytes within the tissue that have yet to complete cell division.[8] During acute inflammatory reactions the number of circulating MC increases, reflecting increased production in the bone marrow;[9] circulation time is shortened due to rapid efflux of cells into inflammatory exudates.[10]

MC are one of two cell types known to differentiate to dendritic cells[11] (DC), the most competent antigen presenting cells known[12] (Figure A.1). *In vitro*, this maturation process is facilitated by the addition of granulocyte-macrophage colony stimulating factor (GM-CSF) and IL-4, which are known to push $CD14^+$ MC toward a DC phenotype.[13,14] *In vivo*, DC are migratory cells that may be found in the blood and lymph (veiled cells), in secondary lymphoid tissues (interdigitating DC), in organs (interstitial DC) and in the epidermis and mucous membranes (Langerhans cells). Like MΦ, DC function and phenotype varies based on the local environment. Collectively and constitutively, DC express more MHC class II and co-stimulatory molecules required for antigen presentation to T cells than MΦ, and this is one of the main distinctions between these two cell types.

A.2 Macrophage morphology

The appearance and size of cells of the mononuclear phagocyte system changes as cells progress toward a fully differentiated mature state. Monoblasts and promonocytes are smaller and less complex in both appearance and function than either MC or MΦ.[1] MΦ possess a single, spherical concentric nucleus containing several nucleoli, and typically exhibit a ruffled margin and many fine cytoplasmic granules.[15] MΦ morphology on

artificial substrates such as two-dimensional cell culture supports is altered. Cells grown on these surfaces display a somewhat distorted and non-physiologically equivalent

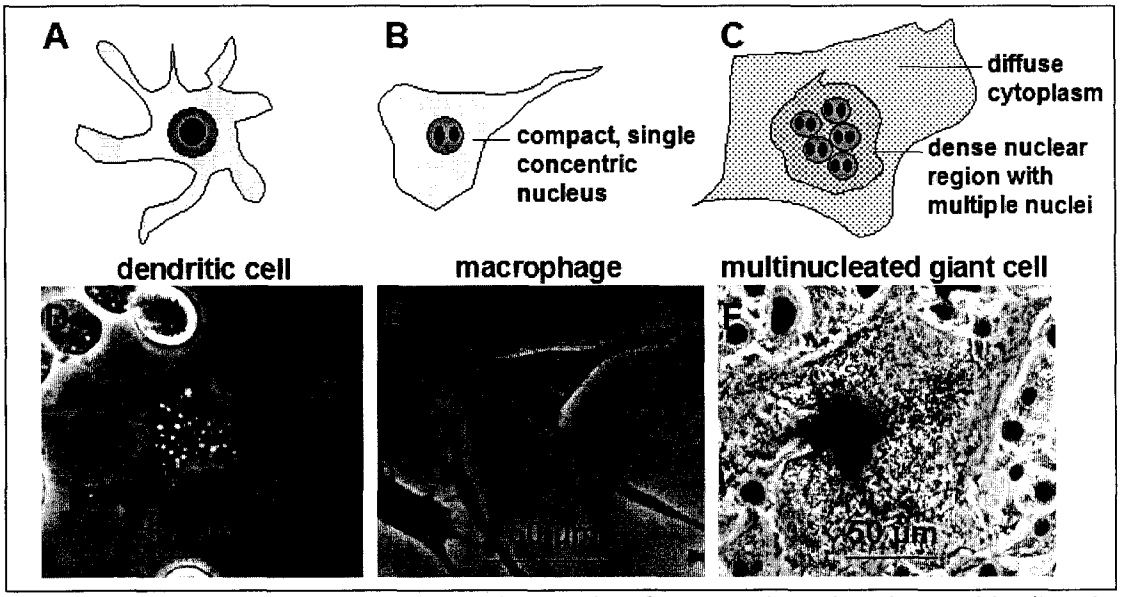

Figure A.2 Cartoon depiction and photomicrographs of cell morphologies observed *in vitro*. A and D) dendritic cells, B and E) macrophage cells, and C and F) multinucleated giant cells. Cell morphology reflects the two-dimensional nature of the culture substrate the cells are grown on. Cells take on a flattened or compressed morphology as compared to the more natural spherical morphologies of cells *in vivo*. D) J774A.1 cells take on the appearance of a dendritic cell in response to exogenous cytokine treatment (10 ng/ml GM-CSF and IL-4). E) An example of IC-21 macrophage morphology on tissue culture polystyrene. F) An example of the fusion product of multiple bone marrow-derived macrophages in the presence of exogenous cytokines (5 ng/ml M-CSF, 10 ng/ml IL-4). Note: cartoons are not to scale.

morphology that is flattened and elongated (Figure A.2). The morphology and growth pattern of each cell type utilized in experiments described in Chapters 2-4 is shown in Figure A.3. In response to exogenous cytokine addition *in vitro*, MΦ cells may fuse to form multinucleated giant cells (MnGC), or develop a "foamy" appearance (Figure A.4). *In vivo*, foamy cells are associated with diseased states and are often described in the literature as a pathological feature. This phenotype may reflect the uptake of an excess of external materials such as cholesterol,[16] surfactants[17] or bacteria.[18]

A.3 Macrophage maturity and activation

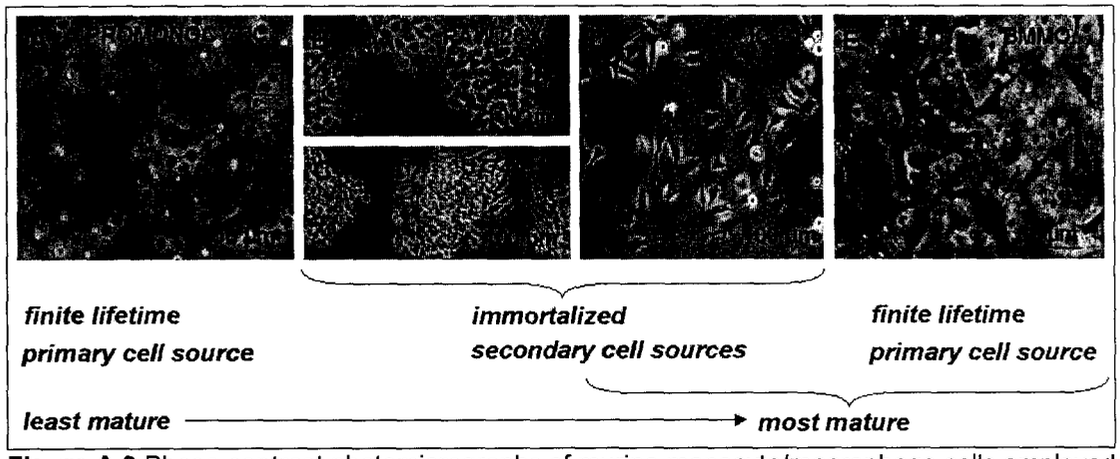

Figure A.3 Phase contrast photomicrographs of murine monocyte/macrophage cells employed in experiments. A) Bone marrow-derived (BMMO) primary culture, consisting of non-adherent monocytes (small white spheres, arrows), adherent monocyte/macrophages (dark spheres, boxes), and adherent macrophages (large cells, circles) 2 days post-seeding. Typical growth patterns and morphologies for sub-confluent cultures of RAW 264.7 (B) and J774A.1 (C) monocyte-macrophages and IC-21 (D) macrophages. All three cell lines demonstrate motile phenotypes, indicated by the presence of filopodia [2] and membrane ruffling. E) BMMO matured 7 days in complete growth medium. Note the difference in cell size compared to primary derived culture shown in panel A at day 2. All cells were grown on tissue culture polystyrene.

MΦ mature in response to local cues, resulting in their heterogeneous distribution throughout the body. Upon terminal differentiation, cells exhibit altered or enhanced effector cell functions. Physical surfaces employed for cell culture are often relied upon to differentiate precursor cells (MC) to MΦ cells *in vitro*, as surfaces alone may serve as sufficient stimuli to promote MΦ phenotype development. Further, it has been reported that MΦ maturity effects the formation of MnGC *in vitro.*[19]

Generally, MΦ activation can be described as the enhancement of a pre-existing characteristic and/or the acquisition of new or enhanced biochemical or functional activity. Activated MΦ display more class II major histocompatibility complex (MHC), are more phagocytic, and release more cytokines (e.g., interleukin-1, IL-1) than their un-

activated counterparts.[20] As a sentinel of the immune system, MΦ play a critical role in host defense against a diverse group of environmental challenges.[21,22] MΦ activation is an essential part of the response to and clearance of harmful entities. Extreme activation leads to the overproduction of chemical mediators, which may in turn result in systemic imbalances often leading to tissue damage/necrosis, anaphylactic shock and death.

Cytokines are potent MΦ activators capable of modulating MΦ function. Cytokines are low molecular weight regulatory proteins or glycoproteins secreted by numerous cell types involved in cell-to-cell communication.[23] Importantly, MΦ produce many cytokines, which may act on various cell types including other MΦ. Inflammatory cytokine production may be the consequence of exposure to bacterial endotoxins (e.g., lipopolysaccharide, LPS), viral particles, or priming factors (e.g., interferon γ, IFN-γ).[24] A list of cytokines produced by MΦ and their biological actions can be found in Table A.1.

'Cytokine' is the general name implied to include the more specific monokines and lymphokines (cytokines secreted by MC and MΦ, and lymphocytes, respectively). Many of the cytokines are interleukins, which are secreted by and act on leukocytes.[23] Cytokines can be effective in picomolar concentrations due to high binding affinities (typical $K_D = 10^{-10}$ to 10^{-12}) [23] and are generally known to have specific effects on, and thus elicit specific responses from, MΦ. IFN-γ,[25] IFN-α,[26] TNF,[27] IL-2,[28] IL-4,[29] M-CSF[30] and GM-CSF[31] have all been shown to be activating to MΦ.

MΦ Cytokine Product[a]	Stimulus for Production[a]	Biological Action[a]	T_H1/T_H2[a]	Induces Production of[a]	Cell Type(s) Affected[a]
G-CSF	IL-1, LPS	Granulocyte colony stimulation, terminal differentiation of myeloid cells, enhanced neutrophil function	----	----	Granulocytes, myeloid stem cells, neutrophils
GM-CSF	IL-1, TNF, LPS, retroviral infection	Granulocyte, eosinophil and MΦ colony stimulation, enhanced neutrophils/eosinophil function	T_H1	IL-1, TNF, PGE_2, O_2	MΦ, eosinophils, granulocytes
M-CSF	IL-1, LPS	MΦ colony stimulation, antiviral	----	IL-1, IFN-γ, TNF-α, PGE_2, PA	MΦ
TNF-α	IL-1, IL-2, GM-CSF, LPS	Tumor necrosis, endotoxic shock-like syndrome, cachexia, fever, acute phase protein response	T_H1	IL-1, IL-6, GM-CSF, MHC I, MHC II	MΦ
IL-1	IL-2, TNF, GM-CSF, antigen presentation	Fever, acute phase protein response, hypotension; increased ICAM-1 expression (endothelial cells)	----	IL-2, IL-4, IL-6, TNF, PGE_2, collagenase	MΦ, endothelial cells
IL-6	IL-1, TNF, PDGF	Hemopoietic cell proliferation, fever, acute phase protein response	T_H2	IL-2R (T-cells), IgG (B-cells)	MΦ, T-cells, B-cells
IL-10	T and B cell activation, LPS	Inhibitory to T cell proliferation & cytokine production	T_H2	MHC II	MΦ, T-cells, B-cells
IL-12	T cell activation, LPS	Promotion of cell mediated immunity, activated T and NK cell proliferation	T_H1	IFN-γ	T-cells
TGF-β	----	Fibrosis & wound healing *in vivo*, influences integrin expression & differentiation	----	----	MΦ, T-cells, B-cells, epithelial cells
FGF	----	Angiogenesis *in vivo*, endothelial cell chemotaxis & growth	----	IFN-γ	Endothelial cells, myoblasts
PDGF	LPS, lectins, zymosan, thrombin coagulation	Neutrophil activation, collagen synthesis augmentation, mesenchymal cell proliferation and chemotaxis	----	IL-1, IL-1R, IFN-β, IFN-γ, PGE_2	Neutrophils, mesenchymal cells
EGF	----	Angiogenesis, wound healing, proliferation/differentiation of basal epithelial cells	----	----	Epithelial cells
MIP-1α	----	Neutrophil recruitment, regulation of hemopoiesis	----	----	Neutrophils
MDC	----	Chemoattractant	----	----	DC, T-cells, NK cells

Table A.1 Select MΦ cytokine products and their effects. Other MΦ cytokine products include: IFN-α, IL-8, IL-15, IL-16, and IL-18.[1,23,32-41] [a]Abbreviations as used in text.

In addition to cytokines, chemokines play a role in influencing MΦ populations. Chemokines are a superfamily of small polypeptides that selectively control leukocyte activation, adhesion and chemotaxis[42] and typically have multiple effects on their target cells.[43] More than fifty leukocyte chemoattractant cytokines have been identified in human and murine systems.[44-46] Chemokines are produced by MC, MΦ, neutrophils, eosinophils, platelets, mast cells, natural killer cells, T and B lymphocytes and epithelial, mesothelial and endothelial cells.[47]

Other activators commonly employed to stimulate MC/MΦ cells *in vitro* are LPS, a mitogen, and phorbol esters (e.g., phorbol 12-myristate 13-acetate (PMA), 12-O-tetradecanoylphorbol-13-acetate (TPA), and others), which act as differentiating Agents.[48] LPS is an endotoxin present in gram-negative bacterial cell walls,[49] often associated with systemic bacterial infections, that leads to MΦ activation and subsequent production of inflammatory cytokines.[24] LPS induces cytokine gene expression via numerous transcription factors including members of the AP-1, C/EBP, Ets, and NF-κB/rel families.[50] Other bacterial components including peptidoglycans, trehalose diesters, lipoteichoic acid and lipomannans are all recognized by and activating to MΦ.[50]

Phorbol esters are tumor promoters that are capable of binding to and activating protein kinase C (PKC), one critical component in T-cell activation.[51,52] PMA is a structural analog of diacylglycerol (DAG), an allosteric activator of PKC. PKC activation via phosphorylation leads to calcium release, resulting in a cascade of cellular responses including rapid proliferation.[52] Experimentally, phorbol esters have been used as

chemoattractants (e.g., TPA[51]) and to differentiate monocytic cells to adherent MΦ cultures (e.g., PMA[53-56]). Phorbol esters are metabolized slowly, thus their effects are long lasting.[57]

A.4 Macrophage secretory products

In addition to cytokine and chemokine production, MΦ and cells of the mononuclear phagocyte system are known to produce a wide range of substances (over 100) varying in size (32-440 kD) and biological activity, affecting virtually every aspect of cell behavior from cell growth to cell death.[40] Enzymes such as lysozyme, proteases and lipases, as well as enzyme inhibitors, complement components, adhesive proteins (fibronectin),[40] reactive oxygen intermediates,[40] and coagulation factors are all known secretory products of MΦ.[1,40,58] MΦ secretory profiles may be affected by maturity and local environmental cues.

A.5 Macrophage surface receptors

MΦ response is often modulated though different combinations of effector molecules (e.g., cytokines) acting on specific receptors;[1] thus, the presence of specific receptors on MΦ correlates to specific (acquired) functions and activation profiles. Further, MΦ maturity and/or differentiation state is/are often characterized based on the presence or absence of specific surface receptors (e.g., F4/80, Mac-1).[59] Receptor profiles vary between cells of primary and secondary derivation, and between cell lines.[60] Select maturity markers are shown in Table A.2.

Cell Type	Immaturity Markers[a]	Maturity Markers
Promonocyte	Unknown	FcR
BMMO	Unknown	F4/80+[b], CD11b+[b]
J774A.1	ER-MP12-/20-/54-/58-	F4/80+, Mac-1 +, FcR
RAW 264.7	ER-MP12-/20-/54-/58-	F4/80+, Mac-1 +
IC-21	None known	F4/80+[b], Mac-1 +, FcR

Table A.2 Select characteristics of cells employed in these studies. [a]ER-MP12, ER-MP20, ER-MP54 and ER-MP58 are monoclonal antibodies used to classify immature mouse MΦ as described by the system of Leenan *et al*[59-62]. [b]Preliminary unpublished findings, L. M. Chamberlain.

Among the first surface receptors to be identified on MΦ were Fc from IgG[63] and complement protein C3.[64] Others include lipoprotein, fibronectin, laminin, fibrinogen, hormone, chemokine, lectin-like, adhesion and migration, and advanced glycosylation endproducts [65] receptors.[1] The mannose receptor (MMR) is a classic phagocytic receptor highly upregulated by IL-4 and implicated in IL-4-induced fusion to FBGC.[66] Cytokine receptors include numerous interleukins (IL-1, IL-2, IL-3, IL-4, IL-6, IL-7, IL-10, IL-13, IL-16, IL-17), macrophage-colony stimulating factor (M-CSF/CSF-1) and GM-CSF, interferons (IFN-α, IFN-β, IFN-γ), and many others.[1] Chemokine receptors have also been identified: CCR1, CCR2, CCR5, CCR8, CCR9, CXCR1, CXCR2, CXCR4 and CX3CR1.[1] Significantly, no single marker has been determined to reliably distinguish MΦ from DC.[67]

A.6 Macrophage fusion products-giant cells

An alternate terminal developmental stage exhibited by cells of the mononuclear phagocyte system is the fusion product of multiple cells to produce a multinucleated giant

cell (MnGC, Figure A.4).[1] The first reported observation of these cells dates to 1868[68] by Langhans, and later reports (1912, 1925 and 1927, respectively) by Lambert and the Lewises.[69-71] Three types of giant cells are most commonly referred to in the literature, the osteoclast, the Langhans cell and the foreign body giant cell (FBGC). Each is distinct in location and appearance, but all share common traits: 1) derivation from cells of the mononuclear phagocyte system, 2) a role in tissue remodeling and/or immune defense, 3) an association with disease and tumors.[72] These cells are well known to be the products of fusion, not cell division in the absence of cytokinesis.[72-76]

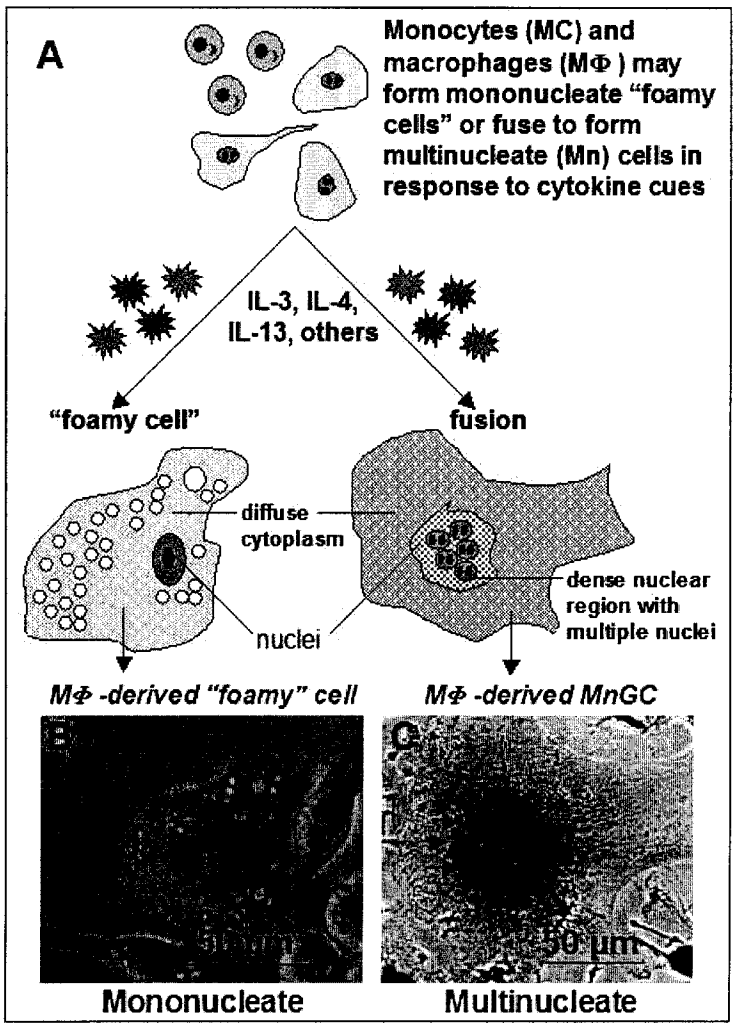

Figure A.4 A) The cellular products of monocyte (MC) and macrophage (MΦ) cells exposed to specific cytokine cues. Cytokine stimulation may result in the production of "foamy" cells, which are characterized by the presence of numerous vesicles and are named for their foamy appearance. Alternatively, MC and MΦ may fuse to produce multinucleated giant cells (MnGC). Photomicrographs of MΦ-derived foamy (E) and MnGC (F) cells are shown. Note: cartoons are not to scale.

Osteoclasts are found on the bone which they resorb, and play a key role in bone tumors, bone transplant rejection and in the pathogenesis of osteoporosis.[72] Langhans

cells (not to be confused with the epithelial dendritic Langerhans cell) are examples of giant cells that are frequently encountered in diseased states involving granulomatous lesions such as tuberculosis, syphilis, sarcoidosis, and deep fungal infections.[68,77] These cells exhibit a nuclear arrangement that is horseshoe- or circular in shape, and the nuclei are found at the periphery of the cells.

The FBGC is the hallmark of the foreign body reaction (FBR) to implant materials and devices, and may contain over a hundred nuclei.[78,79] In contrast to the peripheral nuclear arrangement of the Langhans cell, the nuclei of the FBGC are found in a dense central location.[80] FBGC are not highly phagocytic,[81] possibly due to the relatively large size of the foreign entity that results in a FBR. Despite the fact that FBGC do not phagocytize the implant directly, they do exhibit increased lysosomal and respiratory enzyme activity,[79] and are reported to exhibit fewer cell surface and complement receptors,[82] suggesting a change to a task-oriented phenotype directed toward dismantling and removing the insulting entity. In fact, upon fusing to a giant cell phenotype, the MΦ is thought to redirect its functional role from endocytosis to establishment of a powerful external lysozome.[72] Giant cells and osteoclasts adhere strongly to the substrate they are resorbed to through a "sealing zone" into which lysosomal enzymes and protons are secreted, allowing powerful extracellular resorption.[83]

Giant cell formation *in vivo* is implicated in numerous disease processes including chronic inflammation (FBGC) and osteoporosis (osteoclasts) and clearly occurs only in specific microenvironments.[72] The fusion process is thought to be mediated by the

interaction of transiently expressed cell surface proteins, although the detailed mechanism remains unclear.[72] Recently, several molecular markers that play a role in fusion have been identified; MMR,[66] also known as CD 206, CCR2 (the receptor for monocyte chemoattractant protein-1, MCP-1), the macrophage fusion receptor (MFR), comprising CD44 and CD47,[72,74,84] and the dendritic cell-specific transmembrane protein (DC-STAMP).[85]

In vivo and *in vitro* MΦ studies performed by Vignery *et al* have demonstrated that all cells tested, regardless of origin (species, organ/tissue), express the same functional markers, characteristic of osteoclasts.[83,86-89] To date, no single molecule has been identified with restricted expression to either giant cells or osteoclasts, although it has been postulated that multinucleated MΦ acquire a tissue-specific molecular repertoire.[72]

A.7 References

1. Ross JA, Auger MJ. The biology of the macrophage. In: Burke B, Lewis CE, eds. The Macrophage. Oxford: Oxford University Press, 2002:3-72.

2. Barrows TH. Synthetic Bioabsorbable Polymers. In: Szycher M, ed. High Performance Biomaterials: A Comprehensive Guide to Medical and Pharmaceutical Applications. Lancaster: Technomic Publishing Company, Inc., 1991:243-257.

3. Metcalf D. Transformation of granulocytes to macrophages in bone marrow colonies in vitro. *J Cell Physiol* 1971;**77**:277-80.

4. van Furth R, Sluiter W. Distribution of blood monocytes between a marginating and a circulating pool. *J Exp Med* 1986;**163**:474-9.

5. Meuret G, Hoffmann G. Monocyte kinetic studies in normal and disease states. *Br J Haematol* 1973;**24**:275-85.

6. van Furth R, Cohn ZA. The origin and kinetics of mononuclear phagocytes. *J Exp Med* 1968;**128**:415-35.

7. Whitelaw DM. The intravascular lifespan of monocytes. *Blood* 1966;**28**:455-64.

8. van Furth R. Origin and turnover of monocytes and macrophages. *Curr Top Pathol* 1989;**79**:125-50.

9. van Furth R, Diesselhoff-den Dulk MMC, Mattie H. Quantitative study on the production and kinetics of mononuclear phagocytes during an acute inflammatory reaction. *J Exp Med* 1973;**138**:1314-30.

10. van Furth R. Phagocytic cells: development and distribution of mononuclear phagocytes in normal steady state and inflammation. In: Gallin J, Goldstein IM, Snyderman R, eds. Inflammation: Basic Principles and Clinical Correlates. New York: Raven Press, 1988:281-96.

11. Roth MD, Gitlitz BJ, Kiertscher SM, Park AN, Mendenhall M, Moldawer N, Figlin RA. Granulocyte macrophage colony-stimulating factor and interleukin 4 enhance the number and antigen-presenting activity of circulating CD14+ and CD83+ cells in cancer patients. *Cancer Res* 2000;**60**:1934-41.

12. Banchereau J, Steinman RM. Dendritic cells and the control of immunity. *Nature* 1998;**392**:245-52.

13. Kiertscher SM, Roth MD. Human CD14+ leukocytes acquire the phenotype and function of antigen-presenting dendritic cells when cultured in GM-CSF and IL-4. *J Leukoc Biol* 1996;**59**:208-18.

14. Zhou LJ, Tedder TF. CD14+ blood monocytes can differentiate into functionally mature CD83+ dendritic cells. *Proc Natl Acad Sci U S A* 1996;**93**:2588-92.

15. Douglas SD, Hassan NF. Morphology of monocytes and macrophages. In: Williams WJ, Beutler E, Erslev AJ, Lichtman MA, eds. Haematology. New York: McGraw-Hill, 1990.

16. Kruth HS. Macrophage foam cells and atherosclerosis. *Front Biosci* 2001;**6**:D429-55.

17. Kramer BW, Jobe AH, Ikegami M. Exogenous surfactant changes the phenotype of alveolar macrophages in mice. *Am J Physiol Lung Cell Mol Physiol* 2001;**280**:L689-94.

18. Wang J, Vanley C, Miyamoto E, Turner JA, Peng SK. Coinfection of visceral leishmaniasis and Mycobacterium in a patient with acquired immunodeficiency syndrome. *Arch Pathol Lab Med* 1999;**123**:835-7.

19. Most J, Spotl L, Mayr G, Gasser A, Sarti A, Dierich MP. Formation of multinucleated giant cells in vitro is dependent on the stage of monocyte to macrophage maturation. *Blood* 1997;**89**:662-71.

20. Goldsby RA, Kindt TJ, Osborne BA. Antigens. In: Kuby J, ed. Immunology. New York: W. H. Freeman, 2000:61-81.

21. Adams DO, Hamilton TA. The cell biology of macrophage activation. *Annu Rev Immunol* 1984;**2**:283-318.

22. Nathan CF, Cohn ZA. Cellular components of inflammation: monocytes and macrophages. In: Kelly W, Harris E, Ruddy S, Hedge R, eds. Textbook of Rheumatology. New York: W. B. Saunders, 1995:144.

23. Goldsby RA, Osborne BA, Kindt TJ. Cytokines. In: Kuby J, ed. Immunology. New York: W. H. Freeman and Co., 2000:303-27.

24. Baer M, Dillner A, Schwartz RC, Sedon C, Nedospasov S, Johnson PF. Tumor necrosis factor alpha transcription in macrophages is attenuated by an autocrine factor that preferentially induces NF-kappaB p50. *Mol Cell Biol* 1998;**18**:5678-89.

25. Gonwa TA, Frost JP, Karr RW. All human monocytes have the capability of expressing HLA-DQ and HLA-DP molecules upon stimulation with interferon-gamma. *J Immunol* 1986;**137**:519-24.

26. Dinarello CA. An update on human interleukin-1: from molecular biology to clinical relevance. *J Clin Immunol* 1985;**5**:287-97.

27. Talmadge JE, Phillips H, Schneider M, Rowe T, Pennington R, Bowersox O, Lenz B. Immunomodulatory properties of recombinant murine and human tumor necrosis factor. *Cancer Res* 1988;**48**:544-50.

28. Malkovsky M, Loveland B, North M, Asherson GL, Gao L, Ward P, Fiers W. Recombinant interleukin-2 directly augments the cytotoxicity of human monocytes. *Nature* 1987;**325**:262-5.

29. Paul WE, Ohara J. B-cell stimulatory factor-1/interleukin 4. *Annu Rev Immunol* 1987;**5**:429-59.

30. Flanagan AM, Lader CS. Update on the biologic effects of macrophage colony-stimulating factor. *Curr Opin Hematol* 1998;**5**:181-5.

31. Quesniaux VFJ, Jones TC. Granulocyte-macrophage colony stimulating factor. In: Thomson A, ed. The Cytokine Handbook. San Diego: Academic Press, 1998:635-70.

32. Bagby GC, Jr., Dinarello CA, Wallace P, Wagner C, Hefeneider S, McCall E. Interleukin 1 stimulates granulocyte macrophage colony-stimulating activity release by vascular endothelial cells. *J Clin Invest* 1986;**78**:1316-23.

33. Broudy VC, Kaushansky K, Segal GM, Harlan JM, Adamson JW. Tumor necrosis factor type alpha stimulates human endothelial cells to produce granulocyte/macrophage colony-stimulating factor. *Proc Natl Acad Sci U S A* 1986;**83**:7467-71.

34. Cannistra SA, Rambaldi A, Spriggs DR, Herrmann F, Kufe D, Griffin JD. Human granulocyte-macrophage colony-stimulating factor induces expression of the tumor

necrosis factor gene by the U937 cell line and by normal human monocytes. *J Clin Invest* 1987;**79**:1720-8.

35. Dustin ML, Rothlein R, Bhan AK, Dinarello CA, Springer TA. Induction by IL 1 and interferon-gamma: tissue distribution, biochemistry, and function of a natural adherence molecule (ICAM-1). *J Immunol* 1986;**137**:245-54.

36. Essner R, Rhoades K, McBride WH, Morton DL, Economou JS. IL-4 down-regulates IL-1 and TNF gene expression in human monocytes. *J Immunol* 1989;**142**:3857-61.

37. Lee JD, Swisher SG, Minehart EH, McBride WH, Economou JS. Interleukin-4 downregulates interleukin-6 production in human peripheral blood mononuclear cells. *J Leukoc Biol* 1990;**47**:475-9.

38. Metcalf D. The molecular control of cell division, differentiation commitment and maturation in haemopoietic cells. *Nature* 1989;**339**:27-30.

39. Munker R, Gasson J, Ogawa M, Koeffler HP. Recombinant human TNF induces production of granulocyte-monocyte colony-stimulating factor. *Nature* 1986;**323**:79-82.

40. Nathan CF. Secretory Products of Macrophages. *J Clin Invest* 1987;**79**:319-326.

41. Wu CY, Demeure C, Kiniwa M, Gately M, Delespesse G. IL-12 induces the production of IFN-gamma by neonatal human CD4 T cells. *J Immunol* 1993;**151**:1938-49.

42. Goldsby RA, Kindt TJ, Osborne BA. Leukocyte migration and inflammation. In: Kuby J, ed. Immunology. New York: W. H. Freeman and Co., 2000:371-93.

43. Miller MD, Krangel MS. Biology and biochemistry of the chemokines: a family of chemotactic and inflammatory cytokines. *Crit Rev Immunol* 1992;**12**:17-46.

44. Keane MP, Strieter RM. The role of CXC chemokines in the regulation of angiogenesis. *Chem Immunol* 1999;**72**:86-101.

45. Lukacs NW, Hogaboam C, Campbell E, Kunkel SL. Chemokine function, regulation and alteration of inflammatory responses. *Chem Immunol* 1999;**72**:102-20.

46. Rollins BJ. Chemokines. *Blood* 1997;**90**:909-28.

47. DiPietro LA, Strieter RM. Macrophages in wound healing. In: Burke B, Lewis CE, eds. The Macrophage. Oxford: Oxford University Press, 2002:434-56.

48. Helinski EH, Bielat KL, Ovak GM, Pauly JL. Long-term cultivation of functional human macrophages in Teflon dishes with serum-free media. *J Leukoc Biol* 1988;**44**:111-21.

49. Rietschel ET, Brade H. Bacterial endotoxins. *Sci Am* 1992;**267**:54-61.

50. Sweet MJ, Hume DA. Endotoxin signal transduction in macrophages. *J Leukoc Biol* 1996;**60**:8-26.

51. Davis GE. The Mac-1 and p150,95 beta 2 integrins bind denatured proteins to mediate leukocyte cell-substrate adhesion. *Exp Cell Res* 1992;**200**:242-52.

52. Teixeira C, Stang SL, Zheng Y, Beswick NS, Stone JC. Integration of DAG signaling systems mediated by PKC-dependent phosphorylation of RasGRP3. *Blood* 2003;**102**:1414-20. Epub 2003 May 1.

53. Balsinde J, Balboa MA, Insel PA, Dennis EA. Differential regulation of phospholipase D and phospholipase A2 by protein kinase C in P388D1 macrophages. *Biochem J* 1997;**321**:805-9.

54. Garcia JE, Lopez AM, de Cabo MR, Rodriguez FM, Losada JP, Sarmiento RG, Lopez AJ, Arellano JL. Cyclosporin A decreases human macrophage interleukin-6 synthesis at post-transcriptional level. *Mediators Inflamm* 1999;**8**:253-9.

55. Gomez-Cambronero J, Huang CK, Yamazaki M, Wang E, Molski TF, Becker EL, Sha'afi RI. Phorbol ester inhibits granulocyte-macrophage colony-stimulating factor binding and tyrosine phosphorylation. *Am J Physiol* 1992;**262**:C276-81.

56. Lai JM, Lu CY, Yang-Yen HF, Chang ZF. Lysophosphatidic acid promotes phorbol-ester-induced apoptosis in TF-1 cells by interfering with adhesion. *Biochem J* 2001;**359**:227-33.

57. Wolfe SL. The Cell Cycle, Cell Cycle Regulation, and Cancer Molecular and Cellular Biology. Belmont: Wadsworth, Inc., 1993:910-950.

58. Bogdan C, Nathan C. Modulation of macrophage function by transforming growth factor beta, interleukin-4, and interleukin-10. *Ann N Y Acad Sci* 1993;**685**:713-39.

59. Leenen PJ, de Bruijn MF, Voerman JS, Campbell PA, van Ewijk W. Markers of mouse macrophage development detected by monoclonal antibodies. *J Immunol Methods* 1994;**174**:5-19.

60. Yagnik DR, Hillyer P, Marshall D, Smythe CD, Krausz T, Haskard DO, Landis RC. Noninflammatory phagocytosis of monosodium urate monohydrate crystals by mouse macrophages. Implications for the control of joint inflammation in gout. *Arthritis Rheum* 2000;**43**:1779-89.

61. Leenen PJ, Melis M, Slieker WA, Van Ewijk W. Murine macrophage precursor characterization. II. Monoclonal antibodies against macrophage precursor antigens. *Eur J Immunol* 1990;**20**:27-34.

62. Leenen PJ, Slieker WA, Melis M, Van Ewijk W. Murine macrophage precursor characterization. I. Production, phenotype and differentiation of macrophage precursor hybrids. *Eur J Immunol* 1990;**20**:15-25.

63. Berken A, Benacerraf B. Properties of antibodies cytophilic for macrophages. *J Exp Med* 1966;**123**:119-44.

64. Lay WH, Nussenzweig V. Receptors for complement of leukocytes. *J Exp Med* 1968;**128**:991-1009.

65. Laustriat S, Geiss S, Becmeur F, Bientz J, Marcellin L, Sauvage P. Medical history of Teflon. *Eur Urol* 1990;**17**:301-3.

66. McNally AK, DeFife KM, Anderson JM. Interleukin-4-induced macrophage fusion is prevented by inhibitors of mannose receptor activity. *Am J Pathol* 1996;**149**:975-85.

67. Hume DA. The mononuclear phagocyte system. *Curr Opin Immunol* 2006;**18**:49-53.

68. Langhans T. Uber Riesenzellen mit Wandstandigen Kernen in Tuberkeln und die fibrose Form des Tuberkels. *Arch Pathol Anat* 1868;**42**:382-404.

69. Lambert RA. The production of foreign body giant cells *in vitro*. *J Exp Med* 1912;**15**:510-515.

70. Lewis MR. Origin of phagocytic cells of the lung of the frog. *Bull Johns Hopkins Hosp* 1925;**36**:361-75.

71. Lewis WH. The formation of giant cells in tissue cultures and their similarities to those in tuberculosis lesions. *Ann Rev Tuberc* 1927;**15**:616-28.

72. Vignery A. Osteoclasts and giant cells: macrophage-macrophage fusion mechanism. *Int J Exp Pathol* 2000;**81**:291-304.

73. Murch AR, Grounds MD, Marshall CA, Papadimitriou JM. Direct evidence that inflammatory multinucleate giant cells form by fusion. *J Pathol* 1982;**137**:177-80.

74. Han X, Sterling H, Chen Y, Saginario C, Brown EJ, Frazier WA, Lindberg FP, Vignery A. CD47, a ligand for the macrophage fusion receptor, participates in macrophage multinucleation. *J Biol Chem* 2000;**275**:37984-92.

75. Saginario C, Qian HY, Vignery A. Identification of an inducible surface molecule specific to fusing macrophages. *Proc Natl Acad Sci U S A* 1995;**92**:12210-4.

76. Chambers TJ, Spector WG. Inflammatory giant cells. *Immunobiology* 1982;**161**:283-9.

77. Postlethwaite AE, Jackson BK, Beachey EH, Kang AH. Formation of multinucleated giant cells from human monocyte precursors. Mediation by a soluble protein from antigen-and mitogen-stimulated lymphocytes. *J Exp Med* 1982;**155**:168-78.

78. Mariano M, Spector WG. The formation and properties of macrophage polykaryons (inflammatory giant cells). *J Pathol* 1974;**113**:1-19.

79. Anderson JM. Multinucleated giant cells. *Curr Opin Hematol.* 2000;**7**:40-7.

80. McNally AK, Anderson JM. Interleukin-4 induces foreign body giant cells from human monocytes/macrophages. Differential lymphokine regulation of macrophage fusion leads to morphological variants of multinucleated giant cells. *Am J Pathol.* 1995;**147**:1487-99.

81. Papadimitriou JM, Robertson TA, Walters MN. An analysis of the phagocytic potential of multinucleate foreign body giant cells. *Am J Pathol* 1975;**78**:343-58.

82. Papadimitriou JM, van Bruggen I. Evidence that multinucleate giant cells are examples of mononuclear phagocytic differentiation. *J Pathol* 1986;**148**:149-57.

83. Baron R. Molecular mechanisms of bone resorption. An update. *Acta Orthop Scand Suppl* 1995;**266**:66-70.

84. Cui W, Ke JZ, Zhang Q, Ke HZ, Chalouni C, Vignery A. The intracellular domain of CD44 promotes the fusion of macrophages. *Blood* 2006;**107**:796-805. Epub 2005 Sep 29.

85. Yagi M, Miyamoto T, Sawatani Y, Iwamoto K, Hosogane N, Fujita N, Morita K, Ninomiya K, Suzuki T, Miyamoto K, Oike Y, Takeya M, Toyama Y, Suda T. DC-STAMP is essential for cell-cell fusion in osteoclasts and foreign body giant cells. *J Exp Med* 2005;**202**:345-51.

86. Vignery A, Niven-Fairchild T, Ingbar DH, Caplan M. Polarized distribution of Na+,K+-ATPase in giant cells elicited in vivo and in vitro. *J Histochem Cytochem* 1989;**37**:1265-71.

87. Vignery A, Raymond MJ, Qian HY, Wang F, Rosenzweig SA. Multinucleated rat alveolar macrophages express functional receptors for calcitonin. *Am J Physiol* 1991;**261**:F1026-32.

88. Vignery A, Wang F, Qian HY, Benz EJ, Jr., Gilmore-Hebert M. Detection of the Na(+)-K(+)-ATPase alpha 3-isoform in multinucleated macrophages. *Am J Physiol* 1991;**260**:F704-9.

89. Vignery A, Wang F, Ganz MB. Macrophages express functional receptors for calcitonin-gene-related peptide. *J Cell Physiol* 1991;**149**:301-6.

APPENDIX B: EXPERIMENTAL

B.1 Preliminary studies of murine monocyte/macrophage fusion *in vitro*

B.1.1 Gross morphological observations for J774A.1 monocyte-macrophage cells treated with exogenous cytokines IL-4 and GM-CSF

The objective of this set of experiments was to examine the effects of exogenous cytokine addition to the J774A.1 monocyte-macrophage cells. The effects of cytokine cocktails on this particular cell line were unknown, as it had not been utilized in any previously reported fusion studies. The RAW 264.7 cells had been tested, and fusion was unsuccessful.[1]

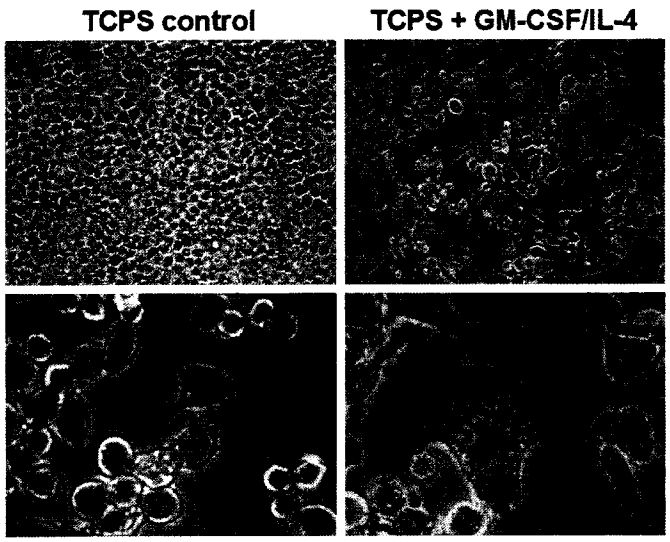

Figure B.1 Phase contrast photomicrographs of J774A.1 murine monocyte-macrophage cells on TCPS without (control) and with cytokine treatments as indicated. A and C) TCPS controls, A) 7 days post-seeding, B) 3 days-post-seeding. Cells progressed to 100% confluence and adopted a tightly packed "cobblestone-like" growth pattern. B and D) Cytokine treatments: 10 days post-seeding on TCPS, 7 days post-cytokine treatment, 10 ng/ml each IL-4 and GM-CSF. B) Cells were more diffuse, exhibited unusual morphologies with lengthy filopodia, a diffuse cytoplasm, and multiple nuclei (D, arrows). No cells with more than five nuclei were detected. Magnifications: A and B, 100 x, C and D, 400 x.

Fusion results with this cell line were poor,[2] although morphological variants were plentiful (Figures B.1 and B.2). Cells of the J774A.1 lineage appear to be easily pushed to a dendritic phenotype (E.g., Figure B.2, C). Generally, multinucleate cells did not possess more than five nuclei (Figure B.1, D, Figure B.2, A, B, D and F). Data presented

here is representative of specific morphologies observed repeatedly in response to exogenous cytokine addition to the J774A.1 cell line.

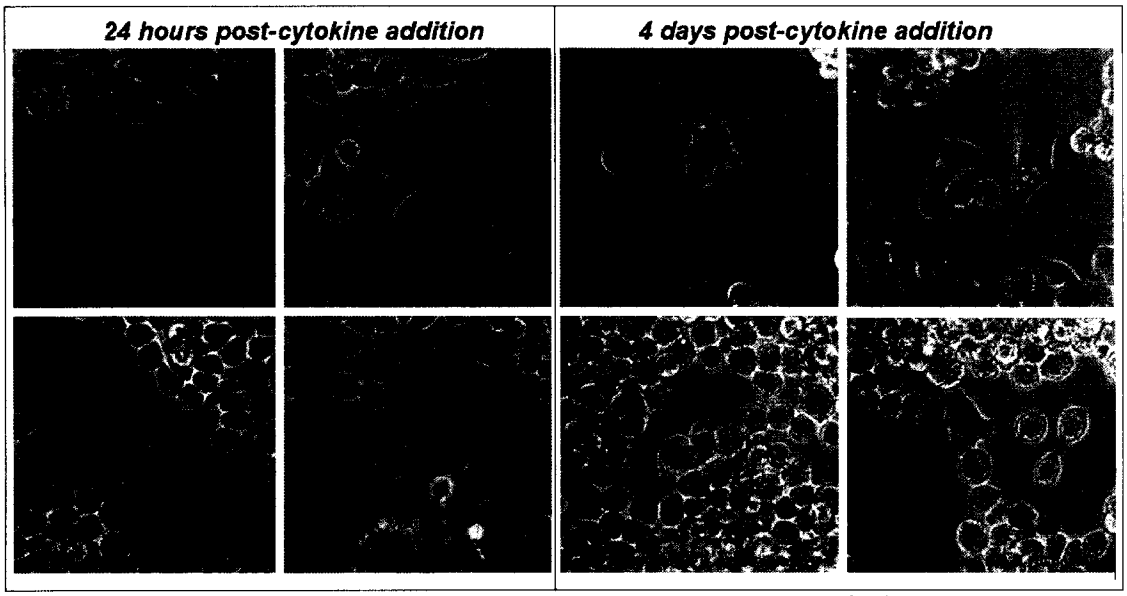

Figure B.2 Phase contrast photomicrographs of live J774A.1 cells on TCPS surfaces exhibiting cell fusion and morphologies commonly observed after cytokine treatment. At early time points (24 hours) cultures of J774A.1 cells appeared to be responding favorably to cytokine treatments (A-D), adopting multinucleate (A,B,D) or dendritic-like (C) morphologies. E-H) Cells maintained altered morphologies as cultures progressed (day 4 shown). By day 7 of cytokine addition, cells appeared stressed and apoptotic (data not shown). Cells were seeded at a density of 100 cells/mm^2. Scale bar is relevant to all images.

B.1.2 RNase Protection Assays

Limited RNase protection assays (RPA, BD Pharmingen, mCK-4 and mCK-1 template sets) were undertaken to profile mRNA species present in control (cells grown on TCPS without exogenous cytokine addition) and IL-4/GM-CSF treated cells on TCPS and 0.5% PLA surfaces. Figure B.3 shows results for select mCK-4 data. J774A.1 grown on TCPS substrates were positive for mRNA for the following species: IL-9 (mCK-1 template set), G-CSF and LIF (mCK-4 template set). J774A.1 grown on TCPS and exposed to IL-4 and GM-CSF (R & D Systems, 10 ng/ml each) were positive for IL-9 (mCK-1 template set),

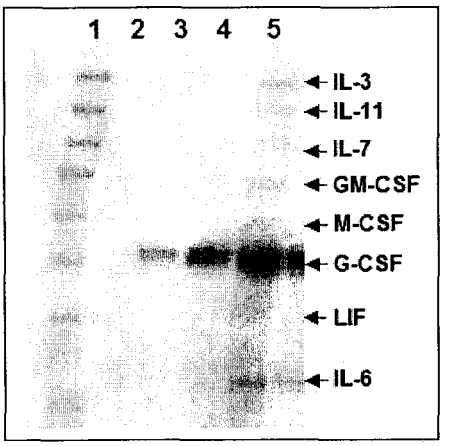

Figure B.3 Autoradiogram of samples of total RNA from J774A.1 cells analyzed for distinct mRNA species using RiboQuant™ Multi-Probe Ribonuclease Protection Assay System (BD Pharmingen) with the mCK-4 Multi-Probe Template Set. Lane 1: mCK-4 template set, not treated with RNases. Lane 2: mouse control RNA; lane 3: cells grown on TCPS, no cytokines (20 µg); lane 4: cells grown on 0.5% PLA with IL-4 and GM-CSF (20 µg); lane 5: cells grown on TCPS with IL-4 and GM-CSF (10 µg). Cytokine treatments were 10 ng/ml each, started 3 days post-seeding and continued through total RNA harvest at day 21.

IL-3, IL-11, IL-7, GM-CSF, M-CSF, G-CSF and LIF (mCK-4 template set). J774A.1 grown on 0.5% PLA substrates were positive for IL-9 and G-CSF; when exposed to cytokines IL-4 and GM-CSF, IL-9 production decreased and G-CSF production increased.

B.1.3 BMMO response to exogenous cytokine cocktails

The objective of this experiment was to examine the effects of IL-4 in combination with one additional cytokine or stimulatory factor (IL-3, M-CSF or GM-CSF) on fusion rates of BMMO cells matured two days prior to treatment. The cytokine cocktails consisted of combinations of M-CSF, GM-CSF, IL-3 and IL-4, in various amounts. These treatment conditions were selected based on positive fusion results in an initial screening of numerous cytokines and combinations thereof. The effects of using a standard (5 or 10 ng/ml) versus an excess of cytokine (50 or 100 ng/ml) were assessed to determine if increasing the cytokine concentration would improve fusion yields. An outline of the experimental procedure is shown in Figure B.4, A.

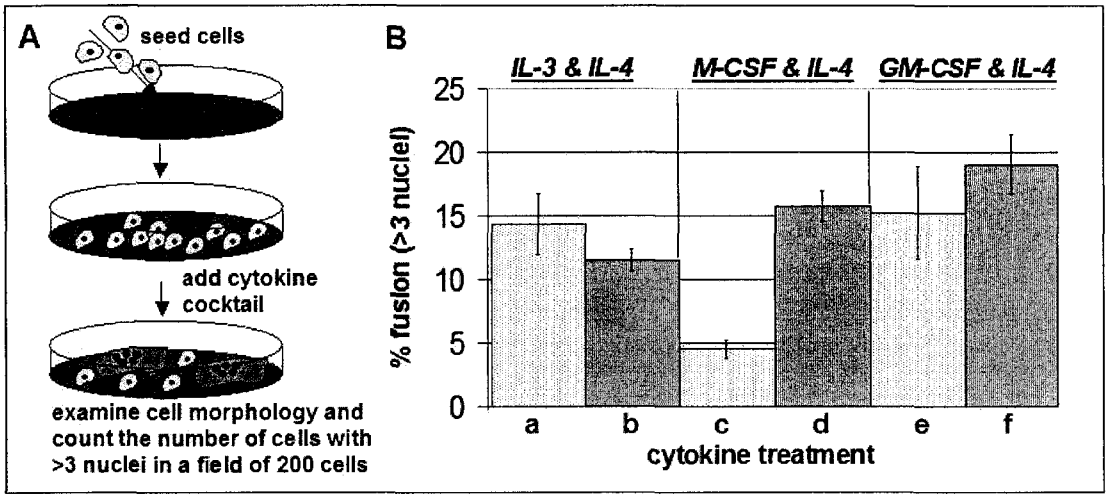

Figure B.4 Bone marrow macrophage fusion to multinucleated giant cells in response to exogenous cytokine cocktail treatments (as indicated). A) Schematic of experimental procedure. Cells were harvested from the femurs and tibias of C57BL/6 mice (n=4), counted, and seeded into TCPS wells at a density of 5000 cell/mm2. Cells were allowed to adhere/mature for 48 hours in complete bone marrow medium before exogenous cytokine addition took place. Media and cytokines were replaced every third day, and the experimental endpoint was 10 days after the first cytokine treatment. Cells were fixed and stained using the Wright-Giemsa method. A minimum of three fields of 200 cells each were counted to determine fusion rates for cells with >3 nuclei per cell.
B) Fusion results for BMMO treated with exogenous cytokines IL-3 and IL-4 at concentrations of 10 ng/ml (a) and 100 ng/ml (b), M-CSF and IL-4 at concentrations of 5 (c) or 50 ng/ml (d) of M-CSF and 10 (c) or 100 (d) ng/ml of IL-4, respectively, and GM-CSF at concentrations of 5 (e) or 50 ng/ml (f) and 10 (e) or 100 (f) ng/ml of IL-4, respectively.

Results (Figure B.4, B) indicate that the majority of the cytokine treatments do not differ significantly. (Error bars represent standard error of the mean). A significant difference was observed between the standard and excess cytokine treatments for M-CSF and IL-4 (Figure B.4 B, c and d). However, these fusion rates are generally low (> 25%) compared to reported literature fusion values for cells of primary derivation.[3] Thus these conditions will not be pursued further, and efforts will focus on establishing a reliable *in vitro* fusion protocol using other cytokine combinations (a combination of GM-CSF, IL-4 and IL-13 is most successful to date).

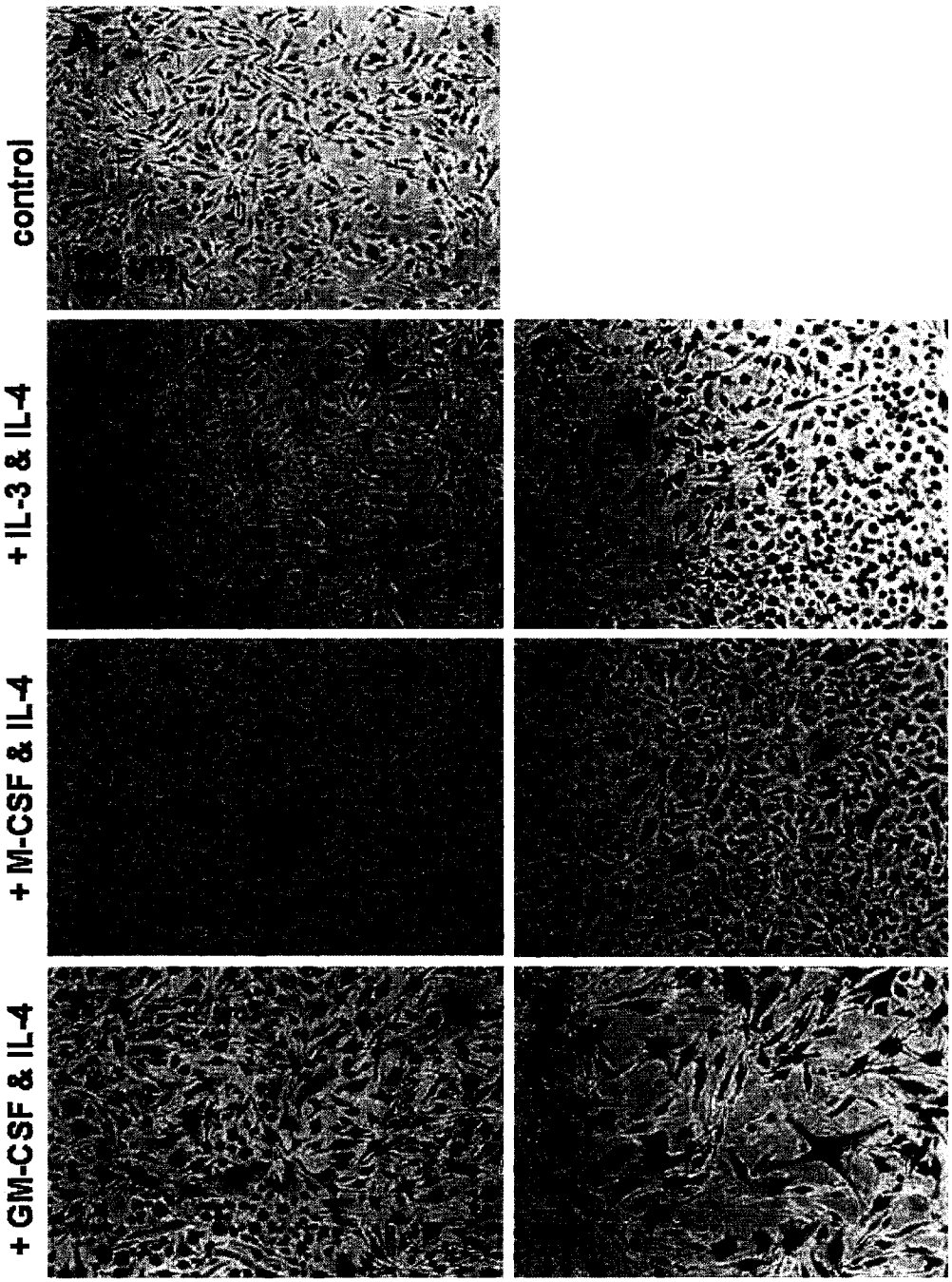

Figure B.5 Photomicrographs of bone marrow macrophage fusion to multinucleated giant cells in response to exogenous cytokine cocktail treatments as indicated. Fusion results for BMMO treated with exogenous cytokines IL-3 and IL-4 at concentrations of 10 ng/ml (A) and 100 ng/ml (B), M-CSF and IL-4 at concentrations of 5 (C) or 50 ng/ml (D) of M-CSF and 10 (C) or 100 (D) ng/ml of IL-4, and GM-CSF at concentrations of 5 (E) or 50 ng/ml (F) and 10 (E) or 100 (F) ng/ml of IL-4. Cells harvested from 4 C57/Black6 mice (n=4) were seeded at a density of 5000 cell/mm^2 on TCPS surfaces and treated on day 3. Media and cytokines were replaced every third day, and the experimental endpoint was 10 days after the first cytokine treatment. Cells were fixed and stained using the Wright-Giemsa method. Scale bar is relevant to all images.

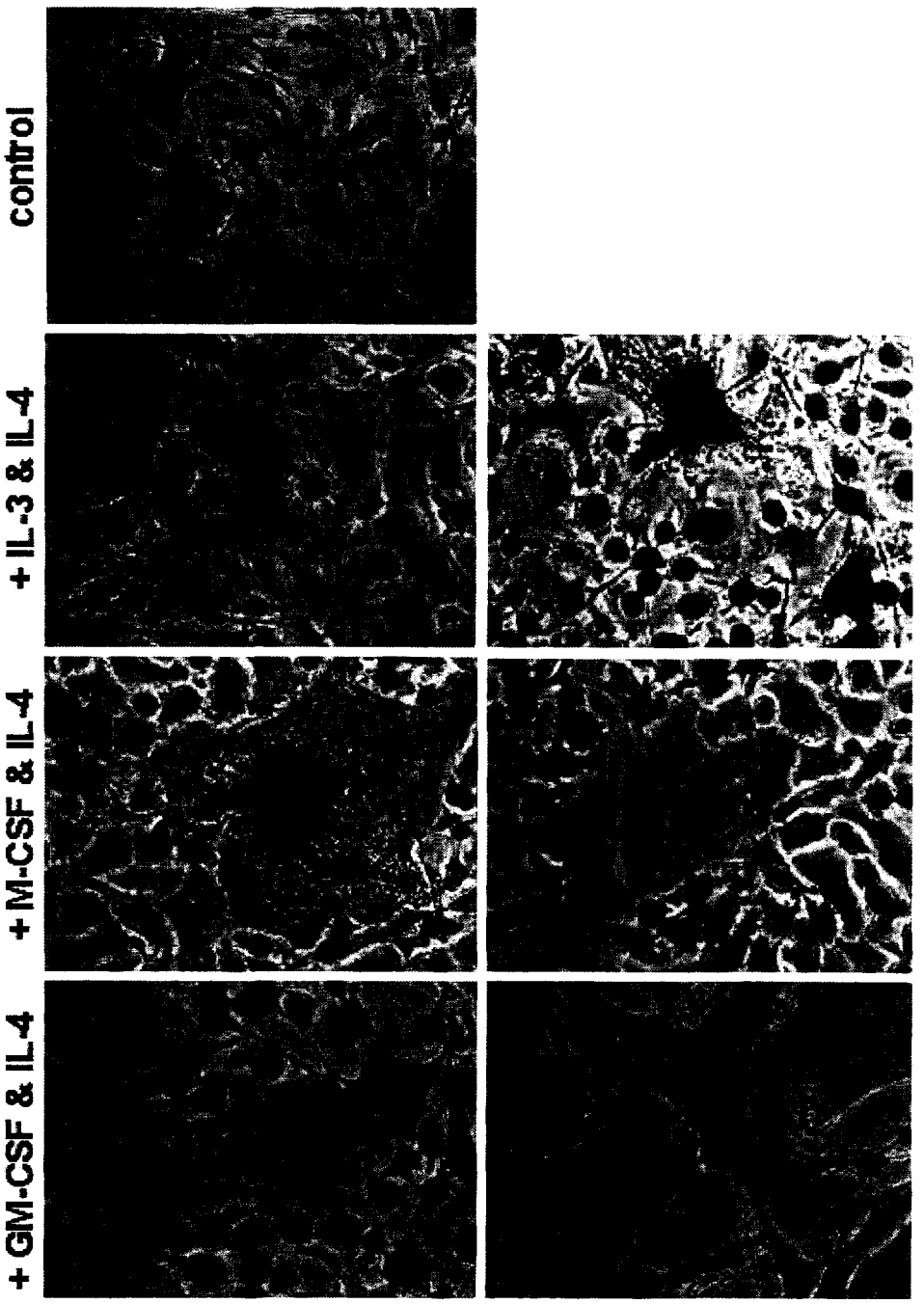

Figure B.6 Phase contrast photomicrographs of bone marrow macrophage fusion to multinucleated giant cells in response to exogenous cytokine cocktail treatments as indicated. Fusion results for BMMO control (A) and treated with exogenous cytokines IL-3 and IL-4 at concentrations of 10 ng/ml (B) and 100 ng/ml (C), M-CSF and IL-4 at concentrations of 5 (D) or 50 ng/ml (E) of M-CSF and 10 (D) or 100 (E) ng/ml of IL-4, and GM-CSF at concentrations of 5 (F) or 50 ng/ml (G) and 10 (F) or 100 (G) ng/ml of IL-4. Cells harvested from 4 C57/Black6 mice (n=4) were seeded at a density of 5000 cell/mm^2 on TCPS surfaces and treated on day 3. Media and cytokines were replaced every third day, and the experimental endpoint was 10 days after the first cytokine treatment. Cells were fixed and stained using the Wright-Giemsa method. Scale bar is relevant to all images.

The surface coverage (Figure B.5) and individual cell morphologies (Figure B.6) of BMMO cells grown without (Figures B.5 and B.6, panel A) or with exogenous cytokine addition (as indicated, Figures B.5 and B.6, B-G). Cell sizes were larger in cells treated with excess GM-CSF and IL-4 (Figure B.6, B-G). Although fusion is thought to be a density-dependent phenomenon, fusion was observed in both very dense and very moderately populated areas. This suggests that our seeding density (5000 cells/$mm^{2)}$ is adequate to achieve fusion. The size and morphology of cells varies in each culture (Figure B.6) even on TCPS, likely related to both the culture age (10 days) and the cell density (virtually all cells exhibit a motile phenotype in the TCPS culture, Figure B.6, A). The majority of fused cells exhibit a compact, central, dense nuclear region, with a diffuse amorphous cytoplasm (Figure B.6, C-G). This can also be easily observed in live cells (data not shown), but the staining method dramatically improves the contrast making these cells easy to visualize even at lower magnifications (Figure B.5 C, D and F).

B.2 Inflammatory cytokine profiles obtained for BMMO, IC-21, RAW 264.7 and J774A.1 (multiplex polymerase chain reaction (MPCR) method)

Here the experimental objective was to perform a preliminary assessment of inflammatory cytokine expression in the BMMO and the three cell lines to assess macrophage activation on TCPS surfaces; a "quick and dirty" MPCR evaluation was performed. This assessment was made using a multiplex format using commercially designed primers (MPCR, Maxim Biotech, Inc.) that employs a one pot PCR reaction to obtain information for numerous amplicons. (The "mouse inflammatory cytokine kit" is

designed to amplify IL-1, IL-6, TNF-α, TGF-β and GM-CSF. GAPDH is employed as a control).

TCPS

Amplicon	Cell type			
	BMMO	IC-21	RAW 264.7	J774A.1
GAPDH	+	+	+	+
IL-6	+	-	-	-
TNF-alpha	+	+	+	+
IL-1 beta	-	-	-	-
TGF-beta	+	+	+	+
GM-CSF	-	-	+	-

LPS

Amplicon	Cell type			
	BMMO	IC-21	RAW 264.7	J774A.1
GAPDH	+	+	+	+
IL-6	+	+	+	+
TNF-alpha	+	+	+	+
IL-1 beta	+	+	+	+
TGF-beta	+	+	+	+
GM-CSF	+	+	+	+

PMA

Amplicon	Cell type			
	BMMO	IC-21	RAW 264.7	J774A.1
GAPDH	+	+	+	+
IL-6	+	-	-	-
TNF-alpha	+	+	+	+
IL-1 beta	-	-	+	-
TGF-beta	+	+	+	+
GM-CSF	-	-	+	-

LPS/PMA

Amplicon	Cell type			
	BMMO	IC-21	RAW 264.7	J774A.1
GAPDH	+	+	+	+
IL-6	+	+	+	-
TNF-alpha	+	+	+	+
IL-1 beta	+	+	+	-
TGF-beta	+	+	+	+
GM-CSF	+	+	+	-

Table B.1 Summarized "inflammatory cytokine" MPCR data by treatment condition. All data shown are representative of ≥3 more trials.

The inflammatory triad includes IL-1, TNF-α and IL-6. IL-1 induces TNF-α and IL-6 production, activates the vascular endothelium and increases vascular permeability. IL-1β is a pro-inflammatory and pro-wound healing cytokine that can activate monocytes, lymphocytes and fibroblasts. TNF-α also activates the vascular endothelium and increases vascular permeability. IL-6 is upregulated during sepsis. It promotes terminal differentiation of proliferating B cells into plasma cells, stimulates antibody secretion in plasma cells, facilitates differentiation in myeloid stem cells and induces the synthesis of acute phase proteins in hepatocytes.

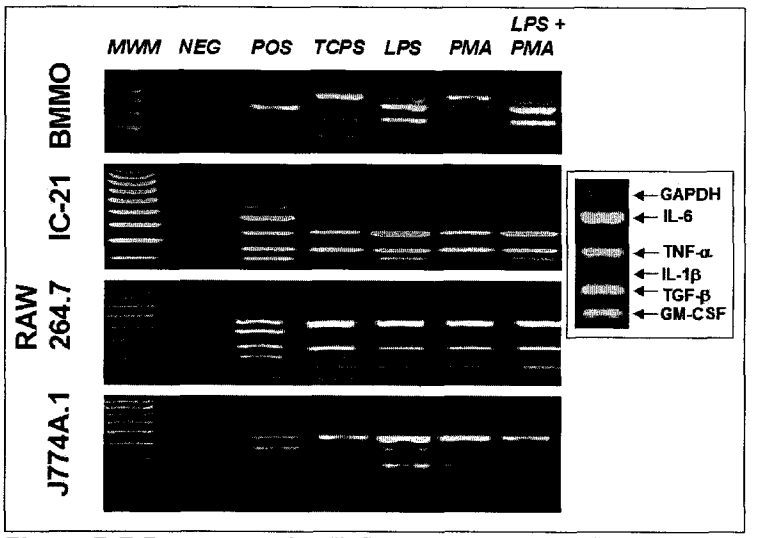

Figure B.7 Representative "inflammatory cytokine" multiplex PCR (MPCR, Maxim Biotech, Inc.) agarose gel electrophoresis results for murine monocyte/macrophages of primary (BMMO) or secondary-derived (IC-21, RAW 264.7, J774A.1) origin treated with chemical activators lipopolysaccharide (LPS) and/or phorbol 12-myristate 13-acetate (PMA), both at 1 μg/ml for 6 hours prior to RNA collection. MWM (100bp molecular weight marker, Bio-Rad); NEG (negative control, MPCR); POS (positive control, MPCR); TCPS (samples grown on TCPS without additional activators); LPS (cells treated with the activator LPS, 6 hours); PMA (cells treated with activator PMA, 6 hours), LPS/PMA (cells treated with a combination of LPS and PMA). All data shown are representative of 2 or more trials. Inset: Positive control with bands defined.

Results (Table B.1 and Figure B.7) indicate that all TCPS "surface controls" were positive for TNF-α and TGF-β. TGF-β plays a role in chemotaxis, growth factor release and macrophage deactivation and it is known to be pro-fibrogenic. Profiles for these two cytokines did not change regardless of activating treatment, i.e. the addition of LPS, PMA or LPS and PMA. Among this test group, *TCPS surfaces incite IL-6 production in primary-derived BMMO exclusively.* All TCPS "surface controls" were negative for IL-1β and GM-CSF transcripts. GM-CSF is implicated in granulocyte, eosinophil and macrophage colony stimulation and enhanced neutrophil and eosinophil function.

All LPS and LPS/PMA treated samples were positive for each cytokine tested except J774A.1 IL-1β and GM-CS, which suggests that LPS is the critical activating factor in the combination treatment. Results for PMA treated samples are nearly identical to

results obtained for TCPS surfaces, and differ only for RAW 264.7 (positive for TGF-β with PMA treatment. This suggests that TCPS surfaces (physical stimulus) and PMA (chemical stimulus) stimulation pathways stimulate the same pathways or pathways that converge on a common target. The most significant differences between cells of primary and secondary derivation are the production of IL-6 by BMMO in response to 1) the TCPS surface alone or 2) stimulation with PMA. In these instances the cell lines show no response.

B.3 Bone marrow macrophage growth to extended time points *in vitro*

The ability of Teflon® AF and pp-FC surfaces to support BMMO growth over extended culture times (36 days) *in vitro* was examined. Results for pp-FC surfaces were presented in Chapter 4, Figures 4.3 and 4.4. Photomicrographs of BMMO growth on Teflon® AF surfaces are shown in Figure B.8. These substrates were cell supportive through Day 36 when cultures were terminated. BMMO cells (Day 36, Figure B.8, panels B-C, E-F) were large by comparison to early time points (24 hours, Figure B.8, panels A, D). Cells exhibited unusual morphologies with large areas of membrane ruffling and lengthy filopodia (Figure B.8, panels E-F). Not all areas of the plates were densely populated. Figure B.9 shows one cell with an unusually lengthy filopodium.

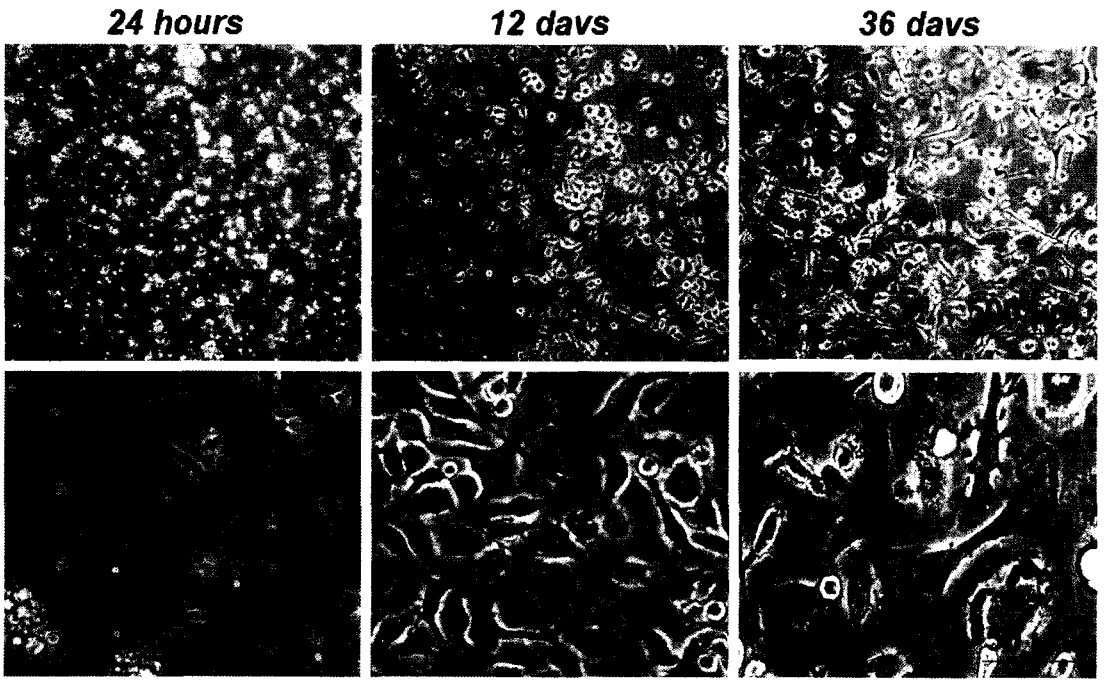

Figure B.8 Photomicrographs of live bone marrow macrophage cells at various time points (as indicated) on Teflon® AF surfaces pre-treated with 10% serum for ≥ 24 hours prior to cell seeding at a density of 6.2 x 10^6 cells per 15 x 100 mm plate. Cell density was very low at 24 hours (A, D), but cells were able to efficiently colonize these surfaces (B, E) and remained adherent through Day 36 (C, F) when the culture was terminated.

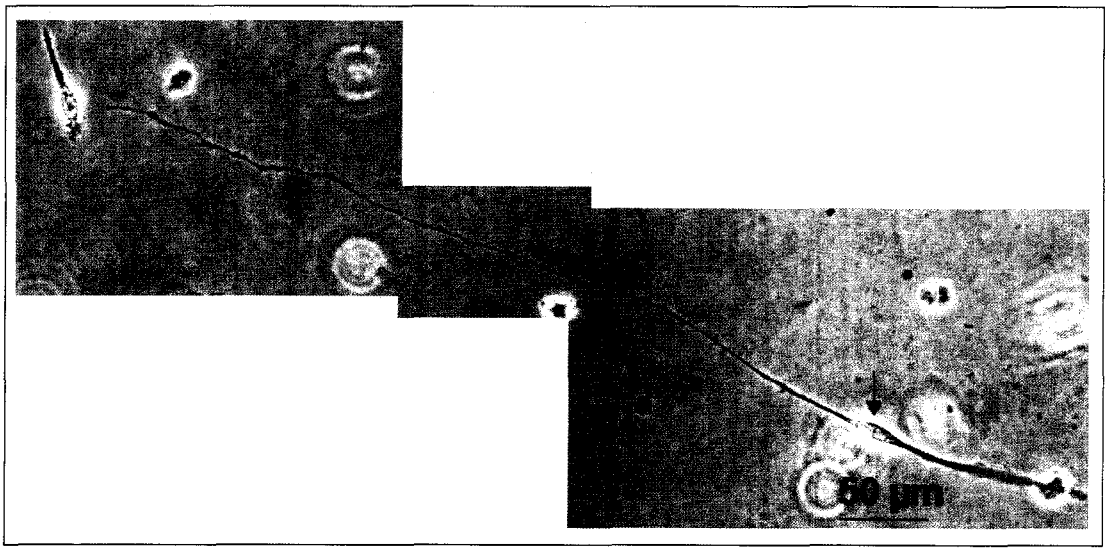

Figure B.9 Photomicrograph of bone marrow macrophage cells at Day 36 on Teflon® AF (pre-treated with 10% serum for ≥ 24 hours prior to cell seeding at a density of 6.2 x 10^6 cells per 15 x 100 mm plate). Arrow indicates cell body.

B.4 Function-blocking integrin studies

These studies examined effects of integrin-directed (α_M, β_1 and β_2) mAb on cell adhesion to Teflon® AF (Table B.2). All mAb employed were sterile-filtered, low-azide and endotoxin-free. (See section C.12.1 for experimental notes). mAb from eBioscience performed better in function-blocking assays. 96- and 24- well plate formats were

Antibody	Clone	Source	Control	Cell type	Block/Sig Block	Morph Changes
Beta 1 Integrin	**Ha2/5**	**Pharmingen**	**N**	**IC-21**	**Y/N**	**N**
Beta 1 Integrin	**Ha2/5**	**Pharmingen**	**N**	**BMMO**	**Y/N**	**N**
Hamster IgM	G235-1	Pharmingen	Y	IC-21	**Y/N**	N
Hamster IgM	G235-1	Pharmingen	Y	BMMO	**Y/N**	N
Beta 2 Integrin	**M18/2**	**Pharmingen**	**N**	**IC-21**	**Y/Y**	**Y**
Beta 2 Integrin	**M18/2**	**Pharmingen**	**N**	**BMMO**	**Y/Y**	**Y**
Rat IgG2a, κ	R35-95	Pharmingen	Y	IC-21	N/N	N
Rat IgG2a, κ	R35-95	Pharmingen	Y	BMMO	N/N	N
Beta 2 Integrin	**M18/2**	**eBioscience**	**N**	**IC-21**	**Y/Y**	**Y**
Beta 2 Integrin	**M18/2**	**eBioscience**	**N**	**BMMO**	**Y/Y**	**Y**
Rat IgG2a, κ	unknown	eBioscience	Y	IC-21	N/N	N
Rat IgG2a, κ	unknown	eBioscience	Y	BMMO	N/N	N
Alpha M Integrin	**M1/70**	**eBioscience**	**N**	**IC-21**	**Y/N**	**N**
Alpha M Integrin	**M1/70**	**eBioscience**	**N**	**BMMO**	**Y/N**	**N**
Rat IgG2b, κ	eB149/10H5	eBioscience	Y	IC-21	N/N	N
Rat IgG2b, κ	eB149/10H5	eBioscience	Y	BMMO	N/N	N

Table B.2 Summary of integrin blocking studies performed. Function blocking mAb (bold) and their isotype controls are matched by row. "Significant blocking (Sig Block)" is defined as ≥80% removal of function-in this case the function is cell adhesion to FC substrates pre-conditioned with 3 mg/ml BSA, 10% HI FBS or 10% FBS for 24 hours prior to cell-seeding.

employed for blocking assays. However, Teflon® AF delaminated readily from 96-well plates and this format was abandoned in favor of the more-stable 24-well format. See optimized protocol in section C.12 for additional experimental details. Initial experiments included Teflon® AF preconditioning with 3 mg/ml BSA, 10 FBS and 10% HI FBS. However, due to various factors (expense, surface delamination and differences in mAb function based on supplier and/or batch to batch variation) a 10% FBS pre-treatment study was focused on exclusively.

B.5 References

1. Personal communication, WJ Kao. Limited fusion experiments were perfomed with cell lines, including the RAW 264.7 lineage; fusion experiments with these cells were unsuccessful and were not reported.

2. Godek ML, Duchsherer NL, McElwee Q, Grainger DW. Morphology and growth of murine cell lines on model biomaterials *Biomed Sci Instrum* 2004;**40**:7-12.

3. McNally AK, Anderson JM. Interleukin-4 induces foreign body giant cells from human monocytes/macrophages. Differential lymphokine regulation of macrophage fusion leads to morphological variants of multinucleated giant cells. *Am J Pathol.* 1995;**147**:1487-99.

APPENDIX C: PROTOCOLS

C.1 Cell culture information sources

Cell information is available online from the American Type Culture Collection (ATCC): www.atcc.org
Biosafety information is available online from the Centers for Disease Control (CDC): http://www.cdc.gov/od/ohs/biosfty/bmbl4/bmbl4toc.htm and in "Biosafety in Microbiological and Biomedical Laboratories (BMBL) 4th Edition".
Biohazard level definitions are available at http://bmbl.od.nih.gov/sect3bsl2.htm.

C.2 Cell line information (*a copy of this information should be posted on the incubator, and updated as new cells are added*)

CELL TYPE:	*MEDIUM:*	*SPLITTING METHOD:*
RAW 264.7 (MC-MΦ)	**RPMI 1640 w/10% FBS**	**HBSS or PBS (Ca^{2+} and Mg^{2+} free)**
ATCC TIB-70		**Biosafety level: 1**

Description: Mouse monocyte-macrophage.

Culture maintenance: RAW 264.7 cells are highly proliferative and require constant attention. They should be split at or below 90% confluence, and medium should be changed frequently as the cells progress towards confluence. Cells may be removed from culture surfaces with (up to 10%) trypsin, although it is best to avoid trypsin when profiling proteins. Medium may be supplemented with 1% penicillin-streptomycin (pen-strep) solution, although this is discouraged*. RAW cells will proliferate under non-adherent conditions, so avoid overgrowth. Changes in adhesive strength (increased adhesion/difficulty in removal cells using divalent cation-free solutions) are an indication of advanced culture age. Discard cells when they fail to respond to removal by this method. Discard cultures if cells grow on top of one another.

J774A.1 (MC-MΦ)	**DMEM w/10% FBS**	**HBSS or PBS (Ca^{2+} and Mg^{2+} free)**
ATCC TIB-67		**Biosafety level: 1**

Description: Mouse monocyte-macrophage.

Culture maintenance: J774A.1 are highly proliferative. Cells should be grown to no more than 90% confluence, and medium changes are as indicated for RAW 264.7. Generally, J774A.1 are easier to remove from culture surfaces than RAW 264.7, and typically "pop" off in HBSS without trypsin. Medium may be supplemented with 1% pen-strep, although this is discouraged*.

IC-21 (MΦ) **RPMI 1640 w/10% FBS** **Scraping, DO NOT USE TRYPSIN**
ATCC TIB-186 **Biosafety level: 2**

Handle as potentially biohazardous material under Biosafety Level 2 containment. Briefly: Never handle without gloves, always use secondary containment (e.g., transport cell flask/tubes/plates on a tray) always autoclave plastics that these cells contact. **Never use trypsin, as it is toxic to IC-21 cells.**

Description: Mouse macrophage. Derived from transformation of normal C57BL/6 mouse peritoneal macrophages with SV40[1]. "This line shares many characteristics with normal peritoneal macrophages and is thus a valuable model in the study of macrophage properties and activities[2]". IC-21 cells are larger than either the RAW 264.7 or J774A.1 cells.

Culture maintenance: IC-21 cells are slow growing acid producers. They will exhibit a medium color change due to acid production in contrast to the RAW 264.7 and J774A.1 cells, where a medium color change is often an indicator of metabolism based on rapid growth. IC-21 medium must be changed religiously. Split IC-21 at 80-90% confluence and ***sub-culture in the same flask***. Leave some of the old medium in the flask, which contains growth factors that facilitate proliferation. When expanding these cultures using medium that contains 20% FBS is helpful. Freeze ample numbers of back-ups at 2 x 10^6 cells per cryotubes; these cells are slow to rebound to usable culture size if contaminated. Generally, IC-21 cultures will not passage as many times as RAW 264.7 and J774A.1, so make plenty of low passage number frozen stocks. If the cells die unexpectedly and cells are needed expeditiously it is best to order a flask of cells from ATCC, which will still take weeks to expand to sufficient quantity for experimental use.

BMMO **BMMO MEDIUM** **HBSS or PBS (Ca^{2+} and Mg^{2+} free)**

Description: C57BL/6 primary-derived mouse monocyte-macrophage.

Culture maintenance: Change medium every three days. Allow cells 7-10 days to mature on TCPS in complete BMMO medium for macrophage phenotype. Cells have a limited lifetime *in vitro*.

NIH/3T3 **DMEM w/10% FBS** **HBSS or PBS (Ca^{2+} and Mg^{2+} free)**
ATCC CRL-1658 **Biosafety level: 1**

Description: NIH Swiss mouse embryo, contact-inhibited.

Culture maintenance: NIH 3T3 are easy to grow and sub-culture. The most significant problem with these cells is clumping. For experimental use, employ a trypsin-containing solution (0.5-1% in HBSS) to aid the removal of cells from the surface/avoid clumping, which prevents accurate cell counts and can affect certain assays. The other potential

problem is cross-contamination of macrophage cells-never work with more than one cell type in the biosafety cabinet (BSC) at once.

*Whereas some groups grow their cell lines in antibiotics we avoid their use. This ensures that the lines we use are "clean". I.e., cells grown in antibiotics may be supporting low levels of microbial contamination-this has important consequences for macrophage cells and is an experimentally unsound system. If contamination becomes problematic almost all cell lines will tolerate 1% penicillin-streptomycin. However, the best fix is a thorough cleaning/autoclaving (where possible) of all cell culture areas, replacement of supplies/filters and starting fresh cultures.

** Flasks should have the same amount of medium added every time. For large flasks (185 cm^2/600 ml) use 50 ml of medium. For the medium flasks (75 cm^2/200 ml) use 25 ml of medium. For the small flasks (25 cm^2/40 ml) use 10 ml of medium. (All V_T). Macrophages respond to altered oxygen content (e.g., hypoxia), affected by medium depth with phenotypic (and presumably genotypic changes).

Labeling Cell Culture containers: Each flask should have the following information:
CELL LINE-***SUB-CULTURE #***
DATE OPERATOR

Example: RAW 264.7-***11***
12/31/02 MLG

C.3 Cell culture procedures

C.3.1 Thawing cells
Rule: THAW QUICKLY

1) Cells should be brought up in medium that contains 20% FBS. To make medium you will need:

-DMEM or RPMI* stored at 4°C (refrigerated) in 500 ml bottles
-FBS stored at -20°C (frozen) in 50 ml aliquots

To make medium: Thaw only enough FBS in a 37°C water bath for the volume of medium you wish to prepare. (e.g., 100 ml total FBS in 500 ml V_T or 200 ml for 1000 ml V_T). Add DMEM (or RPMI) and pen-strep (if used) to a sterile filter cup (0.22-micron cellulose acetate filter) that is already attached to the vacuum pump and pulling a vacuum. Add FBS last. Label as "20% FBS in DMEM (or RPMI) (with Pen-Strep)", the date and your initials. Warm medium to 37°C prior to use. Treat as sterile. Do not leave medium out for extended periods of time.

DMEM for J774A.1 and NIH 3T3, RPMI for IC-21 and RAW 264.7 cells.

2) Prepare T25 TCPS culture flask(s) or 15 x 100 mm TCPS plate(s). Add 9 ml of medium, and place in the incubator to allow medium to adjust to its proper pH (c 30 minutes). Remove cells from liquid nitrogen storage (or from the -70°C freezer) and immediately place in 37°C water bath, taking care to avoid direct contact of the cap area with the water. Allow the sample to thaw. Spray with 70% ethanol (EtOH), transfer to the BSC and immediately transfer (using a 5 or 10 ml pipet and sterile technique) to the flask. Alternatively, you may spin down the cells at (no more than) 1,000 x g for 5 minutes to remove dimethyl sulfoxide (DMSO) and resuspend in medium before adding cells to the flask/plate. Place in the incubator (37°C, 5% CO_2, 98% humidity). Cells should be 90% confluent in 2-5 days. Change the medium after 12-24 hours if you did not spin out the DMSO.

3) Record your activities on the cell culture calendar and be sure to update the freezer or liquid nitrogen storage sheets to allow tracking of the remaining number of frozen aliquots for each cell type.

C.3.2 Sub-culturing cells

-NEVER work with more than one cell type in the BSC at the same time-this invites cross-contamination
-Use sterile technique at all times-if you are unsure about whether you might have contaminated something, assume you did and treat appropriately

1) Determine "% confluence" of the culture by examining the flask/plate using an inverted microscope and a 10x objective. Cells should not be allowed to progress beyond 90% confluence.

2) Set medium out to warm in a water bath (37°C).

3) Disinfect the work area (pay special attention to the aspirator tube) and any reagent bottles to be opened using 70% ethanol (EtOH). Wipe bottles from the top down and reapply EtOH before transferring to the BSC.

4) Work with the BSC blower on, use sterile techniques at all times. Wear gloves and spray your hands regularly with ethanol to protect the cells from contamination. Do not wipe your hands with a towel. If you leave the BSC to do other work, change gloves before returning to cell culture work.

5) Prepare (label) new flasks for RAW 264.7 or J774A.1 cells. Be sure to label the flasks with the complete cell line name (as written above), plus the sub-culture number, the date and your initials. Note: IC-21 cells are sub-cultured in the same flask they are growing in presently. Write small on IC-21 flasks. IC-21 flasks should be changed after approximately 10 passages.

FOLLOW DIRECTIONS FOR THE APPROPRIATE CELL LINE:

IC-21:

6) Remove all but c 10 ml of medium and carefully/gently remove the cells from the flask using a rubber policeman (scraper). There is no need to apply any pressure to the scraper- this results in lower cell viability. Generally the scraping process, even when carefully performed, reduces viability by 40-50%.

Do not aspirate the medium and rinse the cells before scraping unless they are overgrown.

Remove the supernatant and reserve or discard as necessary (the supernatant will contain most of the cells). Replenish the medium in the flask (V_T 50 ml for large flasks) and return to the incubator. IC-21 cells require medium changes every 2-3 days. IC-21 waste should be treated as a biohazard level 2, which means all solids must be autoclaved (e.g., flasks, pipets, tips, etc) and all liquids must be bleached, and preferably autoclaved, before disposal).

OR:

RAW 264.7 and J774A.1:

6) Remove cells from the incubator, transfer to the BSC and aspirate old medium from the flask using sterile technique. (Preferably using a Pasteur pipet with vacuum). Use one sterile Pasteur pipet per flask or plate.

7) Add enough 1x (sterile) HBSS or PBS without divalent cations (Ca^{2+} and Mg^{2+} free) to cover the bottom of the flask (14 ml for a large flask). If the cells are very close to 90% confluence, rock the flask and aspirate this HBSS/PBS as a rinse. Then add a second volume of HBSS/PBS. Place the cells back in the incubator. Allow them to sit 10 minutes before checking for cell lifting (never longer than 30 minutes). For stubborn cells, successive treatments of HBSS/PBS can be employed.

8) Check the progress of cell lifting by examining the flask with an inverted microscope. Tap the flask hard against the back of your hand and check for loosening. Smacking the flask too lightly will result in liberation of too few cells. Smacking the flask too hard will result in damaging the flask and leaking. Most of the cells should be free from the surface after 10 minutes. If cells are not coming off return them to the incubator and check again in five minutes. As the cells age (usually upwards of 50 passages) they will become more resistant to removal.

9) Remove a small aliquot of cells (10-100 µl) to count using Trypan blue if so desired.

10) Remove a small amount of cells and transfer to a new flask containing fresh medium. Plate cells at the desired density (usually 5 x 10^5 cells for experimental 15 x 100 mm plates, 1-2 x 10^6 for cryo vials, and 1 x 10^5 cells for passage flasks). Return flasks to the incubator.

Sources of contamination:

-Avoid double dipping into any reagents or medium containers. Use 1 pipet for each "dip" into the container.

-Avoid adding bubbles to the fresh medium you are aliquoting. Keep the tip of the pipet away from the lip of the flask, and try not to let any medium get on the lip or neck of the flask.

-Avoid tilting the flasks so that medium approaches the cap. Try to keep the flask tilted so that the medium goes to the opposite end of the container. Be especially careful when laying the flasks in the incubator and lifting them out.

-Avoid splashes or medium on the outside of the container. If you get medium on the outside of dishes or flasks clean it off with ethanol and a Kim™ wipe.

-Don't leave medium or cells out at room temperature for longer than is absolutely necessary.

-If cells are suspect or appear contaminated remove them from the incubator immediately and bleach them before disposal. Remove incubator shelves/water pan and autoclave them. Remove all reagents from the BSC and re-filter or toss suspect medium. Change out the aspirator hose-this is often a contamination source. Replace Pasteur pipets and all other opened autoclavables. Typically, contamination from sub-culturing arises within 24 hours.

C.3.3. Freezing cells

Rule: FREEZE SLOWLY

1) Thaw an aliquot of FBS/DMSO (90% FBS should be aliquoted with 10% cell culture grade DMSO and stored frozen in sterile 15 ml Falcon tubes).

2) Remove cells using the procedure outlined in the sub-culturing section. Remove a small amount (10-100 µl) of the cells and count using Trypan blue dye and a hemacytometer[3].

3) Transfer the cell suspension into centrifuge tubes and spin for 5 minutes at 1,000 x g or less.

4) Decant the supernatant and resuspend the cell pellet in the desired amount of 10% DMSO/FBS solution. (Calculate from desired amount of cells per vial as noted above, typically 1-2 x 10^6 cells/ml).

5) Aliquot 1 ml of cell suspension per cryo tube using a 10 ml pipet. Place into a cell freezer container containing EtOH (or Styrofoam container) to provide some insulation.

6) Freeze at -20°C for several hours. Move to -70°C for 24 hours. (Viable for 6 months if left here).

7) Transfer cryotubes to liquid nitrogen storage. They should be viable for 12 months. Update the frozen cell storage records.

C.4 Teflon® AF plate preparation

C.4.1 Materials

-1% Teflon® AF Grade 400S-100-1(DuPont Fluoroproducts)
-Fluorinert™ Electronic Liquid FC-40 (3M #98-0211-3972-4)
-70% tissue culture grade ethanol
-Plates:
Suspension culture (PS) plate (Corning #430591)
Multiwell™ 6 well TCPS flat bottom plate with low evaporation lid (Falcon #351146)
Multiwell™ 12 well TCPS flat bottom plate with low evaporation lid (Falcon #353225)
Multiwell™ 24 well TCPS flat bottom plate with low evaporation lid (Falcon #353935)
96-well, TCPS flat bottom strip plate with lid (Corning #9102)

C.4.2 Plate preparation

1) Preheat a vacuum oven to 65°C.

2) In a sterile glass bottle make a 10:1 dilution of the 1% Teflon® AF (as supplied) in FC-40 solvent to make a 0.1% Teflon® AF solution.

3) Arrange plates to be coated on a clean autoclavable tray.

4) Using the table below, determine the amount of 0.1% Teflon® AF needed to coat the surface used:

Type of plate	Area (cm^2)	Vol. 0.1% Teflon® AF
BPS plate	56	3 ml
6-well plate	9.6	0.5 ml
12-well plate	3.8	200 µl
24-well plate	2	100 µl
96-well plate	0.32	17 µl

*Note: For the 96-well plate, the 0.1% Teflon® AF solution can be diluted 1:1. The multichannel pipet and reagent reservoir can then be used to dispense 34 µl onto the bottom of each well to obtain a 0.1% Teflon® AF coating.

5) Dispense the appropriate amount of 0.1% Teflon® AF into each dish or well. Gently swirl the plate to ensure even distribution of the solution.

6) Remove the lid from each Teflon® AF coated plate and place in the vacuum oven (65° C). Plates should be left in the oven for 3-6 hours, or until all liquid has evaporated from the bottom surface of the plates (wells).

*Note: Check the pressure and the temperature often to ensure that the pressure stays between 20 and 25 mm Hg and the temperature stays at 65°C. When plates are dry, remove plates, place on clean/sterile autoclave tray and replace lids.

7) Transfer plates and lids (facing up) to the BSC, mist with 70% tissue culture grade ethanol and expose to UV light for 20 minutes. Allow plates to dry thoroughly before replacing lids and storing.

C.5 Poly-L-lactide (PLA) plate preparation

C.5.1 Materials

-Poly-L-lactide, Mol. Wt. 50,000, 100,000 or 200,000 (reconstituted, desiccated at 4°C, source: Polysciences, Inc)
-Glass pipettes and plates (plates should be base treated first, *vida infra*)
-Methylene chloride

C.5.2 Preparation of surfaces

1) Base treat plate bottoms in a KOH/EtOH base bath overnight.

2) Rinse each plate with copious amounts of 18 MΩ "Nanopure" grade water.

3) Prepare a treatment solution of poly-L-lactide as follow: Use the 0.2% 50,000 Mol. Wt. poly-L-lactide recipe for cell culture experiments (preferred for microscopic evaluation). Use glass pipets and surfaces for this protocol (methylene chloride will dissolve plastics).

For 50,000 Mol.Wt. poly-L-lactide:
Prepare a 0.2% solution of poly-L-lactide in methylene chloride.
0.2% (w/v) = (g/100ml) = (0.2 g/ 100 ml) = 200 mg per 100 ml of $MeCl_2$.
Note: The smaller molecular weight polymer will yield a clear film.

For 100,000-200,000 Mol.Wt. poly-L-lactide:
Prepare either a 0.1 or a 0.5% (w/v) solution of poly-L-lactide in methylene chloride.
0.1% (w/v) = (g/100ml) = (0.1 g/ 100 ml) = 100 mg per 100 ml of $MeCl_2$.
0.5% (w/v) = (g/100ml) = (0.5 g/ 100 ml) = 500 mg per 100 ml of $MeCl_2$.
This molecular weight range polymer will yield a medium opacity film.

4) Each (20 x 100 mm) glass plate requires 10-15 ml of PLA solution to cover the surface.

5) Allow plates to dry while covered at room temperature. Do not place directly in the oven as $MeCl_2$ will boil off and leave an uneven surface.

6) Place dry plates in the vacuum oven at 65°C for 6 hours. This step is essential to remove residual solvent and prevents surface lifting when exposed to liquids.

7) To sterilize mist with cell culture grade 70% EtOH and expose to UV light for 20 minutes. (Perform in the BSC).

Note: Biodegradable polymers such as poly-L-lactide should be stored desiccated at 4°C. Long-term storage conditions consist of freezing at -70°C with nitrogen or argon (i.e., evacuate a storage bag with nitrogen gas).

C.6 Seeding polymer surfaces

24 hours prior to cell seeding:
Condition plates (6 hours to overnight) with medium containing 10% FBS. Use cell-specific medium except for BMMO cells, instead use 10% FBS in DMEM (to conserve expensive BMMO medium) unless you plan to seed into the medium directly. Conditioning ensures ample time for protein adsorption at the surface to reach equilibrium. Use 10 ml for all plates except Teflon® AF, which will require 15 ml for complete and sustained coverage. Use care when handling plates-especially glass, as they contaminate easily.

Cell seeding:
1) Warm cell-specific medium to 37° C. Spray medium container with 70% ETOH from the top down, and wipe (also from the top down) before transferring to the hood.

2) Transfer cells to the BSC and harvest as appropriate based on cell type. Remove a small volume of cells to count, centrifuge remaining cells at 1000 x g.

3) Count cells using Trypan blue. Determine the seeding concentration and resuspend cells as desired. (E.g., IC-21-500,000 cells per 15 x 100 mm plate).

4) Seed plates by adding an appropriate volume (based on cell count and resuspension volume) to each plate. Swirl each plate clockwise, counter-clockwise, and then cross, being careful not to splash the medium. Return plates to the incubator.

-Check cells daily for contamination-including obvious fungal growth, sudden changes in medium color, flocculation/sediment presence.
-Medium must be refreshed regularly. Do not allow cell overgrowth or medium to turn yellow (overly acidic).

-Record cell growth/proliferative behavior in terms of "% confluence" each day. Note growth trends, abnormal cell behavior, morphological variants, etc.
-Take photos using both 10x (for confluence confirmation and comparison) and 40x (normal and abnormal morphologies) objectives. Be sure to record both the magnification from the objectives (40x, 100x, 400x) and the camera zoom (50, 65, 88,or 100 mm) and include this info in the file name. Save photos as .jpg files. Be as descriptive as possible with file names. Start with the date, then cell line, then experimental surface, magnifications, experimental day, etc.
-Compile photos in power point slide format with labels and descriptive text. Be sure to include date, cell type, surface type, medium, experimental time, treatment conditions, magnification, and " % confluence". Organize slides into folders by cell type and surface type.

C.7 Treatment of cells with chemical stimulants: LPS and PMA[4-7]

C.7.1 Materials

-Lipopolysaccharide (LPS) from *E. coli* 0127:B8, chromatographically purified by gel filtration (Sigma Aldrich # L3137)
-Phorbol 12-myristate 13-acetate (PMA), molecular biology grade (Sigma Aldrich # P1585)
-Cell culture medium, plates, cells, etc.
-RNA or protein extraction reagents

C.7.2 Preparation of LPS stock solution

1) Resuspend 1 mg of LPS in 1 ml of phosphate buffered saline (PBS). (Add liquid directly to LPS powder without weighing, i.e. minimize contact with irritants like LPS).

2) Dilute this solution with an additional 3 ml of PBS to yield a final concentration of 250 μg/ml.

3) Aliquot 250 μl into 1.5 ml Eppendorf tubes. Label with chemical, concentration, date and your initials.

4) Store at -20° C for up to 2 years.

C.7.3 Preparation of PMA stock solution

1) Reconstitute 1 mg of PMA in 1 ml of cell culture grade dimethyl sulfoxide (DMSO).

2) Dilute this solution with an additional 9 ml of DMSO to achieve a final concentration of 100 μg/ml.

3) Aliquot into 1.5 ml Eppendorf tubes. Be sure to label with chemical, concentration, date and your initials.

4) Store in the dark at -20°C for up to 6 months.

C.7.4 Preparation of LPS-containing medium
Prepare the day before treatment. Use 10 ml of the appropriate medium per 15 x 100 mm plate. Adjust volume as necessary for smaller plates/wells. To achieve a **final treatment concentration of 1 μg/ml LPS** add 4 μl of 250μg/ml LPS stock to 10 ml of medium. Label the container with the final concentration and store at 4°C until use.

C.7.5 Preparation of PMA-containing medium
Prepare the day before treatment. Use 10 ml of the appropriate medium per 15 x 100 mm plate. Adjust volume as necessary for smaller plates/wells. To achieve a **final concentration of 100 nM PMA** add 6.18 μl of 100μg/ml PMA stock to 10 ml of medium. Label the container with the final concentration and store at 4°C until use.

C.7.6 Preparation of LPS/PMA-containing medium
Prepare the day before treatment. Use equal volumes of each of the final mixtures and store as noted above.

C.7.7 Plate preparation and cell seeding
1) Label 15 x 100 mm TCPS plates. (E.g. 16- LPS, 16- PMA, 16- LPS+PMA, 16- No RXN= total of 64 plates if you are using 4 cell lines with n = 4 replicates).

2) Harvest cells using appropriate methods and place into sterile Falcon tubes. For multiple replicates keep cells from different flasks separate and labeled. Record which passage number is used for each replicate. Remove an aliquot of cells for counting.

3) Centrifuge cells at 1,000 x g for 5 minutes. Resuspend and divide cells (based on cell count and desired number of cells for each treatment condition) and centrifuge again. Aspirate, resuspend cells in the appropriate (LPS/PMA) medium for each test condition and plate. *Incubate for 6 hours*. Harvest nucleic acids or proteins as desired.

C.8 Cell fixing and staining with the Hema 3® staining system

C.8.1 Materials
-Hema 3® Staining System (Fisher #122-911)
-Four plastic containers, each slightly larger than the plate to be stained

C.8.2 Staining procedure
1) Transfer plates to be fixed and stained from the incubator to the BSC.

2) Remove medium by aspiration-be careful to avoid touching the bottom of the wells. Exercise great caution when working with Teflon® AF surfaces, as they tend to delaminate easily from multi-well plates. For these surfaces it's best to tilt the plate, remove as much media as possible, rinse and then get as close as possible to the bottom of the well on the last aspiration step only.

3) Rinse one time with PBS (with divalent cations). Invert the plate and blot on a paper towel.

4) Add enough fixative (supplied with kit) to cover the bottom of each well. Use a 10 ml pipet and gently add the solution by pipetting down the side of each well. Let the solution sit briefly, 5-10 seconds.

5) Remove the fixative by gently inverting the plate over a plastic container and then blot on a paper towel. Save the fix and dye solutions for reuse.

6) Add approximately 300 µl of solution I (orange, supplied with kit) to each well (12-well plate), using a 10 ml pipet as described above. Let sit 20 seconds. Remove solution I by gently inverting the plate over a different plastic container, blot the plate on a paper towel. *DO NOT LEAVE DYE ON FOR ANY LONGER THAN A MINUTE-results in delamination of Teflon® AF films.

7) Add approximately 300 µl of solution II (purple, supplied with kit) to each well (12-well plate), as described above. Let sit 20 seconds. Remove solution II by gently inverting the plate over a different plastic container and then blot the plate on a paper towel. *DO NOT LEAVE DYE ON FOR ANY LONGER THAN A MINUTE-results in delamination of Teflon® AF films.

8) Wash each well gently two times by running nanopure water down the side of each well and rocking the plate when all wells contain water. Be sure not to spray the water directly on the bottom of the wells. Teflon AF delaminates easily, especially during these rinses-use great care!

9) Blot on a paper towel and allow the plate to air dry upside down overnight.

10) Assess plates microscopically, photograph. Label plates and save for future reference.

C.9 Protein harvest for the GTPase activity assays

C.9.1 Materials

Cell Lysis/binding/wash buffer	
	100 ml
$MgCl_2$	0.1 g
NP-40	1 ml
Glycerol	5 ml
DTT	0.015 g
Tris-HCl	0.3 g
NaCl	0.88 g
NPH_20	QS to 100 ml

Store cell lysis/binding/wash buffer at 4°C.

C.9.2 Procedure

Preparation:

1) Label three sets of microcentrifuge tubes for samples: one set simply the other two with the date, sample name and number, cell line and your initials.

2) Get ice and place in the BSC.

3) Turn microcentrifuge refrigeration unit on to 4°C.

4) Pull out cold PBS (immediately before starting), cell scrapers, 1ml tips and a P1000 pipet. Spray each item with 70% EtOH, wipe and transfer to the BSC.

Procedure:

1) Determine the total volume of lysis buffer needed to harvest plates. For each TCPS or PS plate use 0.5 ml. For each PLA or Teflon® AF plate, use 1 ml.

2) Prepare lysis buffer ***immediately before use*** by adding an appropriate amount of protease inhibitors:

Aprotinin	1 μg/ml.
Leupeptin (in DI water)	1 μg/ml.
PMSF (in EtOH)	1mM final.

For example, if using 12 ml of lysis buffer prepare your final working solution from stock as follows:

Aprotinin stock: 1.5 mg/ml. Desired final [ ]= 1 μg/ml. Thus, use 8 μl of aprotinin stock.

Leupeptin stock: 1 mg/ml. Desired final [ ]= 1 μg/ml. Thus, use 12 μl of leupeptin stock.

PMSF stock: 100 mM. Desired final [ ]= 1 mM. Thus, use 120 μl of PMSF stock.

3) Pull 2-3 plates to be harvested at one time. Aspirate media. Use ice cold Tris-buffered saline (TBS) or PBS to wash plates once (use approximately 5 ml per plate). Aspirate. Add 0.5 -1 ml of lysis buffer prepared as described above. (Invert tube before each addition). Immediately scrape (very gently on PLA and Teflon® AF surfaces) cells and transfer 20 μl of supernatant into a microcentrifuge tube for protein quantification. Transfer the remaining supernatant to another microcentrifuge tube (one per plate). **Vortex briefly**. Immediately place tube on ice for 5 minutes.

4) When all samples have been collected centrifuge at 16,000 x g at 4°C for 15 minutes.

5) **Immediately** proceed to GTP-pulldown procedures (to avoid GTP hydrolysis), per manufacturer's instructions (see Pierce EZ™-detect Rho, Rac and Cdc activation kit instructions). Do not allow samples to warm to room temperature until after the pulldown has been completed. After the pull down samples may be stored at -20°C until analysis by gel electrophoresis.

C.10 Denaturing gel electrophoresis-discontinuous gels

Note: The gel % should be carefully selected based on the protein separation desired. The protocol described here is useful for separating proteins ranging from c 10 to several hundred kD. Many factors affect protein separation, including the gel composition (buffer choice, inclusion of glycine and SDS, ratio of bis/acrylamide, final % acrylamide, etc), the gel temperature during electrophoresis, the separation time and applied voltage.

C.10.1 Solution preparation

5x Tris-Glycine electrophoresis buffer:

7.5 g	Tris*	(Bio-Rad # 161-0716)	Mol. Wt. 121.14
36.0 g	Glycine	(Bio-Rad # 161-0718)	Mol. Wt. 75.07
2.5 g	SDS (sodium dodecyl sulfate)		Mol. Wt. 288.38

QS to 500 ml with nanopure water. Dilute to 1x before using. May be re-used several times. Store at 4°C. (*Tris = THAM: Tris (hydroxymethyl)-aminomethane).
Make sure you use Tris (base), which has a pH c 11. These directions are not appropriate for Tris acid (Tris-HCl).

Acrylamide/bisacrylamide preparation:

Use a pre-mixed (commercially available) solution of 29:1 acrylamide to bisacrylamide, e.g., **40% acrylamide (29:1)** (Bio-Rad catalog # 161-0147). The bis/acrylamide ratio affects cross-linking and final porosity.

1.5 M Tris, pH 8.8

(1.5 M = 181.71 g per liter).
Dissolve 18.17 g of Tris in 100 ml, pH to 8.8 with 7 M HCl (allow ~25% of volume to adjust pH; dissolves readily without pH adjustment).

1 M Tris, pH 6.8

(1 M = 121.14 g per liter).
12.11 g in 100 ml, pH to 6.8 with 7 M HCl (allow ~30% of volume to adjust pH)

10% SDS (w/v)

% weight per volume (w/v) calculations are g/100 ml. Thus, for a 10% solution of SDS weigh out 10 g for every 100 ml. Use care when weighing out SDS-use a mask to avoid breathing this very fine powder in.

10% (w/v) Ammonium persulfate (APS) solution

Weigh out 1g of APS and QS to 10 ml with nanopure H_2O.
Freeze small aliquots (e.g., 50-100 µl). Dry APS can be stored desiccated, but it is very hygroscopic. It's preferable to reconstitute the entire bottle, aliquot and freeze. Frozen aliquots may be used for up to 2 years. When gels fail to polymerize, aged APS stocks are often the culprit.

C.10.2 Pouring gels

1) Prepare glass plates for electrophoresis. Plates should be washed thoroughly with warm water and Alconox soap, rinsed copiously with "nanopure grade" water and dried. Plates should be wiped clean with 70% ethanol, and dried with Kim™ wipes (not paper towels). Don't worry about the outsides (non-gel interfacing sides) of the plates.

Plates should not be handled with bare hands or dirty gloves, and always by the edges. Select appropriate combs (based on sample volumes to be loaded) and make sure comb size matches plate size (both are labeled, e.g., 0.75 mm, 1.5 mm). The well volumes associated with each comb can be found in the Bio-Rad catalog, electrophoresis section. Follow Bio-Rad instructions for plate assembly. Handle plates gently, they break easily.

2) Prepare 2 Falcon tubes. Label one "stacker" and the other "separator". The stacking gel volume will be much smaller than the separator gel volume.

2) Take out all solutions required to prepare the gels. Thaw APS. Place TEMED (N,N,N',N'-di-(dimethylamino)ethane) in a vented chemical fume hood (i.e., never in the BSC). Line up the reagents for each gel component (separator, stacker) on your bench top. E.g., for "separator" you will have sterile DI H_2O, acrylamide, 1.5 M Tris pH 8.8, and 10% SDS. ***Note: Use different Tris solutions for the separator and stacker!*** Use the tables below to determine amounts of each solution to add. The final volume will depend on how many gels you are pouring, and the size of the gels (e.g., 0.75 mm or 1.5 mm). To provide a gauge, 10 ml of separator is typically enough for 2-0.75 mm spaced gels.

3) Mix all components **EXCEPT TEMED**.

4) Place clean tips on P1000 and P200 pipets. Set aside. Have DI water open/available.

5) Take the "separator" gel mixture (only) to the hood. Add TEMED-watch the addition-even though the volume is very small it's easy to see the TEMED as it has a very different viscosity than the separator gel solution. Immediately invert the tube gently 2-3 times, avoid shaking which will result in bubbles. Immediately begin pouring the gel-use the P1000 pipet and pipet deliberately/slowly to avoid introducing bubbles into the solution. Fill plates approximately 65-70%. Rock to remove bubbles. Add a thin layer of DI water to the top and rock again. Allow the gel to set up. Follow the polymerization by checking the solution leftover in the Falcon tube-don't rock plates! Typically, gels will take 45 minutes to set up.

Separating Gel: 12% Acrylamide Gel

	5 ml	10 ml	15 ml
DI H_2O	2.15 ml	4.3 ml	6.4 ml
40% Acrylamide	1.5 ml	3 ml	4.5 ml
*1.5 M TRIS, **pH 8.8***	1.25 ml	2.5 ml	3.8 ml
10% SDS	50 µl	100 µl	150 µl
10% APS	50 µl	100 µl	150 µl
TEMED	2 µl	4 µl	6 µl

Stacking Gel: 5% Acrylamide

	5 ml
DI H_2O	3.6 ml
40% Acrylamide	625 µl
*1.0 M TRIS, **pH 6.8***	630 µl
10% SDS	50 µl
10% APS	50 µl
TEMED	5 µl

6) After polymerization occurs, wick off water. To do this take a Kim™ wipe and place it at the corner of the plates, then tilt the gel rig and allow the Kim™ wipe to wick up the water.

7) Add TEMED to the stacking gel, pour the stacking gel all the way to the top of the plates (eliminates air bubbles) and insert comb. The stacking gel will polymerize *much faster* than the separator gel. (The polymerization rate is controlled by the amount of TEMED added). Be careful to avoid acrylamide splashes when placing the comb(s)-wear safety glasses.

8) Gels may be used immediately, or wrapped in Kim™ wipes soaked in 1x Tris-glycine running buffer and stored in plastic bags at 4°C for up to 10 days. Leave combs in. Be sure to rinse wells of stored gels prior to loading samples.

*DON'T USE PRE-POURED GELS UNLESS YOU NEED A GRADIENT. Commercially prepared gels are VASTLY INFERIOR to fresh gels.

C.11 Western blot

C.11.1 Reagents

Protein sample buffer-denaturing
2 ml Glycerol
2 ml 10% SDS
0.25 mg Bromophenol blue
2.5 ml Tris-glycine running buffer (2x)

Add β-Mercaptoethanol (β-ME or 2-ME) immediately before each use. Store at 4° C in a tube wrapped in aluminum foil or a light sensitive container. If color dissipates add more bromophenol blue (final solution color should be blue, not brown). Note: You may prepare your own sample buffer, or purchase a commercially produced Laemmli sample buffer (e.g., Bio-Rad Catalog # 161-0737). The strength of the buffer you use to make up the dye determines the sample buffer strength. I.e. if you use 5x Tris buffer in your recipe you have 5x sample buffer. Remember that the final concentration of the solution you load into the wells should be 1x).

Western blot blocking buffer
3% Bovine serum albumin (BSA) in Tris-buffered saline (TBS). Weigh out 15 g of BSA, QS to 500 ml with 1x TBS.

Western 1° antibody buffer
(3% BSA, 0.05% Tween-20™ in TBS) Weigh out 15 g of BSA, add 450 ml of TBS, add 250 µl of Tween-20™ (polyoxyethylene (20) sorbitan monolaurate), QS to 500 ml with TBS.

Western 2° antibody buffer
(2.5% Milk, 0.2% Tween-20™ in TBS). Weigh out 12.5 g dry milk add 450 ml of TBS, add 1 ml of Tween-20™, QS to 500 ml with TBS.

TBST (Tris-buffered saline with Tween™)
(0.05% Tween-20 in TBS) Add 1 ml Tween-20™ to 2 L of TBS.

Western blot transfer buffer (pH 8.3)
12.12 g Tris (base)
57.6 g Glycine
800 ml Methanol
QS to 4 L with nanopure grade H_2O

C.11.2 Procedure
Notes: Save the buffers used in all of the steps except the Western blot transfer buffer. Milk or BSA-containing buffers should be prepared once a week. Sodium azide (NaN_3) should NEVER be used in the Western wash buffer as it interferes with some forms of detection.

(Day 1)
1) Prepare a denaturing polyacrylamide gel (SDS-PAGE) as described above.

2) Prepare samples, molecular weight markers, and appropriate positive control(s). ***Positive controls should always be included in Western blotting experiments, to verify experimental procedure and antibody- detection fidelity.***

In detail:

i) Protein samples should be quantified using the Bradford Protein Assay (Bio-Rad). Calculate the amount of protein necessary to load 25 μg of each protein sample per well. Protein quantification should be done as close as possible to the day samples are analyzed by Western blot, as some degradation is likely to occur over time/ due to multiple freeze-thaw cycles.

ii) Use the recommended amount of an appropriate positive control. (Either a nuclear extract or a cell lysate from a cell line we do not routinely employ. These are commercially available and the recommendations for positive controls are typically listed on the information sheet of each antibody). If you are quantifying you must use the same amount of sample protein and control protein.

iii) Prepare molecular weight markers (MWM), Kaleidoscope (Bio-Rad preferred). Use 10 μl per well. Multi-colored pre-stained markers are best for Westerns. *Do not heat denature pre-stained MWM. They will still work but it can reduce the amount of dye bound. Note the slight difference in molecular weights of dye-labeled markers.

Individual sample prep:
i) To each sample add:
1) 1-2 μl of β-ME. Store β-ME at 4°C, dispense in a chemical fume hood.
2) 2 volumes of (2x) sample buffer. (You can purchase this or make your own, *vida supra*).

ii) Vortex each sample briefly, quick spin or tap contents to the bottom of the tube.

iii) Heat samples (except MWM) at 90°C for 2-5 minutes, monitoring carefully to avoid caps popping open.

iv) Quick spin samples again, then load.

Gel prep:
Every 8 samples will require one 10 well SDS-PAGE gel (2 lanes for MWM and positive control samples). Larger gel set-ups also exist-an example is the Criterion set-up from Bio-Rad. (Gel % will vary with the molecular weight of the protein of interest).

Use a buffer dam if running a single gel.

Pre-rinse wells thoroughly with buffer (1x Tris-glycine running buffer). Be careful not to pierce the wells. The best way to remove residual acrylamide from the wells is to get air into the syringe and use it to "rinse" the acrylamide out of the well.

Load samples into each well using a Hamilton Microliter™ syringe. Rinse the syringe 2-3 times with buffer between loadings. The 10 well gels, (0.75mm spacer) should hold 25-30 μl. Top off inner rig chamber and fill outer electrophoresis unit chamber

with buffer, at least to the level where the platinum wire is covered. If running for extended time periods (2+ hours) fill up the outer chamber to keep the gel cool.

Run at 60-100V for approximately 30 minutes-2 hours, depending on desired separation. Increasing the voltage leads to reduced resolution.

Blot Prep: (Note: Protocol is slightly different if you are blotting onto PVDF)
Select an appropriate blotting membrane. PVDF can be charged, so make sure you have PVDF for Western blot applications. NC pore size varies. Use 25μm for the small Rho proteins (or anything 20-30 kD), and 45μm for the NFκ-B proteins (50, 65 and 100kD). If running a blot for the first time you can double up the blotting membrane to make sure that most of the protein hits and remains in the first membrane.

- Pre-soak the filter papers (2 per transfer), nitrocellulose (NC) (1 per transfer), and sponges (2 per transfer) in Western blot transfer buffer.
- When the gels are finished remove them from the chambers and place them in the transfer buffer. Soak briefly, 5 minutes.
- Pour the 1x running buffer back into the storage containers and put back in the refrigerator. (It can be reused several times)
- Rinse the electrophoresis chamber out well.
- Set up the blot as follows:
  Run to red----set up your blot as follows from black to red:
  (BLACK -Sponge-filter paper-gel-NC membrane-filter paper-sponge-RED).
  Double check that your NC is closer to the red side.
  Tips: Be careful not to rip your gel when removing it from the plate. Apply a thin layer of buffer to the gel after placing it on the filter paper and before placing the NC membrane on top of it for proper alignment. **Run your fingers over the top (or use a rolling pin) of the membrane after placing it on top of the gel to remove air bubbles (they will prevent protein transfer).**
- Place holders into blotting chamber, add the ice block and fill inner chamber to the top with Western transfer buffer.
- In the Criterion Blotter™ (Bio-Rad) run the transfer at 100V for 30-40 minutes.
- Mini-Protean™ systems (Bio-Rad) require 100V for three hours, and an ice block change. Place the entire chamber in an ice bucket.

Block:
Remove the NC membrane from the blotting set up (after checking for complete transfer- use the transfer of the MWM nearest to the size of your protein of interest as an indicator). Place in blocking solution for a minimum of one hour at room temperature with agitation (or overnight at 4°C).

Rinse:
3-5 rinses with PBS or TBS solutions. 15-20 ml is sufficient.

Primary Antibody Addition:
Prepare primary antibody solution by diluting the primary antibodies with primary antibody buffer (or Western wash buffer). Each NC membrane should be incubated separately with 10-12 ml (Criterion™ size membrane) or 5 ml (Mini-Protean™ size membrane) of primary antibody solution 3 hours-overnight with agitation at 4°C. Most suppliers indicate a range to try when using an antibody for the first time. Typically 1:500 is sufficient.

(Day 2)
Rinse:
Remove primary antibody solution and save for future use. Store at 4°C. Wash each membrane three times for 5 minutes with c 5-10 ml of (non-sterile) PBS.

Secondary antibody addition:
Prepare secondary antibody solution that is appropriate for use with the primary antibody of interest. (I.e. anti-rabbit if primary was a rabbit, anti-goat if primary was anti-goat, etc). Note: Secondary antibodies will typically be HRP-conjugated. For 1:1000 dilution use 10 µl per 10 ml of Western wash buffer. Incubate while shaking at room temperature for one hour (or longer at 4°C).

Rinse:
Remove and discard secondary antibody solution. Wash each membrane five times for 5 minutes at room temperature with 15-20 ml of PBS.

Develop:
Mix 12 ml of developer per NC (Criterion™ size) membrane OR 5 ml for each Mini-Protean™ size membrane. Use an equal amount of the two solutions found in the Pierce Supersignal® West Pico Kit (Product #s 1856135/6).

** DO NOT ADD DEVELOPER UNTIL YOU ARE AT THE DETECTION INSTRUMENT. Develop for 30 seconds-3 minutes at room temperature. The developing solution is good for up to eight hours. If you can visualize the bands on the NC membrane with your naked eye they are overdeveloped and cannot be quantified.

After scanning save NC membranes in plastic sheets. Do not tape in, as it is difficult to remove them for re-staining if necessary.

C.12 Functional blocking assays with monoclonal antibodies

C.12.1 Notes
Antibody Sourcing: antibody source and preparation has critical implications for blocking experiments, depending on cell type. Antibody production is generally from a B-cell that produces the clone of interest, fused with a tumor cell (thus, a hybridoma). These hybridomas may be grown in flasks, where they secrete antibodies into the media. The media is then collected and affinity purified, which typically leads to a 10-15 x more

concentrated product than the supernatant. Antibodies purified with this method are typically marked as "affinity purified".

Hybridoma cells can also be placed *in vivo* (ascites), where they become hyperactivated and churn out many antibodies. The problem with antibodies from ascites is that they may also contain growth factors and inflammatory cytokines, which is potentially problematic (i.e., activating) for certain cell systems (e.g., monocytes/macrophages).

Isotype control: Ensures that the effect is specific for the antibody employed. When running integrin blocking studies a non-integrin directed antibody should be selected as an isotype control. Using ascites sourced antibodies requires an additional control (to ensure that the effects seen can be attributed to the antibody, rather than to the cocktail the antibody is supplied in).

Control Set Up:
1) Negative control (no antibodies).
2) Isotype control (antibody is not specific for the target of interest).
3) Positive control---test the antibody of interest in a known system.

C.12.2 Reagents

-Function-blocking monoclonal antibodies (MAb) of interest-preferably affinity purified. Must be low endotoxin and azide-free for function blocking assays.
-Matched (to MAb of interest) isotype control antibody. Must be low endotoxin and azide-free for function blocking assays.
-24 and 96 well plates
-Hema 3® staining kit

C.12.3 Procedure

The day before the blocking experiment:
1) Prepare plates to be used in the assay, e.g. Teflon® AF and TCPS. Label plates with cell type, passage number (or age) and blocking information. Pre-treat plates with cell-appropriate medium (or protein solution) overnight. (Do not pre-treat Teflon® AF plates for more than 24 hours, as this facilitates delamination upon staining).

2) Label sterile flip-top 15 ml Falcon tubes for each (cell) replicate as follows: negative control, blocks (e.g., α_M, β_2, $\alpha_M\beta_2$) and isotype controls (as many isotype controls as the number of different antibodies employed to block with, e.g., α_M isotype control, β_2 isotype control).

The day of the blocking experiment:
3) Place PBS (with divalent cations) in a 37° C water bath. Harvest and count cells, as previously described (*vida supra*). Make sure cells are harvested in medium. Separate the cells into the labeled Falcon tubes as appropriate based on the number of cells needed for each assay.

For example, each 24 well plate requires 84,000 cells per well to achieve a seeding density of 500 cells/mm^2. For two replicates, this would require 168,000 cells per Falcon tube. Pay careful attention to volumes, as the final volume per well varies based on the type of surface and the well size and the blocking antibody or isotype control antibody solutions will account for some volume. See the table below for seeding number and volume references.

Surface	Plate/well diameter	Plate/well area	# Cells required to seed at a density of 500 cells/mm^2	Minimum volume required for coverage
TCPS-96 well plate, single well	0.3 cm	30 mm^2	15,000 cells/well	60 µl[Y]
Teflon® AF-96 well plate, single well	0.3 cm	30 mm^2	15,000 cells/well	60 µl[Y]
TCPS-24 well plate, single well	1.5 cm	200 mm^2	84,000 cells/well	200 µl[ς]
Teflon AF®-24 well plate, single well	1.5 cm	200 mm^2	84,000 cells/well	650 µl[ς]
TCPS standard plate	10 cm	78.5 cm^2	3,925,000 cells/well	10 ml[∂]
Teflon AF® standard plate	10 cm	78.5 cm^2	3,925,000 cells/well	15 ml[∂]

[Y]Pre-cell-seeding incubation volumes were 100 µl. [ς]Pre-cell-seeding incubation volumes were 1000 µl. [∂] Pre-cell-seeding incubation volumes were equivalent to the volume of media used for the experiment.

4) Prepare negative controls first, isotype controls second and blocking assays last. Add an appropriate amount of antibody solution (typically supplied as a 1 mg/ml solution, must be a low endotoxin and azide-free formulation). Function-blocking assays may require up to 100 µg/ml of blocking antibody (or as little as 10 µg/ml) to achieve "significant" effects. (For blocking experiments "significant" is ≥ 80%).

5) Incubate the cells at 4° C for 30 minutes, rocking.

6) Aspirate medium or protein solution(s) from the plate(s) to be seeded. Carefully add cell suspensions to each well. Gently rock the plate(s) to ensure that cells are evenly dispersed over the entire surface. Incubate for one hour at 37° C, 98% humidity.

7) Remove plates, aspirate medium and rinse twice with 1 ml of warm PBS (with divalent cations). (Add washes to the side of the well rather than pipetting directly onto the surface).

8) Fix and stain cells using the Hema 3® kit. Dry inverted plates overnight.

9) Evaluate assays by microscopic examination. Photograph a minimum of 3 low magnification (10x objective) fields per well. Examine and record cell morphology using the 40x objective.

10) Count and average fields for each replicate. A minimum of four independent trials should be performed for each test. The blocking assay should be compared to the negative controls. The isotype control and negative control should be highly similar in terms of both cell adhesion numbers and cell morphology. The average of 4 trials should result in 80% blocking or better to be considered a significant positive result.

C.13 References

1. Mauel J, Defendi V. Infection and transformation of mouse peritoneal macrophages by simian virus 40. *J Exp Med* 1971;**134**:335-50.

2. ATCC Cell Lines and Hybridomas. Rockville, MD: American Type Culture Collection, 1994:337.

3. Kaltenbach JP, Kaltenbach MH, Lyons WB. Nigrosin as a dye for differentiating live and dead ascites cells. *Exp Cell Res* 1958;**15**:112-7.

4. Balsinde J, Balboa MA, Insel PA, Dennis EA. Differential regulation of phospholipase D and phospholipase A2 by protein kinase C in P388D1 macrophages. *Biochem J* 1997;**321**:805-9.

5. Chapekar MS, Zaremba TG, Kuester RK, Hitchins VM. Synergistic induction of tumor necrosis factor alpha by bacterial lipopolysaccharide and lipoteichoic acid in combination with polytetrafluoroethylene particles in a murine macrophage cell line RAW 264.7. *J Biomed Mater Res* 1996;**31**:251-6.

6. Gomez-Cambronero J, Huang CK, Yamazaki M, Wang E, Molski TF, Becker EL, Sha'afi RI. Phorbol ester inhibits granulocyte-macrophage colony-stimulating factor binding and tyrosine phosphorylation. *Am J Physiol* 1992;**262**:C276-81.

7. Hitchins VM, Merritt K. Decontaminating particles exposed to bacterial endotoxin (LPS). *J Biomed Mater Res* 1999;**46**:434-7.

List of Abbreviations

AA	acrylic acid
Ag	antigen
AlAm	allylamine
AP-1	activating protein–1
APS	ammonium persulfate
ATCC	American type culture collection
BD	binding domain
β-ME	β-mercaptoethanol
BMMO	bone marrow macrophage
BSA	bovine serum albumin
C3	complement protein 3
CCR	"CC" chemokine receptor
CD	cellular determinant
C/EBP	CCAAT enhancer binding protein
CSF	colony stimulating factor
DAG	diacylglycerol
DC	dendritic cells
DC-STAMP	dendritic cell-specific transmembrane protein
DI	deionized
DMEM	Dulbecco's modification of Eagle's medium
DPBS	Dulbecco's phosphate buffered saline
DTT	dithiothreitol
ECM	extracellular matrix
Ets	e26 transformation-specific sequence
EU	endotoxin units
FBGC	foreign body giant cell

FBR	foreign body reaction/response
FBS	fetal bovine serum
Fc	fragment constant
FC	fluorocarbon
FcR	IgG Fc receptor
FcRN	MHC-related Fc receptor for IgG
Fg	fibrinogen
FGF	fibroblast growth factor
Fn	fibronectin
GAP	guanine activating protein
GAPDH	glyceraldehyde-3-phosphate dehydrogenase
GDI	GDP-dissociation inhibitors
GDP	guanosine diphosphate
GEF	guanine nucleotide exchange factor
GM-CSF	granulocyte macrophage-colony stimulating factor
GST	glutathione S-transferase
GTP	guanosine triphosphate
HBSS	Hank's balanced salt solution
HEP	PDGF-like growth factor
HI	heat inactivated
HRP	horse radish peroxidase
HxAm	hexylamine
ICAM	intracellular adhesion molecule
IFN-γ	interferon gamma
Ig	immunoglobin
IL	interleukin
kD	kilodalton
LFA-1	lymphocyte function associated antigen-1, $\alpha_L\beta_2$, CD11a/CD18
LPS	lipopolysaccharide
MAb	monoclonal antibody
Mac-1	CR3, $\alpha_M\beta_2$, CD11b/CD18

MC	monocyte
(MC-) MΦ	(monocyte-) macrophage
MCP-1	monocyte chemoattractant protein-1
M-CSF	macrophage-colony stimulating factor
MDC	macrophage-derived chemokine
MHC	major histocompatibility complex
MFR	macrophage fusion receptor
MIP	macrophage inflammatory protein
MMP	matrix metalloproteinase
MMR	macrophage mannose receptor
MnGC	multinucleated giant cell
MO	macrophage
MΩ	megaohm
MPCR	multiplex polymerase chain reaction
MWM	molecular weight marker
NC	nitrocellulose
NF-κB	nuclear factor-κB
NK	natural killer
NVFA	N-vinylformamide
NVP	N-vinyl-2-pyrrolidinone
p150,95	$\alpha_X\beta_2$, CD11c/CD18
PA	plasminogen activator
PAF	platelet activating factor
PAGE	polyacrylamide gel electrophoresis
PBS	phosphate buffered saline
PCA	principle component analysis
PCR	polymerase chain reaction
PDGF	platelet-derived growth factor
PE	polyethylene
PET	poly (ethylene terephthalate)
PGA	poly (glycolic acid)

PGD_2	prostaglandin D_2
PGE_2	prostaglandin E_2
PKC	protein kinase C
PLA	poly-l-lactide
PLGA	copoly (lactic-glycolic acid)
PMA	phorbol 12-myristate 13-acetate
PMSF	phenylmethylsulfonyl fluoride
pp	plasma polymerization
PP	polypropylene
PS	polystyrene
PTFE	polytetrafluoroethylene
NO	nitric oxide
RA	receptor antagonist
ROCK	Rho activated kinase
RT-PCR	reverse transcriptase polymerase chain reaction
SAM	scanning Auger microscopy
SIMS	secondary ion mass spectroscopy
SDS	sodium dodecyl sulfate
SE	spectroscopic ellipsometry
SEM	scanning electron microscopy
STM	scanning tunneling microscopy
TBS	Tris-buffered saline
TBST	Tris-buffered saline plus Tween®-20
TCPS	tissue culture polystyrene
TEM	transmission electron microscopy
TEMED	N, N, N', N'-di-(dimethylamino)ethane
TGF-α	transforming growth factor-α
T_H	T helper
TNF-α	tumor necrosis factor alpha
Tof-SIMS	time-of-flight secondary ion mass spectroscopy
TPA	12-O-tetradecanoylphorbol-13-acetate

uPA	urokinase plasminogen activator
UV	ultraviolet
VEGF	vascular endothelial growth factor
VLA-4	very late antigen-4, $\alpha_4\beta_1$, CD49d/CD29
Vn	vitronectin
WCL	whole cell lysate
XPS	X-ray photoelectron spectroscopy